Impact of KIR/HLA-C Interactions on the anti-HIV-1 Activity of NK Cells

Dissertation

with the aim of achieving a doctoral degree at the Faculty of Mathematics, Informatics and Natural Sciences Department of Biology, University of Hamburg

submitted by

Sarah Vollmers

Hamburg, May 2022

The following evaluators recommended the admission of the dissertation:

First reviewer: **Prof. Dr. Marcus Altfeld**
Research Department Virus Immunology, Leibniz Institute of Virology, Hamburg, Germany

Second reviewer: **Prof. Dr. Julia Kehr**
Institute of Plant Science and Microbiology, Department Biology, University of Hamburg, Hamburg, Germany

Date of oral defense: 06.09.2022

Abstract

Background and hypothesis: NK cells play a crucial role in antiviral immunity by utilizing a large array of activating and inhibitory receptors to identify and eliminate virus-infected cells. Killer-cell immunoglobulin-like receptors (KIR) represent a highly polymorphic receptor family, regulating NK cell activity. Human leukocyte antigen (HLA) class I molecules are expressed on almost all somatic cells and serve as a primary ligand for KIRs. HLA-C is the most recently evolved HLA class I molecule and serves as a ligand for the inhibitory KIR2DL receptors. Accumulating evidence indicate that HLA-C/KIR2DL interactions can drive HIV-1-mediated immune evasion and contributes to the intrinsic control of HIV-1 infection. However, little is known about the complex interplay of *HLA-C/KIR2DL* immunogenetics, NK cell-mediated immune pressure and HIV-1 immune escape. Based on the diverse and highly polymorphic combinations of HLA-C and KIR2DL and a potential importance in HIV-1 infection, this thesis aims to assess the impact of *HLA-C* and *KIR2DL* host genetics on NK cell activity in HIV-1 infection and immune evasion.
Methods: Differences in binding affinity and specificity between various HLA-C/KIR2DL allotype combinations were assessed using KIR2DL-Fc fusion proteins and KIR2DL-expressing reporter cell lines. The anti-HIV-1 activity of $KIR2DL^+$ NK cells and role of NK cell education was assessed by using an *in vitro* HIV-1 infection model and CD107a degranulation assays. To investigate the impact of *HLA-C/KIR2DL* combinations on the NK cell repertoire and HIV-1 Vpu protein sequence variations, a phenotypic characterization of NK cells from untreated $HIV\text{-}1^+$ individuals and $HIV\text{-}1^-$ individuals was performed by multi-parameter flow cytometry. In addition, *Vpu* from genomic DNA and plasma samples was analyzed for sequence polymorphisms in context of *HLA-C/KIR2DL* genotypes.
Results: Binding assays of HLA-C and KIR2DL combinations showed large differences in binding affinities between different combinations. CD107a degranulation assays revealed higher frequencies of CD107a in NK cells with inhibitory receptors for self-HLA class I molecules. Moreover, phenotypic characterization of NK cells revealed differences in NK cell receptor profiles between $HIV\text{-}1^+$ and $HIV\text{-}1^-$ individuals and a genotype-dependent expansion of $KIR2DL1^+$ NK cells in $HIV\text{-}1^+$ individuals carrying the respective HLA-C2 ligand. Lastly, *Vpu* sequencing indicated a selection of Vpu sequence variants in association with high HLA-C allele expression and strong KIR2DL/HLA-C binding affinities.
Conclusion: Altogether, the results of this thesis provide evidence that HIV-1 is associated with changes in the KIR repertoire of NK cells that to a certain extent are pre-determined by host *HLA-C/KIR2DL* genotypes. HLA-C expression level and HLA-C/KIR2DL binding affinities might have an impact on HIV-1 Vpu sequence polymorphisms as a potential mechanism to evade the host immune response.

Table of contents

Table of contents

Table of contents

List of publications

Lettau M, Dietz M, **Vollmers S**, Armbrust F, Peters C, Dang TM, Chitadze G, Kabelitz D, Janssen O. Degranulation of human cytotoxic lymphocytes is a major source of proteolytically active soluble CD26/DPP4. Cell Mol Life Sci. 2020, 77, 751-764, doi:10.1007/S00018-019-03207-0.

Schwane V, Huynh-Tran VH, **Vollmers S**, Yakup VM, Sauter J, Schmidt AH, Peine S, Altfeld M, Richert L, Körner C. Distinct Signatures in the Receptor Repertoire Discriminate CD56bright and CD56dim Natural Killer Cells. Front. Immunol. 2020, 11, doi:10.3389/FIMMU.2020.568927.

Vollmers S, Lobermeyer A, Körner C. The New Kid on the Block: HLA-C, a Key Regulator of Natural Killer Cells in Viral Immunity. Cells. 2021, 10, 3108, doi:10.3390/CELLS10113108.

List of abbreviation

AA: amino acid

ADCC: antibody-dependent cellular cytotoxicity

AIDS: acquired immunodeficiency syndrome

APC: antigen presenting cell

ART: antiretroviral therapy

β-TrCP: β-transducin repeat-containing protein

β2m: β2-microglobuline

BC: buffy coat

BCA: bicinchoninic acid

BCR: B cell receptor

CD: cluster of differentiation

cDNA: complementary DNA

DAMPs: damage-associated molecular patterns

DMEM: Dulbecco's Modified Eagle's Medium

DMSO: dimethyl sulfoxide

EDTA: ethylenediaminetetraacetic acid

ER: endoplasmic reticulum

FasL: Fas ligand

FBS: fetal bovine serum

FMO: fluorescence minus one

FSC: forward scatter

fw: forward

gp: glycoprotein

GWAS: genome-wide association study

HBV: hepatitis-B virus

HCV: hepatitis-C virus

HCMV: human cytomegalovirus

HIV: human immunodeficiency virus

HLA: human leukocyte antigen

HSV: herpes simplex virus

IFN-γ: interferon-γ

IL: interleukin

IRF: interferon-response factor

ISRE: interferon stimulated response element

ITAM: immunoreceptor tyrosine-based activating motif

ITIM: immunoreceptor tyrosine-based inhibition motif

KIR: killer-cell immunoglobulin-like receptor

List of abbreviation

KO: knockout

LAMP-1: lysosomal-associated membrane protein-1

LRC: leukocyte receptor complex

MCMV: murine cytomegalovirus

MFI: median fluorescence intensity

miRNA: microRNA

mRNA: messenger-RNA

NCR: natural cytotoxicity receptor

Nef: negative regulatory factor

NGS: Next Generation Sequencing

NK cell: natural killer cell

NKG2: natural-killer group 2 receptors

PAMPs: pathogen-associated molecular patterns

PBMCs: human peripheral blood mononuclear cells

PBS: phosphate buffered saline

PLC: peptide-loading complex

PMT: photomultiplier tube

PRRs: pattern recognition receptors

RFI: relative fluorescence intensity

RPMI: Roswell Park Memorial Institute

RT: room temperature

rv: reverse

SCF: SKP1-cullin1-F-Box

SFM: serum free medium

SIV: simian immunodeficiency virus

SNP: single-nucleotide polymorphism

SSC: side scatter

Tat: trans-activator of transcription

TCR: T cell receptor

TH: T helper

TNF-α: tumor necrosis factor-α

TRAIL: TNF-related apoptosis-inducing ligand

UKE: University Medical Center Hamburg-Eppendorf

UTR: untranslated region

Vif: viral infectivity factor

Vpr: viral protein R

Vpu: viral protein U

VSVG: vesicular stomatitis virus glycoprotein

1 Introduction

1.1 The human immune system

The human immune system is a complex defense network of different organs, cells and proteins that is able to recognize and fight a variety of pathogens such as bacteria, viruses, parasites or fungi, as well as abnormal cell growth. Besides structural and chemical barriers against pathogens, the human immune system is subdivided into two parts: the innate and adaptive immune response (Chaplin, 2010). The innate immune response is the first line of defense and includes the physical barriers of skin and mucous membrane, as well as cells and soluble proteins. Innate immune cells such as dendritic cells, macrophages, monocytes, neutrophils and epithelial cells recognize a broad spectrum of molecular patterns that are expressed by pathogens (pathogen-associated molecular patterns; PAMPs) or released from host cells during cell damage or cell death (damage-associated molecular patterns; DAMPs) by using pattern recognition receptors (PRRs) (Kumar *et al.*, 2011). Another component of the innate immune system is the complement system, which contains a number of plasma proteins that cause the opsonisation and killing of pathogens and induces an inflammatory response to trigger immune cells (Janeway *et al.*, 2001). Moreover, macrophages, neutrophils, monocytes and dendritic cells are professional phagocytes, able to engulf pathogens and "digest" them via phagocytosis. Parts of these ingested pathogens can be presented on the surface of macrophages and dendritic cells to activate the adaptive immune response (Lim *et al.*, 2017). Natural killer (NK) cells are effector cells of the innate immune system that express activating and inhibitory receptors to sense virus-infected or tumor cells (Vivier *et al.*, 2008). Unlike the innate immune response, the adaptive immune response is much slower but highly specific. This system is based on the recognition of foreign proteins, also referred to as antigens, and the induction of an effective and tailored immune response, which leads to an immunological memory (Alberts, 2002). The specific defense mechanisms of the adaptive immune system are carried out by B and T cells. B cells produce antigen-specific antibodies and present antigens on the cell surface. They mature in the bone marrow and circulate through the secondary lymphoid organs. B cells become activated when their B cell receptor (BCR) binds an antigen, which results in proliferation and differentiation into an antibody-secreting plasma cell. The produced antibodies neutralize pathogens by blocking the ability to bind and infect host cells or agglutinate and form cluster with pathogens, which can be recognized by phagocytes of the innate immune system (Hoffman *et al.*, 2016). Moreover, B cells take up the antigen via BCR-mediated endocytosis to present it to T cells. T cells are also produced in the bone marrow and mature in the thymus. In terms of their function, there are different subsets of T cells. The two major types of effector T cells are CD4 and

CD8 T cells, which are named after the expression of the receptor that is involved in antigen recognition. CD4 T cells, are activated by the recognition of exogenous antigens that are presented by HLA class II molecules on the cell surface of antigen presenting cells (APCs) like B cells, dendritic cells and macrophages. By releasing cytokines, including interferon-γ (IFN-γ) or interleukins (IL), T cells shape the activation and differentiation of other immune cells. Based on the expression of cytokines and transcription factors, five major CD4 T cell subsets have been identified: T helper (TH)1, TH2, TH17, regulatory T and follicular helper T cells (Zhu *et al.*, 2020). CD8 T cells are cytotoxic T cells, which are directly involved in killing transformed and infected cells by releasing cytotoxic granules. The membrane bound T cell receptor (TCR) of cytotoxic T cells recognizes antigens that are associated with HLA class I molecules presented on the cell surface of nucleated cells. One of the most important consequences of the adaptive immune response is the creation of an immunological memory, which launches a rapid and more effective immune reaction to a pathogen that has been encountered previously (Pennock *et al.*, 2013).

1.2 Natural killer cells

Natural killer (NK) cells are large granular lymphocytes that are best characterized by their cytotoxic effector and cytokine production function (Vivier *et al.*, 2008). As part of the innate immune system, NK cells are involved in the early defense against pathogens, especially during viral infections, as well as in controlling tumor formation. NK cells develop in the bone marrow and some NK cell subsets also mature in the thymus and in secondary lymphoid tissues, including spleen, tonsils and lymph nodes (Abel *et al.*, 2018) where they undergo differentiation processes that lead to a heterogeneous population of cells with distinct phenotypes and functions. In humans, NK cells are generally defined by the presence of CD56 and the absence of CD3 and can be broadly divided into $CD56^{bright}$ and $CD56^{dim}$ subpopulations. $CD56^{bright}CD16^{-}$ NK cells are efficient cytokine producers and found predominantly in the secondary lymphoid tissues, liver, skin, uterus and bone marrow (Björkström *et al.*, 2016). The majority of NK cells in the peripheral blood are further differentiated into $CD56^{dim}CD16^{+}$ NK cells, which are characterized as a highly diverse cell population with a high cytotoxic potential (Horowitz *et al.*, 2013).

1.2.1 NK cell effector function

NK cells are crucial for the immune response by directly lysing target cells and by producing cytokines. NK cells express a number of different receptor groups, including activating and inhibitory receptors. These receptors interact with ligands that are expressed on the cell surface of healthy cells and with ligands expressed on the surface of virus-infected or tumor cells. Recognition of target cells through activating and inhibitory receptors induces NK cell activation, which leads to a cytotoxic immune response that is characterized by a degranulation of secretory lysosomes and release of cytotoxic molecules such as perforin

and granzymes (Vivier *et al.*, 2008). NK cells can also eliminate target cells through several mechanisms including antibody-dependent cellular cytotoxicity (ADCC), which is induced by the engagement of the low-affinity Fc receptor Fcγ RIIIa (CD16) and the Fc portion of antibodies (Caligiuri, 2008) or through death ligands like Fas ligand (FasL) or TNF-related apoptosis-inducing ligand (TRAIL) (Smyth *et al.*, 2001). Moreover, cytokines release by NK cells and other immune cells, as well as abnormal cells, shape the immune response and allows cross-talk between innate and adaptive immunity. By secreting IFN-γ and tumor necrosis factor-α (TNF-α), NK cells promote the maturation and activation of dendritic cells, T cells and macrophages (Walzer *et al.*, 2005; Nedvetzki *et al.*, 2007), whereas type I IFNs, IL-2, IL-12, IL-15 and IL-18 are potent NK cell activators that promote NK cell proliferation, cytotoxicity and cytokine production (Walzer *et al.*, 2005). **Figure 1** summarizes the described NK cell effector functions.

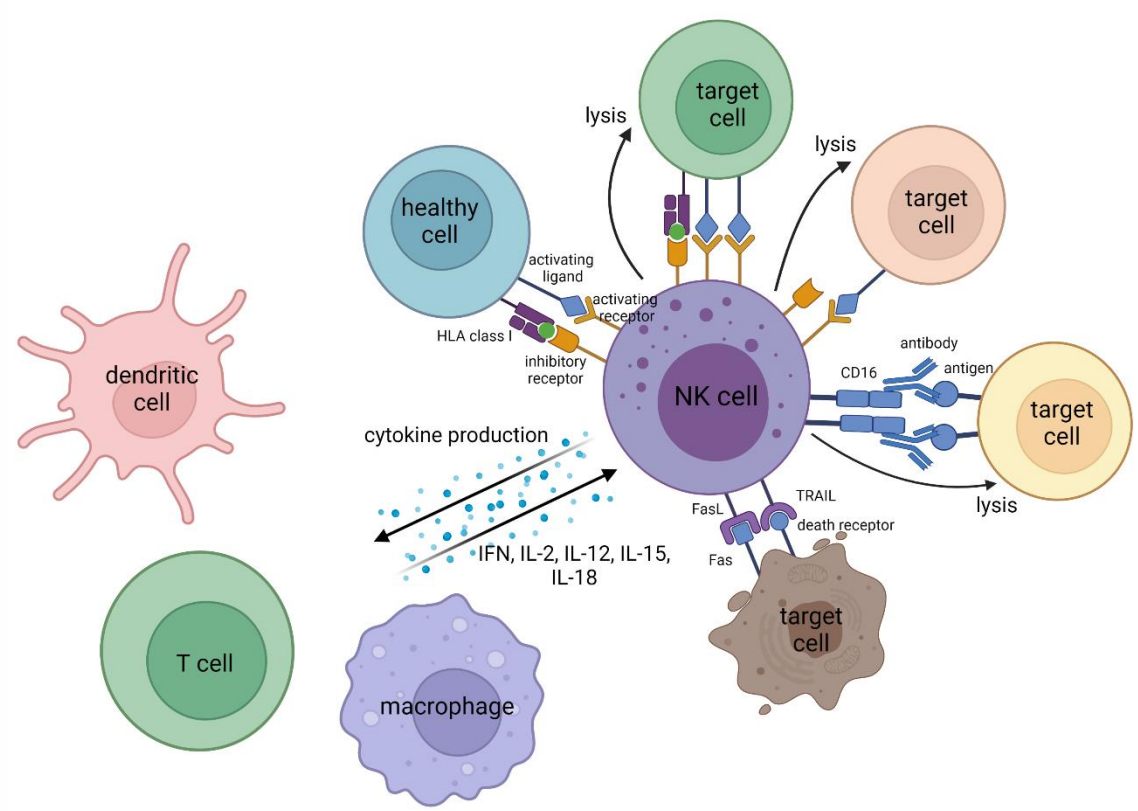

Figure 1: NK cell effector functions. NK cells are large granular lymphocytes that are able to discriminate heathy "self" cells from target cells and to recruit other immune cells by producing cytokines. To regulate NK cell function, NK cells express activating and inhibitory receptors that detect target cells by different mechanisms. Healthy cells do not activate NK cells by expressing ligands for both activating and inhibitory receptors. Changes in the expression profile of activating and inhibitory ligands, induced by stress, virus infections or tumor formation, activates NK cells to kill target cells. Activating receptors recognize the upregulation of activating ligands, whereas inhibitory recognize the absence of inhibitory ligands, mainly HLA class I molecules, by the "missing-self" signal. The low-affinity Fc receptor CD16 detects cells that are coated with antibodies, which induces antibody-dependent cellular cytotoxicity (ADCC). Moreover, NK cells are able to promote apoptosis when death ligands bind their cognate death receptor expressed by target cells. Other immune cells also produce and release cytokines to shape the immune response of NK cells.

1.2.2 NK cell receptors

The cytotoxic function of NK cells is tightly regulated through the expression of germline-encoded activating and inhibitory receptors that are able to discriminate between stressed, transformed or virus-infected and healthy cells (Lanier, 2005; Bryceson *et al.*, 2006). Activating receptors generally detect the presence of stress-induced self ligands that are expressed for example by transformed or virus-infected cells. In contrast, inhibitory receptors recognize surface molecules, mainly HLA class I molecules that are constitutively expressed on the surface by most of the cells. Reduced expression of HLA class I molecules caused for example by viruses triggers NK cell-mediated killing and is referred to as "missing-self signal" (Sivori *et al.*, 2019). Besides CD16, NK cells express a large range of activating receptors, including the natural cytotoxicity receptors (NCRs) NKp30, NKp44 and NKp46 that recognize a broad variety of bacterial, virus-derived and tumor cell ligands (Sivori *et al.*, 1997; Vitale *et al.*, 1998; Pende *et al.*, 1999). In addition, there are generally two more major receptor groups that are expressed by NK cells, comprising activating, as well as inhibitory receptors: the killer-cell immunoglobulin-like receptors (KIRs) and natural-killer group 2 receptors (NKG2) (Pegram *et al.*, 2011). KIRs are type I membrane proteins that recognize various HLA class I alleles. They have either a long (L) or a short (S) cytoplasmic domain, corresponding to their function as inhibitory or activating receptor. NKG2s are members of the C-type lectin-like receptor family and comprise seven members (NKG2-A, -B, -C, -D, -E, -F and -H) with A/B and E/H being splice variants of the same gene. They form homodimers (NKG2D) or heterodimers with CD94 (CD94/NKG2A, -B, -C, -E) and have either activating (e.g. CD94/NKG2C) or inhibitory (CD94/NKG2A) function (Brostjan *et al.*, 2000). **Figure 2** shows the activating and inhibitory receptors that are expressed on NK cells.

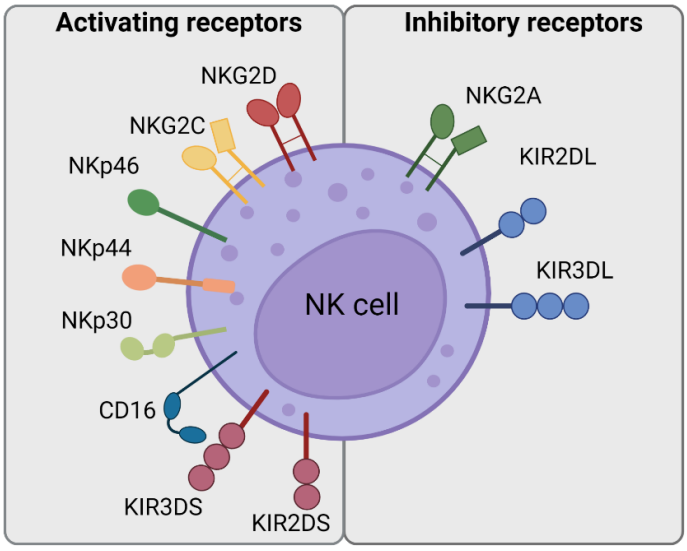

Figure 2: Activating and inhibitory receptors on NK cells. NK cells express a number of activating receptors that can activate the cytotoxic and secretory function of NK cells. Besides CD16, NK cells express three main receptor groups: natural cytotoxicity receptors (NKp30, NKp44 and NKp46), natural-killer group 2 receptors, including NKG2A, NKG2C and NKG2D and killer-cell immunoglobulin-like receptors (KIR).

1.2.3 Killer-cell immunoglobulin-like receptors

Killer-cell immunoglobulin-like receptors (KIRs) are a highly diverse family of receptors that are expressed on the cell surface of NK cells and on subsets of CD8 T cells (Mingari *et al.*, 1995). The diversity of these receptors arises from variability in *KIR* gene content through *KIR* gene copy number variation, allelic polymorphism and absence or presence of *KIR* genes (Shilling *et al.*, 2002; Vilches *et al.*, 2002). *KIR* genes are part of the leukocyte receptor complex (LRC) located on chromosome 19q13.4 and consist of up to 15 genes (*KIR2DL1*, *KIR2DL2*, *KIR2DL3*, *KIR2DL4*, *KIR2DL5A, KIR2DL*5B, *KIR2SD1*, *KIR2DS2*, *KIR2DS3*, *KIR2DS4*, *KIR2DS5*, *KIR3DL1, KIR1DS1*, *KIR3DL2*, *KIR3DL3*) and 2 pseudogenes (*KIR2DP1* and *KIR3DP1*) (**Figure 3**) (Wilson *et al.*, 2000). The *KIR* gene complex has four genes at the 5' centromeric and 3' telomeric end (*KIR3DL3* and *KIR3DL2*) and a central cluster formed by *KIR3DP1* and *KIR2DL4*. Despite the high variability level of *KIR* gene content, two main KIR haplotypes "A" and "B" have been identified (Norman *et al.*, 2009; Jiang *et al.*, 2012). The A haplotypes have a fixed gene content of 6 genes encoding for mainly inhibitory KIR receptors (*KIR2DL1*, *KIR2DL3*, *KIR3DL1*, *KIR3DL2* and *KIR2DL4*) and only one activating KIR (*KIR2DS4*) that in some A haplotypes does not code for a surface molecule (Hsu, Liu, *et al.*, 2002; Maxwell *et al.*, 2002). In contrast, B haplotypes are characterized by the presence of at least one of the following genes: *KIR2DS2*, *KIR2DL2*, *KIR2DL5B*, *KIR2DS3*, *KIR3DS1*, *KIR2DL5A*, *KIR2DS5* and *KIR2DS1*. Consequently, KIR A haplotypes differ from each other predominantly due to *KIR* allelic polymorphism, whereas KIR B haplotypes differ on the basis of their gene content (**Figure 3**). So far, over 1000 *KIR* alleles have been identified (*IPD - KIR Alleles | EBI*). KIRs are named in order to reflect the function and structure of the molecule. They consist of two or three extracellular domains (2D or 3D) and a short or a long cytoplasmic tail (S or L), which consequently reveals the function of the receptor (activating or inhibitory) (**Figure 4A**) (Pende *et al.*, 2019). Activating KIRs possess a charged lysine in their transmembrane region, which allows the association with an adapter protein DAP12 containing immunoreceptor tyrosine-based activating motifs (ITAMs) in its cytoplasmic tail. Ligand binding to activating KIRs results in a phosphorylation of tyrosines within the ITAMs and induces intracellular signaling to activate the NK cell (Lanier *et al.*, 1998). The long cytoplasmic tail of inhibitory KIRs contains immunoreceptor tyrosine-based inhibition motifs (ITIMs). When ligands associate with an inhibitory KIR, the tyrosine in the ITIMs is phosphorylated and binds intracellular phosphatases, which inhibits signaling (**Figure 4B**) (Renard *et al.*, 1997).

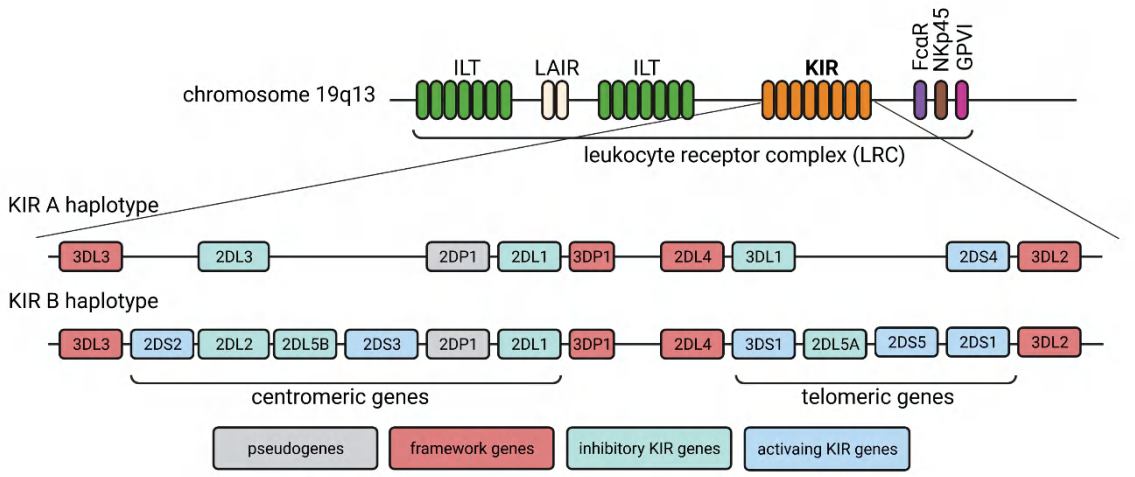

Figure 3: KIR genes and haplotypes. Killer-cell immunoglobulin-like receptors (KIRs) are a group of activating and inhibitory receptors that are mainly expressed by NK cells to regulate NK cell function. The *KIR* gene locus on chromosome 19 comprises a family of highly polymorphic genes within the leukocyte receptor complex (LRC). 15 genes and 2 pseudogenes of *KIR* have been identified and named according to their number of extracellular Ig domains (2D or 3D) and length of the cytoplasmic tail reflecting the activating (short tail; S) or inhibitory (long tail; L) function. The genes are organized as centromeric and telomeric and can be divided into two distinct haplotypes that vary in number and types of *KIR* genes. The framework genes *3DL3*, *3DP*, *2DL4* and *3DL2* are present in all haplotypes. Haplotype A has a nearly fixed combination of seven genes whereas haplotype B have a variable number of inhibitory and activating genes.

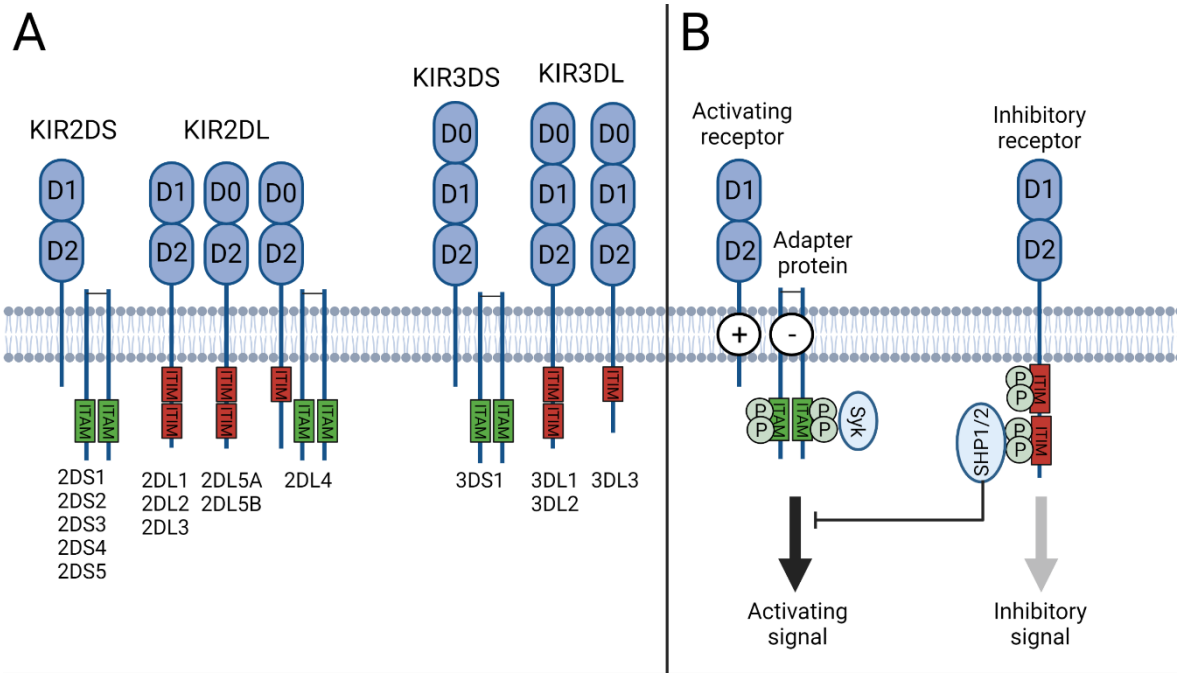

Figure 4: Nomenclature and signaling of KIRs. A KIRs are a group of receptors with activating and inhibitory functions. Activating receptors have a short cytoplasmic tail and contain transmembrane residues that forms a non-covalent association with an adapter protein DAP12, a disulphide-bonded homodimer with immunoreceptor tyrosine-based activating motifs (ITAMs), whereas the cytoplasmic domain of inhibitory KIRs possesses immunoreceptor tyrosine-based inhibitory motifs (ITIMs). **B** Signaling of activating receptors occurs through the phosphorylation of both tyrosines within the ITAMs and recruitment of Syk tyrosine kinases. Engagement of HLA class I molecules to their cognate inhibitory KIR leads to ITIM tyrosine phosphorylation and recruitment of tyrosine phosphatases (SHP1/2) to inhibit NK cell activation. The only exception for the short/long cytoplasmic tail rule is KIR2DL4, which is associated with ITAM-containing adapter protein FcεRI-γ.

1.2.4 Self-tolerance, “missing-self” and NK cell education

Similar to other immune cells, NK cells acquire tolerance towards healthy normal cells of the host (**Figure 5A**). To achieve this self-tolerance it is necessary that NK cells are able to distinguish “self” versus “nonself” or “altered self” (Jaeger *et al.*, 2012). Therefore, NK cells express a set of inhibitory and activating receptors that recognize specific ligands on target cells, including DNA-damage, stress-induced or virus-encoded ligands, as well as molecules on the cell surface that are constitutively expressed (Raulet *et al.*, 2006). The balance of the mentioned inhibitory and activating signals determines the outcome of interactions of NK cells with target cells. Inhibitory receptors mainly interact with HLA class I molecules, which are expressed at high levels by most cells. To avoid recognition by the immune system, especially viruses but also tumors downregulate HLA class I molecules from the cell surface, allowing them to evade T cell-mediated immune response. NK cells are able to sense this “missing-self” signal by their inhibitory receptors and become activated (Ljunggren *et al.*, 1985, 1990; Kärre *et al.*, 1986) (**Figure 5B**). Interaction of HLA class I molecules and inhibitory receptors are key regulators of NK cell function. Engagement of inhibitory receptors such as NKG2A and predominantly KIRs of NK cells with their cognate self-HLA class I molecule results in functional maturation of NK cells termed NK cell education or licensing. Educated NK cells are highly effective in sensing HLA class I-deficient cells and preserve tolerance to healthy cells. In contrast, uneducated NK cells, lacking the expression of inhibitory receptors specific for self-HLA class I molecules, are hyporesponsive and therefore have a low potential to attack healthy cells (Elliott *et al.*, 2011; He *et al.*, 2017) (**Figure 5C**).

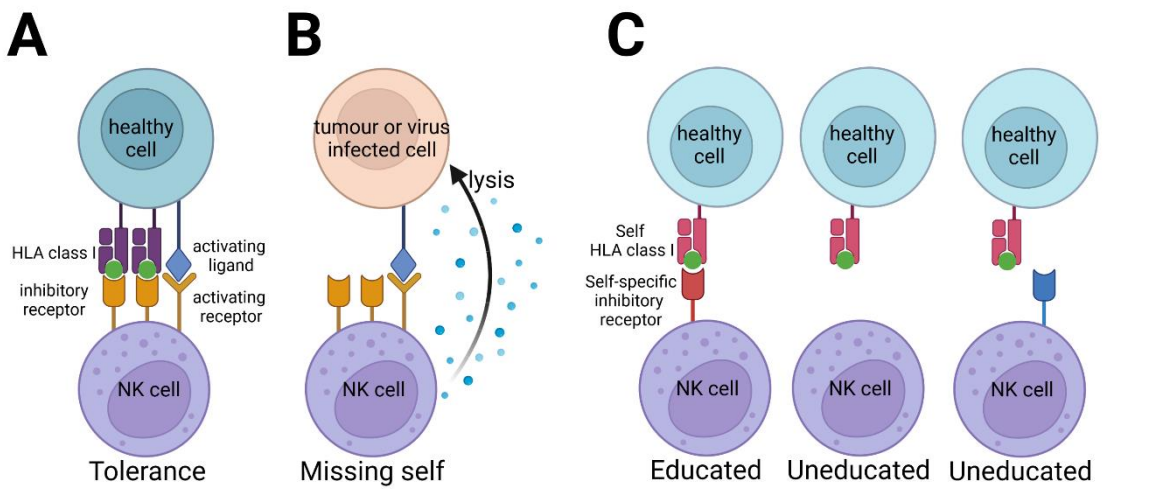

Figure 5: Tolerance, missing-self and education of NK cells. NK cells express activating and inhibitory receptors on their surface that interact with different ligands on host cells. **A** NK cells are tolerant towards healthy cells. **B** Loss of recognition of inhibitory ligands (mainly HLA class I) on target cells induced by virus infection or tumor formation activates NK cells due to the “missing-self” signal. **C** The quality of NK cell response depends on the education of the NK cell. NK cells that express inhibitory receptors that are capable of binding their cognate self-HLA class I ligand are educated and exhibit a low threshold for activation, whereas NK cells that do not express inhibitory receptors for self-HLA class I molecules are uneducated and hyporesponsive towards target cells.

1.3 HLA class I molecules

The human leukocyte antigen (HLA) system is a highly polymorphic gene cluster that is subdivided into two major groups: HLA class I, which comprises of classical (HLA-A, -B and -C) and non-classical (HLA-E, -F and -G), and HLA class II (HLA-DP, -DQ and -DR). HLA class I molecules are key elements in establishing self-tolerance and in triggering innate and adaptive immune responses by presenting endogenous peptides. HLA class I molecules are heterodimers of a transmembrane heavy α-chain and a light soluble β2-microglobuline (β2m). The polymorphic heavy chain is made up of the antigen-binding domains α1, α2 and the α3 domain, anchoring the molecule in the cell surface (Davis *et al.*, 1988). Loading of HLA class I molecules with pathogen-derived or self-peptides occurs in the endoplasmic reticulum (ER). Proteins in the cytosol are degraded in the proteasome, transported into the ER and loaded onto the peptide binding grove of the HLA class I heterodimer. This whole process is facilitated by a multi-subunit complex referred to as peptide-loading complex (PLC). The PLC consists of at least four accessory proteins: the ABC transporter TAP, enabling the transport of peptides from the cytosol into the ER; the type 1 transmembrane glycoprotein tapasin, which mediates the interaction of HLA class I molecules and TAP; the thiol oxidoreductase ERp57 and calreticulin, which are both involved in protein folding by promoting the formation of disulfide bounds (Higgins, 1992; Cresswell *et al.*, 1999; Farmery *et al.*, 2000). HLA class I molecules that have bound peptides with high affinity are released from the ER and transported through the Golgi apparatus to the cell membrane to present the endogenously-generated peptides to immune cells (Williams *et al.*, 2002). Presentation of pathogen-derived peptides by HLA class I molecules are recognized through the TCR of cytotoxic T cells, however NK cells use opposing mechanisms by sensing alterations in HLA class I surface expression. The whole expression pathway of HLA class I molecules is illustrated in **Figure 6**.

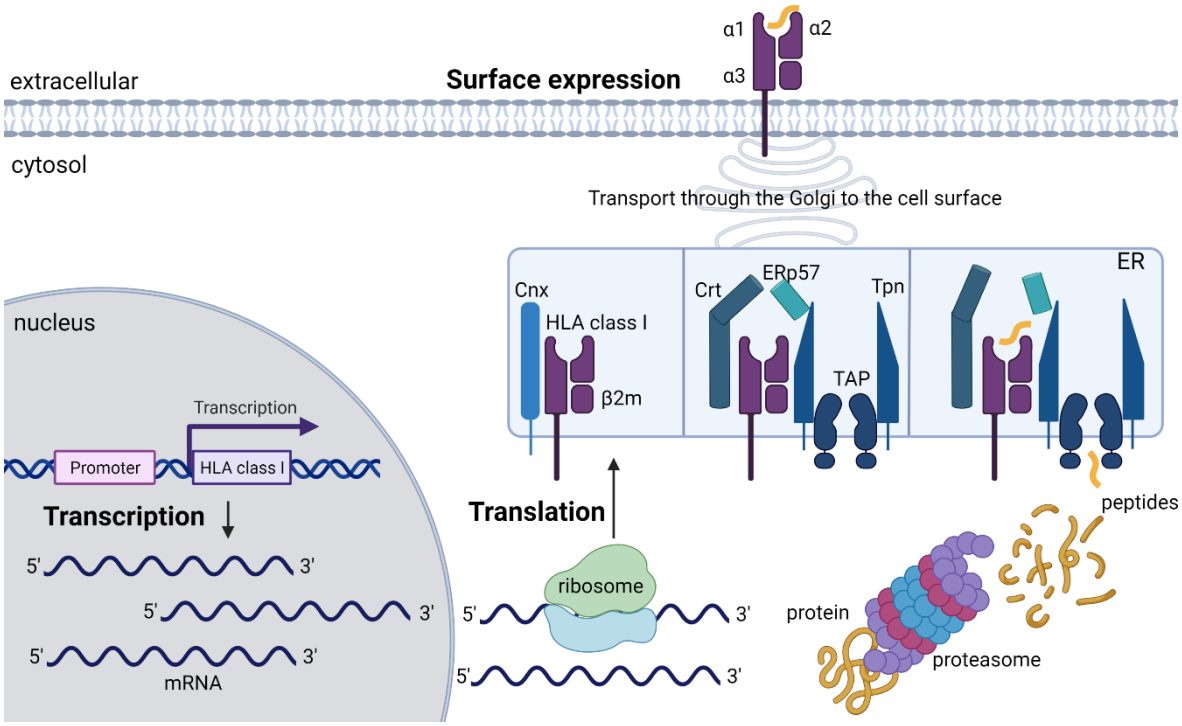

Figure 6: Protein synthesis pathway of HLA class I molecules. HLA class I genes are transcribed into mRNA in the nucleus and transported into the cytosol for translation. The assembly and peptide loading occur in the endoplasmic reticulum (ER), which is facilitated by a multi-subunit complex of Cnx (calnexin), TAP (transporter associated with antigen processing), Tpn (type I transmembrane glycoprotein tapasin) the thiol oxidoreductase ERp57 and Crt (calreticulin). Proteasomes degrade endogenous proteins in the cytosol that are translocated into the ER and loaded onto HLA class I molecules. The mature HLA class I:peptide complex leaves the ER through the Golgi apparatus to the cell surface to present the peptide to immune cells. This figure was created based on (Vollmers *et al.*, 2021).

1.3.1 HLA class I molecule C

In comparison to HLA-A and -B, HLA-C is the most recently evolved HLA class I molecule, only present in humans and great apes. HLA-C is the only HLA class I molecule that is expressed on trophoblasts and a key molecule for maternal-fetal immune tolerance (Papúchová *et al.*, 2019). Due to its considerably lower cell surface expression (Apps *et al.*, 2015) compared to HLA-A and -B, it was thought to have a minor role in adaptive T cell immune response (Falk *et al.*, 1997), but a major role in NK cell recognition and activation as a ligand for multiple members of the KIR family has been elucidated. The expression of HLA-C is tightly regulated by elements in the proximal and distal promoter region on the gene. Two examples of such regulatory elements are the interferon stimulated response element (ISRE) and EnhancerA, which are both relevant for cytokine induced HLA class I expression (Gobin *et al.*, 1998; Carey *et al.*, 2019). IFN-γ, for example, mediates the expression and binding of interferon-response factors (IRFs) to ISRE to induce HLA class I transcription. Compared to *HLA-A* and *-B*, *HLA-C* does not have functional binding sites for NFκB, a transcription factor regulating gene expression for multiple human genes (Wan *et al.*, 2009). The absence of these binding sites is associated with the lower transcription of *HLA-C*, compared to *HLA-A* and *-B* due to a weaker induction of transcription by the inflammatory cytokines IFN-γ and TNF-α (Gobin *et al.*, 1997). Moreover, a SNP (rs2395471)

in the OCT1 transcription factor binding site in the distal promoter region ~800 bp upstream the *HLA-C* transcription start site is associated with differential HLA-C expression levels. The rs2395471_A SNP results in a higher surface expression level of HLA-C compared to the rs2395471_G SNP (Vince *et al.*, 2016). Another SNP (rs9264942) 35 kb away from the transcription initiation of *HLA-C* is also associated with HLA-C expression level (Shimizu *et al.*, 1989). Another mechanism to regulate gene expression on a post-transcriptional level are microRNAs (miRNA). These small single-stranded non-coding RNAs bind to the 3'-untranslated region (UTR) of their target mRNA and repress translation (Cannell *et al.*, 2008). *HLA-C* alleles with an intact binding site of miRNA-148 have a lower surface expression due to the miRNA binding to the mRNA (Kulkarni *et al.*, 2011). *HLA-C* alleles with a more permissive binding groove are able to bind a larger range of distinct peptides and therefore have a higher surface expression (Kaur *et al.*, 2017). NK cells have an NK cell-specific HLA-C promoter element with an ETS-binding site. Polymorphisms in this binding site generate *HLA-C* alleles with a reduced expression and increased NK cell activity (Li *et al.*, 2018). HLA-C allotypes serve as major ligands for one or more KIRs, whereas only a limited number of HLA-A and -B allotypes are able to recognize KIRs (Parham *et al.*, 2013). Generally, HLA-C allotypes interact with seven different inhibitory and activating KIRs: KIR2DL1, KIR2DL2, KIR2DL3, KIR2DS1, KIR2DS2, KIR2DS4 and KIR2DS5. KIR/HLA-C integration relies on a dimorphism at position 80 of the HLA-C α1 domain: the C1 epitope is characterized by an asparagine (N) and the C2 epitope by a lysine (K) (Mandelboim *et al.*, 1996). Inhibitory KIR2DL1, the activating KIR2DS1 and some KIR2DS5 allotypes have a methionine at position 44 and recognize the HLA-C2 epitope exclusively (Biassoni *et al.*, 1997; Hilton *et al.*, 2015; Blokhuis *et al.*, 2017). In contrast, inhibitory KIR2DL2 and KIR2DL3 and some KIR2DS2 allotypes carry a lysine at position 44 and bind to HLA-C1 epitopes (Hilton *et al.*, 2015). In addition, certain KIR2DL2, KIR2DL3 allotypes exhibit binding affinity to selected HLA-C2 allotypes (Moesta *et al.*, 2008; Hilton *et al.*, 2015) and the activating KIR2DS4 is cross-reactive with some HLA-C1 and -C2 allotypes (Graef *et al.*, 2009). All HLA-C and KIR interactions are shown in **Figure 7**.

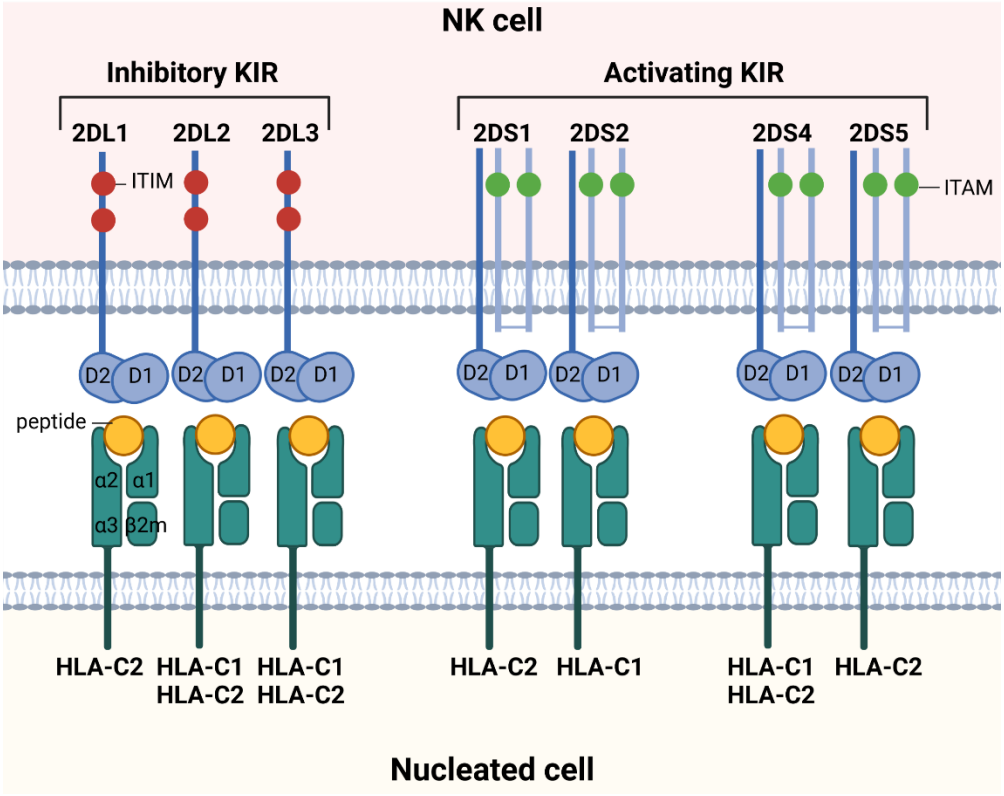

Figure 7: HLA-C interacts with KIRs on NK cells. All nucleated healthy cells express HLA class I molecules on their cell surface to present self and non-self peptides to the environment. Based on a dimorphism at position 80 in the α1 domain, HLA-C can be grouped in HLA-C1 and -2. HLA-C1 interacts with the inhibitory KIR2DL2 and KIR2DL3 and the activating KIR2DS2, whereas HLA-C2 recognizes the inhibitory KIR2DL1 and the activating KIRSDS1. In addition, HLA-C2 molecules can recognize some KIR2DL2, KIR2DL3, KIR2DS4 and KIR2DS5 alleles and HLA-C1 some KIR2DS4 alleles.

1.4 Human immunodeficiency virus

The human immunodeficiency virus (HIV) is a lentivirus that causes HIV infection and can, if not treated, lead to acquired immunodeficiency syndrome (AIDS). Phylogenetic and epidemiological studies assume that HIV spread from non-human primates in west-central Africa to the human population in the early 1900s. The first clinically observation of the virus was made in 1981 in gay men with an impaired immunity (Gottlieb *et al.*, 1981). Two years later, two research groups discovered the virus that causes the disease (Barré-Sinoussi *et al.*, 1983; Gallo *et al.*, 1983). Since then, it is a major global health issue with currently around 40 million people living with HIV and no effective cure (*Global HIV & AIDS statistics — Fact sheet | UNAIDS*). The virus is transmitted by direct contact with certain body fluids (blood, semen, rectal fluids, vaginal fluids and breast milk) from a person with detectable viral load directly into the bloodstream of a HIV-negative person (*How Is HIV Transmitted? | HIV.gov*). In the first stage of infection, most HIV-infected individuals show flu-like symptoms within days to weeks after infection. During this acute infection stage, the virus spreads very quickly, resulting in a decreasing number of CD4 T cells and a high viral load in the blood, which increases the risk of transmitting the virus. The second stage, also known as chronic HIV infection or latent/asymptomatic stage, is characterized by the reproduction of the virus at a very low level and normally progresses asymptomatically.

This phase usually advances to AIDS over 10 years or longer (*The Stages of HIV Infection | NIH*). In this final and most severe stage, the virus has caused extensive damage to the immune system and is characterized by a low CD4 T cell count, which leads to death within a few years (*The Stages of HIV Infection | NIH*). One of the hallmarks of HIV is a high mutation rate caused by the viral reverse transcriptase during the replication process, which allows rapid adaptation to the host immune response (Overbaugh *et al.*, 2001). Moreover, HIV integrates its DNA into the host genome, creating a viral reservoir within long-living memory cells, which makes it challenging to eradicate the virus from the host. However, treatment with multiple drugs can slow down or prevent HIV progression to AIDS. Antiretroviral therapy (ART) can suppress the virus to very low and even undetectable viral load. People with such an undetectable viral load have effectively no risk to transmit the virus to others (Arts *et al.*, 2012).

1.4.1 Classification and structure of HIV

HIV is a family member of retroviruses and belongs to the subgroup of lentiviruses. These type of viruses are characterized as single-stranded, positive-sense, enveloped RNA viruses, which are reverse transcribed into double-stranded DNA in the target cell. HIV includes HIV type 1 (HIV-1) and type 2 (HIV-2) that both originated from cross-species transmission of simian immunodeficiency virus (SIV) from chimpanzees and sooty mangabeys (Deeks *et al.*, 2015). Compared to HIV-2, HIV-1 is more prevalent and pathogenic and responsible for the majority of HIV infections worldwide. The reduced pathogenicity of HIV-2 in humans is possibly due to an incomplete adaptation of SIV to the human host. HIV-2 shows only a low transmission rate and is therefore mainly confined in West Africa. Moreover, HIV-1 can be subdivided into a major group (M) and three minor groups (N, O and P) (Simon *et al.*, 1998; Vallari *et al.*, 2011). The two identical copies of the HIV genome are enclosed by a conical capsid of the viral protein p24 (Gu *et al.*, 2013). The single-stranded RNA is bound to nucleocapsid proteins p7 and a number of enzymes that are necessary for the development of the virion like the reverse transcriptase, proteases and integrases. The outer shell of HIV is composed of a lipid membrane with host proteins and the HIV envelope protein. This envelope glycoprotein (gp) 120 is anchored to the membrane via a non-covalent bond with the transmembrane gp41 (Prabakaran *et al.*, 2007). The inner part of the envelope is layered by matrix protein p17 to ensure the integrity of the virion (Cannon *et al.*, 1997). **Figure 8** shows the described structure of HIV-1. The HIV-1 RNA genome contains nine genes (*gag*, *pol*, *env*, *tat*, rev, nef, *vif*, *vpr* and *vpu*), encoding for 19 proteins with structural and regulatory functions. All genes, proteins and functions are summarized in **Table 1**.

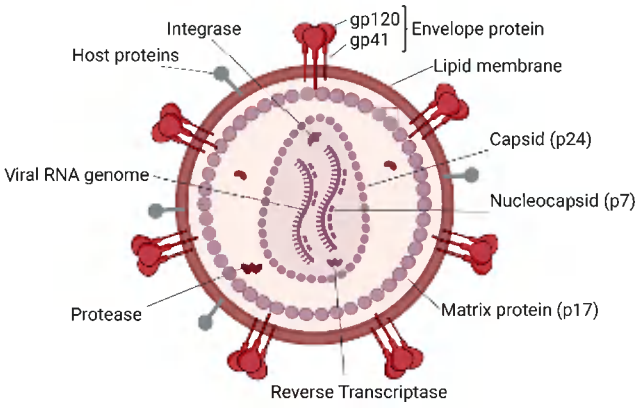

Figure 8: Structure of HIV-1. The human immunodeficiency virus (HIV) is composed of two single stands of RNA that encode for several structural/accessory proteins and viral enzymes. The viral genome is bound to the nucleocapsid (p7) and enclosed by a capsid (p24). A matrix (p17) surrounds the capsid, which is in turn surrounded by an envelope, composed of a lipid membrane with host proteins and viral envelope proteins (gp120 and gp41). Moreover, HIV-1 virions contain viral enzymes (reverse transcriptase, integrase and proteases) that are needed to produce new virions.

Table 1: Overview of HIV-1 gene products and functions.

Class	Gene	Protein	Function	References
Structural proteins	*gag*	p24 (capsid protein)	Formation of conical capsid	(Pornillos *et al.*, 2011)
		p17 (matrix protein)	Formation of inner matrix membrane layer	(Cannon *et al.*, 1997)
		p7 (nucleocapsid)	Formation of nucleocapsid	(De Baar *et al.*, 1999)
		p6	Involved in virus particle release	(Demirov *et al.*, 2002)
	env	Gp120	Attachment of virus to the target cell	(Sullivan *et al.*, 1998)
		Gp41	Anchoring gp120 to membrane; fusion of viral and target cell membrane	(Salzwedel *et al.*, 1999)
Viral enzymes	*pol*	Reverse Transcriptase	Transcription of HIV RNA in proviral DNA	(Hu *et al.*, 2012)
		Integrase	Integration of proviral DNA into host genome	(Craigie *et al.*, 2012)
		Protease	Release of structural proteins and viral enzymes	(Gulnik *et al.*, 2000)
		RNase H	Degradation of viral RNA in the viral RNA/DNA replication complex	(Beilhartz *et al.*, 2010)
Regulatory proteins	*tat*	Tat (transactivator of transcription)	Activates transcription of viral genes	(Das *et al.*, 2011)
	rev	Rev (regulator of viral protein expression)	Regulates export of non-spliced and partially spliced viral mRNA	(Blissenbach *et al.*, 2010)
Accessory proteins	*nef*	Nef (negative regulating factor)	Enhances infectivity of viral particles Downregulation of CD4 and HLA-A and -B on target cells	(Basmaciogullari *et al.*, 2014)
	vpr	Vpr (viral protein r)	Component of virus particles, integration with p6, facilitates virus infectivity	(Hrimech *et al.*, 1999)
	vif	Vif (viral infectivity protein)	Production of infectious virus	(Rose *et al.*, 2004)
	vpu	Vpu (viral protein u)	Efficient release of virus particles, control of CD4 degradation, modulation of intracellular trafficking, Downregulation of HLA-C	(González, 2015; Apps *et al.*, 2016)

1.4.2 HIV-1 replication cycle

HIV-1 uses CD4 as its primary receptor for target cell entry. CD4 is expressed by a number of immune cells, including astrocytes, macrophages and dendritic cells but the preferred targets of HIV-1 are activated CD4 T cells. Besides the CD4 receptor, HIV-1 requires a co-receptor to attach and enter the host cell. These co-receptors are typically the chemokine receptors CCR5 and CXCR4. Depending on the co-receptor used by HIV-1 for entry, HIV-1 can be subdivided into X4- (using CXCR4 for entry) and R5-tropic (using CCR5 for entry) strains (Dean *et al.*, 1996; Feng *et al.*, 1996). Strains that are able to use both CXCR4 and CCR5 are referred to as dual tropic HIV-1 strains. To attach to target cells, the HIV-1 envelope protein interacts with CD4 and the expressed co-receptor on the cell surface of the target cell. Once bound to the target cell, the envelope protein of HIV-1 undergoes conformational changes to form a hairpin structure. This hairpin structure pulls the virus and target cell membrane closer together and thereby allows the fusion of the membranes and the subsequent release of viral content into the target cell (Chan *et al.*, 1998). After entering the cell, the single-stranded viral RNA is reverse transcribed into a linear double-stranded DNA by the HIV-1 enzyme reverse transcriptase. Subsequently, the viral DNA is imported into the nucleus where it integrates into the host genomic DNA. This integration process is mediated by the viral enzyme integrase (Craigie *et al.*, 2012). For the production of new HIV-1 virions the host cell replication machinery is hijacked by HIV-1. In detail, the integrated viral DNA is transcribed by the host cell polymerase and the transcription of the viral DNA is furthermore dependent on target cellular transcription factors like NFκB (Schiralli Lester *et al.*, 2012). Moreover, the viral transactivator protein Tat allows an efficient HIV-1 transcription, resulting in the generation of a number of different viral mRNAs. These viral mRNAs are alternatively spliced and are subdivided into unspliced (serving as genomic RNA and Gag and Pol precursors), incomplete spliced (encoding for the viral proteins Vif, Vpr, Vpu and Env) and fully spliced mRNAs (encoding for the viral proteins Tat and Rev and Nef) (Kirchhoff, 2013). Fully spliced mRNA is transported into the host cell cytosol where it is translated into HIV-1 proteins. Typically, unspliced and partially spliced mRNAs are degraded in the host cell nucleus. The viral Rev protein facilitates the transport of unspliced and partially/incomplete spliced mRNA from the nucleus into the cytosol by interacting with the rev responsive element (RRE) encoded within the viral RNA (Sodroski *et al.*, 1986; Malim *et al.*, 1989). The final assembly and release of new HIV-1 virions is a complex process, including binding to the plasma membrane, creating protein-protein interactions and packaging of the genomic RNA (Sundquist *et al.*, 2012). The budded virions are immature and non-infectious. To become activated, the viral protease cleaves the precursor Gag polyprotein into its final mature proteins. Additionally, some HIV-1-infected cells do not produce new virions but go into a long-term resting state, forming a latent reservoir of HIV-1. In this state the virus stays mainly as genetic information in the

infected cell but can be reactivated (Cohn *et al.*, 2020). The full HIV-1 replication cycle is illustrated in **Figure 9**.

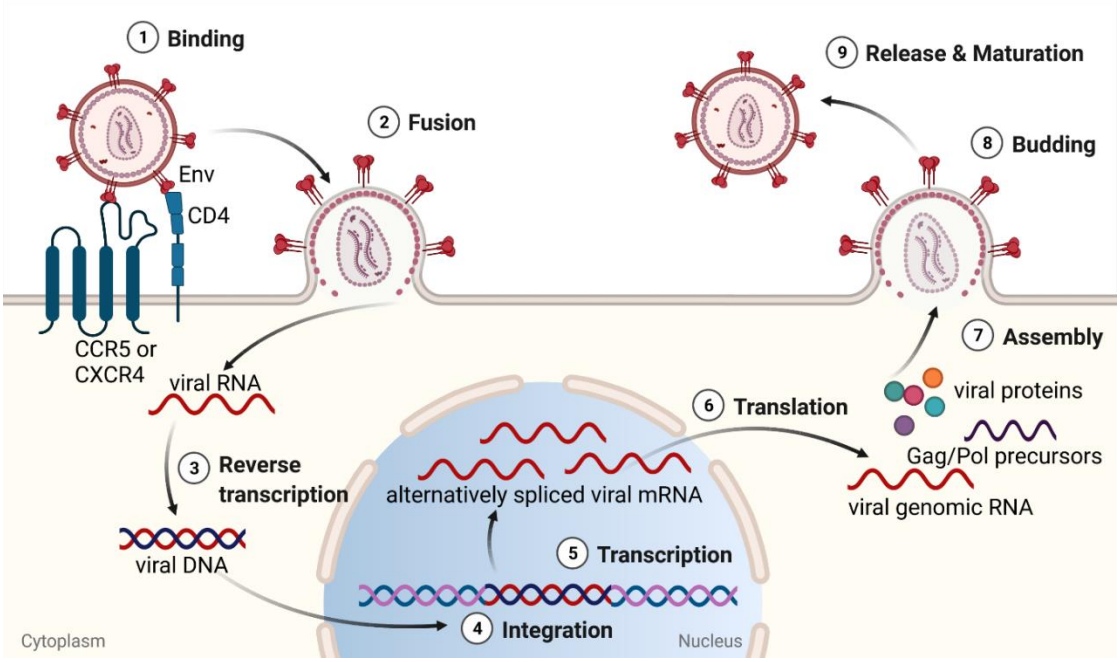

Figure 9: HIV-1 replication cycle. To enter and infect host cells, the HIV-1 envelope protein (Env) binds to CD4 and a co-receptor (CCR5 or CXCR4) on the host cell (1), which leads to a conformational change and fusion of the viral and target cell membranes (2). Viral content is released into the cytoplasm and the viral single-stranded RNA is transcribed to double-stranded DNA by the viral reverse transcriptase (3). The viral DNA is transported into the nucleus, integrated into the host-cell genome (4) and transcribed into alternatively spliced mRNA (5). Fully spliced mRNA can leave the nucleus and is translated to produce HIV-1 proteins (6), whereas unspliced or incomplete spliced mRNA requires Rev for the export from the nucleus. The assembly of new HIV-1 virions occurs at the plasma membrane of the host cell (7). The budded immature virion (8) contains the gag polyprotein which needs to be cleaved into its actual structural proteins. Only mature virions are then able to infect other host cells (9).

1.4.3 Vpu

The HIV-1 Viral protein U (Vpu) is a type I transmembrane phosphoprotein, which belongs to the family of viroporins that are characterized as viral proteins involved in the promotion and release of viral particles (Cohen *et al.*, 1988; Gonzalez *et al.*, 2003). *Vpu* is only present in the genome of HIV-1 and in some SIV strains but not in the HIV-2 genome (Dazza *et al.*, 2005; Sharp *et al.*, 2010). The translated protein is 81 amino acids long and consists of three distinct α-helices (**Figure 10**). *Vpu* encodes for a short luminal N-terminal domain, a transmembrane domain with an α-helix (helix-1) and a C-terminal cytoplasmic domain with two α-helices (helix-2 and -3) and a pair of constitutively phosphorylated serine residues (S52 and S56) (Federau *et al.*, 1996; Wittlich *et al.*, 2008). In HIV-1 infection, Vpu has a key function in the degradation of CD4 and release of newly formed virions (González, 2015). After HIV-1 infection, the HIV-1 protein Nef downregulates CD4 from the plasma membrane, whereas Vpu prevents surface expression of CD4 by targeting newly synthesized CD4 in the ER (Willey *et al.*, 1992). The cytoplasmic domain of Vpu contains a DSGXXS motif with the two phosphoserine residues S52/S56 that interact with β-transducin repeat-containing protein (β-TrCP), which is an adapter for the SKP1-cullin1-F-Box (SCF)

E3 ubiquitin ligase complex (Margottin *et al.*, 1998). The recruitment of the SCF/β-TrCP complex results in poly-ubiquitination of lysine, serine and threonine residues of the cytoplasmic tail of CD4 inducing degradation of CD4 by cellular proteasomes (Magadán *et al.*, 2010). Crucial for the enhancement of HIV-1 release is the downregulation of tetherin (BST-2/CD317) from the cell surface of the infected cell (Van Damme *et al.*, 2008). Tetherin is a glycosylated type II integral membrane protein, which is expressed constitutively by several cell types and induced by type-I interferon and pro-inflammatory signals (Neil, 2013). Tetherin binds to the viral envelope protein and inhibits the release of almost all enveloped viruses, including retroviruses and herpesviruses (le Tortorec *et al.*, 2011). HIV and SIV strains use different antagonists (Vpu, Nef and Env) that counteract the antiviral activity of tetherin by downregulating its cell surface levels (Van Damme *et al.*, 2008; Sauter *et al.*, 2009; Serra-Moreno *et al.*, 2011). However, the exact mechanism of this process is not fully understood. Similar to CD4, Vpu induces ubiquitination of the cytoplasmic tail of tetherin through transmembrane interactions leading to lysosomal degradation (Iwabu *et al.*, 2009). Taken together, Vpu targets the surface expression of several molecules that are involved in an efficient immune response, which highlights the important role of Vpu in HIV-1 immune evasion.

In addition to the downregulation of tetherin, Vpu also mediates the downregulation of HLA-C, an important molecule for immune cell recognition of infected cells (Apps *et al.*, 2016). For a long time, HIV-1 was thought to evade cytotoxic T cell responses via Nef-mediated downregulation of HLA-A and -B but not -C to inhibit NK cell activation. However, recent studies have described that some primary HIV-1 clones and transmitted/founder viruses are able to downregulate HLA-C from the cell surface (Apps *et al.*, 2016). Moreover, the degree of HLA-C downregulation depends on the *HLA-C* genotype of the individual (Bachtel *et al.*, 2018). Although residues in the transmembrane domain of Vpu and HLA-C that mediate an interaction between both molecules have been identified, the precise mechanisms of HLA-C downregulation by Vpu remains unknown. Studies suggest that Vpu targets HLA-C primarily at the protein level, which possibly involves ubiquitination of HLA-C (Hopfensperger *et al.*, 2020). HIV-2, which does not encode for Vpu, uses the accessory protein Vif to downregulate HLA-C surface expression without affecting HLA-C mRNA levels (Hopfensperger *et al.*, 2020).

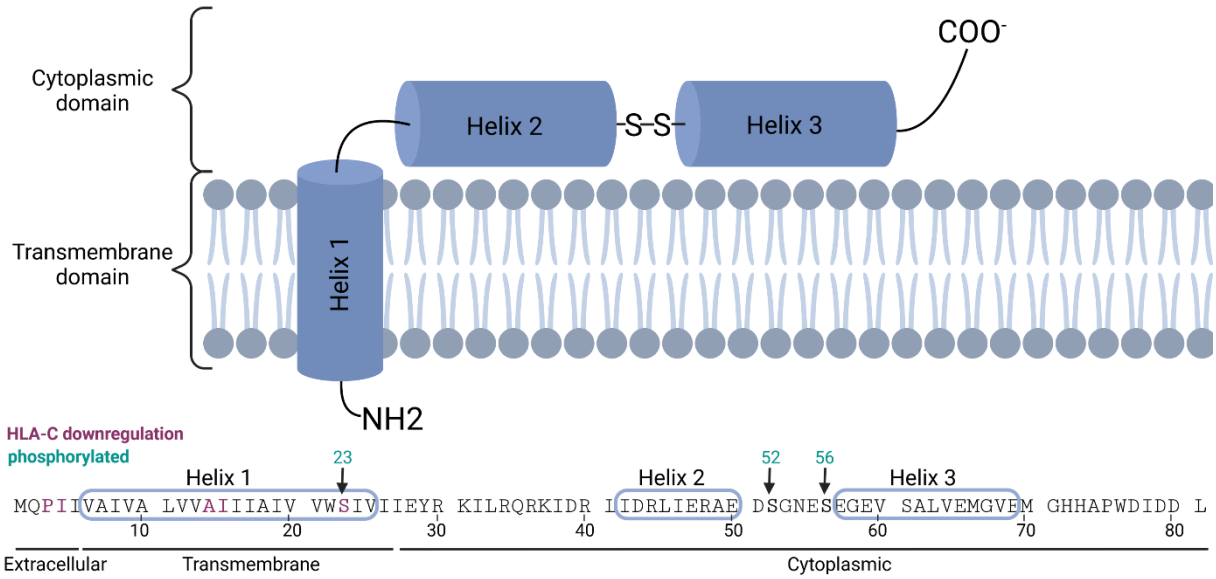

Figure 10: Structure and amino acid sequence of the HIV-1 accessory protein Vpu. Vpu is composed of three alpha helices: one N-terminal transmembrane alpha helix (helix 1) and two cytoplasmic alpha helices (helix 2 and 3), which are connected by two phosphorylated serine residues (52 and 56). Phosphorylated serines and residues that are involved in HLA-C downregulation are highlighted in blue and purple in the amino acid sequence.

1.5 The role of HLA-C in HIV-1 infection

Among HIV-1-infected people, the clinical disease progression varies between individuals. Without treatment, most HIV-1-infected individuals develop AIDS slowly in a span of 3 to 10 years after infection. However, it was observed that a minority of HIV-1 infected individuals rapidly progressed to AIDS, whereas others showed no signs of disease progression (Gaardbo *et al.*, 2012). This small group (<1%) of long-term nonprogressors (LTNPs) or elite controllers are able to suppress viral replication to undetectable levels and maintain high CD4 T cell counts without receiving antiviral therapy (Berg *et al.*, 2021). Host and viral genetic variability as well as differences in immune cell functions have been described as potential underlying reasons for different disease outcomes. Functional studies support the role of potent HIV-1-specific CD8 T cells (Migueles *et al.*, 2008), effects of *HLA* genetic variation, as well as genetic associations with *KIR* genes in controlling HIV-1 infection (Martin *et al.*, 2007). In addition, studies have shown that an effective NK cell response contributes to early control of HIV-1 replication (Naranbhai *et al.*, 2013; Walker-Sperling *et al.*, 2017). Genome-wide association studies (GWAS) revealed an important role of HLA-C in HIV-1 progression (Fellay *et al.*, 2007; International HIV Controllers Study *et al.*, 2010). These studies identified two independent HLA class I polymorphisms. The first one was associated with the *HLA-B*5701* allele, which is known to have a protective effect on HIV-1 progression (Migueles *et al.*, 2000) and the second one was located 35 kb (-35C/T) away from the transcription start site of *HLA-C*. The -35C allele is associated with high mRNA and surface expression levels and slower disease progression compared to the -35T allele with low mRNA and surface expression levels (Stranger *et al.*, 2005, 2007; Fellay

et al., 2009; Thomas *et al.*, 2009). In addition, high HLA-C surface expression is associated with increased likelihood of HLA-C-restricted cytotoxic T cell response and a higher mutation frequency in HLA-C-presented HIV-1 epitopes (Blais *et al.*, 2012; Apps *et al.*, 2013). Besides cytotoxic CD8 T cells, KIR^+ NK cells are also able to exert immunological pressure on HIV-1. To evade the NK cell-mediated immune response, HIV-1 selects for KIR2DL2-associated polymorphisms to enhance the binding of inhibitory KIR to HIV-1-infected cells and reduce the antiviral activity of these NK cells (Alter *et al.*, 2011). Compared to healthy individuals, NK cells of individuals with a primary HIV-1 infection have been shown to have a higher expression of KIR2DL1-3 in the presence of their corresponding HLA-C ligand and to be more polyfunctional (Körner *et al.*, 2014). Moreover, a number of studies have revealed a protective, as well as deleterious effect of specific *HLA-C* and *KIR* genotype combinations in HIV-1 infection (Jennes *et al.*, 2006; Ravet *et al.*, 2007; Paximadis *et al.*, 2011; Lin *et al.*, 2016; Mori *et al.*, 2019). To prevent the cytotoxic T cell recognition and NK cell activation, HIV-1 downregulates HLA-A and -B but not -C from the cell surface of infected CD4 T cells via the accessory protein Nef (Schwartz *et al.*, 1996; Collins *et al.*, 1998; Le Gall *et al.*, 1998). However, many primary HIV-1 clones are also able to downregulate HLA-C from the cell surface to different extents via the accessory protein Vpu (Apps *et al.*, 2016). Downregulation of HLA-C expression levels in HIV-1-infected CD4 T cells are sensed by NK cells, which results in an increased antiviral activity of NK cells (Körner *et al.*, 2017). Besides the missing-self signal, NK cell function can also be modulated by HLA-C peptide presentation. Certain HLA-C*01:02-restricted HIV-1 p24 Gag epitopes modulate NK cell function via KIR2DL2 binding (Fadda *et al.*, 2012) and sequence polymorphisms in p24 Gag can enable binding of KIR2DL2/L3 to HLA-C*03:04 to inhibit NK cell activation (Van Teijlingen *et al.*, 2014; Hölzemer *et al.*, 2015). A recent study observed that HIV-1 is able to induce changes in HLA-C*03:04-presented peptides, which leads to a reduced binding of KIR2DL3 and an enhanced recognition by NK cells (Ziegler *et al.*, 2020).

2 Working hypothesis and aims

Based on the important role of HLA-C and KIR in HIV-1 infection, I hypothesize that the host genetics of HLA-C and KIRs have a functional impact on NK cell activity during HIV-1 infection and that HIV-1 evades immune pressure by selecting Vpu sequence polymorphisms to modulate HLA-C surface expression (**Figure 11**).

To test this hypothesis the following aims were proposed:

- Assessment of KIR2DL/HLA-C binding affinities between various allotype combinations.
- Assessment of the anti-HIV-1 activity of KIR2DL^{+} NK cells.
- Phenotypic characterisation of NK cells from HIV-1^{+} and HIV-1^{-} individuals.
- Identification of Vpu sequence polymorphisms.

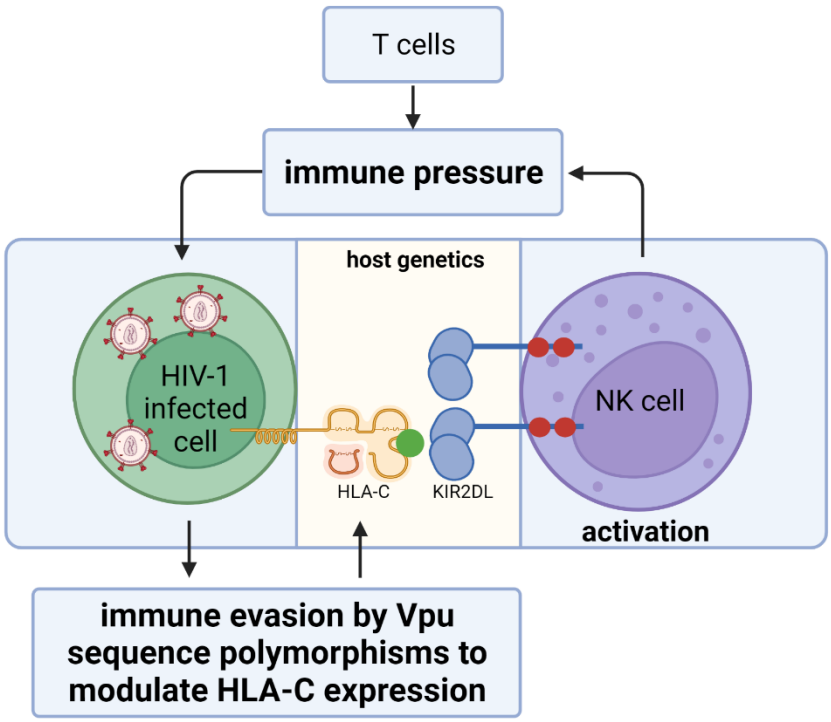

Figure 11: Woking hypothesis. Host genetics predefine the binding affinity between HLA-C and KIR2DL, as well as the presented peptide. The given HLA-C/KIR2DL combination has a functional impact on the anti-HIV-1 activity of NK cells and the overall immune pressure by NK cells and T cells leads to HIV-1 immune evasion by selecting for Vpu sequence polymorphisms to modulate the HLA-C expression on the infected cell.

3 Materials

3.1 Biological samples

Biological sample	Source
Peripheral blood from buffy coats (BC)	Institute of Transfusion Medicine, University Medical Center Hamburg-Eppendorf, Hamburg, Germany
Peripheral blood	Hamburg Healthy Cohort (HHCH), University Medical Center Hamburg-Eppendorf, Hamburg, Germany
Frozen human peripheral blood mononuclear cells (PBMCs) from therapy-naïve HIV-1-infected individuals	DZIF TP-HIV cohort, Hanover, Cologne, Munich, Germany
Frozen plasma from therapy-naïve HIV-1-infected individuals	DZIF TP-HIV cohort, Hanover, Cologne, Munich, Germany

3.2 Demographic and clinical information of HIV-1$^+$ and HIV-1$^-$ individuals

		HIV$^+$ individuals	HIV$^-$ individuals
demographic data	**Number total**	122	60
	Age in years Median (Min, Max)	n=116 37 (20, 73)	n=43 30 (22, 64)
	Sex **Male**, number (%) **Female**, number (%)	n=122 114 (93.4) 8 (6.6)	n=44 21 (47.7) 23 (52.3)
Clinical data	**Viral load in copies/ml** Median (Min, Max)	n=121 516000 (40, 170000000)	n.d
	CD4 absolute Median (Min, Max)	n=118 438 (22, 2601)	n.d
	CD4 in % Median (Min, Max)	n=116 24.6 (3, 54)	n.d
	CD8 absolute Median (Min, Max)	n=84 936 (177, 6636)	n.d
	CD8 in % Median (Min, Max)	n=81 50 (29, 85.9)	n.d
	CD4/CD8 ratio Median (Min, Max)	n=84 0.49 (0.1, 1.86)	n.d
	NK absolute Median (Min; Max)	n = 122 22,253 (374, 199,014)	n.d

Detailed demographic and clinical information, as well as HLA and KIR genotyping of all HIV-1$^-$ and HIV-1$^+$ individuals are provided in the appendix.

3.3 Cell lines

Cell line	Characterisation	Source and Research Resource Identifier (RRID)	Usage
721.221	Human HLA negative B-Lymphoblastoid cell line	Ragon Institute of MGH, MIT and Harvard, Cambridge, MA, USA; CVCL_6263	Production of stable HLA-C expressing cell lines
721.221 HLA-C*01:02	721.221 cell line transduced with HLA-C*01:02	This thesis	KIR2DL/HLA-C binding assays
721.221 HLA-C*03:03	721.221 cell line transduced with HLA-C*03:03	This thesis	KIR2DL/HLA-C binding assays
721.221 HLA-C*03:04	721.221 cell line transduced with HLA-C*03:04	This thesis	KIR2DL/HLA-C binding assays
721.221 HLA-C*07:01	721.221 cell line transduced with HLA-C*07:01	This thesis	KIR2DL/HLA-C binding assays
721.221 HLA-C*07:02	721.221 cell line transduced with HLA-C*07:02	This thesis	KIR2DL/HLA-C binding assays
721.221 HLA-C*12:03	721.221 cell line transduced with HLA-C*12:03	This thesis	KIR2DL/HLA-C binding assays
721.221 HLA-C*14:02	721.221 cell line transduced with HLA-C*14:02	This thesis	KIR2DL/HLA-C binding assays
721.221 HLA-C*16:01	721.221 cell line transduced with HLA-C*16:01	This thesis	KIR2DL/HLA-C binding assays
721.221 HLA-C*02:02	721.221 cell line transduced with HLA-C*02:02	This thesis	KIR2DL/HLA-C binding assays
721.221 HLA-C*04:01	721.221 cell line transduced with HLA-C*04:01	This thesis	KIR2DL/HLA-C binding assays
721.221 HLA-C*05:01	721.221 cell line transduced with HLA-C*05:01	This thesis	KIR2DL/HLA-C binding assays
721.221 HLA-C*06:02	721.221 cell line transduced with HLA-C*06:02	Leibniz Institute of Virology, Hamburg, Germany; Anais Chapel	KIR2DL/HLA-C binding assays
Jurkat_E6.1-∆βm (following described as β2m-KO-Jurkat)	Human acute T-cell Leukaemia cell line, Clone E6-1, stable β2m knockout (KO)	Ragon Institute of MGH, MIT and Harvard, Cambridge, MA, USA; CVCL_0367	Production of stable KIR2DL-CD3ζ expressing cell lines
β2m-KO-Jurkat KIR2DL1*001	β2m-KO-Jurkat cell line transduced with KIR2DL1*001 and CD3ζ	This thesis	KIR2DL/HLA-C binding assays
β2m-KO-Jurkat KIR2DL1*004	β2m-KO-Jurkat cell line transduced with KIR2DL1*004 and CD3ζ	This thesis	KIR2DL/HLA-C binding assays
β2m-KO-Jurkat KIR2DL1*020	β2m-KO-Jurkat cell line transduced with KIR2DL1*020 and CD3ζ	This thesis	KIR2DL/HLA-C binding assays
β2m-KO-Jurkat KIR2DL1*022	β2m-KO-Jurkat cell line transduced with KIR2DL1*022 and CD3ζ	This thesis	KIR2DL/HLA-C binding assays
β2m-KO-Jurkat KIR2DL2*001	β2m-KO-Jurkat cell line transduced with KIR2DL2*001 and CD3ζ	This thesis	KIR2DL/HLA-C binding assays
β2m-KO-Jurkat KIR2DL2*003	β2m-KO-Jurkat cell line transduced with KIR2DL2*003 and CD3ζ	This thesis	KIR2DL/HLA-C binding assays
β2m-KO-Jurkat KIR2DL2*009	β2m-KO-Jurkat cell line transduced with KIR2DL2*009 and CD3ζ	This thesis	KIR2DL/HLA-C binding assays

β2m-KO-Jurkat KIR2DL3*001	β2m-KO-Jurkat cell line transduced with KIR2DL3*001 and CD3ζ	This thesis	KIR2DL/HLA-C binding assays
β2m-KO-Jurkat KIR2DL3*002	β2m-KO-Jurkat cell line transduced with KIR2DL3*002 and CD3ζ	This thesis	KIR2DL/HLA-C binding assays
β2m-KO-Jurkat KIR2DL3*009	β2m-KO-Jurkat cell line transduced with KIR2DL3*009 and CD3ζ	This thesis	KIR2DL/HLA-C binding assays
β2m-KO-Jurkat KIR2DL3*016	β2m-KO-Jurkat cell line transduced with KIR2DL3*016 and CD3ζ	This thesis	KIR2DL/HLA-C binding assays
HEK-293T	Immortalised cell line derived from human embryonic kidney cells from a female fetus in 1973 expressing the SV40 large T antigen	DSMZ; CVCL_0063	Production of HIV-1 and lentivirus stocks
Sf9	Insect cell line originated from the Clonal isolate of *Spodoptera frugiperda* Sf21 cells	Thermo Fisher Scientific #11496015; CVCL_0549	Production of baculovirus
Hi5	Insect cell line originated from the ovarian cells of *Trichoplusia ni*	Leibniz Institute of Virology, Hamburg, Germany; Jürgen Müller-Guhl; CVCL_C190	Production of KIR2DL-Fc fusion proteins

The sequences for the β2m-KO Jurkat-KIR2DL-CD3ζ cell lines contain the signal peptide, extracellular and transmembrane domain of the respective KIR2DL allotype and the cytoplasmic domain of CD3ζ. All cloned sequences of HLA-C and KIR2DL are provided in the appendix.

3.4 KIR2DL-Fc fusion proteins

KIR-Fc protein	Characterisation	Source	Usage
KIR2DL1*001-Fc	D1, D2 and stem domains of KIR2DL1*001 and the Fc region of a human IgG1 antibody	This thesis	KIR2DL/HLA-C binding assays
KIR2DL1*003-Fc	D1, D2 and stem domains of KIR2DL1*003 and the Fc region of a human IgG1 antibody	Stanford University, Stanford, CA, USA; Dr. Paul Norman	KIR2DL/HLA-C binding assays
KIR2DL1*004-Fc	D1, D2 and stem domains of KIR2DL1*004 and the Fc region of a human IgG1 antibody	This thesis	KIR2DL/HLA-C binding assays
KIR2DL1*020-Fc	D1, D2 and stem domains of KIR2DL1*020 and the Fc region of a human IgG1 antibody	This thesis	KIR2DL/HLA-C binding assays
KIR2DL1*022-Fc	D1, D2 and stem domains of KIR2DL1*022 and the Fc region of a human IgG1 antibody	This thesis	KIR2DL/HLA-C binding assays
KIR2DL2*001-Fc	D1, D2 and stem domains of KIR2DL2*001 and the Fc region of a human IgG1 antibody	Stanford University, Stanford, CA, USA; Dr. Paul Norman	KIR2DL/HLA-C binding assays
KIR2DL2*003-Fc	D1, D2 and stem domains of KIR2DL2*003 and the Fc region of a human IgG1 antibody	This thesis	KIR2DL/HLA-C binding assays
KIR2DL2*009-Fc	D1, D2 and stem domains of KIR2DL2*009 and the Fc region of a human IgG1 antibody	This thesis	KIR2DL/HLA-C binding assays
KIR2DL3*001-Fc	D1, D2 and stem domains of KIR2DL3*001 and the Fc region of a human IgG1 antibody	Stanford University, Stanford, CA, USA; Dr. Paul Norman	KIR2DL/HLA-C binding assays
KIR2DL3*002-Fc	D1, D2 and stem domains of KIR2DL3*002 and the Fc region of a human IgG1 antibody	This thesis	KIR2DL/HLA-C binding assays
KIR2DL3*009-Fc	D1, D2 and stem domains of KIR2DL3*009 and the Fc region of a human IgG1 antibody	This thesis	KIR2DL/HLA-C binding assays
KIR2DL3*016-Fc	D1, D2 and stem domains of KIR2DL3*016 and the Fc region of a human IgG1 antibody	This thesis	KIR2DL/HLA-C binding assays

3.5 Cultivation medium and supplements

Cell type	Media	Supplements
PBMC 721.221 β2m-KO Jurkat	RPMI -1640	10% (v/v) FBS 100 U/ml penicillin 100 µg/ml streptomycin
Transduced 721.221 Transduced β2m-KO Jurkat	RPMI -1640	10% (v/v) FBS 100 U/ml penicillin 100 µg/ml streptomycin 1 µg/ml puromycin
Primary CD4 T cell	RPMI -1640	10% (v/v) FBS 100 U/ml penicillin 100 µg/ml streptomycin 100 U/ml IL-2
Primary NK cells	RPMI -1640	10% (v/v) FBS 100 U/ml penicillin 100 µg/ml streptomycin 50 U/ml IL-2 5 ng/ml IL-15
HEK-293T	DMEM	10% (v/v) FBS 100 U/ml penicillin 100 µg/ml streptomycin
Sf9	Sf-900 II serum free	10% (v/v) FBS 100 U/ml penicillin 100 µg/ml streptomycin 1% L-Glutamine
Hi5	Express Five serum free	1% L-Glutamine

Name	Company	Catalogue Number
Roswell Park Memorial Institute (RPMI)-1640	Thermo Fisher Scientific	#21875091
Dulbecco's Modified Eagle's Medium (DMEM)	Thermo Fisher Scientific	#31966047
Sf-900 II SFM	Thermo Fisher Scientific	#10902-096
Express Five SFM	Thermo Fisher Scientific	#10486025
Fetal bovine serum (FBS)	Capricorn Scientific	#FBS-11A
Penicillin-Streptomycin	Sigma-Aldrich	#P4333-100ML
Interleukin-2 (IL-2)	PeproTech	#200-02-500
Interleukin-15 (IL-15)	PeproTech	#200-15-100
Puromycin	InvivoGen	#ANT-PR-1
L-Glutamine	Sigma-Aldrich	#G7513

3.6 Antibodies

Name	Flurochrome	Clone	Channel	Company	Cataloge Nr.
α-human CD3	APC-Cy7	OKT3	R1	BioLegend	#317334
α-human CD3	PE-Cy5	UCHT1	YG2	BioLegend	#300410
α-human CD3	PerCP-Cy5.5	UCHT1	B1	BioLegend	#300430
α-human CD3	Pacific Blue (PB)	UCHT1	V7	BD Bioscience	#558117
α-human CD4	BV650	RPA-T4	V3	BioLegend	#300536
α-human CD4	APC	OKT4	R3	BioLegend	#317416
α-human CD8	AF700	SK1	R2	BioLegend	#344724
α-human CD14	APC-Cy7	HCD14	R1	BioLegend	#325620
α-human CD16	BUV785	3G8	V1	BioLegend	#302046
α-human CD19	APC-Cy7	HIB19	R1	BioLegend	#302218
α-human CD56	BUV395	NCAM16.2	UV2	BD Optibuild	#563554
α-human CD57	PerCP-Cy5.5	QA17A04	B1	BioLegend	#393312
α-human CD57	BV510	QA17A04	V6	BioLegend	#393314
α-human CD69	BV421	FN50	V7	BioLegend	#310930
α-human CD107a	BV510	H4A3	V6	BioLegend	#328632
α-human KIR2DL1/S5	PE	143211	YG4	R&D	#FAB1844P
α-human KIR2DL1/S1	Biotin	11PB6	-	Miltenyi	130-092-683
α-human KIR2DL1/S1	APC	EB6B	R3	Beckman	#A22332
α-human KIR2DL1/S1	PE	11PB6	YG4	Miltenyi	#130-092-684
α-human KIR2DL2/L3	PE	DX27	YG4	Miltenyi	#130-092-618
α-human KIR2DL2/L3/S2	BV711	DX27	V2	BD Optibuild	#745442
α-human KIR2DL3	AF488	180701	B2	R&D	#FAB2014G
α-human KIR2DL3	Biotin	REA147	-	Miltenyi	130-100-127
α-human KIR3DL1	AF700	CX9	R2	BioLegend	#312712
α-human KIR3DL1	BV605	NKB1	V4	BD Bioscience	#742981
α-human KIR3DL1/L2	PE-Vio770	5.133	YG1	Milenyi	#130-099-941
α-human KIR2DS4	Biotin	JJC11.6	-	Miltenyi	#130-092-898
α-human NKG2A	PE-Vio615	REA110	YG3	Miltenyi	#130-120-035
α-human NKG2C	BUV563	134591	UV1	BD Optibuild	#749842
α-human CCR5	BV421	J418F1	V7	BioLegend	#359118
α-human HIV-1 p24	FITC	KC57	B2	Beckamn Coulter	#6604665
α-human HLA-ABC	PE	W6/32	YG4	BioLegend	#311410
α-human HLA-C	PE	DT9	YG4	BD Bioscience	#566372
α-human HLA-C purified	-	DT9	-	Sigma-Aldrich	#MABF233
α-human IgG	PE	-	YG4	Fisher Scientific	#H10104
α-mouse IgG	PE	-	YG4	Sigma-Aldrich	#P8547

3.7 Buffer, media and solutions

Prepared buffer/medium	Composition
Cryopreservation medium (cell lines and primary cells)	FBS supplemented with 10% (v/v) DMSO
Cryopreservation medium (insect cell lines)	45% (v/v) conditioned cultivation medium, 45% (v/v) fresh cultivation medium and 10% (v/v) DMSO
Enrichment buffer	PBS supplemented with 2% (v/v) FBS and 1 mM EDTA
Staining buffer	PBS supplemented with 2% (v/v) FBS
Fixation buffer	Deionized water supplemented with 10% (v/v) CellFix
LB medium	20 g LB Broth Base in 1 L water; autoclaved
LB agar	32 g LB Agar in 1 L water; autoclaved
100 mM glycine buffer, pH 2.7	7.5 g glycine (75 g/mol) in 1 L distilled water
1 M Tris buffer, pH 9.0	121,1 g Tris (121,14 g/mol) in 1 L distilled water

Buffer/ medium	Company	Catalogue Number
Dulbecco's Phosphate Buffered saline (PBS)	Sigma-Aldrich	#D8537
HEPES buffer (1 M)	Thermo Fisher Scientific	#15630056
Brilliant Stain Buffer	BD Bioscience	#566349
CellFIX (10x concentrate)	BD Bioscience	#340181
Fluorofix Buffer	BioLegend	#422101
S.O.C medium	Life Technologies	#1544034

3.8 Chemicals and reagents

Name	Company	Catalogue Number
LB Agar, powder (Lennox L agar)	Thermo Fisher Scientific	#22700025
LB Broth Base	Thermo Fisher Scientific	#12780052
Ampicillin	Sigma-Aldrich	#A5354-10ML
Benzonase Nuclease, purity > 99%	Merck Milipore	#70664-3
Cellfectin II	Thermo Fisher Scientific	#10362100
CS&T Research Beads	BD Bioscience	#655041
Dynabeads M-280 Streptavidin	Thermo Fisher Scientific	#11205D
Ethylenediaminetetraacetic acid (EDTA), 0.5 M	Promega	#V4231
Ethanol absolute reinst.	Th. Geyer	#2273-5L
Glycine	Serva	#23390.03
ImmunoCult Human CD3/CD28 T-Cell Activator	Stemcell Technologies	#10991
Lenti-X concentrator	Clonect	#631232
Lipofectamine 3000	Thermo Fisher Scientific	#L3000150
Opti-MEM	Thermo Fisher Scientific	#31985047
Tris	Carl Roth	#A411.3
Trypsin-EDTA solution	Sigma-Aldrich	#T3924-100ML
Trypan blue solution, 0.4%	Sigma-Aldrich	#T8154-100ML
One Shot Stbl3 Chemically Competent E. coli	Thermo Fisher Scientific	#C737303
Protein A Sepharose	Fisher Scientific	#10727673
Lymphoctes Separation Medium	Capricorn Scientific	#LSM-A
Streptavidin-BV421	BioLegend	#405225

3.9 Plasmids

Name	Description/ usage	Source
pLVX-SIP	Lentiviral transfer vector for HLA-C and KIR2DL cell lines	Ragon Institute of MGH, MIT and Harvard, Charlestown, MA, USA; Dr. Thomas Pertel
psPAX2	HIV-1 gag-pol packaging plasmid for lentiviral production	NIH Aids Research Program, ARP-11348
pCMV-VSVG	VSV-G expression plasmid for lentiviral production	Addgene, #8454
pAcGP67a	Baculovirus transfer vector for KIR2DL-Fc fusion protein	Stanford University, Stanford, CA, USA; Dr. Paul Norman
BestBac 2.0 Δ c-cath/chiA Linearized Baculovirus DNA	Linearized Baculovirus DNA with a v-cath/chiA deletion for generating recombinant Baculovirus	Expression System, #91-002
HIV-1 NL4-3 wt	Full-length, replication-competent, infectious HIV-1; subtype B; CXCR4 tropic	NIH HIV Reagent Program, ARP-114; contributed by Dr. Malcom Matrin
HIV-1 JRCSF wt	Full-length, replication-competent, infectious HIV-1; subtype M; CCR5 tropic	NIH HIV Reagent Program, ARP-2708; contributed by Dr. Irvin SY Chen and Dr. Yoshio Koyanagi
HIV-1 JRCSF Vpu_L4IQ5del mutant (following described as JRCSF Vpu mut)	Mutagenesis of JRCSF wt Vpu sequence: Leucine (L) at amino acid position 4 was exchanged to Isoleucine (I). Glutamine (Q) at position 5 was deleted.	Leibniz Institute of Virology, Hamburg, Germany; Dr. Philipp Schommers

Vpu sequences of HIV-1 NL4-3 wt, JRCSF wt and JRCSF Vpu_L4IQ5del are provided in the appendix.

3.10 Kits

Name	Company	Catalogue Number
DNeasy Blood & Tissue Kit	Qiagen	#69504
EasySep Human $CD4^+$ T Cell enrichment Kit	Stemcell Technologies	#19052
EasySep Human NK cell Enrichment Kit	Stemcell Technologies	#19055
EasySep Human CD4 Positive Selection Kit II	Stemcell Technologies	#17852
HiSpeed Plasmid Maxi Kit	Qiagen	#12663
SuperScript III One-Step RT-PCR System with Platinum Taq DNA Polymerase	Thermo Fisher Scientific	#12574-026
Platinum SuperFi DNA Polymerase	Thermo Fisher Scientific	#12351-010
High Pure Viral RNA Kit	Roche	#11858882001
QIAprep Spin Minipep Kit	Qiagen	#27106
LIVE/DEAD fixable near-IR dead cell stain kit	Thermo Fisher Scientific	#L34976
QuikChange II XL Site-Directed Mutagenesis Kit	Agilent Technologies	#200521
Cytofix/Cytoperm Fixation/Permeabilisation Solution Kit	BD Bioscience	#554714
ArC Amine Reactive Compensation Bead Kit	Thermo Fisher	#A10346
CompBeads Anti-mouse Ig, κ/negative control compensation particles set	BD Bioscience	#552843
Anti-human Igκ, MACS Comp Bead Kit	Miltenyi	#130-104-187
NEBuilder HiFi DNA Assembly Master Mix Kit	New England BioLabs GmbH	#E2621L
Pierce BCA Protein Assay Kit	Thermo Fisher Scientific	#23227
Vybrant CFDA SE Cell Tracer Kit	Thermo Fisher Scientific	#V12883

3.11 Primer

Primer	Sequence (5'-> 3')
pLVX-SIP sequencing fw	GCGCCTTATTTGAATTAACC
pLVX-SIP sequencing rv	ACACCGGCCTTATTCCAAGC
KIR sequencing fw	TTTACTGTTTTCGTACACGTTTTG
KIR sequencing rv	GGAAGCTGTCTTCCATGAGCG
Vpu amplification fw	CCTAGACTAGAGCCCTGGAAGCAT
Vpu amplification rv	TTCTTGTGGGTTGGGGTCTGT
Vpu adapter fw	**TCGTCGGCAGCGTCAGATGTGTATAAGAGACAG**TAATACGACTCACTATAGG CAGGAAGAAGCGGAGACA
Vpu adapter rv	**GTCTCGTGGGCTCGGAGATGTGTATAAGAGACAG**CAGGAAACAGCTATGACC CCATAATAGACTGTGAC

fw: forward
rv: reverse

3.12 Software and websites

Software/ website	Company
BD FACS Diva Software, version 7.0	BD Bioscience
FlowJo_v10.7.1	BD Life Science
GraphPad Prism, version 9	GraphPad Software Inc.
Mendeley Desktop 1.19.4.	Mendeley Ltd
Microsoft Office 2016	Microsoft
Inkscape	Inksape Community
BioRender	BioRender

4 Methods

4.1 General handling information

Depending on the safety level of the cell lines or viruses used, the work was performed under sterile conditions in a biological safety cabinet with laminar flow under S2 or S3** biosafety conditions. The compositions of cultivation media for cell lines and primary cells, as well as for used buffers and solutions is summarized in the material section. Cultivation medium was warmed up to room temperature (RT) or small aliquots were warmed up in a 37 °C water bath before usage. All experimental work was planned and performed to achieve equal conditions for all samples. Work with proteins was performed on ice or at 4 °C. All centrifugation steps, except the density gradient centrifugation, were performed at maximum acceleration and deceleration.

4.2 Biological sample acquisition

Peripheral blood mononuclear cells (PBMCs) were isolated from buffy coats (concentrated whole blood that contains most of the leukocytes and platelets) from the Institute of Transfusion Medicine, University Medical Center Hamburg-Eppendorf (UKE) or from EDTA whole blood tubes from the healthy cohort (HHCH) of the UKE. The usage of the buffy coats and peripheral blood from the HHCH was approved by the ethics committee of the German Medical Association and the ethic committee of the Ärztekammer Hamburg (PV4780). Cryopreserved PBMCs and plasma samples from untreated HIV-1 positive donors were provided by the Translational Platform (TP-HIV) Cohort by the German Center for Infection Research (DZIF) and complies by the ethics committee of the Ärztekammer Hamburg **(**MC-316/14).

4.3 Cell biology

4.3.1 Cultivation of cell lines

All cell lines, except the insect cell lines Sf9 and Hi5, were cultured in respect of their cell number and viability in cell culture flasks (T25, T75, T175) or plates (6-, 12-, 24-well) in cultivation medium at 37 °C and 5% CO_2. The 721.221 and Jurkat cells with a β2-microglobuline-knockout (β2m-KO) were used for HLA-C/KIR binding assays and therefore stably transduced with HLA-C and KIR2DL allotypes. 721.221, as an HLA class I devoid cell line was used for the expression of HLA-C, whereas β2m-KO Jurkats were transduced with KIR2DL-CD3ζ and used as a reporter cell line. Both cell lines were cultivated at 0.5-1x10^6 cells/ml and passaged every 2-3 days depending on the cell density and viability. HEK-293T cells were cultured in an adherent monolayer and if not used for lentivirus or HIV-1 production, passaged at a confluence about 90%. Therefore, old medium was carefully removed and cells were washed with PBS to remove dead/non-adherent cells

and incubated for 5 min at 37 °C and 5% CO_2 with 0.05% (v/v) trypsin-EDTA. After the incubation, cells were washed off with cultivation medium and centrifuged to remove the trypsin-EDTA. Between 1:2 and 1:10 of the cells were used for further cultivation and complemented with fresh cultivation medium.

Generally, Sf9 and Hi5 insect cells were cultured in suspension in vented sterile Erlenmeyer flasks at 27 °C and 120 rpm. Depending on the growth rate, cells were passaged every 2-5 days at a cell density between $2x10^6$ to $4x10^6$ cells/ml and seeded between $3x10^5$ to $5x10^5$ viable cells/ml.

4.3.2 Cell thawing

Cryopreserved cells were thawed at 37 °C in a water bath until only a small frozen pellet remained. The rest of the cell pellet was thawed at RT, transferred into a 15 ml falcon tube and dropwise diluted with 9 ml cultivation medium. After a centrifugation step (200 x g, 10 min, 21 °C), the supernatant was discarded and the cell pellet was resuspended in 10 ml fresh cultivation medium. Cells were counted and cultured at the desired density in a respective cell culture flask or plate at 37 °C and 5% CO_2 until further usage.

Insect cell lines were shortly thawed at 37 °C in a water bath then directly transferred into an Erlenmeyer flask with fresh cultivation medium and cultured at 27 °C and 120 rpm until further usage.

4.3.3 Cryopreservation

For long-term storage, cell lines and primary cells were cryopreserved in liquid nitrogen tanks. Usually $5x10^6$ cells/ml, $10x10^6$ cells/ml or $50x10^6$ cells/ml were cryopreserved. Therefore, viable cells were counted, the respective amount of cells was centrifuged (400 x g, 1 min/ml, 4 °C) and the supernatant was removed. Cells were resuspended in cryopreservation medium. 1 ml aliquots were transferred into cryovials and placed into a 4 °C pre-cooled stratacooler. The stratacooler was stored overnight at -80 °C before the cryovials were transferred into liquid nitrogen tanks.

4.3.4 Cell count and viability assessment

Cells were counted with a Bio-Rad T20 cell counter. The machine automatically detects trypan blue staining and calculates the cell concentration and viability. Trypan blue is a dye that is only absorbed by dead cells through a disrupted cell membrane. The optimal range for calculations is $1x10^5$-$5x10^6$ cells/ml. Depending on the cell density and volume, the samples were diluted 1:1 (25 µl cell suspension mixed with 25 µl trypan blue) or 1:10 (10 µl cell suspension mixed with 90 µl trypan blue). For PBMCs, cells with a diameter from 6-17 µm were counted.

4.3.5 Isolation of peripheral blood mononuclear cells

Peripheral blood mononuclear cells (PBMCs) from peripheral blood were isolated with a density gradient centrifugation (Ulmer *et al.*, 1984). This technique uses centrifugal force and a density gradient medium to separate blood cell populations based on their different density and size (**Figure 12**). Depending on the experimental set-up, PBMCs were either isolated from buffy coats or from EDTA whole blood tubes. Blood from one buffy coat (~60 ml) or ten EDTA blood tubes, was distributed to three 50 ml falcon tubes and filled up with PBS to 50 ml. After layering the blood in a continuous, steady mode over 15 ml lymphocytes separation medium, the samples were centrifuged (900-950 x g, 20 min, 21 °C with acceleration set at one and deceleration on zero). The PBMC layer was carefully removed with a plastic Pasteur pipet and transferred into three 15 ml falcon tubes. The falcon tubes were filled up with PBS and centrifuged (500 x g, 15 min, 21 °C). The supernatant was removed with a 10-ml and 1000-µl pipet and the cells were washed again with 10 ml PBS (300 x g, 13 min, 21 °C). After the centrifugation step, the supernatant was removed as previously described and the PBMC pellet was resuspended in 10 ml (EDTA blood tubes) or 30 ml (buffy coat) cultivation medium and counted. PBMCs were then used for CD4 T cell enrichment or cryopreserved until further usage.

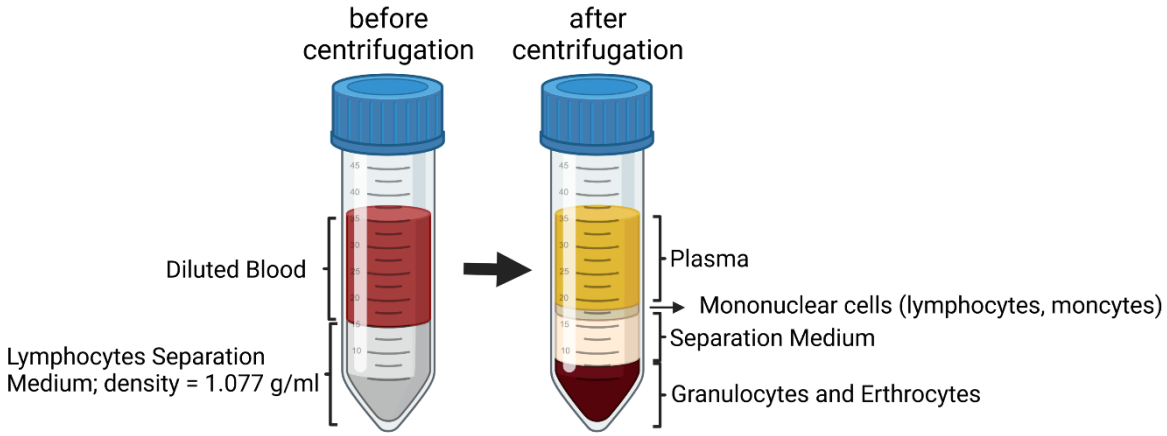

Figure 12: Density gradient centrifugation. Density gradient centrifugation is a method to separate cellular components of human blood by their density and size. After the centrifugation, following layers are visible from top to bottom: plasma, a layer of mononuclear cells, including lymphocytes and monocytes, separation medium and a red pellet of granulocytes and erythrocytes.

4.3.6 Immunomagnetic separation of primary CD4 T and NK cells

Immunomagnetic cell separation is a method to isolate specific cell populations from PBMCs. Therefore, cells are targeted with antibodies and magnetic particles for negative or positive selection with a magnet. A negative selection labels unwanted cell types that are depleted from the final fraction by an incubation in a magnetic field, whereas the supernatant contains the desired and untouched cell population. As an advantage, the isolated cells of interest are not bound by antibodies and magnetic particles. In contrast, the positive selection works with directly magnetic labelling the cell population of interest, which retains in the magnet.

For the enrichment of CD4 T cells or NK cells from PBMCs, the immunomagnetic negative selection kits EasySep Human CD4 T cell and NK Cell Enrichment Kit from Stemcell Technologies were used as described in the manufacturer's protocol with small variations: the isolation process was performed in two rounds. The first round was performed with 1/5 of the recommended amount of enrichment cocktail and magnetic particles and the second round with 1/2 of the kit.

In order to enrich $CD4^-$ HIV-1-infected T cells for functional degranulation assays, a positive selection for $CD4^+$ T cells was performed with the EasySep Human CD4 Positive Selection Kit II from Stemcell Technologies. The selection was executed as indicated in the manufacturer's protocol with the exception that step 7 and 8 were not performed. In addition, the supernatant with the $CD4^-$ T cells was incubated a second time for 3 min in the magnet and poured into a new tube to achieve a clean $CD4^-$ HIV-1-infected T cell population. The CD4 T cell positive selection was only performed for HIV-1-infected CD4 T cells and not for the mock control.

4.3.7 Stimulation of primary CD4 T and NK cells

Isolated primary CD4 T cells were cultured at $4x10^6$ cells/ml in cultivation medium with 100 U/ml IL-2 and 25 µg/ml ImmunoCult Human CD3/CD28 T cell activator for 3 days at 37 °C and 5% CO_2 before HIV-1 infection. The antibody complex provides T cell activation, which increases the efficiency of HIV-1 infection through binding and cross-linking CD3 and CD28 on the cell surface of T cells.

NK cells were isolated from frozen PBMCs one day before functional degranulation assays and after at least 2 hours of resting. NK cells were cultured at $5x10^6$ cells/ml in cultivation medium with 50 U/ml IL-2 and 5 ng/ml IL-15 overnight at 37 °C and 5% CO_2.

4.4 Molecular biology and protein biochemistry

4.4.1 Genomic DNA isolation

Genomic DNA from PBMCs was extracted with a silica-based membrane and microspin technology with the DNeasy Blood & Tissue Kit from Qiagen. For the genomic DNA isolation, $5x10^6$ frozen PBMC were thawed and processed. PBMCs from HIV-1-infected untreated donors were thawed ($5\text{-}10x10^6$ PBMC), 200 µl were taken and directly used for genomic DNA isolation. The isolation was performed as described in the manufacturer's protocol except the elution step. To increase the DNA yield, the DNA was eluted in two steps. 100 µl H_2O was pipetted to the center of the spin column membrane, incubated for 1 min at RT and centrifuged for 1 min at ≥6000 x g. This procedure was repeated and after measuring the concentration with a Nanodrop 100 spectrophotometer, the DNA was frozen at -20 °C until further usage for Vpu sequencing and *HLA/KIR* genotyping.

4.4.2 Viral RNA isolation

For the isolation of viral RNA from plasma samples from HIV-1-infected untreated individuals, the High Pure Viral RNA Kit from Roche was used. The frozen plasma samples were thawed at RT and 200 µl was used for the isolation, which was performed as recommended in the manufacturer's protocol. Briefly, viruses in the plasma were lysed with a detergent and proteinase K and the released viral RNA was selectively bound to the glass fiber fleece in the spin filter tubes. Contaminating substances were washed out and the purified RNA was eluted in 50 µl elution buffer. The concentration of the viral RNA was measured with a Nanodrop 100 spectrophotometer and the samples were stored at -80 °C for later generation of complementary DNA (cDNA) and *Vpu* gene amplification.

4.4.3 Reverse transcription and Vpu amplification

Isolated RNA was reverse transcribed into cDNA and amplified with Vpu-specific primer in a nested PCR. Vpu primers were designed and modified as described by Pickering *et al.* (Pickering *et al.*, 2014). cDNA from viral RNA was synthesized with the SuperScript II One-Step RT PCR System with Platinum Taq DNA Polymerase from Thermo Fisher Scientific and Vpu-outer primer (see methods 3.10 Vpu amplification primer). For *Vpu* sequencing, cDNA was then amplified with the Platinum SuperFi DNA Polymerase from Thermo Fisher Scientific and following Vpu-inner adapter primer (see methods 3.11 Vpu adapter primer). These primers include overhang adapter sequences that allow a dual index barcoding and pooling of the samples for sequencing.

4.4.4 Molecular cloning

Molecular cloning is a set of methods to generate many identical copies of a specific piece of DNA, which is inserted into a circular vector DNA plasmid. In order to replicate the plasmid, it is introduced into bacteria via transformation. Plasmids carry antibiotic resistance genes and therefore bacteria carrying the plasmid can be selected and cultured using these antibiotics. Different options are available to isolate and purify the plasmid DNA from bacteria, which work with a bind-wash-elute procedure where the bacterial culture is lysed and cleared by centrifugation. The plasmid DNA is bound to a silica membrane, contaminating reagents are washed out and pure plasmid DNA is eluted in water. To verify the integrity of the DNA sequence into the vector, plasmids were sequenced with specific sequencing primer by the company Microsynth SEQLAB.

For this project plasmid DNA was generated or mutated for three different approaches (**Figure 13**):

- KIR2DL1*003-Fc, 2DL2*001-Fc and 2DL3*001-Fc sequences cloned into a baculovirus transfer vector (pAcGP67a) were kindly provided by Paul Norman. More KIR2DL allotypes were generated by site-directed mutagenesis and used for KIR2DL-Fc fusion protein production.

- HLA-C allotype sequences were synthesized by GeneArt GeneSynthesis (Thermo Fisher Scientific), cloned into a lentiviral transfer vector (pLVX-SIP) and used to generate HLA-C1 or -C2 expressing 721.221 cell lines.
- Plasmids containing the transmembrane domain of KIR2DL1-3 allotypes and the cytoplasmic domain of the CD3ζ chain were synthesized by GeneArt GeneSynthesis (Thermo Fisher Scentific), cloned into a lentiviral transfer vector (pLVX-SIP) and used to generate KIR2DL-CD3ζ expressing Jurkat reporter cells.

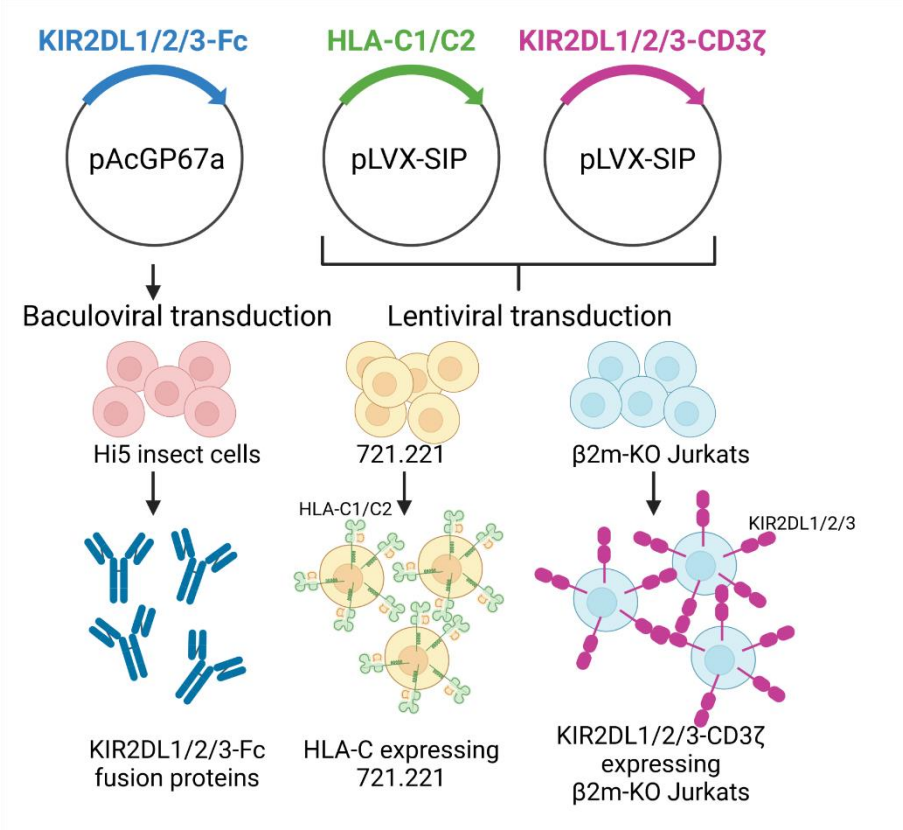

Figure 13: Overview of plasmid preparation and usage. Plasmids containing the sequence of a KIR2DL1/L2/L3 allotype fused with the Fc sequence were generated and used for the production of KIR2D-Fc fusion proteins in a baculovirus expression system. Plasmids with HLA-C1 and -C2 allotype sequences or KIR2DL1/2/3-CD3ζ sequences were used to generate HLA-C expressing 721.221 and KIR2DL-CD3ζ expressing β2m-KO Jurkat cell lines with lentiviral transduction.

The following paragraph summarizes the methods that were used for plasmid generation.

4.4.4.1 Plasmid assembly

KIR2DL-CD3ζ and HLA-C allotype sequences were designed with an EcoRI recognition site (GAATTC) at the 5' end and a NotI recognition site (GCGGCCGC) at the 3' end for the assembly with the lentiviral transfer vector pLVX-SIP. Therefore, vector plasmid DNA was digested with EcoRI and NotI and incubated with HLA-C or KIR2DL-CD3ζ sequences and the NEBuilder HiFi DNA assembly master mix for 1 h at 50 °C. The reaction was diluted 1:10 and stored at 4 °C until bacterial transformation.

4.4.4.2 Site-directed mutagenesis

The provided KIR2DL-Fc plasmids were mutated at specific amino acid positions to generate different allotypes of KIR2DL1/L2 and L3. Therefore, mutagenesis primers were designed with the QuikChange Primer Design from Agilent Technologies and ordered at Integrated DNA Technologies (IDT). The QuickChange II XL Site-Directed Mutagenesis Kit from Agilent Technologies was used as described in the manufacturer's protocol. The mutant strand synthesis reaction was prepared and amplified in a thermo cycler followed by a DpnI digestion for 1 h at 37 °C to get rid of non-mutated plasmids. The reaction was stored at 4 °C until bacterial transformation.

4.4.4.3 Bacterial transformation and selection

Generated plasmids were transformed into chemically competent *E. coli* for replication. To introduce the plasmid into the cells, plasmid DNA was incubated with the competent cells one ice and then briefly heated (42-50 °C), which allows the uptake of plasmid DNA into the cell through cell membrane disruption.

One shot Stbl3 chemically competent *E.coli* from Thermo Fisher Scientific were used for the HLA-C and KIR2DL-CD3ζ constructs as described in the manufacturer's protocol. Mutated plasmid was transformed into XL10-Gold ultracompetent cells, which were provided in the Site-Directed Mutagenesis Kit. Appropriate volumes of the transformation reactions were plated on pre-warmed LB agar plates containing 100 µg/ml ampicillin for both used plasmid vectors pLVX-SIP and pAcGP67a and incubated overnight at 37 °C. The following day, 2-5 colonies were used for further cultivation in LB medium with ampicillin and plasmid preparation.

4.4.4.4 Plasmid preparation

Depending on the later usage of plasmid DNA, transformed bacteria were cultured in 5 ml or in 250 ml LB medium with 100 µg/ml ampicillin overnight at 37 °C shaking at 250 rpm. For purifications of up to 20 µg plasmid DNA the QIAprep Spin Miniprep Kit from Qiagen was used. For larger purification of up to 750 µg plasmid DNA, the HiSpeed Plasmid Kit from Qiagen was used. The purifications were performed as recommended in the manufacturer's protocol with one exception: plasmid DNA was eluted in water and stored at -20 °C until further usage. Isolated plasmid DNA was sequenced by Microsynth SEQLAB.

4.4.5 Production of KIR2DL-Fc fusion proteins

Soluble recombinant KIR2DL1/L2 and L3 proteins that consist of the extracellular part of the KIR2DL receptor and the Fc region of an IgG antibody were generated as described by Hilton *et al.* with a baculovirus expression system (Hilton *et al.*, 2015). Briefly, KIR2DL-Fc plasmids were combined with linearized baculovirus by co-transfection into Sf9 insect cells with Cellfectin II from Thermo Fisher Scientific. Three rounds of Sf9 amplification were

performed to generate high titer of baculovirus (P1-P3) for adequate protein production. A small-scale protein production with following SDS-PAGE was used to quantify the amount of generated baculovirus. Full-scale protein was produced with little variations to the Hilton method. 50 ml Hi5 cells with a density of $2x10^6$ cells/ml with 100 µl P3 baculovirus stock were incubated for 72 h at 120 rpm and 27 °C. Cells were separated by centrifugation (2500 x g, 15 min, 4 °C) and the supernatant was filtered through a 0.2 µm filter. 5 ml HEPES buffer (1 M) and 100 µl protein A Sepharose beads were added to the supernatant and incubated rotating overnight at 4 °C in a 50 ml falcon tube. The following purification of the protein was performed on ice. All solutions were kept at 4 °C. The supernatant/bead mixture was centrifuged (2500 x g, 20 min, 4 °C) and the supernatant was discarded. The beads, that have bound the KIR2DL-Fc fusion proteins, were washed twice with 30 ml PBS (2500 x g, 20 min, 4 °C), resuspended with 10 ml PBS and transferred to an empty 13 ml PD-10 column. As the PBS passes through the column, the beads were collected on the filter and eluted with 4 ml 100 mM glycine (pH 2.7) into 5 fractions of 800 µl into 1.5 ml tubes, which contained 200 µl with 1 M Tris (pH 9) for neutralization. The protein concentration was measured with the Nanodrop 100 spectrophotometer. Lastly, a Sephadex G-25 desalting column was washed with 25 ml PBS and loaded with 2.5 ml of fractions with the highest protein concentration. 3.5 ml PBS was added to the column and collected in seven 0.5 ml fractions in 1.5 ml tubes. The protein concentration was determined with a BCA protein assay and the proteins were stored at -20 °C. The whole fusion protein production is illustrated in **Figure 14**.

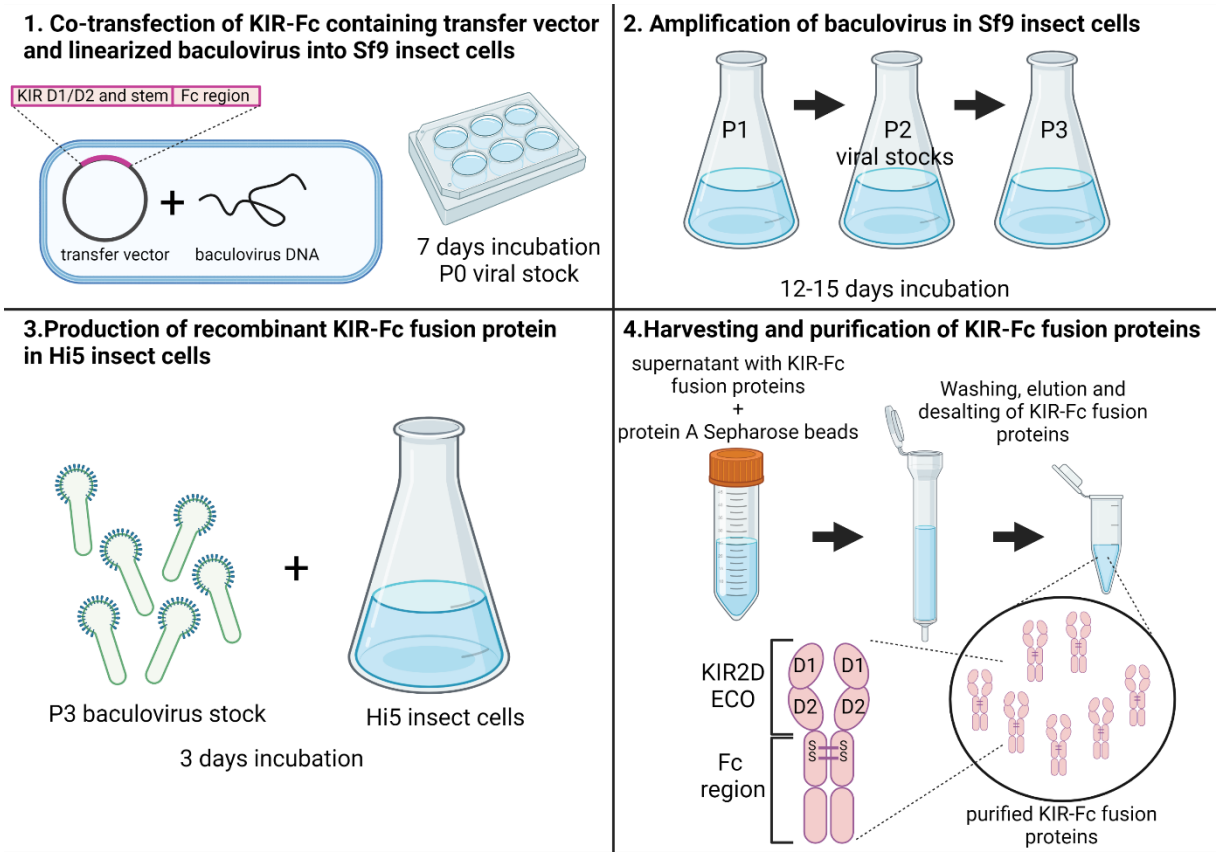

Figure 14: Overview of KIR-Fc fusion protein production. Transfer vector, containing the KIR-Fc sequence, and linearized baculovirus were co-transfected into Sf9 insect cells (1). To produce a high titer of baculovirus stock, the baculovirus was amplified in three rounds (2). P3 baculovirus stock was then used to infect Hi5 insect cells to produce KIR-Fc fusion proteins (3). After 3 days, the supernatant was harvested and the KIR-Fc fusion proteins purified (4).

4.4.5.1 Quantification of KIR2DL-Fc fusion proteins by SDS-PAGE

To confirm a successful production of KIR2DL-Fc fusion proteins from Hi5 cells upon baculovirus infection, the isolated protein fractions (F1-F5) were incubated with 20 µl Laemmli sample buffer containing 5% β-mercaptoethanol (10 min at 95 °C) and loaded onto a 12% SDS-PAGE gel. After running the gel for 1 h at 150 V, the gel was stained with Coomassie reagent to identify the appropriately sized protein bands.

4.4.5.2 Identification of baculovirus-infected Hi5 cells by GP64 staining

As the baculorvirus encoded glycoprotein GP64 is expressed on insect cells after baculovirus infection, GP64 cell surface expression can be used to identify baculovirus-infected Hi5 cells. Therefore, $2x10^6$ Hi5 cells were infected with 100 µl P3 viral stock and incubated for 24 h (120 rpm, 27 °C). Subsequently, Hi5 cells were separated from supernatant by centrifugation (50 x g, 2 min), washed twice with staining buffer (PBS + 2% FBS) and incubated with 25 µl GP64-PE antibody (1:25) for 30 min at 4 °C.

After 30 min incubation, the cells were washed twice with staining buffer and resuspended in 150 µl 1x CellFix and analysed via flow cytometry.

4.4.5.3 Assessment of KIR2DL-Fc integrity by flow cytometry

To determine the integrity of the KIR2DL-Fc fusion proteins, 250 µl KIR2DL-Fc fusion protein were incubated rotating with 20 µl anti-human IgG-coated beads for 30 min at 4 °C. The beads were collected by centrifugation (50 x g, 2 min) and washed twice with PBS. Following, the beads were stained with 25 µl respective KIR2DL-PE antibody (1:25) and incubated rotating for 30 min at 4 °C. Subsequently, the beads were separated by centrifugation (50 x g, 2 min), washed twice with PBS and resuspended in 150 µl PBS. Binding of the KIR2DL antibody was detected by flow cytometry.

4.4.6 BCA protein assay

The BCA (bicinchoninic acid) assay from Thermo Fisher Scientific was used to determine the total protein concentration of the KIR2DL-Fc fusion proteins. The assay based on a color change of the sample solution, which is proportional to the protein concentration and can be measured colorimetrically with a Tecan plate reader at a wavelength of 562 nm. The assay relies on two reactions. Cu^{2+} ions are reduced to Cu^{1+} in the presence of proteins, which reacts with BCA and forms a purple complex. The kit was used as described in the manufacturer's protocol.

4.5 HLA and KIR genotyping

HLA class I and KIR genotyping was performed by the DKMS Life Science Lab GmbH in Dresden, Germany.

4.6 Virology

4.6.1 Lentivirus production

Lentiviral particles were produced with a 2nd generation lentivirus packaging system, which requires generally three components: 1) the lentiviral transfer vector (pLVX-SIP) with the inserted sequence of HLA-C allotypes or KIR2DL1/2/3 allotypes, 2) the packaging plasmid (psPAX2) which contains the HIV-1 proteins Gag and Pol and 3) the envelope plasmid (pCMV-VSVG) expressing vesicular stomatitis virus glycoprotein (VSVG). All three components were transfected into HEK-293T cells. Therefore, HEK-293T cells were cultured in a 6-well plate in 2 ml cultivation medium without antibiotics to a 70-90% confluence for transfection. For one well, 6 µl Lipofectamine 3000 was mixed with 250 µl Opti-MEM and incubated for 5 min. 2 µg of transfer vector, 1 µg of packaging plasmid and 0.5 µg envelope plasmid were diluted in 250 µl Opti-MEM with 7 µl P3000 reagent. Lipfectamine 3000 was diluted dropwise to the DNA mix and incubated for 20 min at RT. During the incubation time, the cultivation medium was removed from the HEK-293T cells

and cells were carefully washed with 2 ml PBS. 2 ml Opti-MEM was added to the cells, as well as the DNA/Lipofectamine mix and incubated at 37 °C and 5% CO_2. After 48 h, the supernatant was collected, centrifuged (500 x g, 5 min, 21 °C) and filtered through a 0.45 µm Steriflip. 2 ml aliquots were stored at -80 °C until further usage for lentiviral transduction.

4.6.2 Lentiviral transduction to generate HLA-C 721.221 and KIR2DL-Jurkat reporter cell lines

Target cell lines (721.221 and β2m-KO Jurkats) were cultured in a 6-well plate ($0.5x10^6$ cells/well) in 2 ml cultivation medium. 2 ml of lentiviral supernatant or 2 ml cultivation medium for the untransduced control were added and incubated at 37 °C and 5% CO_2. After 72 h, surface expression of the respective ligand or receptor was checked via flow cytometry. Cells were selected and expanded with 1 µg/ml puromycin. Only cells that have incorporated the lentiviral genome are resistant to puromycin, while cells without the lentivirus are killed. After 2-3 weeks, cells that express the surface molecule were sorted with a FACS Aria Fusion flow cytometer from BD Bioscience.

4.6.3 Production of HIV-1 stocks

To generate replication-competent HIV-1 stocks, HEK-293T cells were seeded in cultivation medium to be 70-90% confluent for transfection. For one batch of HIV-1 JRCSF wt or JRCSF Vpu mut, five T175 cell culture flasks with HEK-293T cells were used. 600 µl Lipfectamine 3000 was diluted in 10 ml Opti-MEM and mixed gently. 200 µg full-length HIV-1 proviral expression plasmid DNA was diluted in 10 ml Opti-MEM and 400 µl P3000 reagent was added. The diluted DNA was then added dropwise to the diluted Lipofectamine 3000 solution (1:1) and incubated for 15 min at RT. The cultivation medium was removed from the HEK-293T cells and 4 ml per T175 cell culture flask of DNA/Lipofectamine mix was added gently directly onto the cells. In addition, 26 ml DMEM medium supplemented with 2.5% (v/v) FBS was added and the cells were incubated for 72 h at 37 °C and 5% CO_2. The virus was harvested by collecting and centrifuging the cell culture supernatant into 50 ml falcon tubes (500 x g, 15 min, 21 °C). The supernatant was then filtered through a 0.45 µm filter via a vacuum pump, mixed with Lenti-X concentrator (1:4) and incubated overnight at 4 °C. On the next day, the mixture was centrifuged (1500 x g, 45 min, 4 °C) and the visible pellet was resuspended in 5 ml RPMI-1640 medium supplemented with 10% (v/v) FBS, 100 U/ml penicillin and 100 µg/ml streptomycin, from which 1 ml were aliquoted and stored at -80 °C until further usage.

4.6.4 In vitro HIV-1 infection of primary CD4 T cells

After an incubation of 3 days, isolated and stimulated CD4 T cells were transferred into a 15 ml falcon tube and centrifuged (350 x g, 10 min, 21 °C) to wash out the CD3/CD28 antibody complex. The supernatant was discarded and the cells were washed with 10 ml cultivation medium with 100 U/ml IL-2 and counted. Between 10 and $15x10^6$ CD4 T cells were used for HIV-1 infection and $5x10^6$ CD4 T cells for mock control. The respective volume of cells was centrifuged (350 x g, 10 min, 21 °C), resuspended in 1 ml virus stock (JRCSF wt or JRCSF Vpu mut) or cultivation medium with 100 U/ml IL-2 and transferred into a 24-well plate. The cells were spinoculated for 2 h at 1200x g and 37 °C. After the centrifugation, the cells were cultured at $5x10^6$ cells/ml in cultivation medium with 100 U/ml IL-2 for 8 days at 37 °C and 5% CO_2. Every 2 days, approximately half of the cell culture supernatant was aspirated and replaced with freshly prepared cultivation medium with 100 U/ml IL-2.

4.7 Fluorescence staining for flow cytometry

4.7.1 Viability staining

To discriminate live and dead cells, the LIVE/DEAD Fixable Near-IR Dead Cell Kit from Thermo Fisher Scientific was used. The kit uses a near-IR fluorescent amine-reactive dye with an excitation maximum of ~633 nm. Cells with a disrupted cell membrane absorb the dye where it reacts with intracellular free amines and on the cell surface, resulting in a bright fluorescent staining. In intact, viable cells, the dye only reacts with cell surface amines with a low fluorescence. The viability staining was performed at a final dilution of 1:500 or 1:1000 for 10-15 min in the dark before the surface staining.

4.7.2 Staining with fluorochrome conjugated antibodies of surface and intracellular proteins

Antibodies are known for their important role in the immune system by recognizing and binding specific structures (antigens) for example of pathogens, which results in an activation of immune cells or direct neutralization of the pathogen. In research, antibodies are used to identify and locate surface and intracellular proteins. Cells express molecules on their surface that are often referred to as cluster of differentiation (CD), which are characteristic for different cell types. The conjugation of antibodies to fluorochromes allows phenotypic as well as functional characterisation of specific cell subsets with fluorescence microscopy or flow cytometry.

The easiest and most common way to stain surface proteins is a primary, direct staining. This staining works with a primary antibody that is directly conjugated to a fluorochrome and targets the structure of interest. A secondary or indirect staining requires two steps: the first antibody is not conjugated to a fluorochrome and binds the structure of interest.

The second antibody is conjugated to a fluorochrome and targets the first antibody. Examples for secondary stainings are primary biotin-conjugated and secondary streptavidin-flurochrome antibody interactions but also the staining of Fc fusion proteins is possible with secondary antibodies that recognize the Fc part of the fusion protein. For an intracellular staining of proteins, cells need to be fixed and permeabilized after the surface staining. Between the different staining steps, cells are usually washed two times with PBS or staining buffer (PBS + 2% FBS) to wash out unbound antibodies and to avoid unspecific signals.

4.7.3 Preparation of compensation beads for flow cytometry

Compensation beads are species-specific beads that bind fluorochrome conjugated antibodies. They are used to set voltages for flow cytometry to obtain an accurate fluorescence signal. For preparation, a drop of beads was gently mixed with 0.5-1 µl of antibody in a FACS tube and stored at 4 °C. Directly before usage, the bead/antibody mixture was filled-up with 300 µl PBS and vortexed.

4.8 Functional assays

4.8.1 KIR2DL-Fc fusion protein binding assay

In order to assess the binding affinity between different HLA-C1 and -C2 allotypes and allotypes of the inhibitory KIR2DL1/L2 and L3 receptors, KIR2DL-Fc fusion protein binding assays were performed. HLA-C transduced 721.221 cell lines were incubated with the KIR2DL-Fc fusion proteins. These proteins consist of the extracellular part of the KIR2DL receptor which bind to the HLA-C molecule and the Fc region of an IgG antibody. To detect the binding, a secondary anti-human IgG-PE antibody was used, which binds to the Fc part of the fusion protein. For the assay, untransduced and HLA-C transduced 721.221 cell lines were counted and washed with PBS. For each condition, 100,000 cells were used and transferred into a 96-well plate. The plate was centrifuged (350 x g, 3 min, 4 °C) and the supernatant was carefully discarded. The cell lines were resuspended in 50 µl KIR2DL-Fc fusion protein (25 µg/ml) in PBS and incubated for 15 min at 4 °C. After the incubation, the cells were washed twice with cold staining buffer (350 x g, 3 min, 4 °C) and then stained for 15 min at 4 °C in the dark with 50 µl LIVE/DEAD Near-IR viably dye (1:1000) and goat anti-human IgG-PE (1:100). After another round of two washing steps, the cells were resuspended in 150 µl fixation buffer, transferred into cluster tubes and analysed at a BD Fortessa. Besides the KIR2DL-Fc incubation, 721.221 were stained only with the human IgG antibody, without previous fusion protein labelling. This “secondary” only control was used to separate the specific KIR binding from unspecific binding of the antibody. Moreover, the cells were stained with an HLA class I antibody (anti-human HLA-ABC-PE, 1:100) to assess the HLA-C expression level on the cell surface of the transduced cell lines.

4.8.2 KIR2DL-β2m-KO Jurkat reporter assay

In a more physiological approach, the binding affinity between HLA-C and KIR2DL1-3 was assessed in an assay with KIR2DL-β2m-KO Jurkat reporter cells (effector cells) with HLA-C expressing 721.221 cells (target cells). Binding between the two cell lines results in an activation of the Jurkat reporter cells and an increased expression of the activation marker CD69. The co-culture was performed at an effector:target ratio of 1:10 using 25,000 effector and 250,000 target cells. The Jurkat reporter cells were counted, washed with PBS and resuspended at a concentration of $0.25x10^6$ cells/ml in cultivation medium. To differentiate target from effector cells in the later analysis, HLA-C transduced 721.221 were labelled with a CFSE cell tracer. Therefore, 721.221 were counted, washed with 10 ml PBS (500 x g, 10 min, 21 °C) and resuspended in 1 ml pre-warmed PBS. 5 µl aliquoted CFSE was mixed with 20 µl PBS and 2.5 µl diluted CFSE was added to the cells. After an incubation of 8 min at RT, 1 ml FBS was added to the cells and incubated for 1 min at RT. 5 ml of RPMI-1640 medium was added and again incubated for 5 min at RT. Finally, the cells were washed with cultivation medium (500 x g, 7 min, 21 °C) and resuspended at $2.5x10^6$ cells/ml in cultivation medium. For the assay, 100 µl of target cells (250,000 cells) were incubated with 100 µl of effector cells (25,000 cells) in a 96-well plate for 5 h at 37 °C and 5% CO_2. Following, the cells were washed with PBS and resuspended in 50 µl antibody mix with CD3-PE/Cy5 (1:100), CD69-BV421 (1:100) and LIVE/DEAD Near-IR viability dye (1:1000) in PBS and incubated for 20 min at 4 °C in the dark. Lastly, the cells were washed two times with staining buffer before they were resuspended in 100 µl fixation buffer and transferred to cluster tubes for further flow cytometry analysis. In relation to the KIR-Fc fusion protein assay, following controls were used: KIR2DL-β2m-KO Jurkat reporter cells were incubated without target cells as a “no target control” to assess the baseline expression of CD69 and the respective KIR2DL expression on the cell surface. In addition, HLA-C 721.221 were incubated without effector cells and stained for HLA-ABC (1:100 in PBS) to assess the HLA-C expression levels.

4.8.3 CD107a degranulation assay and HIV-1 p24 staining

CD107a is a functional marker, which can be used to identify NK cell activity (Alter *et al.*, 2004). CD107a, also known as lysosomal-associated membrane protein-1 (LAMP-1), is expressed in cells on the membrane of lysosomes. In activated NK cells, these lysosomes are transported to the cell surface where they fuse with the cell membrane and secret cytokines. This fusion results in a surface expression of CD107a and can be used as a marker for NK cell degranulation. After 8 days of infection of CD4 T cells with the HIV-1 strains JRCSF wt and JRCSF Vpu mut, a CD107a degranulation assay with autologous NK cells was performed. Uninfected (mock) and HIV-1-infected CD4 T cells were counted and treated for 20 min at 37 °C and 5% CO_2 with 25 U/ml Benzonase Nuclease to remove

"sticky" DNA from dying cells that can clump cells together. In order to get a high rate of infected cells within the target cell population and to remove uninfected cells, a positive selection of CD4 was performed. The enriched $CD4^-$/HIV-1-infected T cells were used for the co-culture with NK cells at an effector:target ratio of 1:2. Therefore, NK cells were resuspended in cultivation medium with 5 ng/ml IL-15 at a density of $1x10^6$ cells/ml. HIV-1-infected CD4 T cells were resuspended in the same medium at a density of $0.5x10^6$ cells/ml. 100,000 NK cells (100 µl) and 200,000 HIV-1-infected CD4 T cells (100 µl) were incubated with CD107a-BV510 (1:100) for 5 h at 37 °C and 5% CO_2 in a 96-well plate. Following conditions were used for the assay: 1) NK cells without any target cells, 2) NK cells and JRCSF wt infected CD4 T cells, 3) NK cells and JRCSF Vpu mut infected CD4 T cells, 4) NK cells with mock CD4 T cells and 5) NK cells and 721.221. During the incubation time, an intracellular HIV-1 p24 and surface marker staining was performed for following CD4 T cell populations: 1) Mock CD4 T cells, 2) HIV-1-infected CD4 T cells before positive selection, 3) enriched HIV-1-infected $CD4^-$ T cells after positive selection and 4) uninfected CD4 T cells after positive selection. First, cells were stained with 10 µl LIVE/DEAD Near-IR viability dye (1:50 in PBS) for 10 min in the dark at RT. Next, 90 µl of purified HLA-C antibody (1:100 in PBS) was added and incubated for 15 min in the dark at RT. Cells were washed twice with PBS (350 x g, 3 min, 4 °C) and then stained with 100 µl secondary mouse-IgG-PE (1:100 in PBS) for 20 min at 4 °C. Cells were washed two more times with PBS and then permeabilized and fixed for intracellular staining using the Cytofix/Cytoperm kit from BD Bioscience. Therefore, cells were incubated with 100 µl Cytofix/Cytoperm for 20 min at 4 °C, washed twice with 1x PermWash and then stained with 50 µl antibody master mix of CD3-PB (1:100), CD4-APC (1:100) and p24-FITC (1:100) in 1x PermWash for another 20 min at RT in the dark. Lastly, cells were washed twice with PBS, resuspended in 150 µl fixation buffer and transferred into cluster tubes for following flow cytometry analysis. After 5 h, the co-cultures were centrifuged (350 x g, 3 min, 21 °C) and the supernatant was removed. Firstly, cells were resuspended in 30 µl staining buffer, 10 µl LIVE/DEAD Near-IR viability dye (1:50 in PBS) was added and incubated for 10 min at 4 °C. Secondly, a master mix of following antibodies, diluted in brilliant stain buffer, was added and incubated for 20 min at 4 °C (CD56-BUV395, 1:200; CD16-BV785, 1:200; CD14-APC-Cy7, 1:100; CD19-APC-Cy7, 1:200; CD3-APC-Cy7, 1:100; CD57-PerCP-Cy5.5, 1:200; NKG2C-BUV563, 1:100; NKG2A-PE-Vio615, 1:50; KIR2DL1/S1-APC, 1:50; KIR2DL1/S5-PE, 1:50; KIR2DL3-AF488, 1:50; KIR2DL2/L3/S2-BV711, 1:50; KIR3DL1-AF700, 1:50; KIR3DL1/L2-PE-Vio770, 1:40 and KIR2DS4-Biotin, 1:50). Cells were washed twice with PBS and stained for 15 min at 4 °C with 50 µl strepdavidin-BV421 (1:1600). After a further round of two washing steps with PBS, cells were fixed with 200 µl Fluorofix buffer, transferred into cluster tubes and incubated 30 min at RT in the dark before flow cytometry analysis.

4.9 Phenotypic characterisation of NK cells from untreated HIV-1 infected and healthy individuals

Frozen PBMC were thawed in a water bath at 37 °C. The suspension was gently mixed and 200 µl of cells were directly transferred to a 1.5 ml tube for genomic DNA isolation. The remaining cell suspension was transferred to a 15 ml falcon tube and 10 ml pre-warmed cultivation medium with 25 U/ml Benzonase Nuclease was added dropwise. Cells were incubated for 20 min at 37 °C and 5% CO_2, centrifuged (200 x g, 10 min, 21 °C) and resuspended in fresh cultivation medium. During Benzonase Nuclease incubation time, cells were counted. The staining was performed as followed: every experiment had 4 FMO control samples from two healthy donors and an unstained control. FMO controls were performed for NKG2C, KIR2DS4, KIR3DL1 and KIR3DL1/L2. After a centrifugation step (200 x g, 10 min, 21 °C), the supernatant was carefully removed, the cells were resuspended in 30 µl staining buffer and transferred to a 96-well plate. 10 µl LIVE/DEAD Near-IR viability dye (1:50 in PBS) was added and incubated for 10 min at 4 °C in the dark. Afterwards, around 60 µl of antibody master mix (CD56-BUV395, 1:200; CD16-BV785, 1:200; CD14-APC-Cy7, 1:100; CD19-APC-Cy7, 1:200; CD3-PerCP-Cy5.5, 1:100; CD4-BV650, 1:200; CD8-AF700, 1:100; CD57-BV510, 1:500; NKG2C-BUV563, 1:100; NKG2A-PE-Vio615, 1:50; KIR2DL1/S1-APC, 1:50; KIR2DL1/S5-PE, 1:50; KIR2DL3-AF488, 1:50; KIR2DL2/L3/S2-BV711, 1:50; KIR3DL1-BV605, 1:40; KIR3DL1/L2-PE-Vio770, 1:40 and KIR2DS4-Biotin, 1:50; in Brilliant stain buffer) or FMO control mixes (same as mastermix, only without the respective FMO antibody) was added to the appropriate wells and incubated for 30 min at 4 °C in the dark. For the secondary staining, cells were washed twice, 50 µl of strepdavidin-BV421 (1:1600 in PBS) was added and incubated for 15 min at 4 °C in the dark. Lastly, cells were washed two times and fixed with 200 µl Fluorofix buffer. Before flow cytometry analysis, cells were transferred into cluster tubes and incubated for 30 min at RT.

4.10 Vpu sequencing

HIV-1 *Vpu* sequencing from plasma and PBMC samples of untreated HIV-1 patients was performed by the Next Generation Sequencing (NGS) technology platform at the Leibniz Institute of Virology by Dr. Daniela Indenbirken. Bioinformatic analysis were performed by Dr. Sanamjeet Virdi.

4.11 Flow cytometry

4.11.1 Principle

Flow cytometry is a technique to detect physical and chemical characteristic of single cells by light scattering. A common flow cytometer comprises of a 1) fluidic, 2) optical and 3) electronic system. A cell suspension is injected into the fluidic system where the sample is hydrodynamically focused by using a sheath fluid so that the cells travel in a single-cell stream through a laser beam. The optical system consists of lasers, lenses and collection systems (filters and mirrors). If a cell goes through the laser beam, the light is scattered and detected in forward as well as side directions. Forward-scattered light (FSC) is proportional to the size of the cell, whereas the side-scattered light (SSC) is a parameter for cell granularity and complexity. When a fluorochrome-labelled cell passes the laser beam, the fluorochrome absorbs and emits the light. This emitted fluorescence is detected by the optics. A set of mirrors and filters separate specific wavelengths and focus them towards photodetectors (photodiodes or photomultiplier tubes; PMTs). The signals are processed and converted by the electronic system to a digital signals, which can be visualized by a software. Every fluorochrome absorbs and emits light at an optimal excitation and emission wavelength, but it can also be excited and emit light over the whole spectrum. Therefore, it is important to know the spectral information about the used fluorochrome to prevent strong spectral overlay of different fluorochrome (Manohar *et al.*, 2021). **Figure 15** illustrates the structure of a flow cytometer.

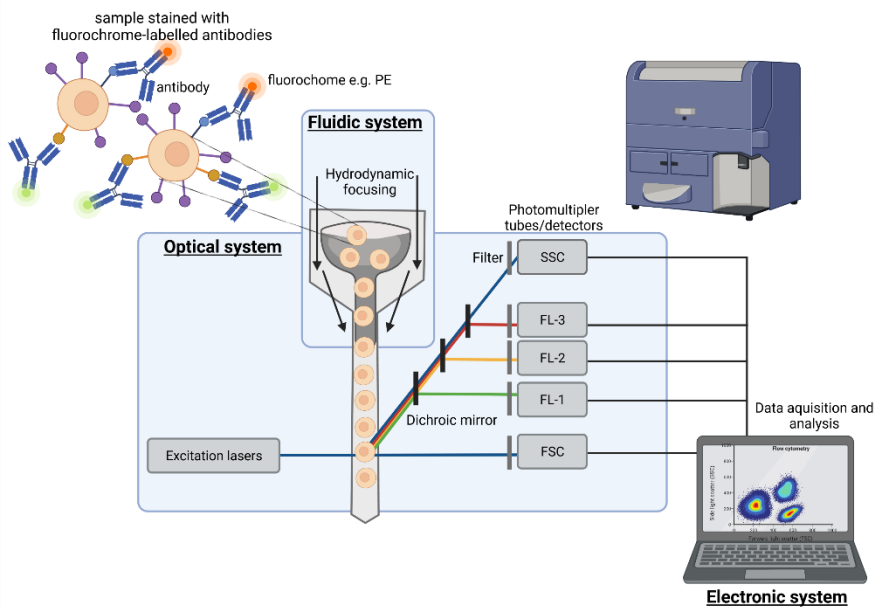

Figure 15: Illustration of a flow cytometer. Generally a flow cytometer composes of a fluidic, optical and electronic system. The fluorochrome-labelled cells are transported through a fluidic system and pass through the excitation lasers and emit the fluorescence and scatter the light. The scattered light is measured in line with the laser beam referred to as forward scatter (FSC) and at a ninety-degree angle ratio to the laser referred to as side scatter (SSC). Both parameters allow for discrimination of a heterogeneous cell population by size and internal complexity of the cells. The emitted light is collected by filters and lenses and captured by detectors. The electronic system converts the excited photons to a digital signal, which represents the expression intensity of the fluorochrome-labelled marker on the cell.

For all experiments, a BD LSR Fortessa flow cytometer with five lasers for up to 18 different parameters (fluorochromes) was used (**Table 2**).

Table 2: Configuration of the BD LSR Fortessa with used fluorochromes.

Detector Array	Laser	Parameter	Channel and BP-Filter	Fluorochrome
Trigon	Ultraviolet 355 nm	1	UV1 740/35	-
		1	UV1 560/40	BUV563
		2	UV2 380/14	BUV395
Octagon	Violet 405 nm	3	V1 780/60	BV785
		4	V2 710/40	BV711
		5	V3 675/50	BV650
		6	V4 610/20	BV605
		7	V5 586/15	-
		8	V6 525/50	BV510
		9	V7 450/50	BV421, Pacific-Blue
Octagon	Blue 488 nm	10	B1 710/50	PerCP-Cy5.5
		11	B2 530/30	AF488, FITC
		SSC	SSC	-
Octagon	Yellow-Green 561 nm	12	YG1 780/60	PE-Vio770
		13	YG2 670/30	PE-Cy5
		14	YG3 610/20	PE-Vio615
		15	YG4 586/15	PE
Trigon	Red 633 nm	16	R1 780/60	APC-Cy7, LIVE/DEAD Near-IR
		17	R2 730/45	AF700
		18	R3 670/14	APC

4.11.2 Analysis of flow cytometric data and hierarchical gating strategies

Flow cytometric data were analysed using the FlowJo software from BD. Fluorochrome-labelling of cells allows the identification and comparison of homogeneous cell populations across samples. This is achieved by hierarchical gating strategies. Control samples like fluorescence-minus one (FMO) or unstained control were used as gating controls.

4.11.2.1 Gating strategy for KIR2DL-Fc fusion protein binding assays

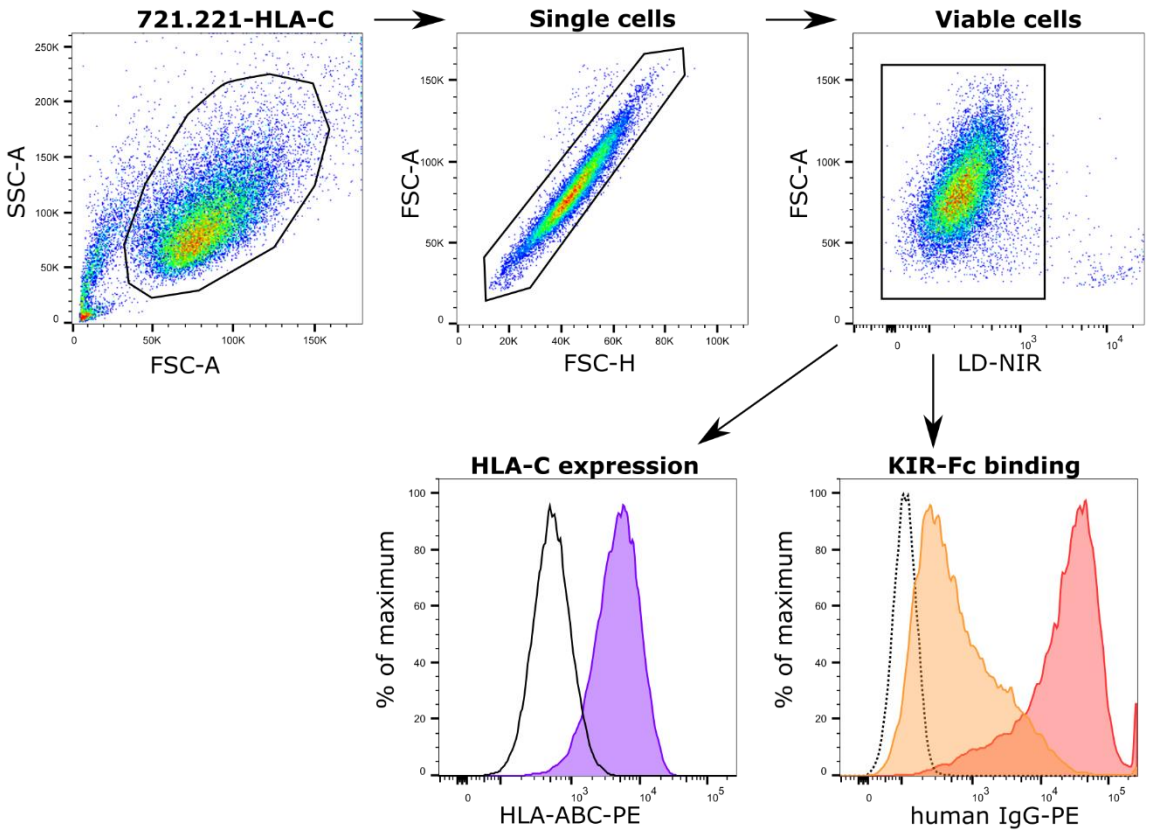

Figure 16: Gating strategy for KIR2DL-Fc fusion protein binding assay. The population of 721.221 was identified by using the forward and side scatter (FSC-A/SSC-A). Only single cells were included for analysis by area and height of the forward scatter (FSC-H/FSC-A). Next, dead cells were excluded by only gating on cells that were negative for the LIVE/DEAD (LD) fixable Near-IR (NIR) dye. Viable/single 721.221 were analyzed for their KIR2DL-Fc fusion protein binding and HLA-C expression.

4.11.2.2 Gating strategy for KIR2DL β2m-KO Jurkat reporter assays

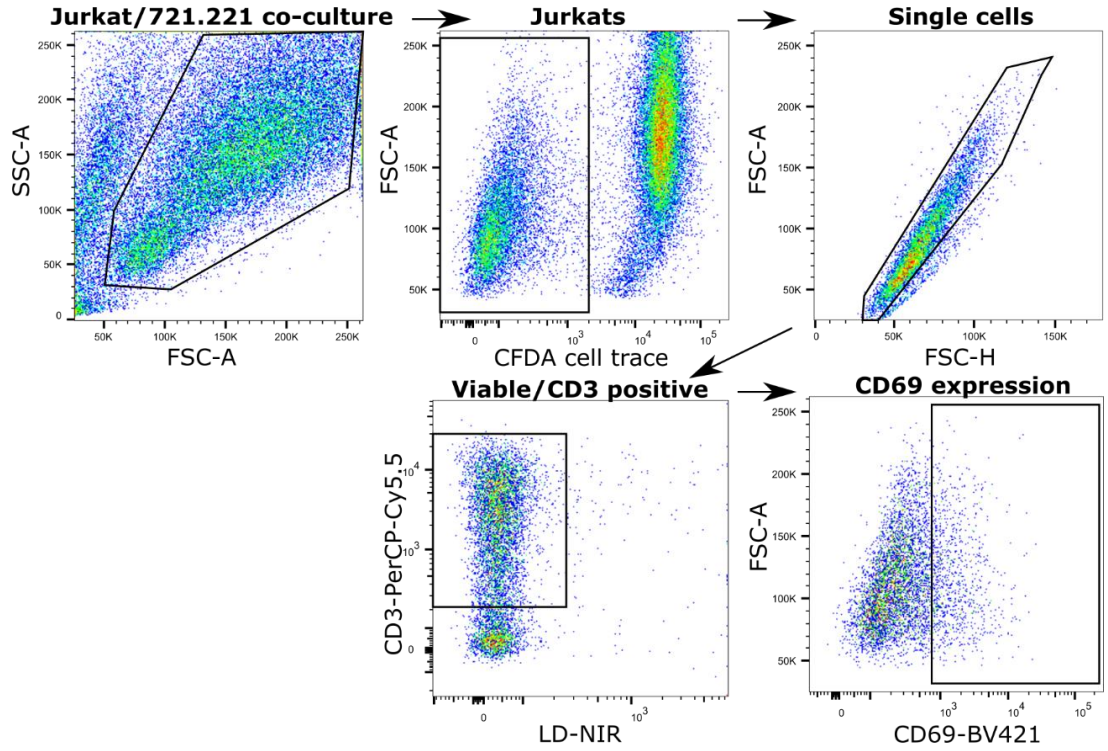

Figure 17: Gating strategy for KIR2DL β2m-KO Jurkat reporter assay. The co-culture of HLA-C expressing 721.221 and KIR2DL1-3 expressing β2m-KO Jurkat reporter cells was identified by using the forward and side scatter (FSC-A/SSC-A). 721.221 cells were excluded by the CFDA cell tracer. Only single reporter cells were included for analysis by area and height of the forward scatter (FSC-H/FSC-A). Next, CD3 negative and dead cells were excluded by only gating on cells that were negative for the LIVE/DEAD (LD) fixable Near-IR (NIR) dye and positive for CD3. Viable/single/CD3$^+$ reporter cells were analysed for their CD69 expression. Moreover, expression of HLA-C on 721.221 and KIR2DL1-3 on β2m-KO Jurkats was analyzed.

4.11.2.3 Gating strategy for p24 staining of HIV-1 infected CD4 T cells

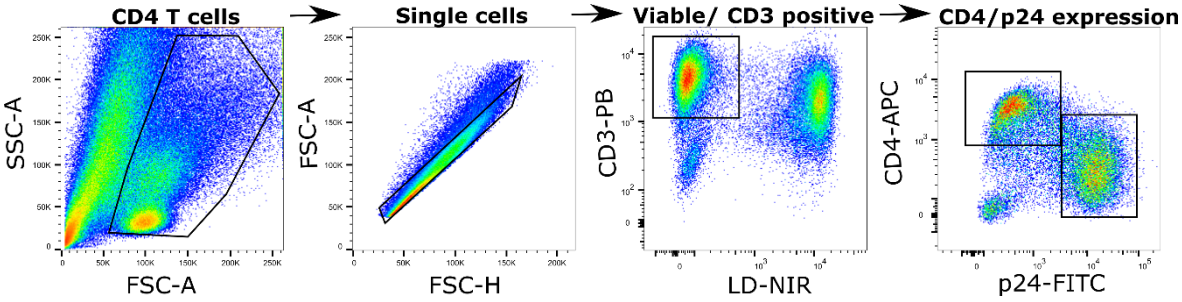

Figure 18: Gating strategy for p24 staining of HIV-1 infected CD4 T cells. PBMCs were isolated from buffy coats or healthy cohort blood and enriched for CD4 T cells. CD4 T cells were stimulated with CD3/CD28 T-Cell activator for 3 days and infected with different HIV-1 strains for 7 days. CD4 T cells were identified by using the forward and side scatter (FSC-A/SSC-A). Only single cells were included for analysis by area and height of the forward scatter (FSC-H/FSC-A). Next, CD3 negative and dead cells were excluded by only gating on cells that were negative for the LD-NIR dye and positive for CD3. Viable/single/CD3$^+$ CD4 T cells were analyzed for HIV-1 infected (CD4$^-$/p24$^+$) and uninfected (CD4$^+$/p24$^-$) cells.

4.11.2.4 Gating strategy for CD107a degranulation assay

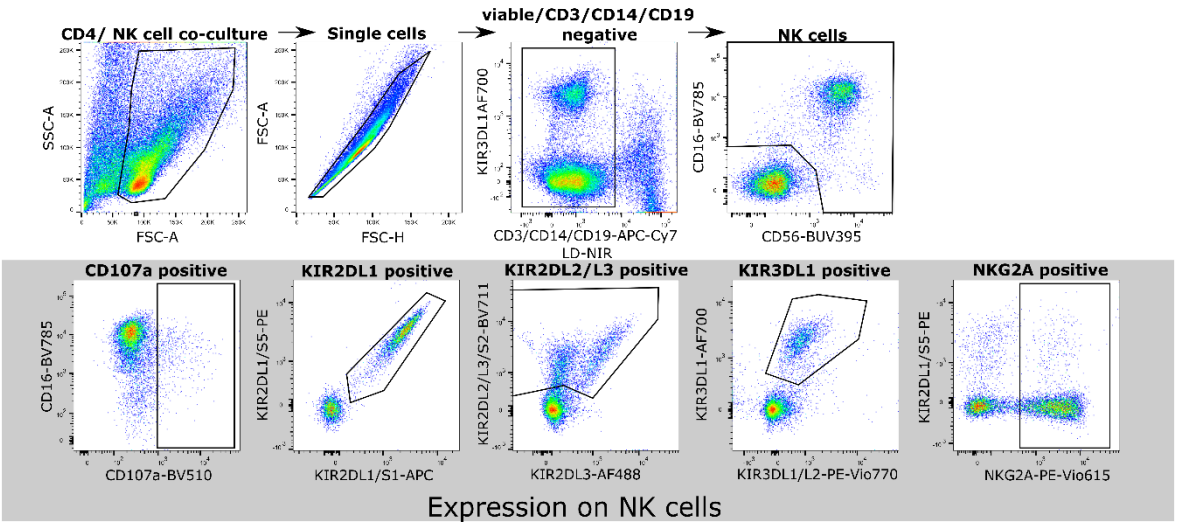

Figure 19: Gating strategy for CD107a degranulation assay. NK cells were incubated with HIV-1 infected CD4 T cells at an E:T ratio of 1:2 for 5 h. The co-culture was identified by using the forward and side scatter (FSC-A/SSC-A). Only single cells were included for analysis by area and height of the forward scatter (FSC-H/FSC-A). Only viable and CD3/CD14/CD19 negative cells were included and NK cells were identified by the expression of CD16 and CD56. NK cells were further analyzed for the expression of following marker: CD107a, KIR2DL1, KIR2DL2/L3, KIR3DL1 and NKG2A.

4.11.2.5 Phenotypic characterisation of NK cells from HIV-1$^+$ and HIV-1$^-$ individuals

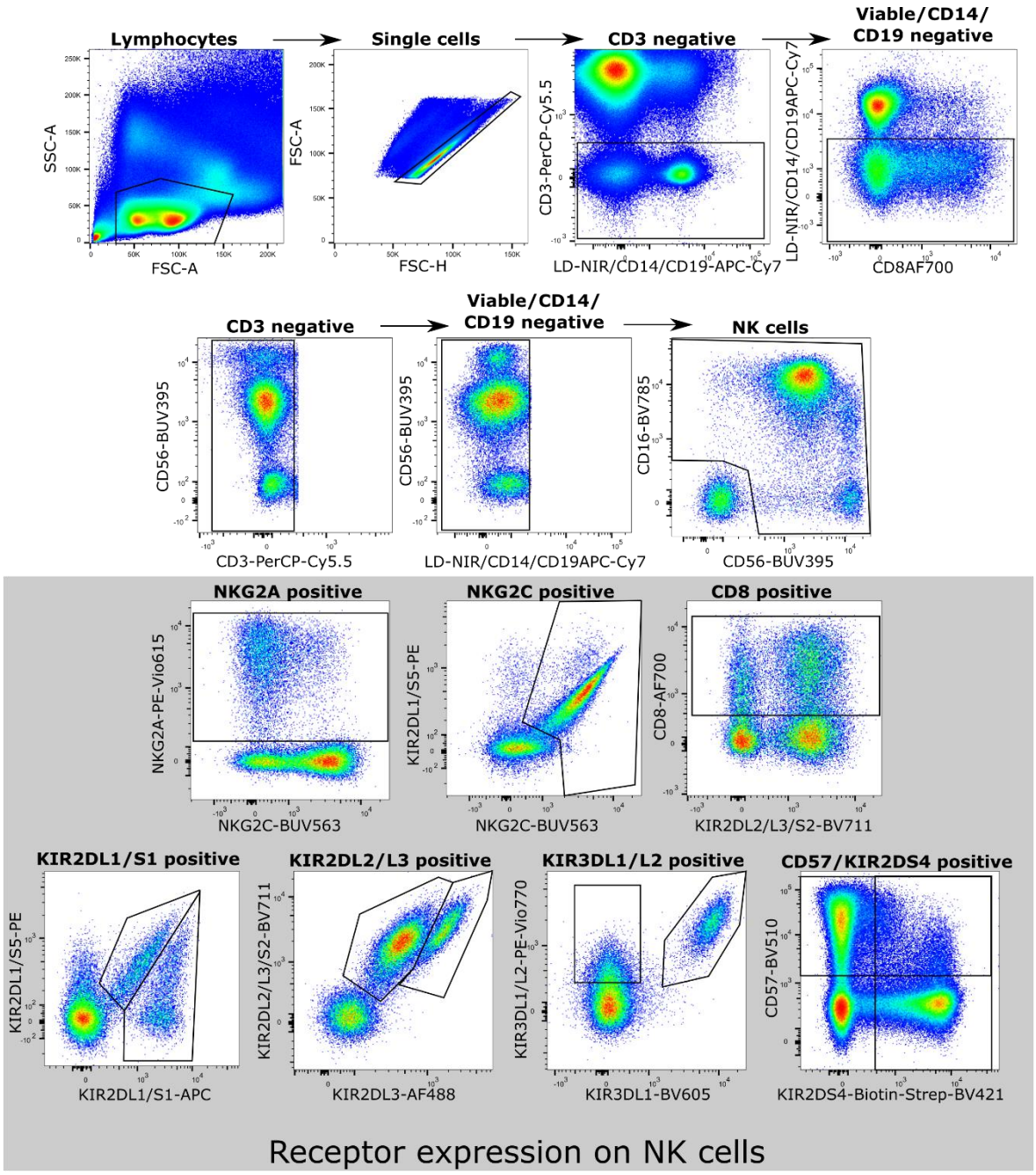

Figure 20: Gating strategy for phenotypic characterisation of NK cells. Lymphocytes were identified by using forward and side scatter (FSC-A/SSC-A). Only single cells were included for analysis by area and height of the forward scatter (FSC-H/FSC-A). Next, CD3/CD14/CD19 negative and dead cells excluded by multiple gating steps. NK cells were identified by the expression of CD56 and CD16 and further analysed for the expression of following maker: NKG2A, NKG2C, CD8, KIR2DL1/S1, KIR2DL2/L3, KIR3DL1/L2, CD57 and KIR2DS4.

4.12 Data analysis

4.12.1 KIR2DL-Fc fusion protein binding assays

Binding between KIR2DL-Fc fusion proteins and HLA-C1 or HLA-C2 expressing 721.221 cell lines was measured with flow cytometry as median fluorescence intensity (MFI) and normalized with the secondary only control to a relative fluorescence intensity (RFI). To consider differential HLA-C allotype expression on the 721.221 cell lines, the cell line with the highest MFI of HLA-ABC was set to 100% and the HLA-ABC expression of the other used cell lines was calculated in relation to the 100%. Finally, the calculated RFI was normalized to the relative HLA-ABC expression of the respective 721.221 HLA-C cell line.

$$\text{RFI} = \frac{\text{MFI (KIR2DL-Fc binding)}}{\text{MFI (secondary only control)}} - 1$$

$$\text{RFI normalized to HLA-ABC expression} = \frac{\text{RFI}}{\text{relative HLA-ABC expression}}$$

4.12.2 KIR2DL β2m-KO Jurkat reporter assays

CD69 expression of KIR2DL β2m-KO Jurkat reporter cell lines after co-culture with HLA-C1 or HLA-C2 expressing 721.221 cell lines was measured with flow cytometry as MFI and normalized with the CD69 expression of the Jurkat reporter cell line without target cells to a RFI. In line with the KIR2DL-Fc fusion protein binding assay, the HLA-C 721.221 cell line with the highest MFI of HLA-ABC was set to 100% and the HLA-ABC expression of the other used cell lines was calculated in relation to the 100%. Finally, the calculated RFI was normalized to the relative HLA-ABC expression of the respective 721.221 HLA-C cell line. KIR2DL expression of all generated β2m-KO Jurkat cell lines was comparably high and not taken into account for calculations.

$$\text{RFI} = \frac{\text{MFI (CD69 expression of reporter cells with target cells)}}{\text{MFI (CD69 expression of reporter cells without target cells)}} - 1$$

$$\text{RFI normalized to HLA-ABC expression} = \frac{\text{RFI}}{\text{relative HLA-ABC expression}}$$

4.12.3 CD107a expression by uneducated and educated NK cells

CD107a expression by NK cells cultured with and without target cells was measured as a percentage using flow cytometry. To assess differences in the frequency of educated and uneducated NK cells expressing CD107a, the frequency of CD107a-expressing NK cells after co-culture with target cells (721.221, uninfected CD4 T cells and HIV-1 infected CD4 T cells) was normalized to the frequency of CD107a-expressing NK cells without target cells and NK cells without inhibitory receptors (iRec) that recognize HLA class I molecules.

$$\begin{aligned}&\text{CD107a}^{+}\text{ NK cells (p.p.) normalized to NK cell alone and NK cells without iRec}\\&=\left(\frac{\text{\% CD107a (target cells)-\% CD107a (NK cells alone)}}{\text{100-\% CD107a (NK cells alone)}}\cdot 100\right)\\&\qquad-\left(\frac{\text{\% CD107a (without iRec)-\% CD107a (NK cells alone)}}{\text{100-\% CD107a (NK cells alone)}}\cdot 1\right)\cdot 100\end{aligned}$$

4.12.4 HLA-C downmodulation of HIV-1 infected CD4 T cells

To assess the ability of HIV-1 strains to downregulate HLA-C of the cell surface of infected CD4 T cells, the MFI of HLA-C of uninfected CD4 T cells was divided by the MFI of infected CD4 T cells.

$$\text{HLA-C downmodulation}=\frac{\text{MFI HLA-C (uninfected CD4 T cells)}}{\text{MFI HLA-C (HIV-1 infected CD4 T cells)}}$$

5 Results

5.1 Production of HLA-C expressing 721.221 cell lines

The human B-lymphoblastoid cell line 721.221 does not express endogenous HLA-A, -B or -C, due to gamma-ray-induced mutations in the HLA complex. Therefore, 721.221 cells can be used to express just one defined HLA class I molecule by inducing the HLA class I gene into the cell (Shimizu *et al.*, 1988, 1989). 12 HLA-C expressing 721.221 cell lines were generated to assess different binding affinities between HLA-C and KIR2DL, namely C*01:02, C*02:02, C*0303, C*03:04, C*04:01, C*05:01, C*06.02, C*07:01, C*07:02, C*12:03, C*14:02 and C*16:01. The HLA-C allotypes were selected based on an *HLA* allele frequency study of 39 689 caucasian individuals (*The Allele Frequency Net Database)*. A list of the 20 highest *HLA-C* allele frequencies is provided in the appendix. HLA-ABC expression of all generated HLA-C 721.221 cell lines was compared to unstained as well as untransduced cell lines using flow cytometry (**Figure 21**). The HLA-ABC staining of untransduced 721.221 cells showed a low expression of HLA class I on their cell surface maybe due to unspecific binding of the antibody. In addition, the transduced cell lines expressed high levels of HLA-C with variations between the different HLA-C allotypes. The generated 722.221 HLA-C-expressing cell lines were used for the KIR2DL-Fc binding assays, as well as for the KIR2DL reporter cell assays.

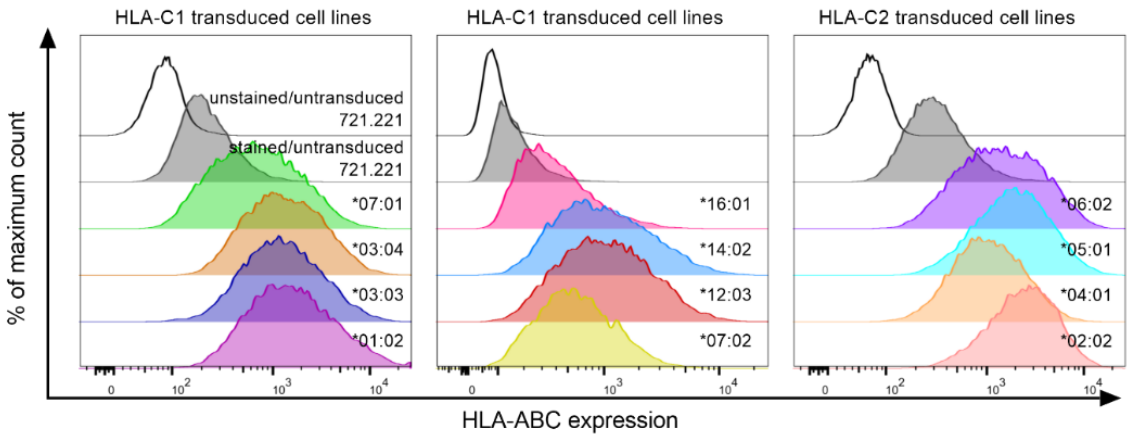

Figure 21: HLA-ABC expression of untransduced and HLA-C transduced 721.221 cell lines. All three histograms compare the HLA-ABC expression of HLA-C transduced 721.221 cell lines to unstained (black, not filled) and stained (grey, filled) untransduced 721.221 cells. The left and middle histograms show the expression of the 8 HLA-C1 transduced cell lines (HLA-C*01:02, *03:03, *03:04, *07:01, *07:02, *12:03, *14:02 and *16:01). The right histogram shows the HLA-C expression of the generated HLA-C2 cell lines (HLA-C*02:02; *04:01, *05:01 and *0602).

5.2 Production of KIR2DL-Fc fusion proteins

KIR2DL-Fc fusion proteins were produced to assess the binding affinities between the fusion proteins and HLA-C transduced 721.221 cell lines. KIR2DL allotypes were selected based on *KIR2DL* allele frequencies that were calculated from the DKMS of 615 630 genotyped caucasian donors. The list of the KIR2DL frequencies is provided in the

appendix. Following KIR2DL-Fc fusion proteins were produced using baculovirus infected insect cells (Hilton *et al.*, 2015): KIR2D1*001, *003, *004, *020, *022, KIR2DL2*001, *003, *009, KIR2DL3*001, *002, *009 and *016. Briefly, the allocated constructs were mutated and co-transfected with baculovirus into Sf9 insect cells. Following this, the baculovirus was amplified to generate high baculoviral titres. The baculovirus amplification was quantified by measuring the amount of baculovirus envelope protein GP64 with flow cytometry, as previously described (Blissard *et al.*, 1989). The GP64 staining of uninfected Hi5 cells and Hi5 cells infected with baculovirus P3 stock of KIR2DL1*022, KIR2DL2*001 and KIR2DL3*009 after 24 h showed that all Hi5 insect cells that were incubated with Sf9 supernatant containing baculovirus stock had an upregulated GP64 expression on the cell surface in comparison to uninfected Hi5 cells, indicating a successful infection of the Hi5 insect cells (**Figure 22A**). To confirm the production of KIR2DL-Fc fusion proteins of Hi5 cells upon baculovirus infection, the isolated protein fractions (F1-F5) were loaded onto a SDS-PAGE gel and stained with Coomassie reagent to identify protein bands (**Figure 22B**). As a positive control, commercially available recombinant KIR2DL1-Fc fusion protein from R&D was used. KIR2DL-Fc exists as a 102 kDa homodimer of two 51 kDa monomers (Hilton *et al.*, 2015). Under reducing conditions, the protein runs as a band of 72-80 kDa. The SDS-PAGE gel showed a very light band of the KIR2DL-Fc fusion protein from R&D around 70 kDa. The eluted and desalted protein fractions (F1-F2) of the produced KIR2DL-Fc protein had the same size as the R&D protein with around 70 kDa. Moreover, to determine the protein integrity (i.e. correct folding), the produced KIR2DL-Fc proteins were incubated with anti-human IgG-coated beads and then stained with anti-human KIR2DL1 or L2/L3 specific antibodies. Flow cytometry was used to detect the anti-KIR2DL antibody binding to the KIR2DL-Fc fusion protein (**Figure 22C**). Beads that were incubated without KIR2DL-Fc fusion protein did not bind the KIR2DL1/L2/L3 antibodies. In contrast, IgG-coated beads that were incubated with KIR2DL1*001-Fc, KIR2DL2*001-Fc or KIR2DL3*001-Fc displayed binding of the respective KIR2DL antibody. Taken together, the results verify a successful establishment and production of KIR2DL-Fc fusion proteins.

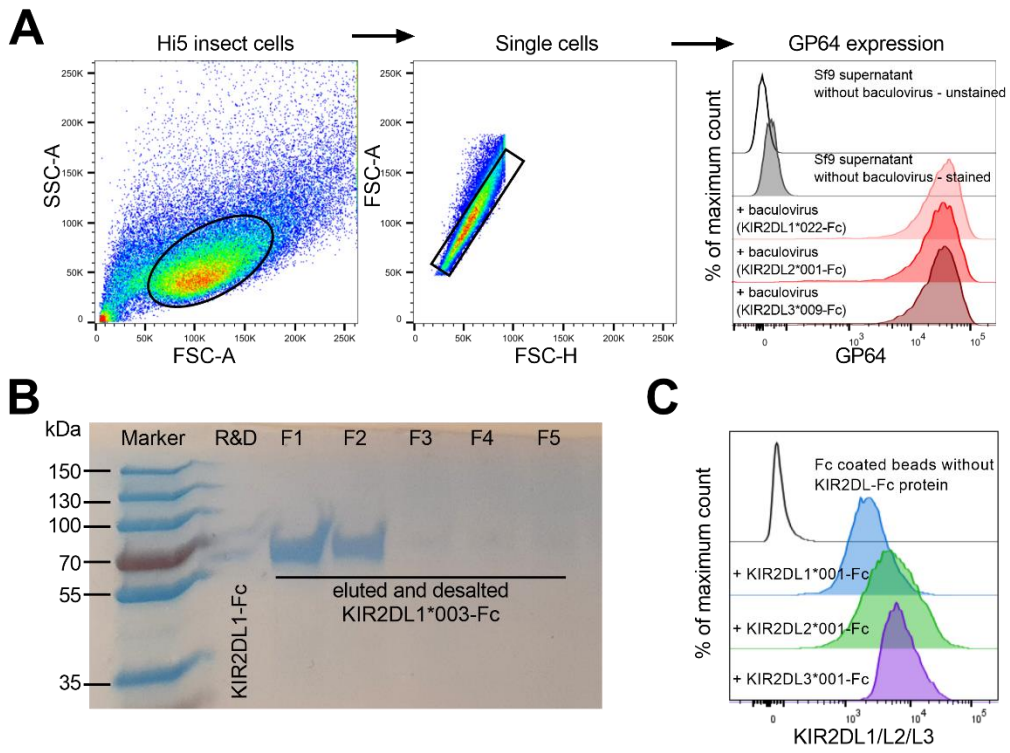

Figure 22: Quantification of KIR2DL-Fc fusion protein production. A Gating strategy for Hi5 cells incubated with Sf9 supernatant without baculovirus and with Sf9 supernatant from P3 viral stocks. Histograms show GP64 expression of Hi5 cells without baculovirus (black) and with baculovirus from KIR2DL1*022-Fc, KIR2DL2*001-Fc or KIR2DL3*009-Fc (red). **B** Reduced SDS-PAGE with a protein ladder on the left (PAGERuler Plus Prestained Protein Ladder 10-250 kDa), KIR2DL1-Fc fusion protein from R&D and F1-F5 of produced KIR2DL1*001-Fc fusion protein. **C** KIR2DL staining of IgG-coated beads without KIR2DL-Fc fusion protein (black, not filled) and with KIR2DL1*001-Fc (blue), KIR2DL2*001-Fc (green) or KIR2DL3*001-Fc (purple) fusion protein.

5.3 Binding assay of KIR2DL-Fc fusion proteins and HLA-C expressing 721.221 cell lines

To determine the strength and specificity of the interaction between HLA-C group 1 (HLA-C1) and HLA-C group 2 (HLA-C2) allotypes and inhibitory KIR2DL1/L2/L3 allotypes, binding assays were performed using KIR2DL-Fc fusion proteins and HLA-C expressing 721.221 cell lines. Therefore, HLA-C expressing 721.221 cell lines were incubated with KIR2DL-Fc fusion proteins. Engagement of HLA-C with KIR2DL-Fc fusion proteins was assessed with a secondary human Fc recognizing antibody and detected via flow cytometry. To ensure no unspecific binding of the secondary antibody, HLA-C transduced and untransduced 721.221 cell lines were stained with the secondary antibody without a previous KIR2DL-Fc incubation step. This negative control is described as secondary antibody control within the following sections and was used to calculate the relative fluorescence intensity (RFI). Moreover, the HLA-C expression of every 721.221 cell line was assessed and RFIs for ever measured HLA-C/KIR2DL interaction was normalized to the HLA-ABC expression of the respective HLA-C transduced 721.221 cell line. **Figure 23** illustrates the work flow for the performed KIR2DL-Fc fusion protein binding assays.

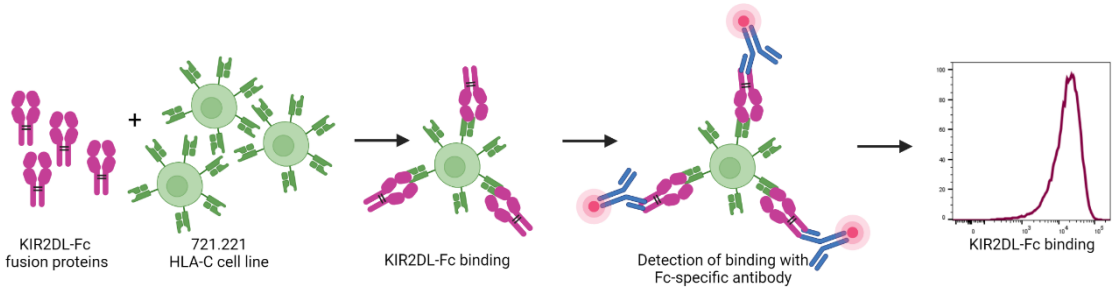

Figure 23: Work flow of KIR2DL-Fc fusion protein binding assays. KIR2DL-Fc fusion proteins were incubated with HLA-C expressing 721.221 cell lines. Binding of KIR2DL-Fc fusion proteins was assessed with a Fc-specific antibody via flow cytometry.

5.3.1 Binding assay of KIR2DL-Fc fusion proteins and HLA-C1 expressing 721.221 cell lines

KIR2DL-Fc binding was assessed for untransduced and HLA-C1 transduced 721.221 cell lines. The three histograms display the binding affinity as median fluorescence intensity (MFI) representative of KIR2DL1*001-Fc (green), KIR2DL3*001-Fc (blue) fusion proteins and secondary only control (black, dotted) with untransduced or HLA-C1 (C*03:04 and C*07:01) transduced 721.221 cell lines (**Figure 24A**). Relative fluorescence intensities (RFI) were calculated and normalized to the HLA-ABC expression of the respective HLA-C1 cell line of the KIR2DL-Fc binding (**Figure 24B**). Generally, untransduced 721.221 cells did not bind the KIR2DL-Fc fusion proteins, whereas the HLA-C1 expressing 721.221 showed binding to KIR2DL2/L3-Fc fusion proteins with strong variations between different allotype combinations. HLA-C1 721.221 cell lines did not bind KIR2DL1 allotypes (Hilton *et al.*, 2015). One exception is KIR2DL1*022, which possess a methionine at position 44 instead of a lysine, giving KIR2DL1*022 a C1 specificity (Hilton *et al.*, 2015). HLA-C*****07:01 showed the highest binding affinities to KIR2DL2/L3 allotypes, HLA-C*03:04, *07:02 and *16:01 a lower affinity and HLA-C*12:03, *C14:02, C*01:02 and C*03:03 almost no binding. In regards to KIR2DL2 allotypes, all HLA-C1 cell lines revealed the highest affinity to KIR2DL2*009 and the lowest to KIR2DL2*003. In addition, KIR2DL3 *001 and KIR2DL3*016 had a high binding affinity to HLA-C1 allotypes in comparison to the other KIR2DL3 allotypes tested. Moreover, binding affinity of HLA-C*07:02 to the KIR2DL-Fc fusion protein varied strongly between the experiments. In summary, HLA-C1 cell lines showed no interaction with KIR2DL1-Fc fusion proteins but displayed binding to KIR2DL2-Fc and KIR2DL3-Fc fusion proteins, in dependency of the allotype combinations of the respective HLA-C and KIR proteins.

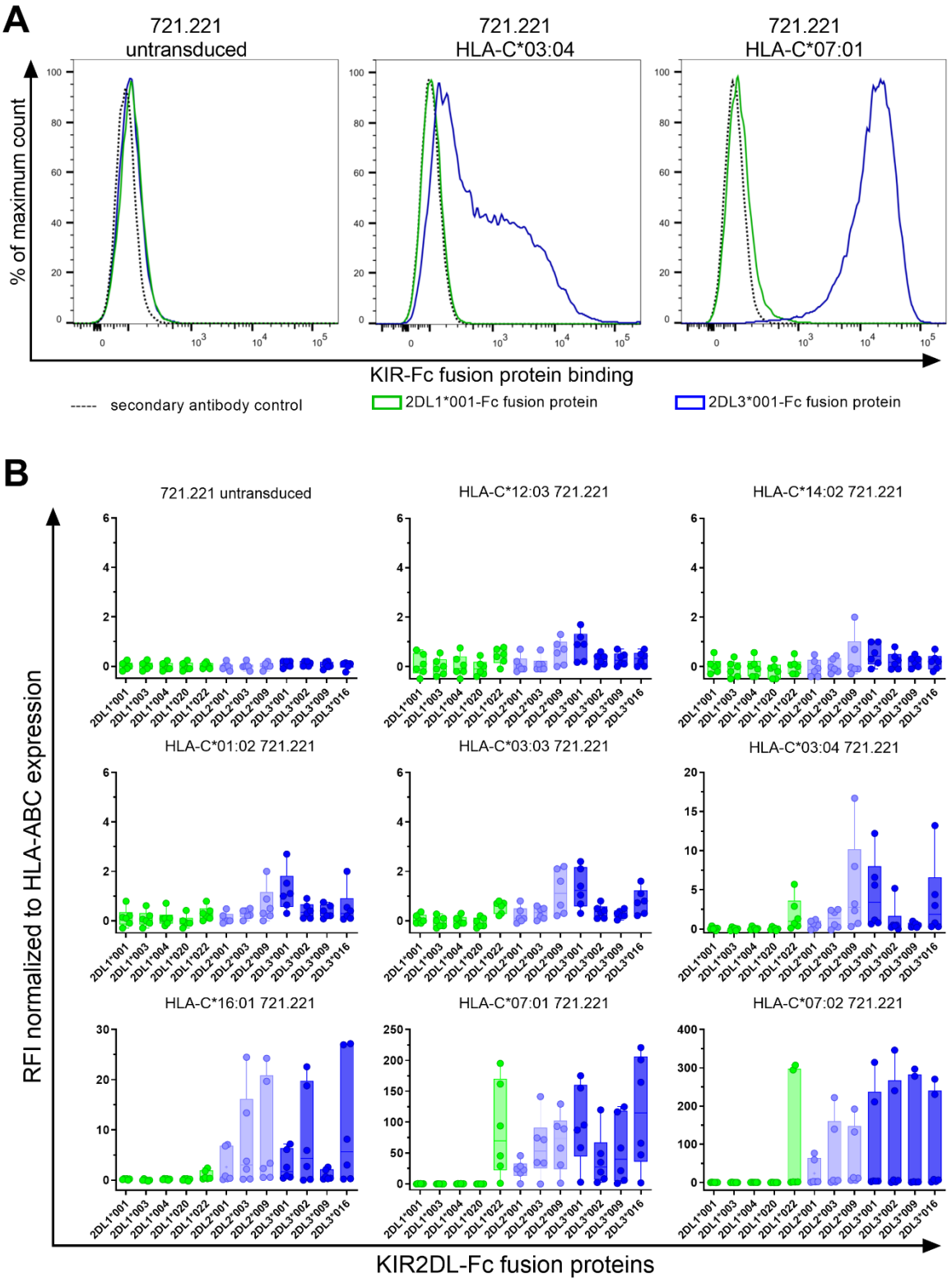

Figure 24: Binding between HLA-C1 721.221 cell lines and KIR2DL-Fc fusion proteins. HLA-C1 transduced 721.221 cell lines were incubated with KIR2DL1/L2/L3-Fc fusion proteins. Binding of the fusion protein was detected with a secondary human-Fc antibody. As a negative control, HLA-C1 721.221 cells were stained without KIR2DL-Fc fusion protein (secondary antibody control). **A** Histograms of KIR2DL1*001-Fc (green), KIR2DL3*001-Fc (blue) and secondary antibody control (black dotted) binding to exemplary two HLA-C1 transduced 721.221 cell lines (C*03:04 and C*07:01) and untransduced 721.221. **B** Box plots show the relative fluorescence intensity (RFI) normalized to the HLA-ABC expression of the 721.221 cell lines upon KIR2DL1-Fc (green), KIR2DL2-Fc (light blue) and KIR2DL3-Fc (dark blue) allotype binding (n ≤ 6). RFI was calculated with the median fluorescence intensity (MFI) with KIR2DL-Fc fusion protein/ MFI of secondary antibody only control.

5.3.2 Binding assay of KIR2DL-Fc fusion proteins to HLA-C2 expressing 721.221 cell lines

In addition to the KIR2DL-Fc fusion proteins binding assays with transduced HLA-C1 721.221 cell lines, binding assays were also performed with transduced HLA-C2 721.221 cell lines (**Figure 25**). Representative binding of KIR2DL and HLA-C are shown for KIR2DL1*001-Fc (green), KIR2DL3*001 (blue) and the secondary antibody control (black, dotted) with untransduced or HLA-C2 (C*06:02 and C*05:01) transduced 721.221 cell lines (**Figure 25A**). KIR2DL-Fc binding of the HLA-C2 cell lines displayed as the RFI normalized to the HLA-ABC expression of the respective HLA-C2 cell line (**Figure 25B**). KIR2DL1-Fc fusion protein had a high binding affinity to HLA-C2 expressing 721.221 cell lines with different extents. The strongest binding to KIR2DL1-Fc allotypes revealed HLA-C*05:01 followed by C*02:02. The lowest affinity had HLA-C*06:02 to the KIR2DL1-Fc allotypes. In addition, all HLA-C2 cell lines showed the highest affinity to the KIR2DL1*003 allotype. KIR2DL1*022 as a C1 specific KIR2DL1 allotype showed no binding to the HLA-C2 expressing cell lines. Moreover, HLA-C2 721.221 cell lines displayed higher binding affinities to KIR2DL1-Fc fusion proteins than HLA-C1 transduced 721.221 to KIR2DL2/L3-Fc fusion proteins. Most of the KIR2DL2-Fc and KIR2DL3-Fc fusion proteins did not bind to HLA-C2. However, KIR2DL2-Fc allotypes interacted with HLA-C*05:01 and C*02:02 but with a very low affinity. Taken together, KIR2DL1-Fc fusion proteins bound strongly to HLA-C2 expressing 721.221 cell lines.

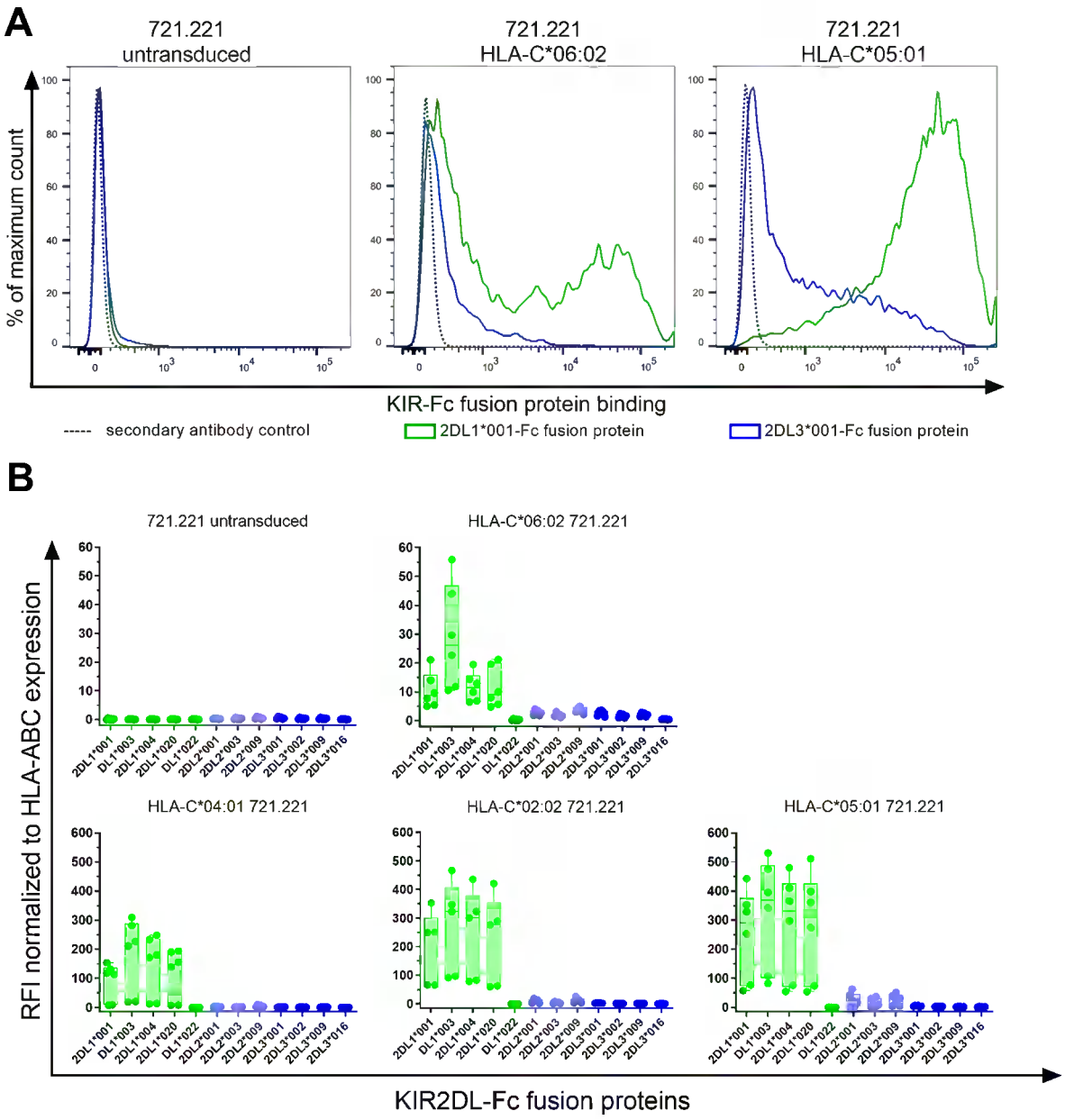

Figure 25: Binding between HLA-C2 721.221 cell lines and KIR2DL-Fc fusion proteins. HLA-C2 transduced 721.221 cell lines were incubated with KIR2DL1/L2/L3-Fc fusion proteins. Binding of the fusion protein was detected with a secondary human-Fc antibody. As a negative control, HLA-C2 721.221 cells were stained without KIR2DL-Fc fusion protein (secondary antibody control). **A** Histograms of KIR2DL1*001-Fc (green), KIR2DL3*001-Fc (blue) and secondary antibody control (black dotted) binding to exemplary two HLA-C2 transduced 721.221 cell lines (C*06:02 and C*05:01) and untransduced 721.221. **B** Box plots show the relative fluorescence intensity (RFI) normalized to the HLA-ABC expression of the 721.221 cell lines upon KIR2DL1-Fc (green), KIR2DL2-Fc (light blue) and KIR2DL3-Fc (dark blue) allotype binding (n ≤ 6). RFI was calculated with the median fluorescence intensity (MFI) with KIR2DL-Fc fusion protein/ MFI of secondary antibody only control.

5.4 Production of KIR2DL β2m-KO Jurkat reporter cell lines

To assess the binding affinities of KIR2DL/HLA-C in a more physiological way, KIR2DL expressing β2m-KO Jurkat reporter cell lines were generated: KIR2DL1*001, *004, *020, *022, KIR2DL2*001, *003, *009, KIR2DL3*001, *002, *009 and *016. Jurkat cells are T cells initially established from a donor with an acute T cell leukemia. The knock-out (KO) of β2m prevents the surface expression of HLA class I molecule on the Jurkat cells and ensures that KIR2DL transduced cells do not activate each other. KIR2DL expression of all produced cell lines was compared to untransduced β2m-KO Jurkats (**Figure 26**). All cell lines expressed high amounts of the respective KIR2DL on the surface.

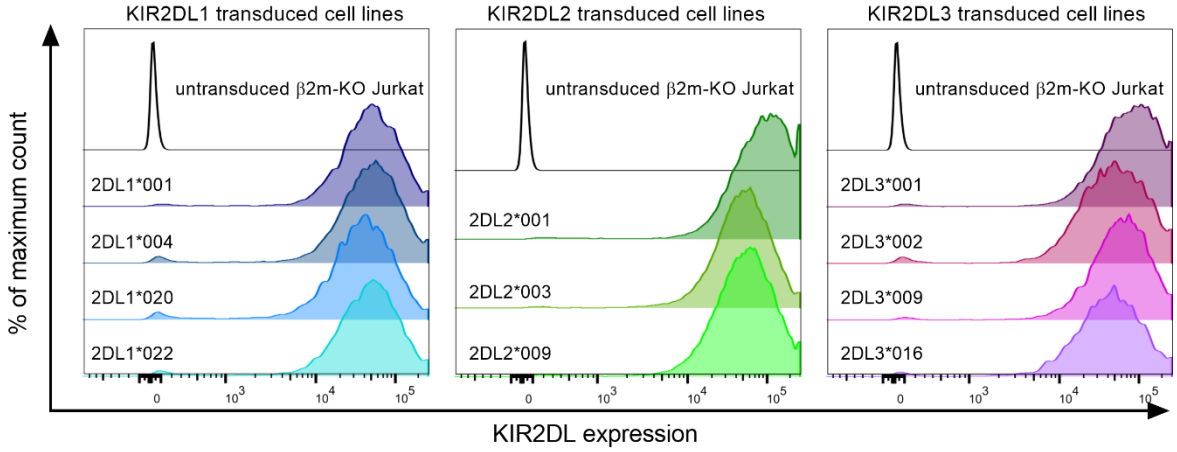

Figure 26: KIR2DL expression of untransduced and KIR2DL transduced β2m-KO Jurkat cell lines. Histograms show the expression of the KIR2DL1 (*001, *004, *020, *022; blue), KIR2DL2 (*001, *003, *009; green) and KIR2DL3 (*001, *002, *009, *016; purple) transduced and untransduced (black, not filled) β2m-KO Jurkat cell lines.

5.5 Reporter assay of KIR2DL β2m-KO Jurkat reporter cells and HLA-C expressing 721.221 cell lines

To confirm the binding pattern observed in KIR2DL-Fc binding assays with HLA-C expressing cell lines and to assess the functional consequences of KIR2DL-HLA-C interactions, reporter cell assays with KIR2DL-CD3ζ transduced β2m-KO Jurkat cell lines and HLA-C1 and -C2 transduced 721.221 cell lines were performed. KIR2DL expressing β2m-KO Jurkat cell lines were co-cultured with HLA-C transduced 721.221 cell lines at an effector and target cell ratio of 1:10 for 5 h. Upon interaction of HLA-C transduced 721.221 cell lines with KIR2DL transduced β2m-KO Jurkat cell lines, KIR2DL β2m-KO Jurkat cells signal intracellularly through CD3ζ, leading to upregulation of the activation marker CD69 on the cell surface (Cibrián *et al.*, 2017). Therefore, CD69 expression of KIR2DL β2m-KO Jurkat cell lines was used to determine the binding between KIR2DL and HLA-C. As CD69 expression of KIR2DL β2m-KO Jurkat cells can also be triggered through other factors such as metabolic stress the “baseline” CD69 expression of KIR2DL β2m-KO Jurkat cell lines was assessed without target cells and set in relation to the induced CD69 expression after incubation with target cells as relative fluorescence intensity (RFI).

Moreover, the expression of KIR2DL on β2m-KO Jurkat cells and the expression of HLA-C on 721.221 cells was quantified. Because of some variations in the HLA-C expression of the 721.221 cell lines, the relative fluorescence intensity was normalized to the assessed HLA-ABC expression of the 721.221 cell lines. The gating strategy for the KIR2DL reporter assays is provided in the methods (4.11.2.2). **Figure 27** illustrates the work flow for the KIR2DL reporter assays.

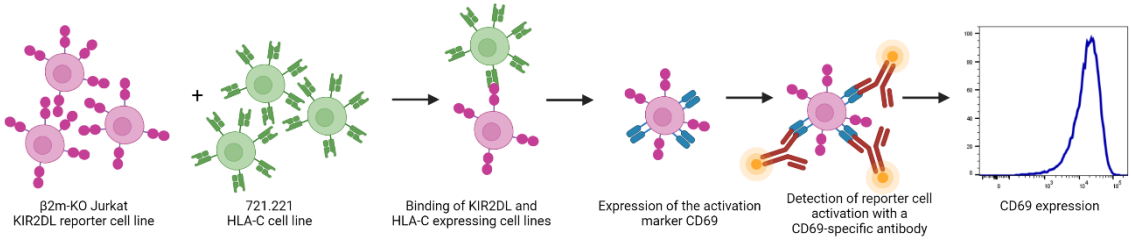

Figure 27: Work flow for KIR2DL β2m-KO Jurkat reporter assay. KIR2DL expressing β2m-KO Jurkat reporter cell lines were incubated with HLA-C expressing 721.221 cell lines. Binding of KIR2DL was assessed with a CD69-specific antibody via flow cytometry.

5.5.1 Reporter assay of KIR2DL β2m-KO Jurkat reporter cells and HLA-C1 expressing 721.221 cell lines

The expression of CD69 of KIR2DL β2m-KO Jurkat cell lines was assessed after co-culture with HLA-C1 expressing 721.221 cell lines. Representative CD69 expression by KIR2DL*001 and KIR2DL3*001 expressing β2m-KO Jurkat cell lines without target cells and with HLA-C*12:03 transduced 721.221 cells is shown in **Figure 28A**. RFI of CD69 expression by KIR2DL β2m-KO Jurkat cell lines upon co-cultures with HLA-C1 expressing 721.221 cell lines were calculated and normalized to HLA-ABC expression by the respective HLA-C1 721.221 cell line (**Figure 28B**). Untransduced β2m-KO Jurkat cell lines did not show any upregulation of CD69 in co-culture with HLA-C1 transduced 721.221 cell line. In general, KIR2DL2 and KIR2D3 expressing β2m-KO Jurkat cell lines upregulated CD69 in co-culture with HLA-C1 721.221 cell lines whereas KIR2DL1 β2m-KO Jurkat cell lines did not display a higher surface expression of CD69 after co-incubation with HLA-C1 expressing cell line. KIR2DL1*022 transduced β2m-KO Jurkats, a C1 specific KIR2DL1, strongly expressed CD69 after incubation with HLA-C*07:02 and C*07:01 but not after co-incubation with HLA-C*16:01 and C*14:02 or only to a low level after co-culture with any of the remaining HLA-C1 721.221 cell lines. HLA-C*07:01 induced the strongest upregulation of CD69 in KIR2DL2 and KIR2DL3 β2m-KO Jurkat cell lines, whereas the other HLA-C1 transduced cell lines induced comparable levels of CD69 in KIR2DL2 and KIR2DL3 β2m-KO Jurkat cell lines. All HLA-C1 cell lines triggered the highest expression of CD69 in KIR2DL3*002 β2m-KO Jurkat cells. In summary, co-cultures between HLA-C1 expressing 721.221 cell lines and KIR2DL expressing β2m-KO Jurkat cell lines confirmed the binding patterns observed within previous KIR2DL-Fc fusion protein assays.

In addition, KIR2DL/HLA-C1 interactions induced functional activity in KIR2DL β2m-KO Jurkat cell lines with high activation in KIR2DL2 and KIR2DL3 β2m-KO Jurkat cell lines after co-incubation with HLA-C1 721.221 cell lines.

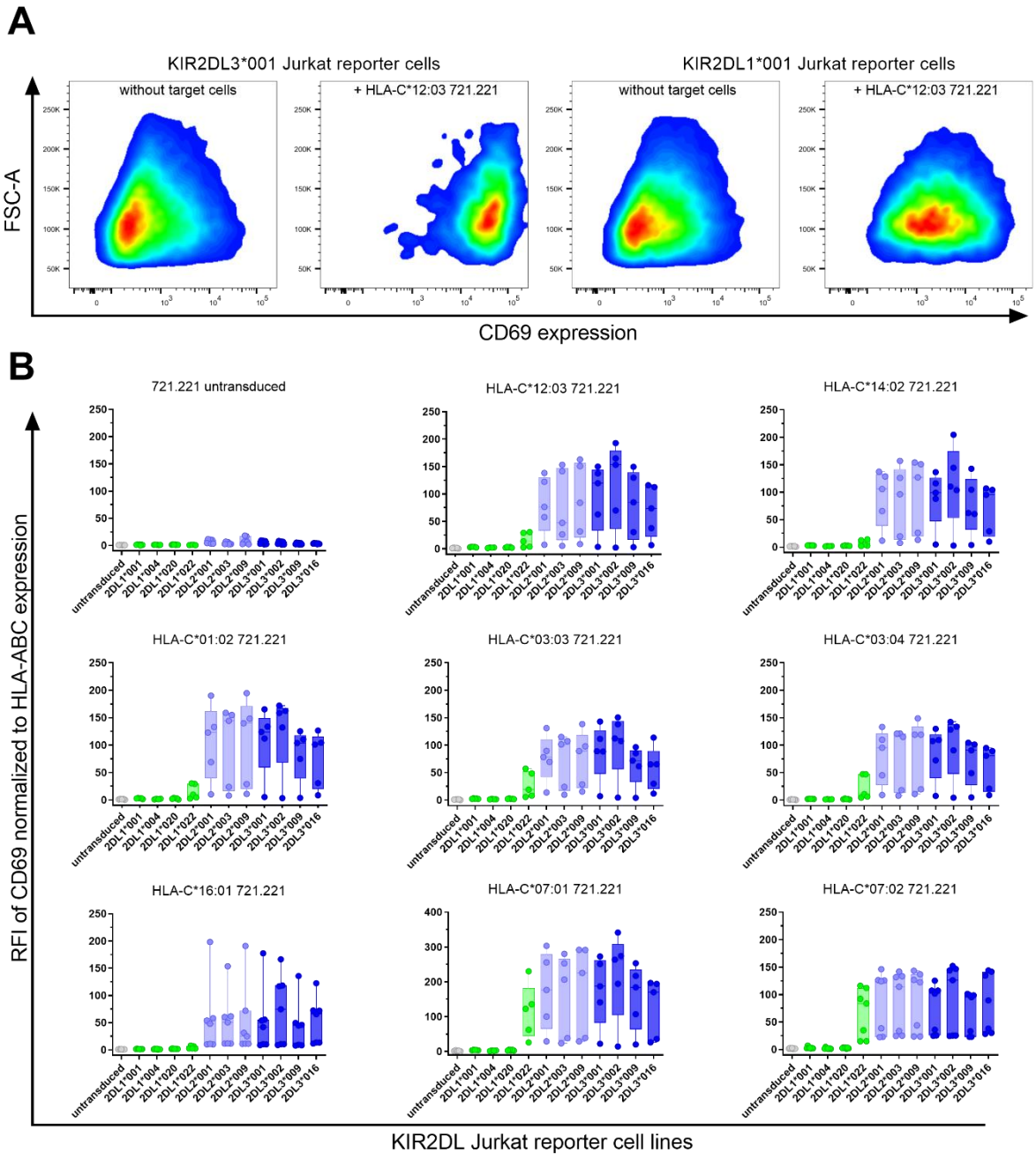

Figure 28: CD69 expression by untransduced and KIR2DL transduced β2m-KO Jurkat cell lines after co-culture with HLA-C1 expressing and untransduced 721.221 cell lines. HLA-C1 transduced 721.221 cell lines were co-cultured with KIR2DL1/L2/L3 β2m-KO Jurkat cell lines at an effector to target cell ratio of 1:10 for 5 h. CD69 expression of the KIR2DL β2m-KO Jurkat cell lines was assessed as marker of interaction between HLA-C and KIR2DL. **A** Representative plot of CD69 expression by KIR2DL3*001 and KIR2DL1*001 transduced β2m-KO Jurkat cells without target cells and with HLA-C*12:03^{+} 721.221 cells. **B** Box plots show the relative fluorescence intensity (RFI) of CD69 normalized to HLA-ABC expression of the respective HLA-C1 721.221 cell line. HLA-C1 721.221 cell lines were co-cultured with untransduced β2m-KO Jurkat cells (grey) or KIR2DL1 (green), KIR2DL2 (light blue) or KIR2DL3 (dark blue) transduced β2m-KO Jurkat cells (n ≤ 6). RFI was calculated with the median fluorescence intensity (MFI) of CD69 expression with target cells/ MFI of CD69 expression without target cells.

5.5.2 Reporter assay of KIR2DL β2m-KO Jurkat reporter cells and HLA-C2 expressing 721.221 cell lines

KIR2DL β2m-KO Jurkat reporter assays were also performed using HLA-C2 transduced 721.221 cell lines. Representative CD69 expression by KIR2DL3*001 and KIR2DL1*001 expressing β2m-KO Jurkat cells without target cells and with HLA-C*04:01 expressing 721.221 cells is illustrated in **Figure 29A**. RFIs of CD69 expression after co-culture of untransduced and KIR2DL transduced β2m-KO Jurkat cell lines with HLA-C2 721.221 cell lines were calculated and normalized to the HLA-ABC expression of the respective 721.221 cell line (**Figure 29B)**. Co-cultures including untransduced β2m-KO Jurkat cells and/or untransduced 721.221 cells did not induce any expression of CD69. KIR2DL1 transduced β2m-KO Jurkat cell lines upregulated CD69 expression after incubation with HLA-C2 expressing 721.221 cell lines, with β2m-KO Jurkat cells transduced with the KIR2DL1*002 allotype displaying the highest surface expression of CD69 after co-culture with almost all HLA-C2 cell lines. KIR2DL1*022 transduced β2m-KO Jurkat cells did not upregulate CD69 after co-incubation with 721.221 cell lines. In addition, some KIR2DL2 or KIR2DL3 transduced β2m-KO Jurkat cell lines upregulated CD69 after exposure to HLA-C2 transduced cell lines, but in general to lower levels compared to KIR2DL1 transduced Jurkat cells. Taken together, co-culture between HLA-C2 expressing 721.221 cell lines and KIR2DL expressing β2m-KO Jurkat cell lines revealed comparable binding patterns observed within previous KIR2DL-Fc fusion protein assays. In addition, HLA-C2 transduced 721.221 cell lines induced CD69 expression in KIR2DL1 expressing β2m-KO Jurkat cell lines and also in some KIR2DL2 and KIR2DL3 β2m-KO Jurkat cell lines.

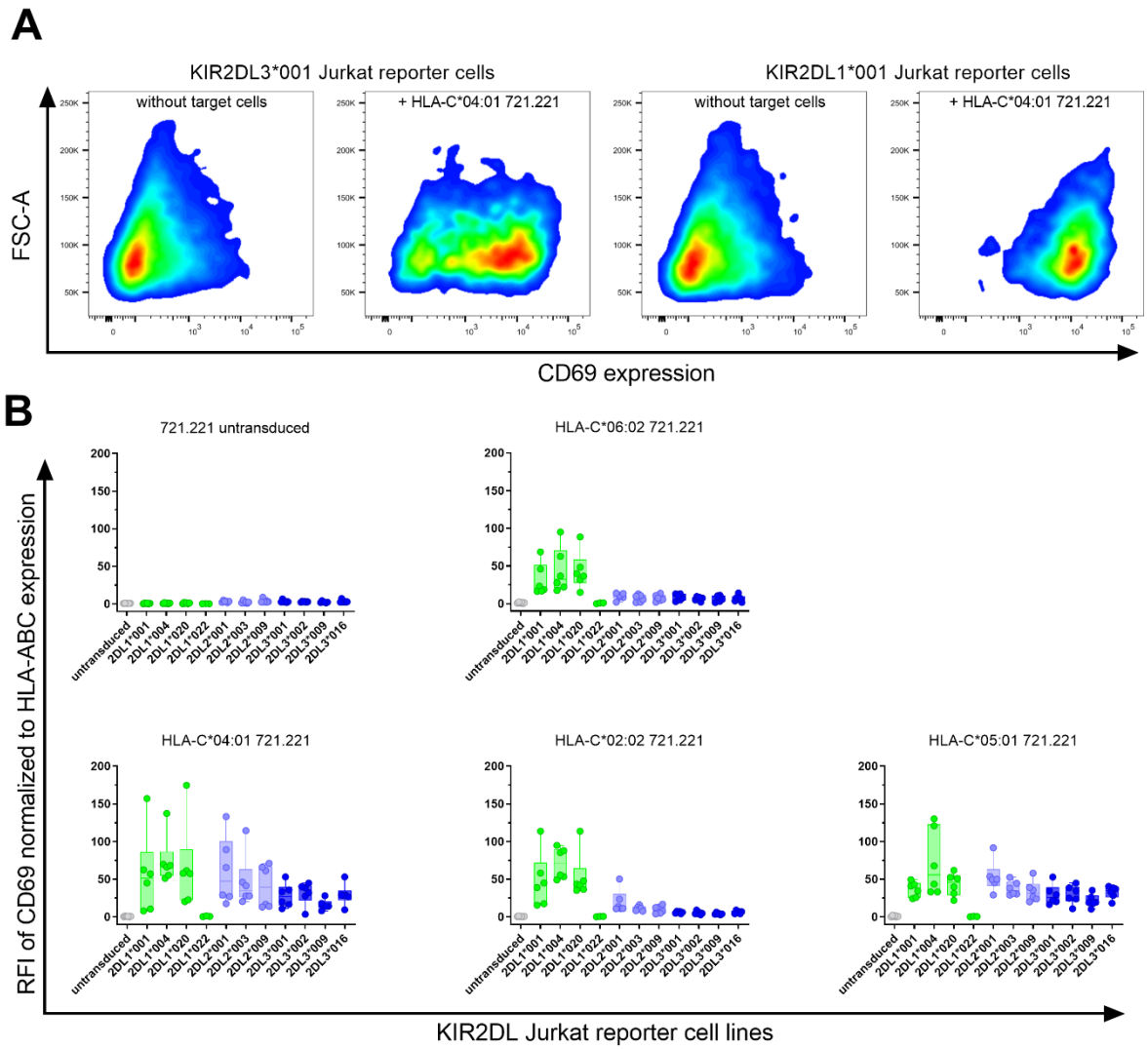

Figure 29: CD69 expression of untransduced and KIR2DL transduced β2m-KO Jurkat cell lines after co-culture with HLA-C2 expressing and untransduced 721.221 cell lines. HLA-C2 transduced 721.221 cell lines were co-cultured with KIR2DL1/L2/L3 β2m-KO Jurkat cell lines at an effector to target cell ratio of 1:10 for 5 h. CD69 expression of the KIR2DL β2m-KO Jurkat cell lines was assessed as marker of interaction between HLA-C and KIR2DL. **A** Representative plot of CD69 expression of KIR2DL3*001 and KIR2DL1*001 transduced β2m-KO Jurkat cells without target cells and with HLA-C*04:01^{+} 721.221 cells. **B** Box plots show the relative fluorescence intensity (RFI) of CD69 normalized to HLA-ABC expression of the respective HLA-C2 721.221 cell line. HLA-C2 721.221 cell lines were co-cultured with untransduced β2m-KO Jurkat cells (grey) or KIR2DL1 (green), KIR2DL2 (light blue) or KIR2DL3 (dark blue) transduced β2m-KO Jurkat cells (n ≤ 6). RFI was calculated with the median fluorescence intensity (MFI) of CD69 expression with target cells/ MFI of CD69 expression without target cells.

5.6 Correlation of KIR2DL/HLA-C binding assays

For a better comparison between the Fc fusion protein binding assay and the Jurkat reporter cell assay, the median of the respective binding assay was calculated for every individual receptor and ligand combination. Following this, the median of the KIR2DL/HLA-C combination with the highest value was set to 100% and all other values of KIR2DL/HLA-C combinations were calculated in relation to the 100% value (**Figure 30A/B)**. The KIR2DL-Fc fusion protein binding assays revealed the highest binding affinities between HLA-C2 expressing 721.221 cell lines and KIR2DL1-Fc fusion proteins, at which HLA-C*05:01 and KIR2DL1*003 displayed the highest affinities and HLA-C*06:02 revealed the lowest affinities to KIR2DL1-Fc fusion proteins. Moreover, HLA-C2 expressing 721.221 cell lines only bound with a very low affinity to KIR2DL2- and KIR2DL3-Fc fusion proteins. HLA-C1 expressing 721.221 did not bind to KIR2DL1-Fc fusion proteins and only with a low affinity to KIR2DL2- and KIR2D3-Fc fusion proteins with the exception of HLA-C*07:01 as the only HLA-C1 721.221 cell line binding to all KIR2DL2- and KIR2DL3-Fc fusion proteins. In contrast, the Jurkat reporter cell assays showed the highest induced CD69 expression in KIR2DL2 and KIR2DL3 expressing β2m-KO Jurkat reporter cell lines in combination with HLA-C1 transduced 721.221 cell lines with the highest activation value for KIR2DL3*002 and HLA-C*07:01. Furthermore, combinations of HLA-C1 and KIR2DL1 induced no upregulation of the activation marker CD69 in Jurkat reporter cell lines. Co-cultures of HLA-C2 expressing 721.221 cell lines induced CD69 expression in all KIR2DL expressing β2m-KO Jurkat reporter cell lines with a slightly higher frequency of CD69 in KIR2DL2 and KIR2DL3 β2m-KO Jurkat reporter cell lines. To compare the results of the two binding assays, correlation analyses were performed for KIR2DL-Fc fusion proteins and KIR2DL expressing β2m-KO Jurkat reporter cells with HLA-C1 and HLA-C2 transduced 721.221 (**Figure 30C**). KIR2DL1-Fc fusion protein assays and KIR2DL1 β2m-KO Jurkat reporter cell assays correlated strongly ($r = 0.89$, $p<0.0001$). In addition, KIR2DL2/L3-Fc fusion protein assays and KIR2DL2/L3 β2m-KO Jurkat reporter cell assays showed a weak correlation ($r = 0.21$, $p=0.033$).

A

KIR-Fc fusion proteins

721.221 HLA-C cell lines		2DL1 *003	2DL1 *004	2DL1 *020	2DL1 *001	2DL1 *022	2DL3 *016	2DL3 *001	2DL2 *009	2DL2 *003	2DL3 *009	2DL2 *001	2DL3 *002
721.221		0.0	0.0	0.0	0.0	0.0	0.0	0.1	0.1	0.1	0.1	0.1	0.1
C*14:02	HLA-C1	0.0	0.0	0.0	0.0	0.0	0.1	0.1	0.0	0.0	0.1	0.0	0.0
C*12:03	HLA-C1	0.0	0.0	0.0	0.0	0.1	0.1	0.2	0.2	0.0	0.1	0.0	0.1
C*01:02	HLA-C1	0.0	0.0	0.0	0.0	0.1	0.1	0.3	0.1	0.1	0.1	0.0	0.1
C*03:03	HLA-C1	0.0	0.0	0.0	0.0	0.2	0.2	0.3	0.3	0.1	0.1	0.0	0.1
C*16:01	HLA-C1	0.0	0.0	0.0	0.1	0.1	1.5	0.5	0.8	0.8	0.1	0.2	1.2
C*03:04	HLA-C1	0.0	0.0	0.0	0.0	0.3	0.5	0.9	0.8	0.4	0.1	0.2	0.1
C*07:02	HLA-C1	0.0	0.1	0.0	0.1	0.5	2.0	1.1	3.3	1.6	0.5	0.7	1.7
C*07:01	HLA-C1	0.0	0.1	0.0	0.1	18.9	31.3	24.8	19.9	14.4	10.8	6.3	7.3
C*06:02	HLA-C2	7.1	3.1	2.4	2.3	0.1	0.1	0.8	0.9	0.4	0.5	0.7	0.4
C*04:01	HLA-C2	59.4	47.7	40.0	31.4	0.1	0.1	0.4	0.7	0.4	0.2	0.5	0.2
C*02:02	HLA-C2	87.5	81.7	75.0	67.6	0.1	0.2	0.7	2.5	1.3	0.5	2.8	0.4
C*05:01	HLA-C2	100.0	89.9	86.2	78.9	0.1	0.6	1.3	7.8	2.5	0.7	5.6	0.8

B

KIR β2m-KO Jurkat reporter cell lines

721.221 HLA-C cell lines		2DL1 *001	2DL1 *004	2DL1 *020	2DL1 *022	2DL2 *001	2DL2 *003	2DL2 *009	2DL3 *001	2DL3 *002	2DL3 *009	2DL3 *016
721.221		0.2	0.3	0.3	0.1	1.3	0.8	1.1	1.0	1.1	0.8	1.0
C*16:01	HLA-C1	0.6	0.4	0.7	1.0	18.2	19.2	9.4	16.0	28.3	17.0	24.8
C*12:03	HLA-C1	1.3	0.8	1.1	5.2	29.0	18.0	31.8	45.3	58.1	32.1	28.0
C*03:03	HLA-C1	1.0	0.6	0.9	7.2	29.7	38.5	33.9	33.7	42.6	27.3	24.7
C*14:02	HLA-C1	1.2	0.8	1.0	1.7	40.1	36.5	48.1	37.6	41.8	23.5	36.1
C*07:02	HLA-C1	0.9	0.6	0.9	31.8	47.1	43.3	46.4	38.5	47.8	36.1	33.9
C*03:04	HLA-C1	0.8	0.6	0.7	4.1	36.1	43.7	45.1	40.8	48.6	34.4	30.6
C*01:02	HLA-C1	1.2	0.8	1.1	3.7	46.6	54.7	53.1	47.0	60.1	39.4	38.3
C*07:01	HLA-C1	1.6	1.1	1.1	46.5	67.0	78.2	85.5	71.0	100.0	69.9	64.6
C*06:02	HLA-C2	8.0	12.2	14.5	0.4	3.8	2.9	2.5	3.5	2.9	2.9	2.7
C*05:01	HLA-C2	14.3	21.1	17.2	0.2	18.9	13.2	11.8	9.8	11.2	7.3	13.3
C*02:02	HLA-C2	16.0	26.7	16.3	0.3	4.7	4.1	3.8	2.3	1.7	1.5	2.6
C*04:01	HLA-C2	19.4	25.5	21.9	0.3	18.0	13.1	14.8	10.2	13.4	5.5	10.9

C

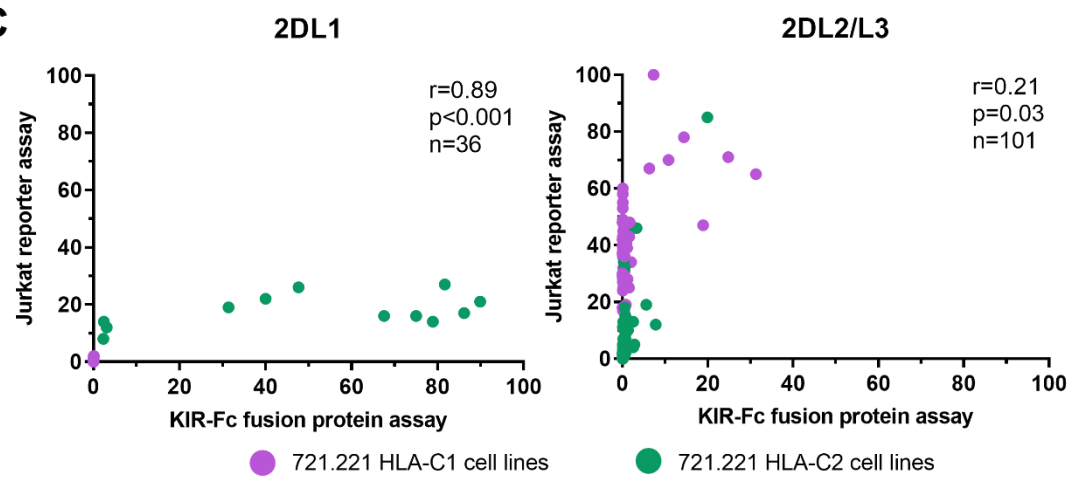

Figure 30: Comparison and correlation of KIR2DL-Fc fusion protein assays and KIR2DL β2m-KO Jurkat reporter cell assays. A Matrix of KIR2DL-Fc fusion protein assays with HLA-C1 and HLA-C2 expressing 721.221 cell lines. **B** Matrix of KIR2DL β2m-KO Jurkat reporter cell assays with HLA-C1 and HLA-C2 expressing 721.221 cell lines. **C** Correlation analysis of KIR2DL-Fc fusion protein assays and KIR2DL β2m-KO Jurkat reporter cell assay with HLA-C1 (purple) and HLA-C2 (green) expressing 721.221 cell lines. Correlations were evaluated using Spearman's rank correlation test.

5.7 Assessment of the activity of KIR2DL$^+$ NK cells

5.7.1 Functional assessment of NK cells expressing inhibitory receptors for self-HLA class I

To achieve functional maturation and self-tolerance towards healthy host cells, NK cells possess a fine-tuning mechanism known as NK cell education in which specific inhibitory receptors interact with self-HLA class I molecules (Anfossi *et al.*, 2006). To analyze the functional impact of NK cells that express inhibitory receptors for self-HLA class I molecules, NK cells isolated from buffy coats were incubated with HLA class I deficient 721.221 cells. NK cell degranulation was assessed with CD107a expression using flow cytometry (**Figure 31**). For NK cell degranulation, median percentage of CD107a$^+$ NK cells and median percentage points (p.p.) of CD107a$^+$ NK cells normalized to NK cells without target cells and NK cells without inhibitory receptors were used as readouts.

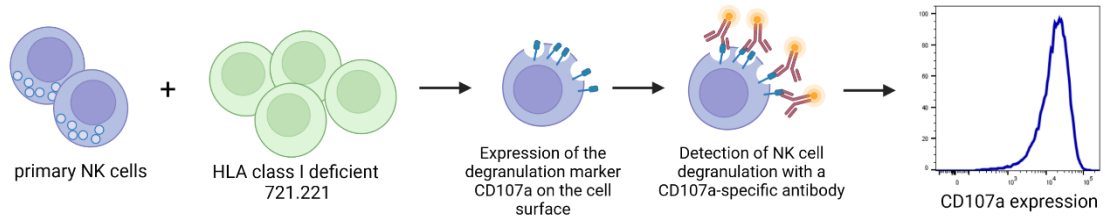

Figure 31: Work flow for CD107a degranulation assay. Primary NK cells were isolated from buffy coats and used for a co-culture with 721.221. NK cell degranulation was assessed with a CD107a-specific antibody and measured via flow cytometry.

Co-cultures of NK cells with 721.221 cells induced high CD107a expression within NK cells (23.6%) in comparison to NK cells incubated without target cells (1.5%) as displayed in **Figure 32A**. NK cells that did not express any of these inhibitory receptors (11.6%) were less responsive to 721.221 than NK cells that expressed inhibitory receptors (**Figure 32B**). NK cells that are single$^+$ for KIR2DL1 (16.2%), KIR2DL2/L3 (18.4%) or KIR3DL1 (18.2%) showed comparable surface expression of CD107a when exposed to 721.221. NKG2A single$^+$ NK cells (26.5%) expressed the highest amount of CD107a in the degranulation assays. Moreover, analysis of uneducated and educated NK cell subsets was performed (**Figure 32C**). The frequency of CD107a$^+$ NK cells single$^+$ for KIR2DL1, KIR2DL2/L3, KIR3DL1 and NKG2A in the presence and absence of their respective HLA class I ligand was assessed and normalized to NK cells alone and NK cells without inhibitory receptors (iRec). Educated NK cells were significantly more responsive to 721.221 than uneducated NK cells. KIR2DL1 single$^+$ NK cells from HLA-C2 heterozygous or homozygous donors expressed CD107a on their cell surface when exposed to 721.221 (C2+: 11.4%, C2-: 0.44%, p=0.0002). In line with that, KIR2DL2/L3 single$^+$ NK cells from HLA-C1

expressing donors (C1+: 11.5%, C1-: 0.44%, p=0.002) and KIR3DL1 single$^+$ NK cells from Bw4$^+$ donors (Bw4+: 16.0%, Bw4-: 1.2%, p=0.001) were highly responsive towards 721.221 cells. NKG2A single$^+$ NK cells showed the highest frequency of CD107a$^+$ NK cells (18.5%). In contrast, uneducated NK cells did not degranulate when co-cultured with 721.221 cells. Taken together, co-culture experiments of HLA class I deficient 721.221 cells and primary NK cells induced an overall high degranulation of educated NK cells in comparison to uneducated NK cells.

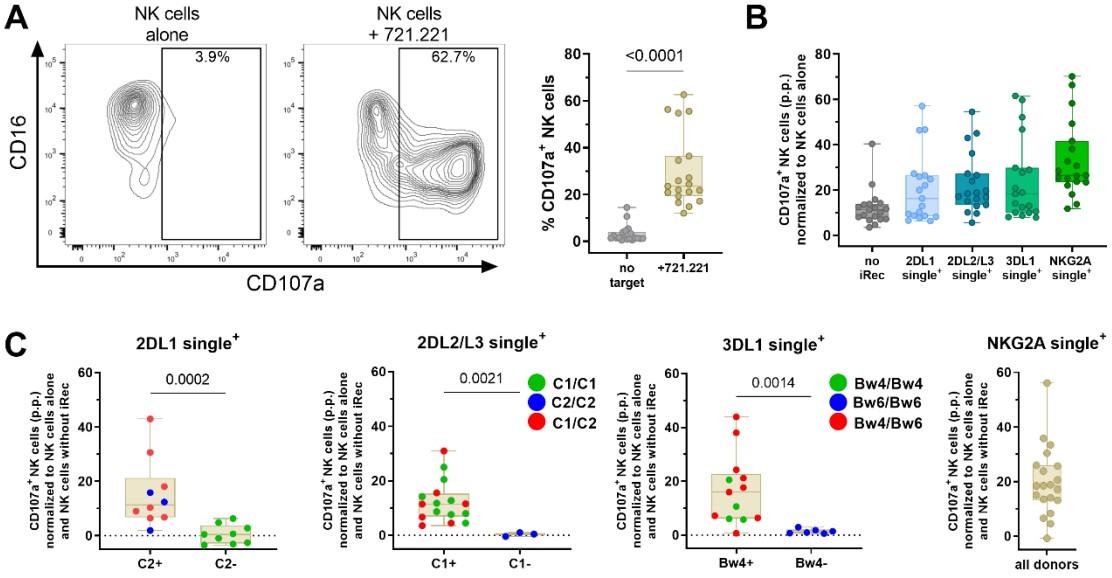

Figure 32: Functional assessment of educated and uneducated NK cells. NK cells were isolated from buffy coats and co-cultured with HLA class I deficient 721.221 for 5 h. **A** Co-culture of NK cells without targets and with 721.221 (n=19). Histograms show CD107a expression of NK cells with and without 721.221 target cells. Box plots show relative frequency of CD107a$^+$ NK cells after incubation without target cells and with 721.221. **B** Comparison of CD107a frequency of NK cells that are single$^+$ for inhibitory receptors that recognize HLA class I molecules (KIR2DL1, KIR2DL2/L3, KIR3DL1, NKG2A) and NK cells without inhibitory receptors (iRec) after 721.221 exposure. Box plots show relative frequency of CD107a$^+$ NK cells normalized to NK cells without target cells. **C** Comparison of CD107a frequency of educated and uneducated NK cells after 721.221 exposure. Box plots show relative frequency of CD107a$^+$ NK cells normalized to CD107a frequency of NK cells without targets and NK cells without iRec. Box plots represent the median and 25%/75% percentile. Each dot represents one donor (n=19). For statistical analysis, Mann-Whitney test was used to check for differences between educated and uneducated NK cells.

5.7.2 Assessment of the anti-HIV-1 activity of KIR2DL$^+$ NK cells

To assess the anti-HIV-1 activity of KIR2DL$^+$ NK cells, primary CD4 T cells were infected with the HIV-1 strain JRCSF wt, a HIV-1 strain that strongly downregulates HLA-C on infected cells, or a JRCSF Vpu mutant (Vpu mut) that lacks the ability to downregulate HLA-C on infected cells (Körner *et al.*, 2017). Uninfected and infected CD4 T cells, as well as 721.221 cells were co-cultured with autologous NK cells and NK cell activity was assessed with the CD107a degranulation marker. Moreover, NK cells were stained for a number of NK cell markers, including KIR2DL receptors. **Figure 33** illustrates the work flow for the CD107a degranulation assay of NK cells with HIV-1 infected CD4 T cells.

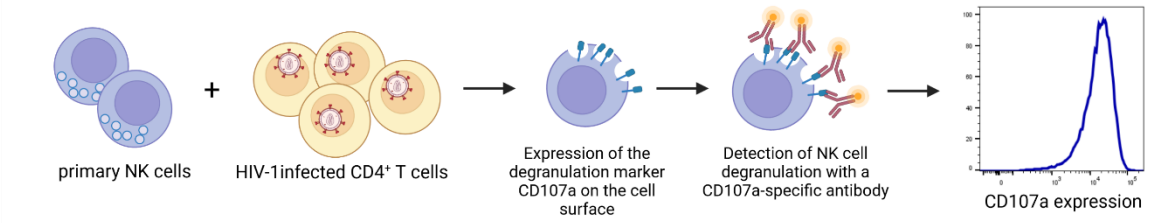

Figure 33: Work flow for CD107a degranulation assays of NK cells with HIV-1 infected CD4 T cells. Primary NK cells and CD4 T cells were isolated and CD4 T cells were infected with HIV-1 JRCSF wt or JRCSF Vpu mut. CD107a degranulation assays were performed with NK cells and autologous HIV-1 infected CD4 T cells and degranulation of NK cells was assessed with a CD107a-specific antibody and measured via flow cytometry.

5.7.2.1 Enrichment of CD4 depleted and HIV-1 infected CD4 T cells and surface expression of HLA-C on HIV-1 infected CD4 T cells

Since HIV-1 infection induces a downregulation of CD4 on the surface of infected cells, HIV-1 infected cells were enriched using a CD4 selection kit. HIV-1 infection of CD4 T cells was confirmed with an intracellular staining with a HIV Gag p24-specific antibody. Moreover, the cells were stained for CD4 and HLA-C surface expression (**Figure 34A**). Uninfected CD4 T cell population were defined as CD4+/p24- and infected CD4 T cells were defined as CD4-/p24+. The full gating strategy of HIV-1 infected CD4 T cells is provided in the methods. Infections with JRCSF wt were generally more effective (median percentage of $p24^+$ cells: 5.7%) than infections with JRCSF Vpu mut (median percentage of $p24^+$ cells: 3.0%) (**Figure 34B**). Enrichment of $CD4^-$ T cells increased the frequency of $p24^+$ cells in JRCSF wt (median percentage of $p24^+$ cells: 28.8%) and JRCSF Vpu mut (median percentage of $p24^+$ cells: 9.6%) infections. Analysis of HLA-C expression verified that JRCSF wt infected CD4 T cells (MFI of HLA-C: 199.5) expressed lower levels of HLA-C compared to CD4 T cells infected with JRCSF Vpu mut (MFI of HLA-C: 656.0) and that JRCSF strongly downregulated HLA-C on CD4 T cells compared to the JRCSF Vpu mut (MFI of HLA-C: 20.8 vs. 6.8), which also showed a weak downregulation of HLA-C (**Figure 34C**).

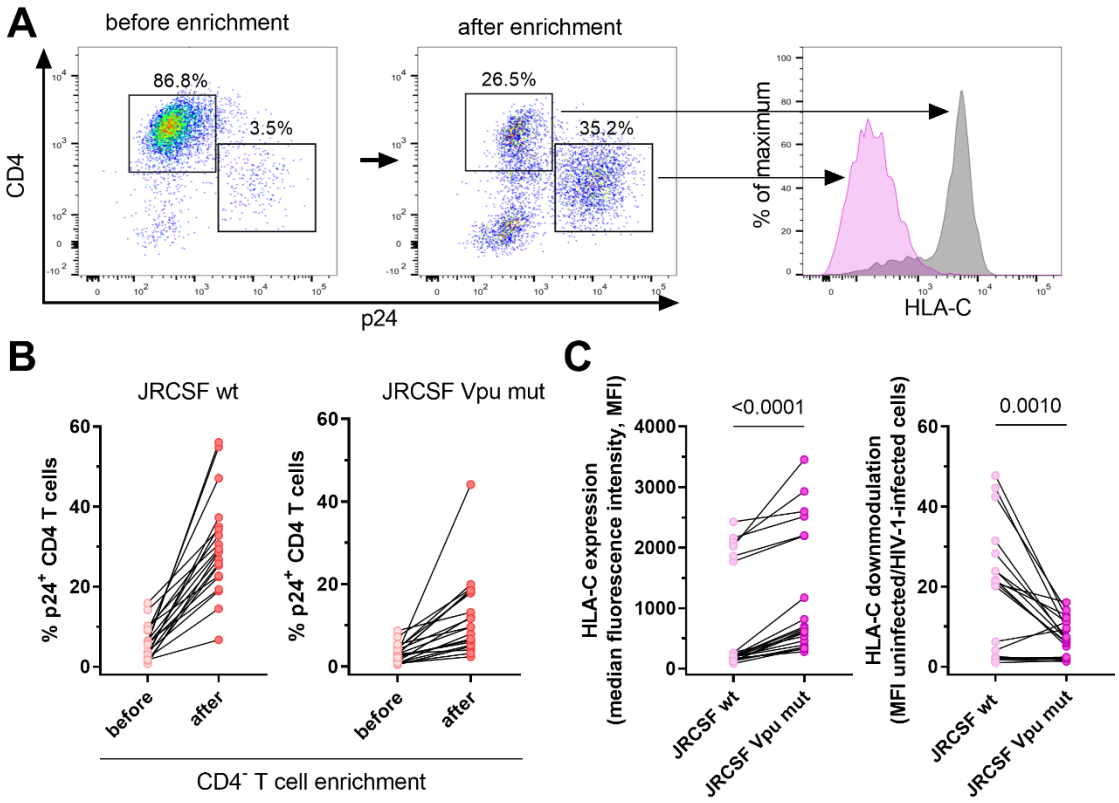

Figure 34: HIV-1 infection of CD4 T cells. CD4 T cells were isolated from buffy coats and infected with HIV-1 JRCSF wt or JRCSF Vpu mut. **A** Representative CD4 and p24 staining of JRCSF wt infected CD4 T cells before and after enrichment of CD4 depleted T cells and histogram of HLA-C expression of uninfected (CD4+/p24-) and infected (CD4-/p24+) cells. **B** Percentages of $p24^+$ JRCSF wt and JRCSF Vpu mut infected CD4 T cells before and after $CD4^-$ T cell enrichment (n=20). **C** HLA-C expression and downmodulation of JRCSF wt and JRCSF Vpu mut infected CD4 T cells (n=20). For statistical analysis, Mann-Whitney test was used to check for differences between before and after $CD4^-$ T cell enrichment and JRCSF wt and JRCSF Vpu mut.

5.7.2.2 CD107a degranulation assay of NK cells with HIV-1 infected CD4 T cells

To assess the anti-HIV-1 activity of NK cells, NK cells were incubated with and without target cells, including uninfected CD4 T cells (mock), JRCSF wt or JRCSF Vpu mut infected CD4 T cells and 721.221 cells, using median percentage of $CD107a^+$ NK cells as a readout (**Figure 35A**). NK cells that were incubated without target cells only showed a low percentage of CD107a expression (1.5%). In contrast, co-culture of NK cells with HLA class I deficient 721.221 induced a high frequency of CD107a (23.6%). Incubation of NK cells with autologous HIV-1 infected CD4 T cells induced CD107a expression (JRCSF wt: 9.2%; JRCSF Vpu mut: 10.1%), however co-culture with uninfected CD4 T cells induced comparable frequencies of CD107a (9.8%) in NK cells (**Figure 35B**). CD107a frequency was also analyzed in educated and uneducated NK cell subsets after co-culture with HIV-1 JRCSF wt and HIV-1 JRCSF Vpu mutant infected CD4 T cells (**Figure 35C/D**). Therefore, $CD107a^+$ NK cells that were $single^+$ for one of the inhibitory receptors (KIR2DL1, KIR2DL2/L3, KIR3DL1 and NKG2A) were normalized to NK cells alone and NK cells without inhibitory receptors (iRec). Higher frequencies of CD107a in educated NK cells compared

to uneducated NK cells, as seen for co-cultures with HLA class I deficient 721.221 cells (**Figure 32**), were not observed for NK cells that were co-cultured with HIV-1 infected CD4 T cells. Only KIR3DL1 educated NK cells with HIV-1 JRCSF wt infected CD4 T cells showed a trend towards higher CD107a frequencies (p=0.08). NKG2A single$^+$ NK cells showed higher frequencies of CD107a$^+$ NK cells compared to inhibitory KIR single$^+$ NK cells. In summary, co-culture experiments of HIV-1 infected and uninfected CD4 T cells with primary NK cells induced degranulation to equal levels. Differences in degranulation between educated and uneducated NK cell subsets were not observed.

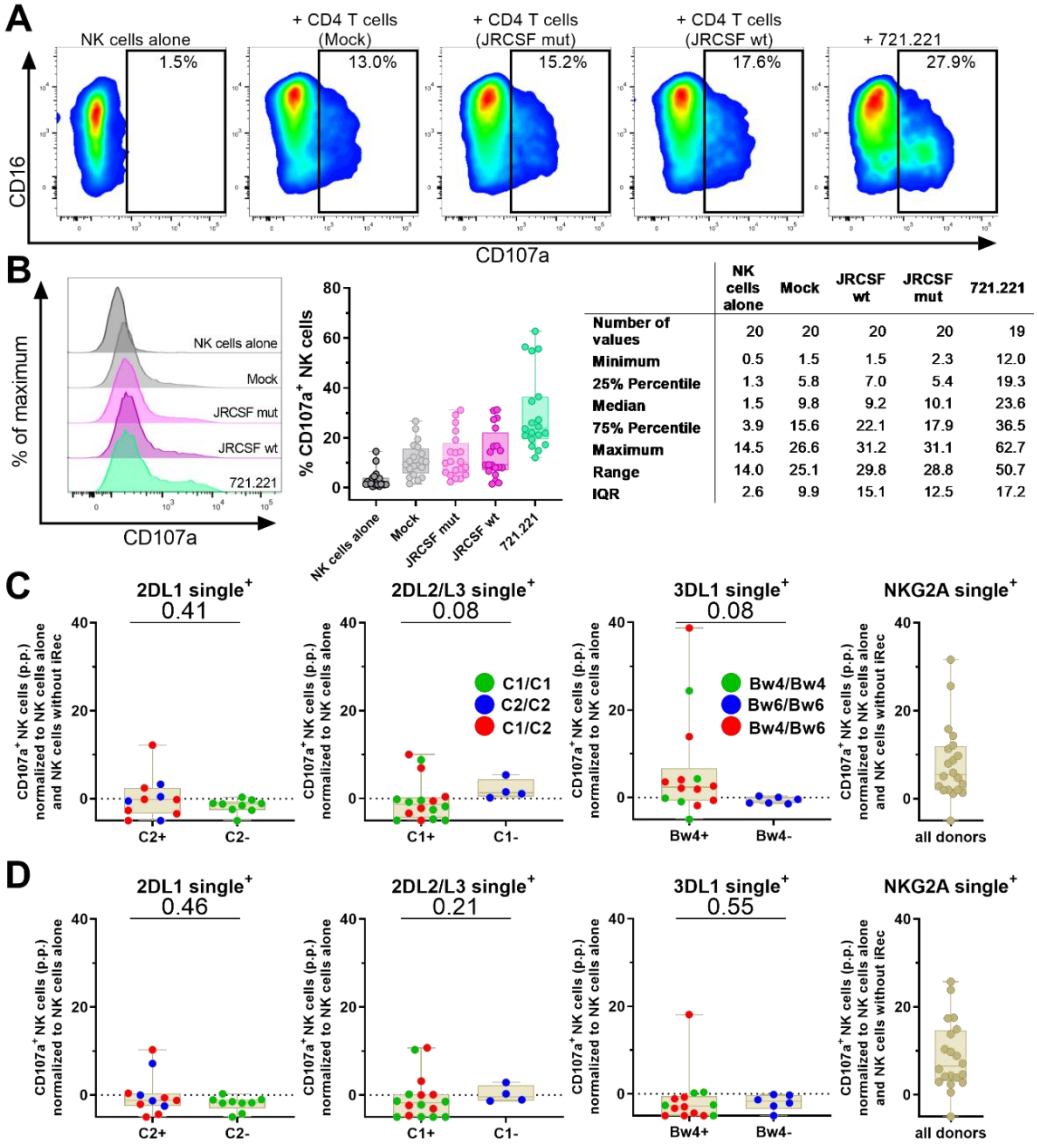

Figure 35: CD107a degranulation assay of NK cells with HIV-1 infected CD4 T cells. A Representative plot of CD107a expression of NK cells without and with target cells (Mock, JRCSF wt, JRCSF Vpu mut and 721.221). **B** Representative histogram of CD107a expression of NK cells with and without target cells, relative frequency of CD107a$^+$ NK cells for all performed CD107a assays and descriptive statistics. **C** Comparison of the frequency of CD107a$^+$ educated and uneducated NK cells after exposure to HIV-1 JRCSF wt infected CD4 T cells. Box plots show relative frequency of CD107a$^+$ NK cells normalized to NK cells without targets and NK cells without iRec. **D** Comparison of CD107a$^+$ educated and uneducated NK cells after exposure to HIV-1 JRCSF Vpu mut infected CD4 T cells. Box plots show relative frequency of CD107a$^+$ NK cells normalized to NK cells without targets and NK cells without iRec. Box plots represent the median and 25%/75% percentile. Each dot represents one donor (n≥19). For statistical analysis, Mann-Whitney test was used to check for differences between educated and uneducated NK cells.

To assess the impact of the KIR2DL/HLA-C interaction on the anti-HIV-1 response of NK cells, CD4 T cells from two donors with strong HLA-C2/KIR2DL1 binding affinity and two donors with weak HLA-C2/KIR2DL1 binding affinity were infected with the lab-adapted HIV-1 strain NL4-3 and a CD107a degranulation assay was performed after 4 days of infection (**Figure 36**). The degranulation assay revealed a high frequency of $CD107a^+$ NK cells from donors with weak HLA-C2/KIR2DL1 binders (median: 22.95%) in comparison to the donors with strong HLA-C2/KIR2DL1 combinations (median: 13.25%). In summary, degranulation assays of NK cells with HIV-1 infected and uninfected CD4 T cells showed that NK cells strongly degranulate in the presence of HLA class I deficient 721.221 cells, whereas NK cells that were incubated without target cells expressed only low levels of the degranulation marker CD107a. Moreover, uninfected and HIV-1 infected CD4 T cells induced CD107a expression to comparable amounts independent from their inhibitory receptor expression. Binding affinities of HLA-C and KIR2DL could have a potential impact on NK cell degranulation but needs to be further investigated.

Donor	binding	HLA-C2 allele	HLA-C1 allele	KIR2DL1 allele
1	strong	**04:01**	07:01	*003/*034+*004/*035|*003/*034+*035|*006+*010
2	strong	**04:01**	03:CEJXD	*001/*002*004/*035
3	weak	**06:02**	01:02	*001/*002+*003/*035
4	weak	**06:02**	03:DJUJX	*001/*002+*003/*034

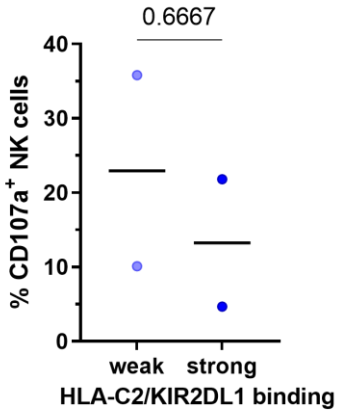

Figure 36: CD107a degranulation assay of donors with strong and weak binding combination of HLA-C2 and KIR2DL1. Table displays the HLA-C and KIR2DL1 allotypes of the donors. Scatter plot displays relative frequency of $CD107a^+$ NK cells for weak and strong HLA-C2/KIR2DL1 combinations and median for each group. For statistical analysis, Mann-Whitney test was used to check for differences between weak and strong combinations.

5.8 Phenotypic characterisation of NK cells from untreated HIV-1$^+$ individuals

To assess the impact of KIR2DL/HLA-C allotype combinations on the NK cell repertoire of HIV-1$^+$ individuals, multi-parameter flow cytometry was performed to profile NK cell receptor expression on untreated HIV$^+$ individuals and healthy controls (**Figure 37**). Receptor frequency on NK cells was assessed as median percentage.

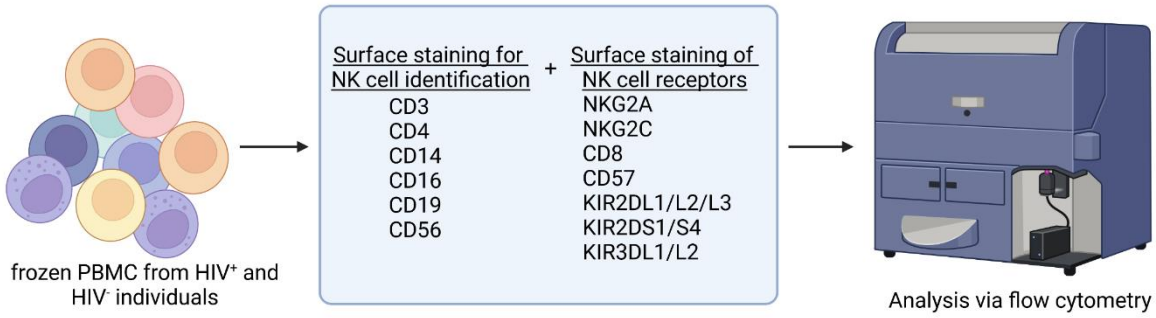

Figure 37: Workflow for NK phenotypic characterisation of NK cells from untreated HIV-1$^+$ individuals. Frozen PBMCs were thawed and stained for various marker for NK cell identification and NK cell receptor expression.

5.8.1 Phenotypic characterisation of bulk NK cells

The phenotypic characterisation of bulk NK cells (**Figure 38**) revealed a decreased frequency of NK cells expressing the inhibitory NKG2A receptor (HIV-1$^+$:42.5%, n=122; healthy control: 54.4%, n=60; p<0.0001) and an increased frequency of NK cells carrying the activating NKG2C receptor (HIV-1$^+$:23.5%, n=122; healthy control: 3.5%, n=60; p<0.0001) in HIV-1$^+$ individuals. Moreover, CD8 (HIV-1$^+$:18.9%, n=122; healthy control: 32.3%; n=60; p<0.0001) on NK cells of HIV-1$^+$ individuals was decreased whereas CD57 (HIV-1$^+$:36.7%, n=122; healthy control: 31.5%, n=60; p=0.05) was increased. Analysis of inhibitory KIR2DL receptors showed no different frequency for KIR2DL1 (HIV-1$^+$: 17.0%, n=118; healthy control: 15.0%, n=59; p=0.22) and KIR2DL2/L3 (HIV-1$^+$:26.3%, n=122; healthy control: 27.0%, n=60; p=0.41). However, separate examination of KIR2DL2 and KIR2DL3 expression showed a higher frequency of KIR2DL2$^+$ cells (HIV-1$^+$:17.5%, n=64; healthy control: 12.1%, n=28; p=0.018) and a lower frequency of KIR2DL3$^+$ cells (HIV-1$^+$:15.3%, n=111; healthy control: 20.7%, n=55; p=0.018). Moreover, the activating receptors KIR2DS1 (HIV-1$^+$: 9.9% n=47; healthy control: 14.8%, n=26; p=0.012) and KIR2DS4 (HIV-1$^+$: 26.5%, n=25; healthy control: 41.6%, n=18; p=0.012) displayed a decreased frequency on NK cells of HIV-1$^+$ individuals compared to healthy control individuals. KIR3DL1 frequency (HIV-1$^+$: 13.3%, n=108; healthy control: 16.2%, n=55; p=0.09) did not differ between HIV-1$^+$ individuals and the healthy control group but KIR3DL2 (HIV-1$^+$: 19.7% n=122; healthy control: 13.4%, n=60; p<0.001) was increased in HIV-1$^+$ individuals. **Table 3** summarizes the descriptive and comparative statistics of all analyzed NK cell markers for HIV-1$^-$ and HIV-1$^+$ individuals.

Table 3: Descriptive statistics of analysed receptors on bulk NK cells.

	HIV-	HIV+	HIV-	HIV+	HIV-	HIV+		
receptor	**n**	**n**	**median (25%/75% percentile)**	**median (25%/75% percentile)**	**Min/Max**	**Min/Max**	**p value**	**Adjusted p value**
NKG2A	60	122	54.4 (45.28/64.25)	42.50 (31.65/53.48)	17.2/81.8	6.44/81.9	<0.0001	<0.0001
NKG2C	60	122	3.47 (1.63/5.54)	23.45 (11.03/84.8)	0.1/56.3	0.1/84.8	<0.0001	<0.0001
CD8	60	122	32.3 (24.58/42.2)	18.9 (13.58/26.13)	5.74/57.9	2.34/55.1	<0.0001	<0.0001
CD57	60	122	31.5 (20.2/42.33)	36.7 (23.55/49.25)	8.85/63.6	6.14/84.4	0.048	0.043
KIR2DL1	59	118	15.0 (12.4/19.4)	17.0 (9.22/31.75)	3.55/56.7	1.6/85.8	0.301	0.221
KIR2DS1	26	47	14.75 (10.6/19.43)	9.86 (6.98/17.1)	6.18/34.6	0.04/43.6	0.009	0.012
KIR2DL2/L3	60	122	27.0 (19.35/32.23)	26.3 (18.7/37.35)	12.9/67.6	3.3/77.3	0.616	0.414
KIR2DL2	28	64	12.1 (7.49/18.73)	17.5 (10.63/28.5)	0.1/32.9	0.1/68.7	0.018	0.018
KIR2DL3	55	111	20.7 (13.7/23.9)	15.3 (9.6/24.4)	8.2/41.3	0.3/61.3	0.016	0.018
KIR2DS4	18	25	41.85 (29.68/45.88)	26.5 (12.85/38.6)	20.6/63.8	0.3/60.7	0.009	0.012
KIR3DL1	55	108	16.2 (11.1/23.9)	13.25 (7.8/19.68)	0.2/69.8	0.1/51.0	0.106	0.086
KIR3DL2	60	122	13.4 (7.83/19.2)	19.65 (12.48/28.75)	2.96/34.7	0.48/78.9	<0.0001	<0.001

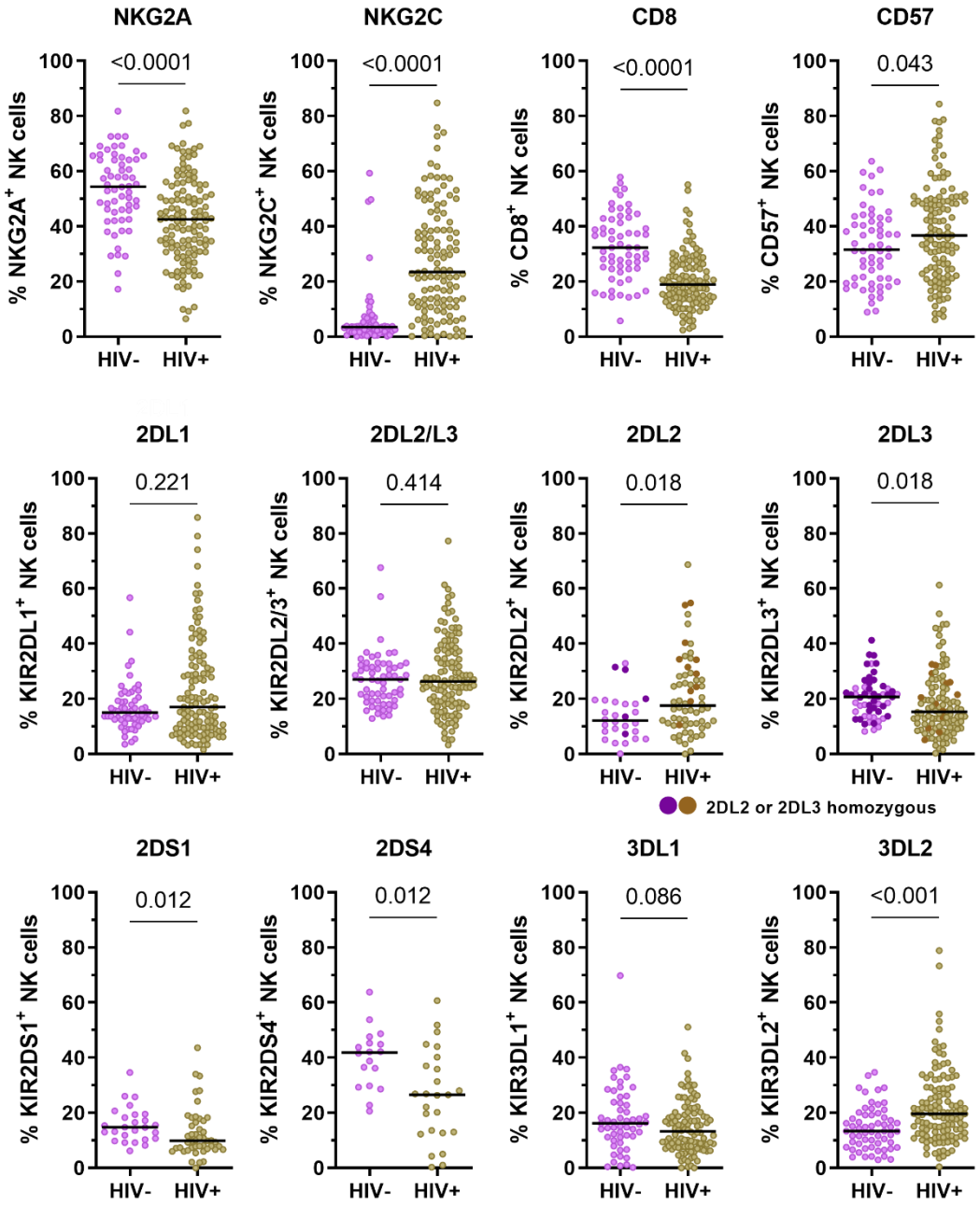

Figure 38: Phenotypic characterisation of NK cells of HIV-1⁻ (HIV-) and HIV-1⁺ (HIV+) individuals. PBMCs from HIV-1⁻ (n=60) and HIV-1⁺ (n=122) individuals were thawed, stained and analyzed via flow cytometry. NK cells were identified as CD3, CD14 and CD19 negative and positive for CD16 and/or CD56. Frequency of following NK cell receptors was analyzed: NKG2A, NKG2C, CD8, CD57, KIR2DL1-3, KIR2DS1/S4 and KIR3DL1/L2. Scatter plots display frequency of NK cell receptor expression in HIV-1⁻ and HIV-1⁺ individuals and median for each group. For statistical analysis, Mann-Whitney test was used to check for differences between HIV-1⁻ and HIV-1⁺ individuals. P values were adjusted for multiple comparisons (Benjamini/Krieger/Yekutieli).

5.8.2 Phenotypic characterisation of CD56 subpopulations

As HIV-1 infection has been associated with altered CD56 subset distribution (Björkström *et al.*, 2010), bulk NK cells of HIV-1$^+$ and HIV-1$^-$ individuals were further analyzed based on their CD56 expression into CD56 negative, dim and bright (**Figure 39**). The detailed analysis of the median percentage of CD56 NK cell subsets displayed a significantly reduced frequency of CD56 bright NK cells within HIV-1-infected individuals (HIV-1$^+$: 3.6%; healthy control: 6.2%, p<0.0001) and a significantly increased population of CD56 negative NK cells (HIV-1$^+$: 9.0%; healthy control: 4.5%, p<0.0001) in HIV-1$^+$ individuals compared to a HIV-1$^-$ individuals. The frequency of CD56 dim NK cells (HIV-1$^+$: 86.9%; healthy control: 88.1%, p=0.08) did not differ. Because of the different frequencies of CD56 NK cell subsets within HIV-1$^+$ and HIV-1$^-$ individuals, the expression of the KIR2D1, KIR2DL2, KIR2DL3, KIR2DL2/L3, KIR2DS1, KIR2DS4, KIR3DL1, KIR3DL2, CD8, CD57, NKG2A and NKG2C was analyzed separately for each of the CD56 NK cell subsets (bright, dim, negative) (**Figure 40**). The statistical analysis revealed significant differences in the CD56 NK cell subsets for all assessed marker expression between HIV-1$^-$ and HIV-1$^+$ individuals. KIR2DL1-3 and KIR2DS1 expression was significantly increased in CD56 bright NK cells in HIV-1$^+$ individuals. In addition, KIR2DL3 frequency was decreased in CD56 dim NK cells and KIR2DS1 and KIR2DS4 expression was reduced in dim and negative CD56 subsets of HIV-1$^+$ individuals. CD56 bright NK cells of HIV-1$^+$ individuals had an increased frequency of KIR3DL1, whereas KIR3DL1 was increased in CD56 dim and CD56 negative NK cell subsets of HIV-1$^+$ individuals. NKG2C showed an increased frequency in HIV-1$^+$ individuals, but NKG2A and CD8 were decreased in all three CD56 NK cell subsets. In addition, CD57 was only significantly increased in HIV-1$^+$ individuals in CD56 bright and CD56 negative NK cells. **Table 4** summarizes the descriptive analysis (median, 25%/75% percentile) and adjusted p values for all eleven NK cell receptors in the CD56 bright, dim and negative NK cell subsets for HIV-1$^-$ and HIV-1$^+$ individuals.

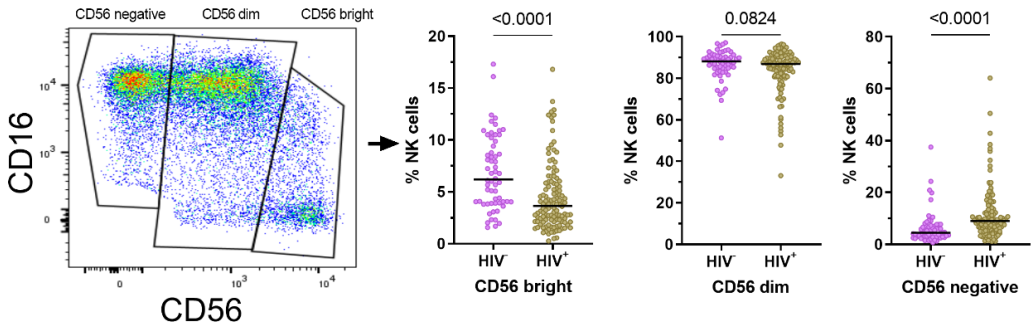

Figure 39: Differentiation of CD56 NK cell subsets in HIV-1$^-$ and HIV-1$^+$ individuals. Gating strategy for flow cytometry analyses of CD56 NK cell subsets. NK cells were identified as CD3, CD14 and CD19 negative and positive for CD16 and/or CD56. NK cell subsets were further identified based on CD56 expression as CD56 negative, CD56 dim and CD56 bright. Comparison of the percentage of bulk NK cells and the three subsets in HIV-1$^-$ (n=60) and HIV-1$^+$ (n=122) individuals. For statistical analysis, Mann-Whitney test was used to check for differences between HIV-1$^-$ and HIV-1$^+$ individuals.

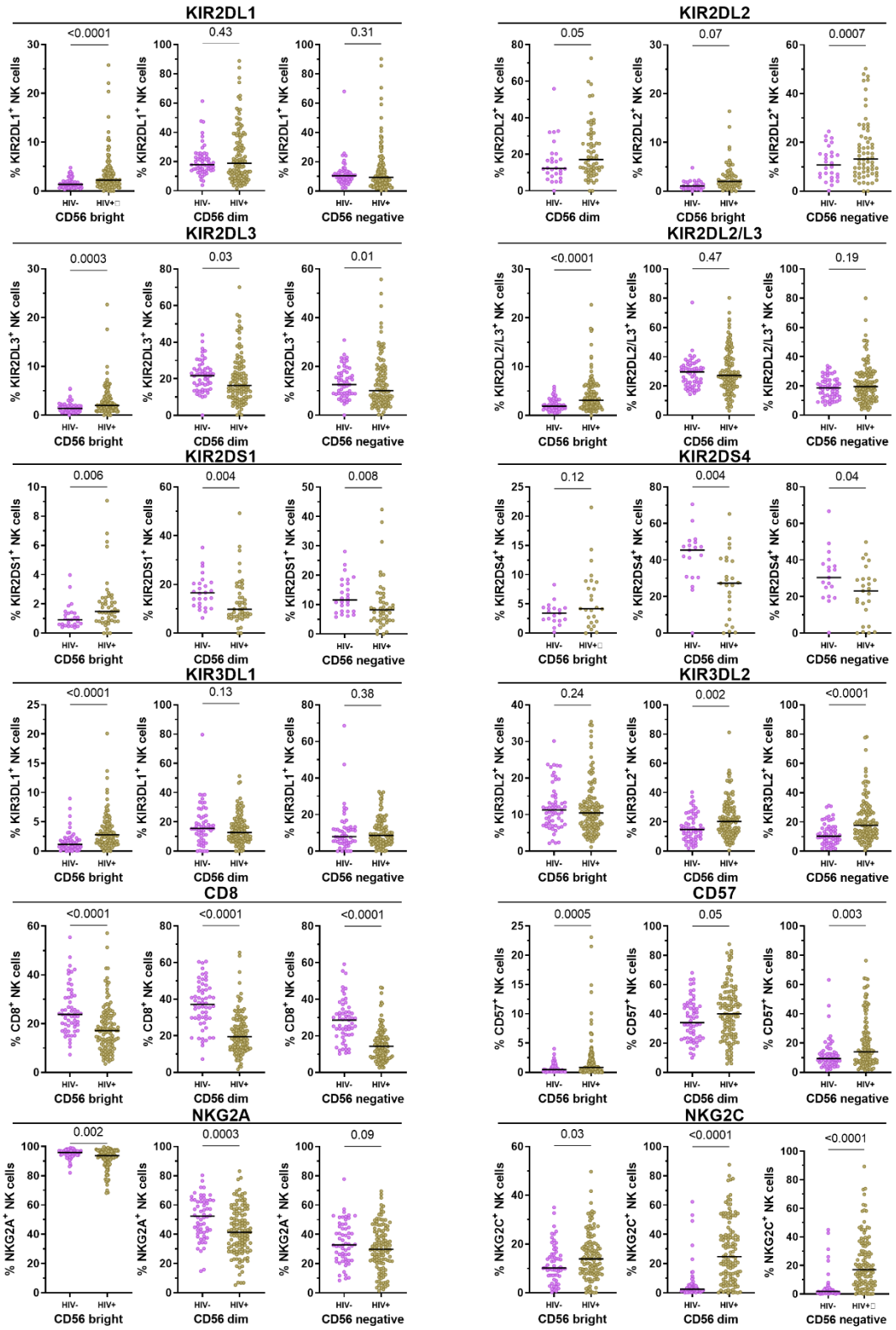

Figure 40: Phenotypic characterisation of CD56 NK cell subsets of HIV-1$^-$ (HIV-) and HIV-1$^+$ (HIV+) individuals. PBMCs from HIV-1$^-$ (n=60) and HIV-1$^+$ (n=122) individuals were thawed, stained and analyzed via flow cytometry. NK cells were identified as CD3, CD14 and CD19 negative and positive for CD16 and/or CD56. NK cell subsets were further identified based on CD56 expression as CD56 negative, CD56 dim and CD56 bright. Expression of following NK cell markers was analysed: NKG2A, NKG2C, CD8, CD57, KIR2DL1-3, KIR2DS1/S4 and KIR3DL1/L2. Scatter plots display frequency of NK cell receptor expression in HIV-1$^-$ and HIV-1$^+$ individuals for all three CD56 subsets and median for each group. For statistical analysis, Mann-Whitney test was used to check for differences between HIV-1$^-$ and HIV-1$^+$ individuals. P values were adjusted for multiple comparisons (Benjamini/Krieger/Yekutieli).

Table 4: NK cell marker expression on CD56 subsets.

			CD56^{Bright}			CD56^{Dim}			CD56^{Negative}		
	HIV-	HIV+	HIV-	HIV+		HIV-	HIV+		HIV-	HIV+	
receptor	**n**	**n**	**median (25%/75% percentile)**	**median (25%/75% percentile)**	**p value***	**median (25%/ 75% percentile)**	**median (25%/ 75% percentile)**	**p value***	**median (25%/ 75% percentile)**	**median (25%/ 75% percentile)**	**p value***
NKG2A	60	122	95.9 (94.1/97.1)	93.7 (89.7/96.9)	0.002	52.5 (41.3/63.2)	41.4 (29.6/54.7)	0.0003	32.9 (23.4/45.3)	29.9 (20.6/42.7)	0.09
NKG2C	60	122	10.2 (7.1/15.9)	14.0 (8.0/20.1)	0.03	2.6 (1.7/5.4)	24.9 (11.0/42.0)	<0.0001	1.8 (1.0/3.4)	17.1 (6.9/33.9)	<0.0001
CD8	60	122	23.8 (18.7/31.1)	17.2 (11.0/23.3)	<0.0001	37.1 (29.4/45.8)	19.5 (13.3/28.0)	<0.0001	28.6 (20.7/33.1)	14.3 (8.4/19.2)	<0.0001
CD57	60	122	0.5 (0.2/1.0)	0.8 (0.4/2.2)	0.0005	34.2 (23.4/46.2)	40.2 (26.0/52.9)	0.05	9.5 (6.4/13.8)	14.0 (7.5/27.1)	0.003
KIR2DL1	59	118	1.4 (0.8/1.9)	2.2 (1.2/4.0)	<0.0001	17.9 (14.2/23.6)	18.9 (9.9/36.8)	0.43	10.4 (7.7/13.1)	9.3 (4.4/17.7)	0.31
KIR2DS1	26	47	0.9 (0.6/1.4)	1.5 (0.8/2.4)	0.006	16.5 (11.2/20.5)	9.8 (6.8/18.5)	0.004	11.6 (7.7/17.5)	8.2 (4.7/12.6)	0.008
KIR2DL2/L3	60	122	1.9 (1.5/2.9)	3.2 (1.8/6.1)	<0.0001	29.7 (21.2/33.8)	27.2 (20.0/39.0)	0.47	18.6 (12.6/24.0)	19.6 (12.3/28.1)	0.19
KIR2DL2	28	64	1.1 (0.6/1.9)	2.0 (1.1/3.4)	0.0007	12.3 (8.3/19.6)	17.2 (10.8/29.8)	0.05	10.8 (5.8/15.8)	13.2 (7.6/22.3)	0.07
KIR2DL3	55	111	1.4 (0.8/1.9)	2.0 (1.1/3.5)	0.0003	21.7 (14.4/25.5)	16.4 (10.1/26.3)	0.03	12.6 (8.8/17.6)	10.1 (6.1/18.9)	0.01
KIR2DS4	19	25	3.4 (2.1/4.3)	4.2 (1.9/8.8)	0.12	45.4 (30.5/49.7)	27.3 (10.3/40.3)	0.004	30.4 (20.1/37.9)	23.1 (8.2/29.8)	0.04
KIR3DL1	55	108	1.2 (0.6/2.0)	2.8 (1.5/4.3)	<0.0001	15.5 (9.0/24.0)	12.8 (8.0/20.4)	0.13	8.0 (4.7/12.6)	8.6 (5.1/14.1)	0.38
KIR3DL2	60	122	11.3 (7.3/15.0)	10.5 (6.9/13.8)	0.24	14.9 (9.0/22.9)	20.4 (13.2/29.2)	0.002	10.4 (6.4/16.6)	17.6 (10.5/27.1)	<0.0001

* p values were adjusted for multiple comparison (Benjamini/Krieger/Yekutieli).

5.8.3 Stratification of KIR2DL1-3$^+$ NK cells by *HLA-C* genotypes

For a more detailed analysis of KIR2DL1-3 expression patterns, healthy and HIV-1 infected individuals were divided by their *HLA-C* genotype. Therefore, individuals were grouped in C1 homozygous (C1/C1), C1/C2 heterozygous (C1/C2) and C2 homozygous (C2/C2) (**Figure 41**). Stratification along *HLA-C* genotypes revealed significant differences in KIR2DL1$^+$ NK cell frequency between C2- and C2+ HIV-1$^+$ individuals towards an increased frequency of KIR2DL1$^+$ NK cells with increased number of HLA-C2 alleles (C1/C1: 14.8%, C1/C2: 20.1%, C2/C2: 34.75%; p<0.0001), whereas HIV-1$^-$ individuals showed no significant differences in relative KIR2DL1 expression between different *HLA-C* genotypes (C1/C1: 13.3%, C1/C2: 15.5%, C2/C2: 16.35%; p=0.163). Moreover, stratification of *HLA-C* genotypes revealed no different proportion of KIR2DL2/L3$^+$ NK cells in HIV-1$^-$ (C1/C1: 26.4%, C1/C2: 25.0%, C2/C2: 29.4%; p>0.99) and HIV-1$^+$ individuals (C1/C1: 27.6%, C1/C2: 25.3%, C2/C2: 25.5%; p=0.97). Differentiated analysis of KIR2DL2$^+$ and KIR2DL3$^+$ NK cell frequency for *HLA-C* genotypes displayed also no differences in KIR2DL3 frequency neither in HIV-1$^+$ (C1/C1: 19.6%, C1/C2: 13.1%, C2/C2: 16.8%; p=0.27) nor in HIV-1$^-$ individuals (C1/C1: 21.7%, C1/C2: 21.0%, C2/C2: 17.9%; p=0.57). Only KIR2DL2$^+$ NK cells of HIV-1$^-$ individuals (C1/C1: 8.2%, C1/C2: 12.5%, C2/C2: 18.9%; p=0.04) showed a trend towards an increased frequency in C2+ individuals comparable with KIR2DL1 frequency in HIV-1$^+$ individuals.

In addition, absolute cell numbers of KIR2DL1-3 expressing NK cells in cells/µl were calculated for HIV-1$^+$ individuals based on the flow cytometry NK cell analysis and absolute

CD4 T cell counts then correlated with the relative KIR2DL expression (**Figure 42**). Analysis of absolute cell numbers of KIR2DL$^+$ NK from HIV-1$^+$ individuals (**Figure 42A**) displayed a significant difference in KIR2DL1$^+$ NK cells with an increased number of HLA-C2 alleles (C1/C1: 15 cells/µl, C1/C2: 39 cells/µl, C2/C2: 52 cells/µl; p=0.012), however analysis of absolute KIR2DL2/L3$^+$ as well as KIR2DL2$^+$ and KIR2DL3$^+$ NK cell numbers showed no differences between *HLA-C* genotypes (KIR2DL2/L3: p>99, KIR2DL2: p=0.86, KIR2DL3: p=0.88). Correlation analysis of absolute and relative KIR2DL$^+$ NK cells from HIV-1$^+$ individuals showed a significant positive correlation for KIR2DL1 (r=0.73, p<0.0001), KIR2DL2/L3 (r=0.54, p<0.0001), KIR2DL2 (r=0.46, p=0.0002) and KIR2DL3 (r=0.67, p<0.0001) (**Figure 43B**). In summary, relative frequencies of KIR2DL$^+$ NK cells and absolute KIR2DL$^+$ NK cell numbers are comparable and revealed the same results for KIR2DL$^+$ NK cell expression in different *HLA-C* genotypes. Moreover, *HLA-C* genotypes seem to have an influence on the frequency of KIR2DL1$^+$ NK cells.

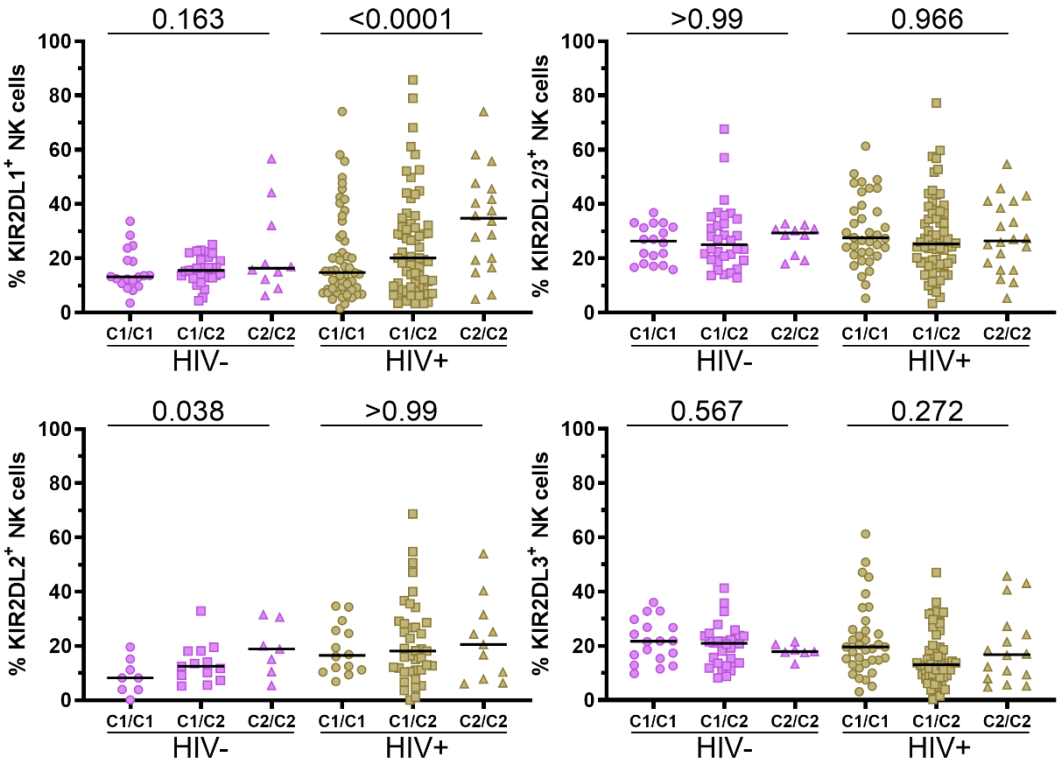

Figure 41: KIR2DL1-3$^+$ NK cell frequencies in HIV-1$^-$ (HIV-) and HIV-1$^+$ (HIV+) individuals stratified by their HLA-C haplotypes. A Percentage of KIR2DL1$^+$, KIR2DL2/L3$^+$, KIR2DL2$^+$ and KIR2DL3$^+$ NK cells in HIV-1$^-$ and HIV-1$^+$ individuals grouped by *HLA-C* genotypes (C1 homozygous: C1/C1, C1/C2 heterozygous: C1/C2 and C2 homozygous: C2C2). Scatter plots display frequency of KIR2DL$^+$ NK cells in HIV-1$^-$ and HIV-1$^+$ individuals and median for each group. For statistical analysis, one-way ANOVA, test for linear trend was used to check for differences between HLA-C genotypes and HIV-1$^-$ and HIV-1$^+$ individuals. P values were adjusted for multiple comparison (Bonferroni).

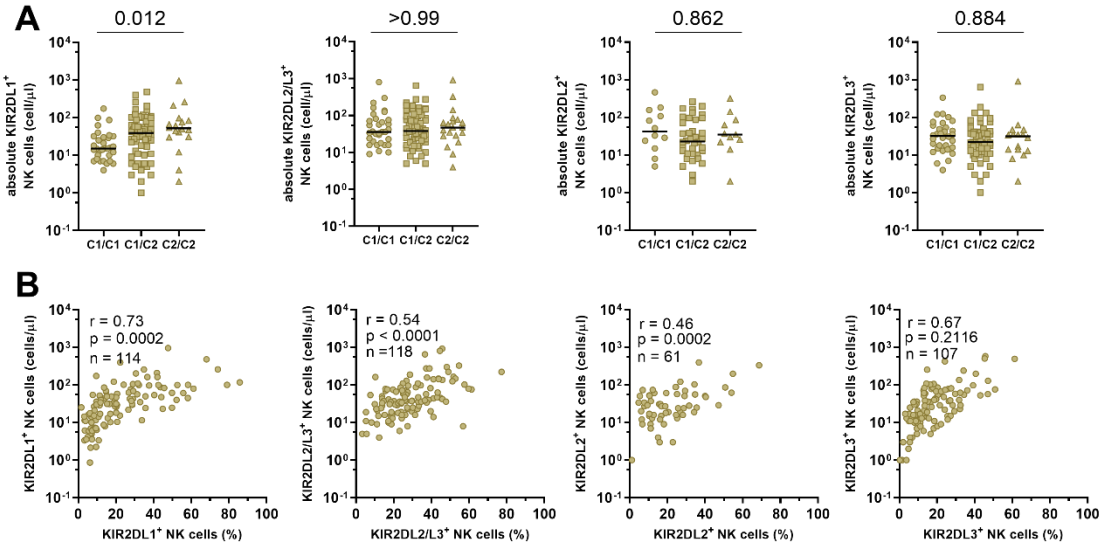

Figure 42: Absolute KIR2DL1-3$^+$ NK cells in HIV-1$^+$ individuals stratified by their *HLA-C* genotypes and correlation of relative and absolute KIR2DL1-3 expression. A Absolute cell numbers of KIR2DL1$^+$, KIR2DL2/L3$^+$ KIR2DL2$^+$ and KIR2DL3$^+$ NK cells in HIV-1$^+$ individuals grouped by HLA-C genotypes (C1 homozygous: C1/C1, C1/C2 heterozygous: C1/C2 and C2 homozygous: C2C2). **B** Correlation of absolute and relative KIR2DL1-3 expression on NK cells of HIV-1$^+$ individuals. Scatter plots display absolute cell numbers of KIR2DL$^+$ NK cells in HIV-1$^+$ individuals and median for each group. For statistical analysis, one-way ANOVA, test for linear trend was used to check for differences between HLA-C genotypes. P values were adjusted for multiple comparison (Bonferroni). Correlations were evaluated using Spearman's rank correlation test.

5.8.4 Correlation of KIR2DL1-3$^+$ NK cells and HIV-1 clinical parameters

As CD4 T cell count and viral load play a central role in HIV-1 progression, association of KIR2DL1 and KIR2DL2/L3 expression on NK cells from HIV-1$^+$ individuals with CD4 T cell count and HIV-1 viral load were performed (**Figure 43**). Correlation analysis of viral loads (**Figure 43A**) showed a significant negative correlation with absolute CD4 T cell counts (r=-0.24, p=0.008) and a significant positive correlation with absolute NK cell counts (r=0.31, p=0.0007). Subsequently, a significant positive correlation was observed between absolute CD4 T cell and NK cell count (r=0.23, p=0.001). In addition, correlation studies of KIR2DL1$^+$ and KIR2DL2/L3$^+$ relative NK cell frequencies (**Figure 43B** and **C**) revealed no correlation with either absolute CD4 T cell count (KIR2DL1: r=0.12, p=0.21; KIR2DL2/L3: r=0.09, p=0.34) or HIV-1 viral load (KIR2DL1: r=0:02, p=0.83; KIR2DL2/L3: r=0.09, p=0.32). Overall, high viral loads are associated with a lower number of CD4 T cells and an increased number of NK cells. Furthermore, there is no association between KIR2DL$^+$ NK cells and clinical parameter for HIV-1.

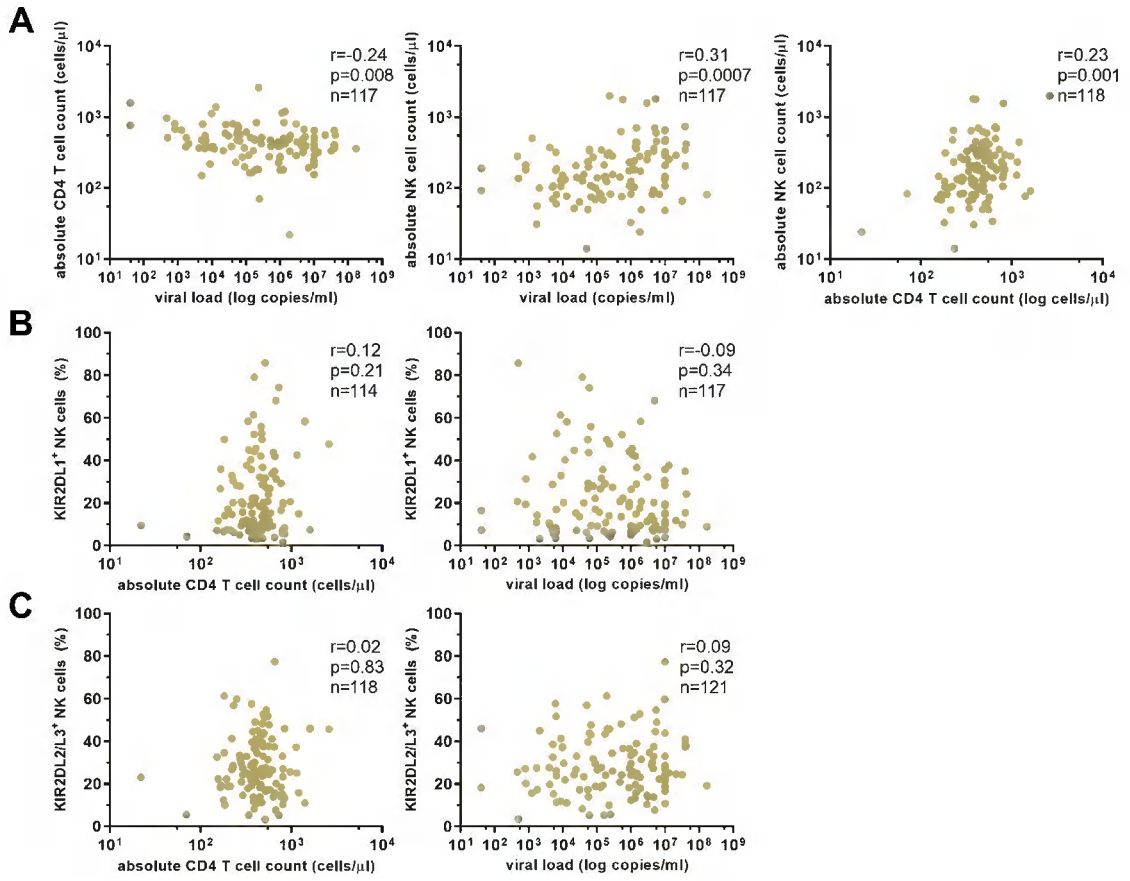

Figure 43: Correlation between the frequencies of KIR2D1$^+$ and KIR2DL2/L3$^+$ NK cells and CD4 T cell count and viral load in HIV-1$^+$ individuals. A Correlation between absolute CD4 T and NK cell count and viral load. **B** Correlation between the frequency of KIR2DL1$^+$ NK cells with CD4 T cell count and viral load. **C** Correlation between the frequency of KIR2DL2/L3$^+$ NK cells with CD4 T cell count and viral load. Correlations were evaluated using Spearman's rank correlation test.

5.8.5 Correlation of HLA-C/KIR2DL binding affinities and KIR2DL$^+$ NK cells

To examine a possible relationship between the genotype of HLA-C and KIR2DL and the frequency of KIR2DL$^+$ NK cells, correlation analysis of KIR2DL$^+$ NK cell frequencies and HLA-C/KIR2DL binding affinities, which were assessed in the KIR2DL-Fc binding assays (5.3), were assessed for HIV-1$^+$ individuals (**Figure 44A)** and HIV-1$^-$ individuals (**Figure 44B**). Therefore, only individuals with a heterozygous C1/C2 genotype and KIR2DL/HLA-C combinations that were analysed in the KIR2DL-Fc binding assays were included. Correlation of KIR2DL1$^+$ NK cell frequency with HLA-C2/KIR2DL1 binding affinities displayed a significant positive correlation in HIV-1$^+$ individuals (r=0.3, p=0.004) but not in HIV-1$^-$ individuals (r=0.16, p=0.36). Moreover, no correlations of KIR2DL2/L3$^+$ NK cells and HLA-C1/KIR2DL2/L3 binding affinities were detected in HIV-1$^+$ (r=0.18, p=0.17) and HIV-1$^-$ (r=0.15, p=0.39) individuals. Taken together, binding affinities of KIR2DL1 and HLA-C2 has an impact on the relative frequency of KIR2DL1$^+$ NK cells in HIV-1$^+$ individuals.

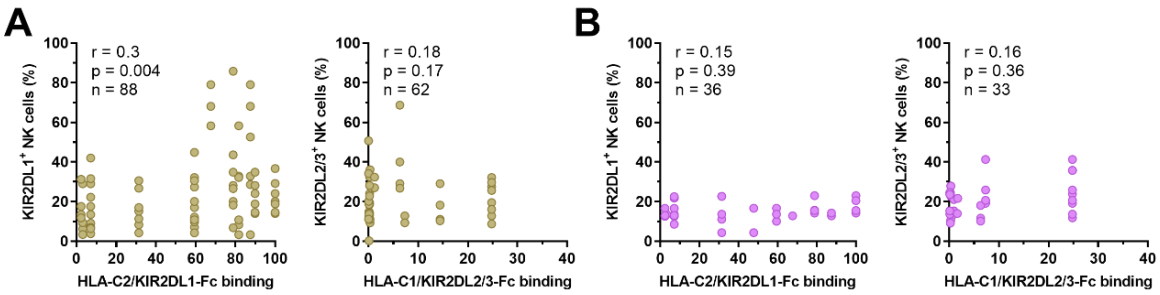

Figure 44: Correlation between the frequencies of KIR2DL1$^+$ and KIR2DL2/L3$^+$ NK cells and KIR2DL/HLA-C binding affinities in HIV-1$^+$ and HIV-1$^-$ individuals . A Correlation between percentage of KIR2DL1$^+$ NK cells and HLA-C2/KIR2DL1-Fc, KIR2DL2/3$^+$ NK cells and HLA-C1/KIR2DL2/3-Fc in HIV-1$^+$ individuals stratified by KIR/HLA binding affinities. **B** Correlation between percentage of KIR2DL1$^+$ NK cells and HLA-C2/KIR2DL1-Fc, KIR2DL2/3$^+$ NK cells and HLA-C1/KIR2DL2/3-Fc in HIV-1$^-$ individuals stratified by KIR/HLA binding affinities. Correlations were evaluated using Spearman's rank correlation test.

5.9 Sequencing of Vpu isolated from viral RNA and genomic DNA from untreated HIV-1$^+$ individuals

HIV-1 is able to modulate HLA-C expression on infected CD4 T cells via the accessory HIV-1 protein Vpu. A recent study identified five amino acid (AA) positions in Vpu at which specific AA residues were associated with HLA-C downregulation (Bachtel *et al.*, 2018). Proline (P) at position 3, glutamic acid (E) at position 5, glycine (G) or threonine (T) at position 16 and serine (S) at position 24 were independently associated with downmodulation of HLA-C. In addition, alanine (A) at position 15 was negatively associated with HLA-C downmodulation. In order to investigate the influence of HLA-C/KIR2DL allotype combinations on Vpu sequence variations, viral RNA and genomic DNA from 122 HIV-1$^+$ individuals was isolated and sequenced with next-generation sequencing (NGS) for *Vpu*. Sequences that passed the quality control (plasma: n=95, PBMC: n=67) were translated into amino acid sequences, aligned to the Vpu proteins sequences from the lab-adapted HIV-1 strains JRCSF and NL4-3 and analysed for the five AA positions (**Figure 45A**). **Figure 45B** shows a representative alignment of Vpu from two matching PBMC and plasma samples with the lab adapted HIV-1 strains JRCSF and NL4-3. The analysed AA positions are highlighted in red.

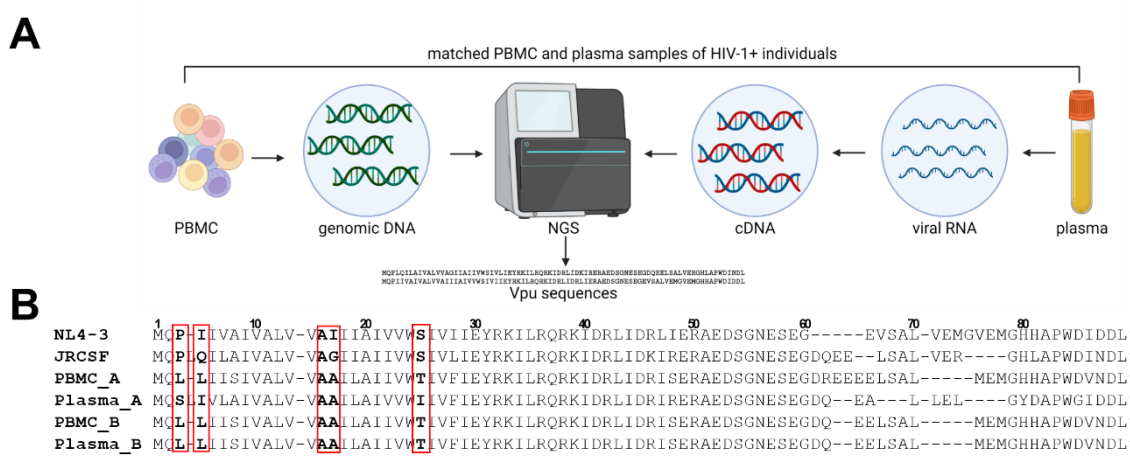

Figure 45: Work flow for Vpu sequencing. A Genomic DNA was isolated from frozen PBMC and viral RNA was isolated from frozen plasma samples from 122 HIV-1$^+$ individuals. Viral RNA was reverse transcribed into cDNA and cDNA and genomic DNA were prepared and sequenced for Vpu with NGS. **B** Sequences that passed the quality control were translated into amio acid sequences and aligned to the Vpu sequences of the lab-adapted HIV-1 strains NL4-3 and JRCSF. Vpu sequences were analyzed for the five amino acid positions highlighted in red.

5.9.1 Comparison of Vpu amino acid residues from PBMC and plasma samples

Vpu sequences of matching PBMC and plasma samples (n=53) were analyzed for their similarity in the five AA positions (3, 5, 15, 16, 24) (**Figure 46**). Moreover, all Vpu sequences from PBMC (n=67) and plasma (n=97) samples were analyzed for the frequency of amino acid residues at the five specific AA positions (**Figure 46**). Comparison of the similarity of the five amino acid positions between matching plasma and PBMC samples revealed a frequency of matching AA residues between 0.64 and 0.92 with the lowest frequency at position 16 and the highest frequency at position 5 (**Figure 46**). Examination of the AA residue frequencies for the five AA positions displayed the highest variation of AA residues for position 5 (12 different AA residues) and the lowest variation for positon 24 with only three different AA residues (**Figure 46**). For position 3, the most common AA residue was proline (PBMC: 0.69, plasma: 0.61) followed by serine and leucine. Position 5 had the highest frequency for isoleucine (PBMC: 0.63, plasma: 0.45) followed by leucine and position 15 had the highest frequency for alanine (PBMC: 0.92, plasma: 0.73) and valine as the second most common AA residue at this position. Furthermore, position 16 showed comparable frequencies for the AA residues alanine (PBMC: 0.29, plasma: 0.36), isoleucine (PBMC: 0.28, plasma: 0.14) and glycine (PBMC: 0.33, plasma: 0.36). Lastly, the most common AA residue at position 24 was serine (PBMC: 0.61, plasma: 0.32) followed by a threonine. Taken together, matching PBMC and plasma samples had quite similar AA residues at the analyzed positions. Moreover, variations of AA residues differed strongly between the five AA positions.

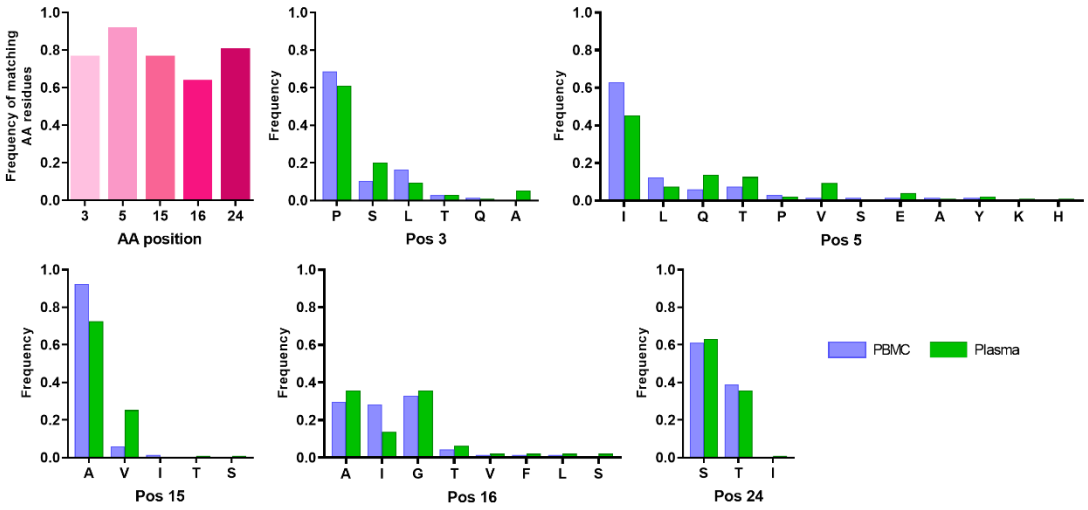

Figure 46: Comparison of AA residue similarity and frequency. Frequency of matching AA residues at position 3, 5, 15, 16 and 24 between matching PBMC and plasma samples (n=53) and frequency of AA residues at position 3, 5, 15, 16 and 24 for PBMC (n=67, blue) and plasma (n=95, green) samples.

5.9.2 Correlation of Vpu amino acid residues and HLA-C genotypes

In a next step, the frequency of AA residues in Vpu that are involved in HLA-C downregulation were analyzed based on the *HLA-C* genotypes (C1 homozygous: C1/C1, C1/C2 heterozygous: C1/C2, C2 homozygous: C2/C2) of the HIV-1$^+$ individuals from PBMC and plasma samples (**Figure 47**). In PBMC samples, individuals with one or two *HLA-C1* alleles had a median of three AA residues that were associated with HLA-C downregulation, whereas *HLA-C2* homozygous donors had a median of two AA residues in their Vpu sequence (p=0.593) (**Figure 47A**). Analysis of Vpu sequences from plasma samples revealed a higher number of HLA-C downregulation associated AA residues in individuals with one or two *HLA-C2* alleles (median: 3) (**Figure 47B**). *HLA-C1* homozygous donors had a median of two AA residues (p=0.205). Further stratification of *HLA-C* genotypes for all five AA positions and the associated AA residues showed no influence of the *HLA-C* genotype on Vpu sequence polymorphisms towards AA residues that were associated with HLA-C expression in either Vpu sequences isolated from PBMC or from plasma samples.

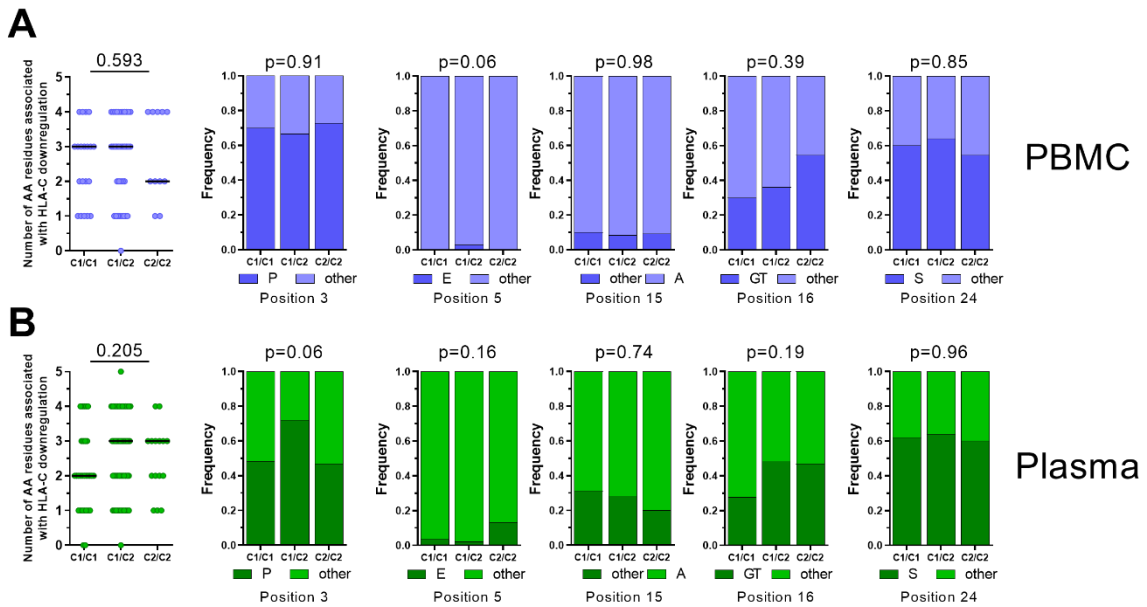

Figure 47: Impact of *HLA-C* genotypes on AA residue variations associated with HLA-C downmodulation in Vpu sequences isolated from PBMC (A) and plasma (B) samples. Dot plots display the cumulative number of AA residues associated with HLA-C downmodulation in Vpu stratified by *HLA-C* genotypes (C1 homozygous: C1/C1, C1/C2 heterozygous: C1/C2, C2 homozygous: C2/C2) and median of each group. Stacked bars show frequency of AA residues that are associated with HLA-C expression level for the five relevant positions in different *HLA-C* genotypes. For statistical analysis, one-way ANOVA, test for linear trend was used to check for differences between numbers of AA residues in *HLA-C* genotypes. In addition, Chi square test was used to analyze differences in AA residues of the five positions between the *HLA-C* genotypes.

5.9.3 Correlation of Vpu amino acid residues and HLA-C expression level

Surface expression levels of HLA-C differs between HLA-C allotypes (Apps *et al.*, 2013).To identify a potent impact of HLA-C surface expression level on Vpu sequence polymorphisms, the Vpu sequences of PBMC and plasma samples were analyzed for the five AA positions that are associated with HLA-C downregulation based on the average MFI of the HLA-C allele expression (**Figure 48**). As a reference previously reported HLA-C allele expression levels, were used (**Table 5**) (Bachtel *et al.*, 2018).

Table 5: Average expression level of HLA-C alleles.

HLA-C allele	Average MFI expression	n (PBMC)	n (plasma)
01	254	5	4
02	164	11	14
03	114	24	30
04	200	21	22
05	154	8	12
06	225	10	21
07	111	32	46
08	176	1	2
12	193	9	16
14	294	3	4
15	223	6	8
16	180	2	5
17	115	2	2
18	239	0	0

AA residue 3P was found to be more frequent in Vpu sequences from PBMC (p=0.038) and plasma (p=0.03) samples from HIV-1$^+$ individuals with HLA-C alleles that have a high surface expression level. The four other AA positions showed no association between HLA-C surface expression level and AA residues that are associated with HLA-C expression level. **Table 6** summarizes the size, median and p values for the five AA positions for PBMC and plasma samples.

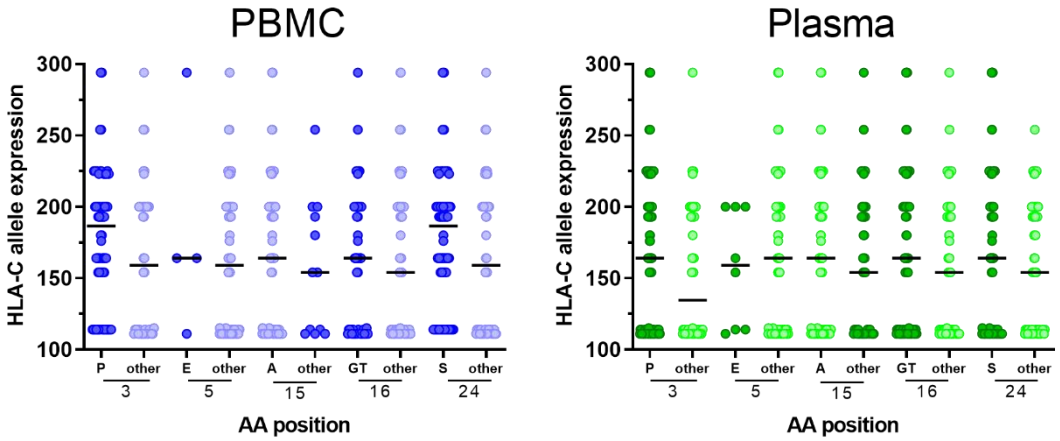

Figure 48: Impact of HLA-C allele surface expression level on AA residue variations associated with HLA-C downmodulation in Vpu sequences isolated from PBMC (blue) and plasma (green) samples. Dot plots display number of individuals positive for the analysed AA residues at the five AA position (3, 5, 15, 16, 24) with their respective HLA-C allele expression. Bars indicate the median for each group. For statistical analysis, Mann-Whitney test was used to identify differences in AA residues at the analysed positions for different HLA-C allele expression levels.

Table 6: Descriptive and comparative statistics for the five analyzed Vpu AA positions.

	AA position	**3**		**5**		**15**		**16**		**24**	
	AA residue	**P**	**other**	**E**	**other**	**A**	**other**	**GT**	**other**	**S**	**other**
PBMC	n	70	42	4	130	122	12	50	84	62	52
	median	186.5	159.0	164.0	159.0	164.0	154.0	164.0	154.0	186.5	159.0
	p value	0.038		0.774		0.682		0.744		0.078	
Plasma	n	122	74	8	178	136	52	78	108	116	70
	median	164.0	134.5	159.0	164.0	164.0	154.0	164.0	154.0	164.0	154.0
	p value	0.030		0.980		0.369		0.223		0.558	

5.9.4 Correlation of Vpu amino acid residues and HLA-C/KIR2DL binding affinities

As a final step of investigating variations in Vpu sequences from PBMC and plasma samples from HIV-1$^+$ individuals, differences in AA residues for the five AA positions were analyzed based on the assessed HLA-C/KIRDL allotype binding affinities of the KIR2DL-Fc binding assays. Therefore, all Vpu sequences from HIV-1$^+$ individuals with HLA-C1/KIR2DL2/L3 and HLA-C2/KIR2DL1 allotype combinations that were used for the KIR2DL-Fc binding assay were analyzed for their AA residues at the five positions and the assessed HLA-C binding affinities (**Figure 49**). Vpu sequences from plasma samples showed a higher frequency of AA residues other than an alanine at position 15 (15 other) (p=0.007) or a glycine or threonine at position 16 (16GT) (p=0.016) in individuals with strong

HLA-C/KIR2DL binding affinities, whereas HLA-C/KIR2DL binding affinities showed no associations with specific AA residues in Vpu sequences from PBMC samples. **Table 7** summarizes the size, median and p values for the five AA positions for PBMC and plasma samples.

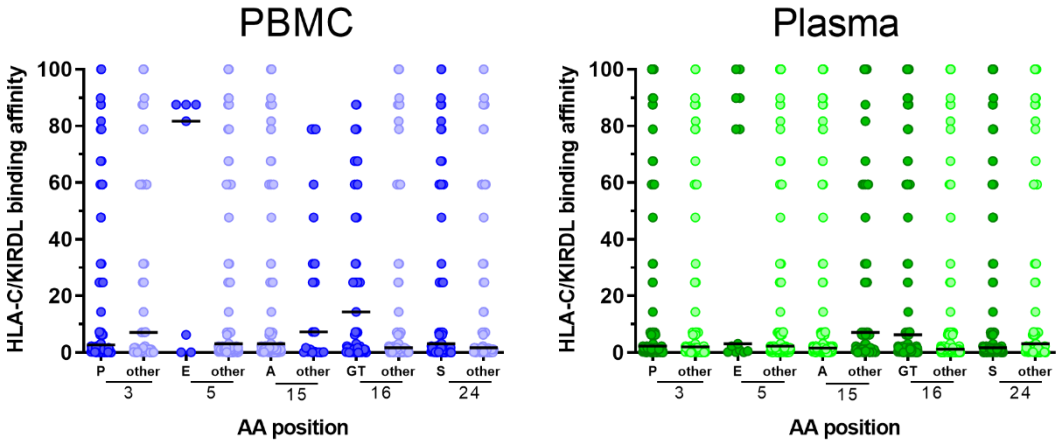

Figure 49: Impact of HLA-C/KIR2DL binding affinities on AA residue variations associated with HLA-C downmodulation in Vpu sequences isolated from PBMC (blue) and plasma (green) samples. Dot plots display number of individuals positive for the analyzed AA residues at the five AA position (3, 5, 15, 16, 24) with their respective HLA-C/KIR2DL binding affinity. Bars indicate the median for each group. For statistical analysis, Mann-Whitney test was used to identify differences in AA residues at the analysed positions for different HLA-C/KIR2DL binding affinities.

Table 7: Descriptive and comparative statistics for the five analysed Vpu AA positions.

	AA position	**3**		**5**		**15**		**16**		**24**	
	AA residue	**P**	**other**	**E**	**other**	**A**	**other**	**GT**	**other**	**S**	**other**
PBMC	n	124	68	7	185	172	21	67	126	117	75
	median	2.7	7.1	81.7	3.1	3.1	7.3	14.4	1.7	3.1	1.7
	p value	0.423		0.172		0.849		0.069		0.790	
Plasma	n	171	108	1	266	188	90	122	157	164	113
	median	2.3	2.0	3.1	2.3	1.7	7.1	6.3	1.2	1.7	3.1
	p value	0.641		0.183		0.007		0.016		0.538	

6. Discussion

HIV-1 developed numerous strategies to overcome the antiviral host immune response. HIV-1 is able to downregulate HLA-A and -B from the cell surface using the accessory protein Nef (Le Gall *et al.*, 1998). In addition, the HIV-1 accessory protein Vpu is able to downregulate HLA-C, yet Vpu proteins from lab-adapted strains and primary isolates exhibit differential abilities to downregulate HLA-C from the cell surface (Collins *et al.*, 1998; Apps *et al.*, 2016). The fact that HLA-A/-B and -C expression is targeted by different viral proteins and HLA-C downregulation diversifies across lab-adapted HIV-1 strains and primary isolates emphasizes differences in the biological role of these HLA molecules in HIV-1 infection, as well as in immune responses. Although HLA class I downregulation is associated with loss of recognition by cytotoxic T cells, reduced HLA class I expression triggers NK cell activation as HLA class I molecules are natural ligands for inhibitory NK cell receptors. All HLA-C allotypes are recognized by the inhibitory KIR2DL receptors of NK cells, whereas only specific HLA-A and -B epitopes are recognized by KIRs (Parham, 2005). Thus, HLA-C has been assumed to be an essential regulator of NK cell activity.

HLA class I molecules are encoded by genes within the major histocompatibility complex which displays a high degree of polymorphism (Williams, 2001). Similarly, KIRs are a highly polymorphic family of inhibitory and activating receptors and to date, there are 173 *KIR2DL1*, 34 *KIR2DL2* and 64 *KIR2DL3* alleles identified (*IPD-KIR Database*) which display distinct functional properties in respect to ligand binding. As both the receptor (KIR) and ligand (HLA) molecules are highly polymorphic, KIR2DL and HLA-C allotype combinations have been identified to have an influence on a variety of disease outcomes, including HIV-1 infection (Mori *et al.*, 2015; Lin *et al.*, 2016). However, the functional consequences of different receptor and ligand combinations between KIR2DL and HLA-C for NK cell education, as well as anti-HIV-1 activity of NK cells remain unknown. Under healthy conditions, HLA-C expression level varies across different allotypes. In HIV-1 infection high HLA-C expression levels are associated with an increased HLA-C-restricted cytotoxic T cell response (Apps *et al.*, 2013) and an increased frequency of mutations in HLA-C-presented HIV-1 epitopes (Blais *et al.*, 2012). In addition to the observed T cell pressure during HIV-1 infection, NK cells have also been shown to mediate immune pressure on HIV-1 and HIV-1 adapts or escapes from this immune pressure by specific sequence polymorphisms (Alter *et al.*, 2011; Hölzemer *et al.*, 2015). Specifically, KIR2DL$^+$ NK cells are able to sense alterations in HIV-1 mediated HLA-C expression levels suggesting a crucial role of KIR2DL$^+$ NK cells in early HIV-1 control (Körner *et al.*, 2017). Nevertheless, the influence of KIR2DL/HLA-C allotype combinations as a potential determinant for the magnitude of NK cell mediated immune pressure during HIV-1 infection and subsequent Vpu escape variants have not been investigated so far.

Based on the current knowledge, I hypothesized that differential binding affinities of KIR2DL/HLA-C allotype combinations predetermine KIR2DL$^+$ NK cell induced immune pressure and affect Vpu-associated viral escape. Therefore, this thesis aimed to assess the KIR2DL/HLA-C binding affinities and specificity with two different approaches. KIR2DL-Fc fusion protein binding assays and KIR2DL-expressing reporter cells were used for a comprehensive evaluation of the binding affinities of multiple KIR2DL allotypes and their cognate HLA-C ligands. Moreover, the antiviral activity and education status of KIR2DL$^+$ NK cells were investigated. To gain more information about alterations in NK cell receptor profiles in HIV-1 infection, PBMC of HIV-1$^+$ and HIV-1$^-$ individuals were analyzed for differential NK cell receptor expression and differences in KIR2DL expression based on *KIR2DL/HLA-C* genotypes. Furthermore, *Vpu* was sequenced from genomic DNA and plasma samples of the HIV-1$^+$ individuals to identify possible Vpu sequence polymorphisms in individuals with different *KIR2DL/HLA-C* allotype combinations.

The assessment of the binding affinities of various KIR2DL/HLA-C allotype combinations, using first HLA-C expressing 721.221 cells in combination with KIR2DL-Fc fusion proteins and then KIR2DL reporter cell lines demonstrated a hierarchy of affinities along the various combinations for both types of binding assays and confirmed the distinct binding specificities of KIR2DL1 for HLA-C2, of KIR2DL3 for HLA-C1 and the cross-binding of KIR2DL2 for HLA-C1 and -C2 (Winter *et al.*, 1998), especially for the KIR2DL-Fc fusion protein binding assays. KIR2DL reporter assays showed a higher variability and less stringent binding specificity compared to the KIR2DL-Fc fusion protein binding assay. The herein observed binding affinities of KIR2DL to distinct HLA-C molecules are mostly consistent with the results from Hilton *et al.* who used a cell-free system, more specifically a panel of microbeads, in which each bead was coated with one of 97 HLA class I allotype to test the binding of KIR2DL1/L2/L3-Fc fusion proteins. It has been shown that polymorphisms in different structural domains of KIR2DL can impact the function of the respective KIR molecule. Substitutions in the D2 domain change the avidity of KIR2DL1 for HLA-C, whereas changes in the hinge region connecting the D1 and D2 domain usually affect the avidity of KIR2DL2/L3 for HLA-C (Hilton *et al.*, 2015). A primary specificity of KIR2DL1 for HLA-C2 or KIR2DL2/L3 for HLA-C1 has been attributed to the amino acid position 44 in the D1 domain, which is a methionine in KIR2DL1 compared to lysine in KIR2DL2 and KIR2DL3 (Winter *et al.*, 1997). KIR2DL1*022 possesses a lysine at position 44 that determines the C1 specificity of the KIR molecule which has also been confirmed by the performed binding assays (Hilton *et al.*, 2015). High variability in *KIR* gene content is the consequence of gene duplication and deletion throughout evolution (Pyo *et al.*, 2010; Traherne *et al.*, 2010).

For example, KIR2DL2 is an evolutionally newer fusion gene consisting of unequal crossing of the intracellular domain of KIR2DL1 and the extracellular domains of KIR2DL3 (Wilson *et al.*, 2000). While KIR2DL2/L3 receptors share over 90% sequence identity and segregation analysis revealed that *KIR2DL2* and *KIR2DL3* behave as alleles at a single gene locus, they are inherited on different KIR haplotypes, which influences NK cell function (Uhrberg *et al.*, 1997; Hsu, Chida, *et al.*, 2002; Parham, 2005). Generally, studies suggested that KIR2DL2 has a greater binding affinity for HLA-C compared to KIR2DL3 (Moesta *et al.*, 2008; Schönberg *et al.*, 2011). This lower affinity of KIR2DL3 has been associated with an arginine at position 16 in the N-terminus of the D1 domain and a cysteine at position 148 in the D2 domain that the hinge angle of the KIR2DL3 molecule and the relative orientation of the extracellular D1 and D2 domains thereby influencing the binding to HLA-C (Moesta *et al.*, 2008). Moreover, a study from Hilton *et al*. that compared the strength and specificity of mutant KIR2DL1 and KIR2DL3 receptors revealed that KIR2DL3 has a lower avidity and broader specificity than KIR2DL1. In comparison to KIR2DL1, KIR2DL3 is a weaker and less selective receptor, retaining a greater potential for improvement and change. In contrast, KIR2DL1 is more specialized but less flexible and adaptable compared to KIR2DL3 (Hilton *et al.*, 2012). In addition to structural differences between the KIR molecules, the endogenous HLA-C peptide repertoire can modulate the specific binding of KIR2DL and HLA-C allotypes. KIR2DL2/L3 binding to HLA-C1 showed a higher peptide selectivity than that of KIR2DL1/HLA-C2 binding, providing another possible explanation for the weaker interaction of KIR2DL3/HLA-C2. Moreover, cross-reactive binding of KIR was also characterized by an even higher peptide selectivity (Sim *et al.*, 2017).

KIR2DL/HLA-C combinations have been associated with clinical outcome of virus infections. For instance, the presence of *KIR2DL3* and the respective *HLA-C1* ligand was associated with clearance of hepatitis-C virus (HCV) infection (Khakoo *et al.*, 2004), a protective effect in ulcerative colitis (Jones *et al.*, 2006) and individuals with HLA-C*16:01/KIR2DL3 were observed to have more rapid progression to AIDS than individuals without this genotype (Mori *et al.*, 2019). Several studies investigated the influence of KIR2DL and HLA-C on HIV-1 infection and demonstrated the importance of the HLA-C presented peptide for NK cell activation. Fadda *et al.* showed that HLA-C*01:02 restricted HIV-1 p24 epitope variants modulate the binding of KIR2DL2 and thereby impact NK cell function (Fadda *et al.*, 2012). HIV-1 p24 Gag consensus sequence peptides enabled KIR2DL2/HLA-C*03:04 binding, resulting in inhibition of $KIR2DL2^{+}$ NK cells (Van Teijlingen *et al.*, 2014), whereas another study showed that HIV-1 induced changes in HLA-C*03:04-presented peptides can reduce the interaction to KIR2DL3 and enhance the activation of NK cells by virus-infected cells (Ziegler *et al.*, 2020). Therefore, differential binding affinities of KIR2DL/HLA-C allotype combinations might impact the anti-HIV-1 activity of NK cells.

Discussion

The specificity and strength of an NK cell response is determined by the inhibitory receptor repertoire of each NK cell and the corresponding HLA class I genotype and is termed NK cell education (Boudreau *et al.*, 2018). It is well established that NK cell education is critical for the generation of functional effector NK cells, however the molecular mechanism of how educated NK cells remain self-tolerant but also deliver spontaneous, well-tuned functional responses in case of activation remain insufficiently understood (Pfeifer *et al.*, 2018). In addition to the performed binding assays, the consequence of HLA-C/KIR2DL combinations on NK cell activation was investigated. As NK cells are triggered by the loss of recognition of HLA class I molecules that interact with inhibitory KIRs, co-cultures of NK cells with the HLA class I deficient 721.221 cell line induced a high frequency of $CD107a^+$ NK cells compared to NK cells that were cultured without target cells. Functional assessment of NK cells in co-culture assays with HLA class I deficient 721.221 cells revealed an increased degranulation of KIR2DL1, KIR2DL2/L3 and KIR3DL1 $single^+$ NK cells compared to their uneducated KIR^- counterparts in donors carrying the corresponding HLA class I epitope. These results are in line with previous studies where educated NK cells displayed a much higher frequency of $CD107a^+$ NK cells than uneducated NK cells after exposure to 721.221 or K562 target cells (Körner *et al.*, 2017; Pfeifer *et al.*, 2018). Educated NK cells expressing self-HLA class I specific inhibitory KIRs had a different structural organization of the endolysosomal compartment, allowing an accumulation of granzyme B in dense-core secretory lysosomes and may serve as a molecular memory of receptor signaling during NK cell education (Goodridge *et al.*, 2019). A common strategy of viruses to evade immune responses is to downmodulate HLA class I expression on the surface upon infection, however the loss of HLA class I expression triggers NK cell activation through the “missing self” signal (Bonaparte *et al.*, 2004). It is still unknown if viral HLA class I modulation is a dynamic process to adapt to specific host immune responses. HLA-C expression, which has been described to undergo dynamic changes after HIV-1 infection with differences in downmodulation of HLA-C expression level across different HIV-1 strains. HLA-C downmodulation has also been described for other viral diseases including herpes simplex virus (HSV) and human cytomegalovirus (HCMV), thereby being a potential target for $KIR2DL^+$ NK cell activation (Barel *et al.*, 2003; Elboim *et al.*, 2013). In order to analyze the influence of HLA-C expression on HIV-1 infected CD4 T cells to NK cell activation, an *in vitro* infection model with HIV-1 strains with different abilities to downmodulate HLA-C surface expression was used. CD107a degranulation assays with NK cells and autologous CD4 T cells infected with HIV-1 JRCSF wt or JRCSF Vpu mutant showed no differences in CD107a degranulation between uninfected (mock) CD4 T cells and HIV-1 infected CD4 T cells, however exposure to 721.221 target cells induced high frequency of $CD107a^+$ NK cells.

Moreover, assessment of the anti-viral activity of educated and uneducated NK cell subsets revealed no differences in CD107a frequency between these subsets. Previous data from my group has shown differences in CD107a expression by NK cells upon co-culture with uninfected and HIV-1 infected CD4 T cells with JRCSF wt infection leading to a higher frequency of CD107a$^+$ NK cells compared to JRCSF Vpu mutant infection due to the missing-self signal (Körner *et al.*, 2017). Possible reasons why no differences in CD107a expression by NK cells after exposure to uninfected and HIV-1 infected CD4 T cells were detectable are diverse and challenging to identify. It is possible that the supplements or stimulators used or long culture conditions for CD4 T cells induced the expression of stress ligands that are detected by activating NK cell receptors. NK cells that were exposed to HIV-1 infected CD4 T cells showed no differences in CD107a frequency between educated and uneducated NK cell subsets. This is possible due to an insufficient downregulation of HLA-B and HLA-C, which are the natural ligands for KIR2DL1-3 and KIR3DL1. High CD107a frequencies were observed for NKG2A single$^+$ NK cells possibly induced by HLA-E downregulation or HIV-1-derived peptides presented by HLA-E on infected CD4 T cells, resulting in a loss of recognition of NKG2A$^+$ NK cells (Davis *et al*., 2016). Direct assessment of the antiviral activity of HLA-C educated KIR2DL$^+$ NK cells revealed a reduced capacity to inhibit HIV-1 replication as compared to uneducated NK cells due to residual KIR2DL/HLA-C binding. Blocking experiments of HLA-C and its corresponding KIR2DL receptors improved the antiviral activity of NK cells (Bonaparte *et al.*, 2004; Davis *et al.*, 2011; Otten *et al.*, 2013; Körner *et al.*, 2017). Additionally, NK cells are not able to kill CD4 T cells that have been infected with HIV-1 strains unable to downregulate HLA class I molecules, indicating that NK cell-mediated killing of HIV-1 infected CD4 T cells depends on the HIV-1 strain to modulate HLA class I expression (Bonaparte *et al.*, 2004). However, NK cells are able to sense alterations in HLA class I expression, which results in an increased antiviral activity (Körner *et al.*, 2017). In this context, it has previously been shown that NK cells from individuals with acute and primary HIV-1 infection had increased frequencies of self-inhibitory KIR (Alter *et al.*, 2009; Körner *et al.*, 2014). For HIV-1, studies have shown that NK cell education is directly associated to the extent of viral control. Strong allotype combination of KIR3DL1 and HLA-Bw80I are associated with HIV-1 control, whereas HLA-Bw negative individuals with uneducated KIR3DL1$^+$ NK cells had the most rapid progression to AIDS (Martin *et al.*, 2002; Boudreau *et al.*, 2016).

In conclusion, educated primary NK cells were highly functional towards HLA class I deficient 721.221 cells, however functional activity of KIR2DL$^+$ NK cells was not observed upon stimulation with HIV-1 infected cells.

Discussion

Virus infection affects NK cell homoeostasis, phenotype as well as their functional activity. In turn, many studies have revealed that NK cell receptor profiles or the expansion of specific NK cell subsets are associated with viral susceptibility (Strauss-Albee *et al.*, 2016). For example, presence of *KIR2DL2* or *KIR2DS2* has been associated with progression to symptomatic HSV-1 infection (Estefanía *et al.*, 2007) and KIR2DL2 or KIR2DS2 were more abundant in RNA$^+$ HCV patients compared to patients who cleared the virus (Paladino *et al.*, 2007). Moreover, HCMV infection results in a clonal expansion of NKG2C in NK cells, persisting throughout life (Gumá *et al.*, 2004) and HIV-1$^+$ women with an impaired NK cell IFN-γ response were more likely to acquire HIV infection (Naranbhai *et al.*, 2012). In the context of HIV-1 infection, several studies have shown significant changes in the NK cell receptor repertoire, including the expansion of KIR$^+$ NK cells (Ahmad *et al.*, 2001; De Maria *et al.*, 2003; Mavilio *et al.*, 2003; Alter *et al.*, 2007, 2009; Pelak *et al.*, 2011). This thesis, revealed significant differences in the NK cell receptor repertoire of HIV-1$^+$ individuals. In agreement with the observed results, a lower frequency of CD8$^+$ NK cells in untreated HIV-1$^+$ individuals compared to healthy controls and ART treated HIV-1$^+$ individuals have been observed in a previous study (Ahmad *et al.*, 2014). In a longitudinal, retrospective study of 117 untreated HIV-1$^+$ individuals, they also showed that a higher frequency and absolute number of CD8$^+$ NK cells were linked to a delayed HIV-1 progression and that an increased frequency of CD8$^+$ NK cells was associated with a lower viral load and increased frequency of CD4 T cells. Moreover, CD8$^+$ NK cells had also higher frequencies of CD57 and exhibited more functional activity in terms of cytokine production and degranulation. CD57 is described as a marker for NK cell differentiation and final stage of NK cell maturation. Stimulation of NK cells with IL-2 or co-cultures with target cells results in an increased expression of CD57 on NK cells and is correlated with maturation of the CD56^{dim} NK cell subset, lower expression of NKp46, NKp30 NKG2D and NKG2A and an increased expression of CD16 and KIRs (Lopez-Vergès *et al.*, 2010). The increased frequency of CD57$^+$ NK cells in viral infection was first described in HCMV$^+$ individuals (Gratama *et al.*, 1988). In addition, recent studies of hematopoietic stem cell transplantations in HCMV-infected and uninfected transplant recipients showed that HCMV infection drives the expansion of NKG2C$^+$ NK cells, which preferentially acquired CD57, express KIR2DL2/L3 and lack the expression of NKG2A (Foley, Cooley, Verneris, Curtsinger, *et al.*, 2012; Foley, Cooley, Verneris, Pitt, *et al.*, 2012). In chronic HIV-1 infection, one study reported higher CD57$^+$ to CD57$^-$ NK cell ratio compared to uninfected individuals due to a loss of CD57$^-$ NK cells (Hong *et al.*, 2010). However, the HCMV status of the subject was not reported. Data from studies with HIV-1$^+$ individuals and information about HCMV status of the patients concluded that an increased proportion of NKG2C$^+$ NK cells in HIV-1$^+$ individuals is related to a concomitant HCMV infection (Gumá *et al.*, 2006). Yet, the frequency of CD57$^+$/NKG2C$^+$ NK cells was shown to be higher in HCMV seropositive co-infected with HIV-1 than HCMV

seropositive individuals without HIV-1 infection (Mela *et al.*, 2007), suggesting that HIV-1 infection either drives the expansion of HCMV-induced NKG2C$^+$ NK cell subsets or favors reactivation of HCMV, leading to an expansion of the NKG2C$^+$ NK cell population. Hantavirus-infected individuals had an elevated level of NKG2C$^+$ NK cells but no detectable levels HCMV DNA in their plasma and no increased numbers of HCMV-specific CD8$^+$ cells (Björkström *et al.*, 2011), indicating that other virus can also drive the expansion of the NKG2C$^+$ NK cell subset. Unfortunately, data on HCMV status of the HIV-1$^+$ cohort presented in this thesis was not available so that predictions or associations between NKG2C$^+$ NK cells, HIV-1 infection and HCMV status were not possible. NKG2C$^+$ NK cells have been linked to NK cell memory and antigen specific memory NK cells were first described in mice with murine cytomegalovirus (MCMV) infection (Sun *et al.*, 2009). Since then, memory-like NK cell responses have also been reported in humans and non-human primates. A study with SHIV-infected and SIV-infected macaques found that splenic and hepatic NK cells lysed Gag- and Env-pulsed dendritic cells in an NKG2C-dependent manner, in contrast to NK cells from uninfected macaques (Reeves *et al.*, 2015).

The observed NKG2 receptor expression switch from the inhibitory to the activating NKG2 receptors has been previously described not only for HIV-1 (Mela *et al.*, 2005) and HCMV (Foley, Cooley, Verneris, Pitt, *et al.*, 2012) but also for HBV, HCV (Oliviero *et al.*, 2009) and chikungunya virus infection (Petitdemange *et al.*, 2011). NKG2A and NKG2C form heterodimers with CD94, both recognizing the non-classical HLA class I molecule HLA-E, which plays a specialized role in NK cell recognition (Braud *et al.*, 1998). HLA-E binds a restricted subset of leader peptides derived from sequences of HLA-A, -B, -C and -G or pathogens (Braud *et al.*, 1997; Lee *et al.*, 1998). Engagement of HLA-E by the inhibitory NKG2A prevents NK cell activation, whereas binding of the activating NKG2C to HLA-E results in NK cell activation. Although several studies have shown a decreased frequency of NKG2A$^+$ NK cells and an increased frequency of NKG2C in HIV-1 infection (Mavilio *et al.*, 2003; Mela *et al.*, 2005), analysis of NK cell subsets of HIV-1$^+$ individuals at different stages of disease progression revealed an increase of cytotoxic NKG2A$^+$ NK cells within patients with advanced clinical status (Zhang *et al.*, 2007). In the context of HIV-1 immune escape, HLA-E surface expression level has been reported to vary substantially between HIV-1 strains with unchanged (Bonaparte *et al.*, 2004), increased (Nattermann *et al.*, 2005) or also decreased (van Stigt Thans *et al.*, 2019) expression on HIV-1 infected cells. However, beneficial effects and the influence of certain immune pressures on HLA-E modulation by HIV-1 need further investigation.

Discussion

Analysis of KIR$^+$ NK cells within the HIV-1$^+$ cohort revealed a decreased frequency of the activating receptors KIR2DS1 and KIR2DS4, whereas inhibitory receptors KIR2DL1 and KIR2DL2/L3 showed no changes in NK cell expression profile when comparing HIV-1$^+$ and HIV-1$^-$ individuals. Previous studies have investigated KIR expression profiles in HIV-1 infection and their impact on disease progression. Chronically and treatment-naïve HIV-1$^+$ individuals in South Africa had a decreased expression of KIR2DL1 and KIR2DS1, which was associated with increased HIV-1 viral load (Wong *et al.*, 2010). Another study of chronic HIV-1 infection showed that full-length KIR2DS4 promoted HIV-1 pathogenesis possibly through the maintenance of an excessively pro-inflammatory state (Merino *et al.*, 2014). Several gene-association studies have linked *KIR* genes, including *KIR2DS4* (Hong *et al.*, 2013), *KIR2DL2* (Mhandire *et al.*, 2016) and *KIR2DL3* (Naranbhai *et al.*, 2016) with differential outcomes of HIV-1 infection. Combined effects of HLA and KIR variants have been reported to influence NK cell education and function in association with effects on HIV-1 infection. For example, KIR3DL1 and KIR3DS1 in combination with their putative ligand, an *HLA-B* allele with isoleucine at position 80 (HLA-Bw4-80I), have been shown to be associated to slower disease progression (Martin *et al.*, 2002). Additionally, it was shown that KIR3DS1$^+$ and KIR3DL1$^+$ NK cells selectively expand during acute HIV-1 infection in individuals positive for HLA-B Bw4-80I demonstrating for the first time an HLA class I subtype dependent expansion of KIR$^+$ NK cells in an acute viral infection in humans (Alter *et al.*, 2009). While *HLA-B* alleles have been described as an important determinant of HIV-1 disease progression, there is less information about HLA-C. A Genome Wide Association Study (GWAS) identified a SNP in the 5' region of HLA-C, which explains 6.5% variation in set point viral load in the study population (Fellay *et al.*, 2007) and high HLA-C expression on T cells was associated with lower viral loads, indicating an important role for HLA-C in direct HIV-1 control (Thomas *et al.*, 2009). Also, genetic combination of *KIR2DL* and *HLA-C* have been shown to be relevant for HIV-1 progression (Lin *et al.*, 2016; Mhandire *et al.*, 2018). Stratification of KIR2DL1/L2 and L3 frequency based on the *HLA-C* and *KIR2DL* genotypes indicated that HIV-1 infection changes the proportion of KIR2DL$^+$ NK cells within the NK cell repertoire pre-determined by the *HLA-C* genotype. The frequency of KIR2DL1$^+$ NK cells was associated with the number of cognate *HLA-C2* alleles, in line with previous studies of individuals with HIV-1 infection (Körner *et al.*, 2014). The increased frequency is potentially linked to a higher surface expression of the respective HLA-C2 ligand. Furthermore, linking the results from the KIR2DL-Fc/HLA-C binding assays with the frequency of KIR2DL1$^+$ NK cells of HIV-1$^+$ individuals revealed a positive correlation between both determinants. However, correlations between KIR2DL frequency on bulk NK cells with viral load or absolute CD4 T cell count showed no influence of KIR2DL$^+$ NK cells on these parameter of HIV-1 infection.

Taken together, most *KIR* gene association studies focus on absence and presence of *KIR* genes. However, *KIR2DL1* and *KIR2DL2/L3* genes are present in the majority of humans, *KIR* genes and also *HLA* genes are highly polymorphic making *KIR* and *HLA* combinations highly diverse. Every combination of KIR2DL/HLA-C displays a differential binding affinity and therefore impacts NK cell function. Moreover, not only do receptor and ligand combinations influence NK cell activation, the presented peptide is also relevant for NK cell function. All factors together need to be taken into account and make it challenging to develop a prediction model for HIV-1 disease progression.

Finally, a detailed analysis of CD56 NK cell subsets revealed a significant decrease of $CD56^{bright}$ but increase in $CD56^{negative}$ NK cells. It has been previously reported that viral infections, including HCMV and HIV-1 are linked to a pathological redistribution of NK cell subsets, in particular the presence of dysfunctional $CD56^{negative}$ NK cells. It is still under debate where $CD56^{negative}$ NK cell subsets during HIV-1 infection originate from. Indeed, associations between high frequencies of $CD56^{negative}$ NK cell subsets in the presence of chronic and systemic inflammation in HIV-1 infection have been made (Fauci *et al.*, 2005; Jost *et al.*, 2013). Moreover, high levels of viremia negatively influence NK cell function and thereby contribute to a defective viral control and HIV-1 disease progression due to a reduced INF-γ and TNF-α secretion, as well as decreased expression of granzyme B and perforin in $CD56^{negative}$ NK cells (Cao *et al.*, 2022).

The accessory HIV protein Nef mediates HLA-A and -B downmodulation to prevent recognition by CD8 T cells (Roeth *et al.*, 2004). In addition, Nef also mediates CD4 (Ross *et al.*, 1999) and CXCR4 (Venzke *et al.*, 2006) downmodulation and enhances viral replication and infectivity (Münch *et al.*, 2007). HLA-C surface expression is manipulated by the accessory HIV-1 protein Vpu to different extents (Apps *et al.*, 2016), which impairs adaptive as well as innate antiviral immune responses (Apps *et al.*, 2016; Körner *et al.*, 2017). Another function of Vpu is to counteract the host restriction factor tetherin, which prevents the budding process of newly formed virions from the cell surface (McNatt *et al.*, 2013). Vpu also suppresses the cellular antiviral immune response through the inhibition of NFκB (Hotter *et al.*, 2017). *Vpu* is one of the most variable regions in the HIV-1 genome with high variations in different genetic subtypes and primary isolates that explain subtype-specific differences in biological activity of the distinct HIV-1 strains (Lee *et al.*, 2000; Yusim *et al.*, 2002; Pacyniak *et al.*, 2005). To gain an understanding of selection pressures and resulting viral immune evasion of HIV-1 targeting HLA-C surface expression, Bachtel *et al.* characterized HLA-C downregulation in primary HIV-1 infection (Bachtel *et al.*, 2018) and showed that the capacity of Vpu to downmodulate HLA-C levels varies due to an adaptation to the host *HLA-C* genotype. Moreover, they identified five amino acid positions at which

specific residues were associated with HLA-C modulation. In this thesis, high HLA-C allele expression in HIV-1$^+$ individuals was associated with a higher frequency of proline at position 3 compared to other amino acid residues at this position, whereas the other amino acid positions showed no correlation with HLA-C allele expression level. Analysis of *KIR2DL/HLA-C* genotypes and binding affinities on Vpu sequence polymorphism revealed an increased frequency of glycine or threonine at amino acid position 16 in individuals with strong HLA-C/KIR2DL binding combinations in comparison to other amino acid residues at this position. This observation might be an indication that binding affinities of different HLA-C/KIR2DL combinations influence Vpu sequence polymorphisms. This high variability of HLA-C downregulation is possibly attributed to a viral adaptation to different immune responses. Downregulation of HLA-C results in an inhibition of HLA-C restricted CTL response, but also leads to NK cell activation. Analysis of HLA-C revealed a strong downregulation of HLA-C in one third of the infectious Vpu clones. Two third of the Vpu clones showed only weak HLA-C downregulation, suggesting an advantage of the virus to preserve HLA-C expression (Bachtel *et al.*, 2018). Stratification of HLA-C alleles by presence of C1 and C2 alleles revealed no differences in the frequency of Vpu clones that strongly downregulate HLA-C. However, strong HLA-C downregulation was previously associated with high HLA-C surface expression level (Körner *et al.*, 2017; Bachtel *et al.*, 2018). The observed association of high HLA-C expressed HLA-C alleles and strong HLA-C/KIR2DL binding combinations with amino acid residue that are involved in HLA-C downregulation is potentially a mechanism of HIV-1 to find a “sweet spot” to avoid CTL as well as NK cell immune response. Downregulation of high HLA-C alleles reduces CTL response but still prevents NK cell activation. In addition, downregulation of HLA-C with strong KIR2DL binding affinities possibly still results in NK cell inhibition, whereas NK cells with weak HLA-C/KIR2DL combinations are more sensitive to alterations in HLA-C surface expression.

Although, due to the high diversity of HLA-C and KIR2DL and ambiguity of the *KIR* allele typing there is a certain ambiguity of these findings and the influence of HLA-C/KIR2DL combinations on Vpu sequences needs further investigation within larger cohorts of HIV-1 infected individuals. The enormous variance of HLA-C and KIR combinations and binding affinities and the impact on NK cell activity and resulting immune evasion strategies of HIV-1 make it challenging to create a prediction model for specific Vpu sequence polymorphisms and consequences on the anti-HIV-1 activity of NK cells based on *HLA-C/KIR2DL* genotype combinations. Regardless, the generated results of this thesis indicate that KIR2DL$^+$ NK cells are involved in the intrinsic control of HIV-1.

In summary, the aim of this thesis was to gain a deeper understanding of the complex interplay between *KIR2DL/HLA-C* immunogenetics and resulting consequences of anti-HIV-1 activity of NK cells as well as HIV-1 induced changes in NK cell receptor repertoire. Moreover, Vpu sequence polymorphisms induced by *KIR2DL/HLA-C* genotype combinations were analyzed as a possible HIV-1 immune escape mechanism. Altogether, this thesis demonstrated that HIV-1 infection shapes NK cell receptor expression and influences the KIR2DL NK cell repertoire depending on the underlying *KIR2DL/HLA-C* genotype. Additionally, the results indicate that binding affinities of KIR2DL/HLA-C allotype combinations impact Vpu-associated viral escape.

References

Abel, A.M., Yang, C., Thakar, M.S. and Malarkannan, S. (2018) 'Natural Killer Cells: Development, Maturation, and Clinical Utilization', *Frontiers in Immunology*, 9(AUG), p. 1869.

Ahmad, F., Hong, H.S., *et al.* (2014) 'High Frequencies of Polyfunctional CD8 + NK Cells in Chronic HIV-1 Infection Are Associated with Slower Disease Progression', *Journal of Virology*, 88(21), pp. 12397–12408.

Ahmad, R., Sindhu, S.T.A.K., *et al.* (2001) 'Modulation of expression of the MHC class I-binding natural killer cell receptors, and NK activity in relation to viral load in HIV-infected/AIDS patients.', *Journal of medical virology*, 65(3), pp. 431–40.

Alberts B, Johnson A, Lewis J, *et al*. (2002) Molecular Biology of the Cell. 4th edition. New York: Garland Science. Chapter 24, The Adaptive Immune System

Alter, G., Heckerman, D., *et al.* (2011) 'HIV-1 adaptation to NK-cell-mediated immune pressure', *Nature*, 476(7358), pp. 96–101.

Alter, G., Malenfant, J.M. and Altfeld, M. (2004) 'CD107a as a functional marker for the identification of natural killer cell activity', *Journal of Immunological Methods*, 294(1–2), pp. 15–22.

Alter, G., Martin, M.P., *et al.* (2007) 'Differential natural killer cell-mediated inhibition of HIV-1 replication based on distinct KIR/HLA subtypes', *The Journal of experimental medicine*, 204(12), pp. 3027–3036.

Alter, G., Rihn, S., *et al.* (2009) 'HLA class I subtype-dependent expansion of KIR3DS1+ and KIR3DL1+ NK cells during acute human immunodeficiency virus type 1 infection', *Journal of virology*, 83(13), pp. 6798–6805.

Anfossi, N., André, P., *et al.* (2006) 'Human NK cell education by inhibitory receptors for MHC class I', *Immunity*, 25(2), pp. 331–342.

Apps, R., Meng, Z., *et al.* (2015) 'Relative Expression Levels of the HLA Class-I Proteins in Normal and HIV-Infected Cells', *The Journal of Immunology*, 194(8), pp. 3594–3600.

Apps, R., Del Prete, G.Q., *et al.* (2016) 'HIV-1 Vpu Mediates HLA-C Downregulation', *Cell Host and Microbe*, 19(5), pp. 686–695.

Apps, R., Qi, Y., *et al.* (2013) 'Influence of HLA-C expression level on HIV control', *Science*, 340(6128), pp. 87–91.

References

Arts, E.J. and Hazuda, D.J. (2012) 'HIV-1 Antiretroviral Drug Therapy', *Cold Spring Harbor Perspectives in Medicine*, 2(4), p. a007161.

De Baar, M.P., Van Der Horn, K.H.M., *et al.* (1999) 'Detection of human immunodeficiency virus type 1 nucleocapsid protein p7 in vitro and in vivo', *Journal of clinical microbiology*, 37(1), pp. 63–67.

Bachtel, N.D., Umviligihozo, G., *et al.* (2018) 'HLA-C downregulation by HIV-1 adapts to host HLA genotype', *PLoS Pathogens*, 14(9), p. e1007257

Barel, M.T., Ressing, M., *et al.* (2003) 'Human Cytomegalovirus-Encoded US2 Differentially Affects Surface Expression of MHC Class I Locus Products and Targets Membrane-Bound, but Not Soluble HLA-G1 for Degradation', *The Journal of Immunology*, 171(12), pp. 6757–6765.

Barré-Sinoussi, F., Chermann, J.C., *et al.* (1983) 'Isolation of a T-lymphotropic retrovirus from a patient at risk for acquired immune deficiency syndrome (AIDS)', *Science (New York, N.Y.)*, 220(4599), pp. 868–871.

Basmaciogullari, S. and Pizzato, M. (2014) 'The activity of Nef on HIV-1 infectivity', *Frontiers in Microbiology*, 5.

Beilhartz, G.L. and Götte, M. (2010) 'HIV-1 Ribonuclease H: Structure, Catalytic Mechanism and Inhibitors', *Viruses*, 2(4), p. 900.

Berg, M.G., Olivo, A., *et al.* (2021) 'A high prevalence of potential HIV elite controllers identified over 30 years in Democratic Republic of Congo', *EBioMedicine*, 65, p. 103258.

Biassoni, R., Pessino, A., *et al.* (1997) 'Role of amino acid position 70 in the binding affinity of p50.1 and p58.1 receptors for HLA-Cw4 molecules.', *European journal of immunology*, 27(12), pp. 3095–9.

Björkström, N.K., Lindgren, T., *et al.* (2011) 'Rapid expansion and long-term persistence of elevated NK cell numbers in humans infected with hantavirus', *Journal of Experimental Medicine*, 208(1), pp. 13–21.

Björkström, N.K., Ljunggren, H.G. and Michaëlsson, J. (2016) 'Emerging insights into natural killer cells in human peripheral tissues', *Nature reviews. Immunology*, 16(5), pp. 310–320.

Björkström, N.K., Ljunggren, H.G. and Sandberg, J.K. (2010) 'CD56 negative NK cells: origin, function, and role in chronic viral disease', *Trends in Immunology*, 31(11), pp. 401–406.

References

Blais, M.-E., Zhang, Y., *et al.* (2012) 'High Frequency of HIV Mutations Associated with HLA-C Suggests Enhanced HLA-C–Restricted CTL Selective Pressure Associated with an AIDS-Protective Polymorphism', *The Journal of Immunology*, 188(9), pp. 4663–4670.

Blissard, G.W. and Rohrmann, G.F. (1989) 'Location, sequence, transcriptional mapping, and temporal expression of the gp64 envelope glycoprotein gene of the Orgyia pseudotsugata multicapsid nuclear polyhedrosis virus', *Virology*, 170(2), pp. 537–555.

Blissenbach, M., Grewe, B., *et al.* (2010) 'Nuclear RNA export and packaging functions of HIV-1 Rev revisited', *Journal of virology*, 84(13), pp. 6598–6604.

Blokhuis, J.H., Hilton, H.G., *et al.* (2017) 'KIR2DS5 allotypes that recognize the C2 epitope of HLA-C are common among Africans and absent from Europeans.', *Immunity, inflammation and disease*, 5(4), pp. 461–468.

Bonaparte, M.I. and Barker, E. (2004) 'Killing of human immunodeficiency virus-infected primary T-cell blasts by autologous natural killer cells is dependent on the ability of the virus to alter the expression of major histocompatibility complex class I molecules', *Blood*, 104(7), pp. 2087–2094.

Boudreau, J.E. and Hsu, K.C. (2018) 'Natural Killer Cell Education and the Response to Infection and Cancer Therapy: Stay Tuned.', *Trends in immunology*, 39(3), pp. 222–239.

Boudreau, J.E., Mulrooney, T.J., *et al.* (2016) 'KIR3DL1 and HLA-B Density and Binding Calibrate NK Education and Response to HIV', *The Journal of Immunology*, 196(8), pp. 3398–3410.

Braud, V., Jones, E.Y. and McMichael, A. (1997) 'The human major histocompatibility complex class Ib molecule HLA-E binds signal sequence-derived peptides with primary anchor residues at positions 2 and 9', *European journal of immunology*, 27(5), pp. 1164–1169.

Braud, V.M., Allan, D.S.J., *et al.* (1998) 'HLA-E binds to natural killer cell receptors CD94/NKG2A, B and C', *Nature*, 391(6669), pp. 795–799.

Brostjan, C., Sobanov, Y., *et al.* (2000) 'The NKG2 natural killer cell receptor family: comparative analysis of promoter sequences', *Genes and immunity*, 1(8), pp. 504–508.

Bryceson, Y.T., March, M.E., Ljunggren, H.G. and Long, E.O. (2006) 'Activation, coactivation, and costimulation of resting human natural killer cells', *Immunological reviews*, 214(1), pp. 73–91.

Caligiuri, M.A. (2008) 'Human natural killer cells', *Blood*, 112(3), pp. 461–469.

Cannell, I.G., Kong, Y.W. and Bushell, M. (2008) 'How do microRNAs regulate gene expression?', *Biochemical Society Transactions*, 36(6), pp. 1224–1231.

References

Cannon, P.M., Matthews, S., *et al.* (1997) 'Structure-function studies of the human immunodeficiency virus type 1 matrix protein, p17', *Journal of virology*, 71(5), pp. 3474–3483.

Cao, W.J., Zhang, X.C., *et al.* (2022) 'Immune Dysfunctions of CD56 neg NK Cells Are Associated With HIV-1 Disease Progression', *Frontiers in immunology*, 12.

Carey, B.S., Poulton, K.V. and Poles, A. (2019) 'Factors affecting HLA expression: A review', *International Journal of Immunogenetics*, 46(5), pp. 307–320.

Chan, D.C. and Kim, P.S. (1998) 'HIV Entry and Its Inhibition', *Cell*, 93(5), pp. 681–684.

Chaplin, D.D. (2010) 'Overview of the immune response', *Journal of Allergy and Clinical Immunology*, 125(2), pp. S3–S23.

Cibrián, D. and Sánchez-Madrid, F. (2017) 'CD69: from activation marker to metabolic gatekeeper', *European journal of immunology*, 47(6), pp. 946–953.

Cohen, E.A., Terwilliger, E.F., Sodroski, J.G. and Haseltine, W.A. (1988) 'Identification of a protein encoded by the vpu gene of HIV-1', *Nature*, 334(6182), pp. 532–534.

Cohn, L.B., Chomont, N. and Deeks, S.G. (2020) 'The Biology of the HIV-1 Latent Reservoir and Implications for Cure Strategies', *Cell Host & Microbe*, 27(4), pp. 519–530.

Collins, K.L., Chen, B.K., *et al.* (1998) 'HIV-1 Nef protein protects infected primary cells against killing by cytotoxic T lymphocytes.', *Nature*, 391(6665), pp. 397–401.

Craigie, R. and Bushman, F.D. (2012) 'HIV DNA integration.', *Cold Spring Harbor perspectives in medicine*, 2(7), p. a006890.

Cresswell, P., Bangia, N., Dick, T. and Diedrich, G. (1999) 'The nature of the MHC class I peptide loading complex.', *Immunological reviews*, 172, pp. 21–8.

Van Damme, N., Goff, D., *et al.* (2008) 'The interferon-induced protein BST-2 restricts HIV-1 release and is downregulated from the cell surface by the viral Vpu protein', *Cell host & microbe*, 3(4), pp. 245–252.

Das, A.T., Harwig, A. and Berkhout, B. (2011) 'The HIV-1 Tat protein has a versatile role in activating viral transcription', *Journal of virology*, 85(18), pp. 9506–9516

.

Davis, M.M. and Bjorkman, P.J. (1988) 'T-cell antigen receptor genes and T-cell recognition', *Nature*, 334(6181), pp. 395–402.

References

Davis, Z.B., Ward, J.P. and Barker, E. (2011) 'Preparation and Use of HIV-1 Infected Primary CD4+ T-Cells as Target Cells in Natural Killer Cell Cytotoxic Assays', *Journal of Visualized Experiments*, (49).

Davis, Z.B., Cogswell, A., *et al.* (2016) 'A Conserved HIV-1-Derived Peptide Presented by HLA-E Renders Infected T-cells Highly Susceptible to Attack by NKG2A/CD94-Bearing Natural Killer Cells',PLOS PATHOGENS, 12(2), p. e1005421.

Dazza, M.-C., Ekwalanga, M., *et al.* (2005) 'Characterization of a novel vpu-harboring simian immunodeficiency virus from a Dent's Mona monkey (Cercopithecus mona denti)', *Journal of virology*, 79(13), pp. 8560–8571.

Dean, M., Carrington, M., *et al.* (1996) 'Genetic restriction of HIV-1 infection and progression to AIDS by a deletion allele of the CKR5 structural gene. Hemophilia Growth and Development Study, Multicenter AIDS Cohort Study, Multicenter Hemophilia Cohort Study, San Francisco City Cohort, ALIVE Study', *Science (New York, N.Y.)*, 273(5283), pp. 1856–1862.

Deeks, S.G., Overbaugh, J., Phillips, A. and Buchbinder, S. (2015) 'HIV infection', *Nature Reviews Disease Primers*, 1(1), p. 15035.

Demirov, D.G., Orenstein, J.M. and Freed, E.O. (2002) 'The late domain of human immunodeficiency virus type 1 p6 promotes virus release in a cell type-dependent manner', *Journal of virology*, 76(1), pp. 105–117.

Elboim, M., Grodzovski, I., *et al.* (2013) 'HSV-2 specifically down regulates HLA-C expression to render HSV-2-infected DCs susceptible to NK cell killing', *PLoS pathogens*, 9(3).
Elliott, J.M. and Yokoyama, W.M. (2011) 'Unifying concepts of MHC-dependent natural killer cell education', *Trends in immunology*, 32(8), pp. 364–372.

Estefanía, E., Gómez-Lozano, N., *et al.* (2007) 'Influence of KIR gene diversity on the course of HSV-1 infection: resistance to the disease is associated with the absence of KIR2DL2 and KIR2DS2', *Tissue antigens*, 70(1), pp. 34–41.

Fadda, L., Körner, C., *et al.* (2012) 'HLA-Cw*0102-restricted HIV-1 p24 epitope variants can modulate the binding of the inhibitory KIR2DL2 receptor and primary NK cell function', *PLoS Pathogens*, 8(7), p. 40.

Falk, C.S. and Schendel, D.J. (1997) 'HLA-C revisited. Ten years of change', *Immunologic Research*, 16(2), pp. 203–214.

References

Farmery, M.R., Allen, S., Allen, A.J. and Bulleid, N.J. (2000) 'The role of ERp57 in disulfide bond formation during the assembly of major histocompatibility complex class I in a synchronized semipermeabilized cell translation system.', *The Journal of biological chemistry*, 275(20), pp. 14933–8.

Fauci, A.S., Mavilio, D. and Kottilil, S. (2005) 'NK cells in HIV infection: paradigm for protection or targets for ambush', *Nature reviews. Immunology*, 5(11), pp. 835–843.

Federau, T., Schubert, U., *et al.* (1996) 'Solution structure of the cytoplasmic domain of the human immunodeficiency virus type 1 encoded virus protein U (Vpu)', *International journal of peptide and protein research*, 47(4), pp. 297–310.

Fellay, J., Ge, D., *et al.* (2009) 'Common Genetic Variation and the Control of HIV-1 in Humans', *PLOS Genetics*, 5(12), p. e1000791.

Fellay, J., Shianna, K. V., *et al.* (2007) 'A whole-genome association study of major determinants for host control of HIV-1', *Science*, 317(5840), pp. 944–947.

Feng, Y., Broder, C.C., Kennedy, P.E. and Berger, E.A. (1996) 'HIV-1 Entry Cofactor: Functional cDNA Cloning of a Seven-Transmembrane, G Protein-Coupled Receptor', *Science*, 272(5263), pp. 872–877.

Foley, B., Cooley, S., Verneris, M.R., Pitt, M., *et al.* (2012) 'Cytomegalovirus reactivation after allogeneic transplantation promotes a lasting increase in educated NKG2C + natural killer cells with potent function', *Blood*, 119(11), pp. 2665–2674.

Foley, B., Cooley, S., Verneris, M.R., Curtsinger, J., *et al.* (2012) 'Human Cytomegalovirus (CMV)-Induced Memory-like NKG2C + NK Cells Are Transplantable and Expand In Vivo in Response to Recipient CMV Antigen', *The Journal of Immunology*, 189(10), pp. 5082–5088.

Gaardbo, J.C., Hartling, H.J., Gerstoft, J. and Nielsen, S.D. (2012) 'Thirty Years with HIV Infection—Nonprogression Is Still Puzzling: Lessons to Be Learned from Controllers and Long-Term Nonprogressors', *AIDS Research and Treatment*, 2012.

Le Gall, S., Erdtmann, L., *et al.* (1998) 'Nef interacts with the μ subunit of clathrin adaptor complexes and reveals a cryptic sorting signal in MHC I molecules', *Immunity*, 8(4), pp. 483–495.

Gallo, R.C., Sarin, P.S., *et al.* (1983) 'Isolation of Human T-Cell Leukemia Virus in Acquired Immune Deficiency Syndrome (AIDS)', *Science*, 220(4599), pp. 865–867.

References

Gobin, S.J., Peijnenburg, A., Keijsers, V. and van den Elsen, P.J. (1997) 'Site α Is Crucial for Two Routes of IFNγ-Induced MHC Class I Transactivation: The ISRE-Mediated Route and a Novel Pathway Involving CIITA', *Immunity*, 6(5), pp. 601–611.

Gobin, S.J., Keijsers, V., van Zutphen, M. and van den Elsen, P.J. (1998) 'The role of enhancer A in the locus-specific transactivation of classical and nonclassical HLA class I genes by nuclear factor kappa B.', *Journal of immunology*, 161(5), pp. 2276–83.

González, M. (2015) 'Vpu Protein: The Viroporin Encoded by HIV-1', *Viruses*, 7(8), pp. 4352–4368.
Gonzalez, M.E. and Carrasco, L. (2003) 'Viroporins', *FEBS letters*, 552(1), pp. 28–34.

Goodridge, J.P., Jacobs, B., *et al.* (2019) 'Remodeling of secretory lysosomes during education tunes functional potential in NK cells', *Nature communications*, 10(1), p. 514

Gottlieb, M.S., Schroff, R., *et al.* (1981) 'Pneumocystis carinii pneumonia and mucosal candidiasis in previously healthy homosexual men: evidence of a new acquired cellular immunodeficiency', *The New England journal of medicine*, 305(24), pp. 1425–1431.

Graef, T., Moesta, A.K., *et al.* (2009) 'KIR2DS4 is a product of gene conversion with KIR3DL2 that introduced specificity for HLA-A*11 while diminishing avidity for HLA-C.', *The Journal of experimental medicine*, 206(11), pp. 2557–72.

Gratama, J.W., Kluin-Nelemans, H.C., *et al.* (1988) 'Flow cytometric and morphologic studies of HNK1+ (Leu 7+) lymphocytes in relation to cytomegalovirus carrier status.', *Clinical and experimental immunology*, 74(2), pp. 190–5.

Gu, Y., Cao, F., *et al.* (2013) 'Structure of a Novel Shoulder-to-Shoulder p24 Dimer in Complex with the Broad-Spectrum Antibody A10F9 and Its Implication in Capsid Assembly', *PLoS ONE*, 8(4), p. e61314.

Gulnik, S., Erickson, J.W. and Xie, D. (2000) 'HIV protease: enzyme function and drug resistance', *Vitamins and hormones*, 58, pp. 213–256.

Gumá, M., Angulo, A., *et al.* (2004) 'Imprint of human cytomegalovirus infection on the NK cell receptor repertoire', *Blood*, 104(12), pp. 3664–3671.

Gumá, M., Cabrera, C., *et al.* (2006) 'Human cytomegalovirus infection is associated with increased proportions of NK cells that express the CD94/NKG2C receptor in aviremic HIV-1-positive patients.', *The Journal of infectious diseases*, 194(1), pp. 38–41.

He, Y. and Tian, Z. (2017) 'NK cell education via nonclassical MHC and non-MHC ligands', *Cellular & molecular immunology*, 14(4), pp. 321–330.

References

Higgins, C.F. (1992) 'ABC Transporters: From Microorganisms to Man', *Annual Review of Cell Biology*, 8(1), pp. 67–113.

Hilton, Hugo G., Guethlein, L.A., *et al.* (2015) 'Polymorphic HLA-C Receptors Balance the Functional Characteristics of KIR Haplotypes', *The Journal of Immunology*, 195(7), pp. 3160–3170.

Hilton, Hugo G, Moesta, A.K., *et al.* (2015) 'The production of KIR-Fc fusion proteins and their use in a multiplex HLA class I binding assay', *Journal of Immunological Methods*, 425, pp. 79–87.

Hilton, H.G., Vago, L., *et al.* (2012) 'Mutation at Positively Selected Positions in the Binding Site for HLA-C Shows That KIR2DL1 Is a More Refined but Less Adaptable NK Cell Receptor Than KIR2DL3', *The Journal of Immunology*, 189(3), pp. 1418–1430.

Hoffman, W., Lakkis, F.G. and Chalasani, G. (2016) 'B Cells, Antibodies, and More', *Clinical Journal of the American Society of Nephrology*, 11(1), pp. 137–154.

Hölzemer, A., Thobakgale, C.F., *et al.* (2015) 'Selection of an HLA-C*03:04-Restricted HIV-1 p24 Gag Sequence Variant Is Associated with Viral Escape from KIR2DL3+ Natural Killer Cells: Data from an Observational Cohort in South Africa', *PLoS Medicine*, 12(11), pp. 1–27.

Hong, H.A., Paximadis, M., *et al.* (2013) 'KIR2DS4 allelic variants: Differential effects on in utero and intrapartum HIV-1 mother-to-child transmission', *Clinical Immunology*, 149(3), pp. 498–508.

Hong, H.S., Eberhard, J.M., *et al.* (2010) 'HIV infection is associated with a preferential decline in less-differentiated CD56dim CD16+ NK cells', *Journal of virology*, 84(2), pp. 1183–1188.

Hopfensperger, K., Richard, J., *et al.* (2020) 'Convergent Evolution of HLA-C Downmodulation in HIV-1 and HIV-2', *mBio*, 11(4), pp. 1–19.

Horowitz, A., Strauss-Albee, D.M., *et al.* (2013) 'Genetic and Environmental Determinants of Human NK Cell Diversity Revealed by Mass Cytometry', *Science Translational Medicine*, 5(208).

Hotter, D., Krabbe, T., *et al.* (2017) 'Primate lentiviruses use at least three alternative strategies to suppress NF-κB-mediated immune activation', *PLOS Pathogens*, 13(8), p. e1006598

Hrimech, M., Yao, X.-J., *et al.* (1999) 'Human Immunodeficiency Virus Type 1 (HIV-1) Vpr Functions as an Immediate-Early Protein during HIV-1 Infection', *Journal of Virology*, 73(5), pp. 4101–4109.

Hsu, K.C., Chida, S., Geraghty, D.E. and Dupont, B. (2002) 'The killer cell immunoglobulin-like receptor (KIR) genomic region: gene-order, haplotypes and allelic polymorphism', *Immunological reviews*, 190, pp. 40–52.

References

Hsu, K.C., Liu, X.-R., *et al.* (2002) 'Killer Ig-like receptor haplotype analysis by gene content: evidence for genomic diversity with a minimum of six basic framework haplotypes, each with multiple subsets', *Journal of immunology (Baltimore, Md. : 1950)*, 169(9), pp. 5118–5129.

Hu, W.S. and Hughes, S.H. (2012) 'HIV-1 Reverse Transcription', *Cold Spring Harbor Perspectives in Medicine*, 2(10), p. a006882.

International HIV Controllers Study, Pereyra, F., *et al.* (2010) 'The Major Genetic Determinants of HIV-1 Control Affect HLA Class I Peptide Presentation', *Science*, 330(6010), pp. 1551–1557.

Iwabu, Y., Fujita, H., *et al.* (2009) 'HIV-1 accessory protein Vpu internalizes cell-surface BST-2/tetherin through transmembrane interactions leading to lysosomes', *The Journal of biological chemistry*, 284(50), pp. 35060–35072.

Jaeger, B.N. and Vivier, E. (2012) 'Natural killer cell tolerance: control by self or self-control?', *Cold Spring Harbor perspectives in biology*, 4(3), p. a007229.

Janeway CA Jr, Travers P, Walport M, et al. (2001) Immunobiology: The Immune System in Health and Disease. 5th edition. New York: Garland Science. The complement system and innate immunity.

Jennes, W., Verheyden, S., *et al.* (2006) 'Cutting Edge: Resistance to HIV-1 Infection among African Female Sex Workers Is Associated with Inhibitory KIR in the Absence of Their HLA Ligands', *The Journal of Immunology*, 177(10), pp. 6588–6592.

Jiang, W., Johnson, C., *et al.* (2012) 'Copy number variation leads to considerable diversity for B but not A haplotypes of the human KIR genes encoding NK cell receptors', *Genome research*, 22(10), pp. 1845–1854.

Jones, D.C., Edgar, R.S., *et al.* (2006) 'Killer Ig-like receptor (KIR) genotype and HLA ligand combinations in ulcerative colitis susceptibility', *Genes and immunity*, 7(7), pp. 576–582.

Jost, S. and Altfeld, M. (2013) 'Control of human viral infections by natural killer cells', *Annual review of immunology*, 31, pp. 163–194.

Kärre, K., Ljunggren, H.G., Piontek, G. and Kiessling, R. (1986) 'Selective rejection of H–2-deficient lymphoma variants suggests alternative immune defence strategy', *Nature*, 319(6055), pp. 675–678.
Kaur, G., Gras, S., *et al.* (2017) 'Structural and regulatory diversity shape HLA-C protein expression levels', *Nature Communications*, 8(1), p. 15924.

Khakoo, S.I., Thio, C.L., *et al.* (2004) 'HLA and NK cell inhibitory receptor genes in resolving hepatitis C virus infection', *Science*, 305(5685), pp. 872–874.

References

Kirchhoff, F. (2013) 'HIV Life Cycle: Overview', in *Encyclopedia of AIDS*. New York, NY: Springer New York, pp. 1–9.

Körner, C., Granoff, M.E., *et al.* (2014) 'Increased frequency and function of KIR2DL1-3^{+} NK cells in primary HIV-1 infection are determined by HLA-C group haplotypes.', *European journal of immunology*, 44(10), pp. 2938–48.

Körner, C., Simoneau, C.R., *et al.* (2017) 'HIV-1-Mediated Downmodulation of HLA-C Impacts Target Cell Recognition and Antiviral Activity of NK Cells.', *Cell host & microbe*, 22(1), pp. 111-119.

Kulkarni, S., Savan, R., *et al.* (2011) 'Differential microRNA regulation of HLA-C expression and its association with HIV control', *Nature*, 472(7344), pp. 495–498.

Kumar, H., Kawai, T. and Akira, S. (2011) 'Pathogen Recognition by the Innate Immune System', *International Reviews of Immunology*, 30(1), pp. 16–34.

Lanier, L.L. (2005) 'NK cell recognition', *Annual review of immunology*, 23, pp. 225–274.

Lanier, L.L., Corliss, B.C., *et al.* (1998) 'Immunoreceptor DAP12 bearing a tyrosine-based activation motif is involved in activating NK cells.', *Nature*, 391(6668), pp. 703–7.

Lee, C.N., Wang, W.K., *et al.* (2000) 'Determination of human immunodeficiency virus type 1 subtypes in Taiwan by vpu gene analysis', *Journal of clinical microbiology*, 38(7), pp. 2468–2474.

Lee, N., Goodlett, D.R., *et al.* (1998) 'HLA-E surface expression depends on binding of TAP-dependent peptides derived from certain HLA class I signal sequences.', *Journal of immunology*, 160(10), pp. 4951–60.

Li, H., Ivarsson, M.A., *et al.* (2018) 'Identification of an elaborate NK-specific system regulating HLA-C expression', *PLoS Genetics*, 14(1), pp. 1–19.

Lim, J.J., Grinstein, S. and Roth, Z. (2017) 'Diversity and Versatility of Phagocytosis: Roles in Innate Immunity, Tissue Remodeling, and Homeostasis.', *Frontiers in cellular and infection microbiology*, 7(MAY), p. 191.

Lin, Z., Kuroki, K., *et al.* (2016) 'HIV-1 Control by NK Cells via Reduced Interaction between KIR2DL2 and HLA-C∗12:02/C∗14:03', *Cell Reports*, 17(9), pp. 2210–2220.

Ljunggren, H.G. and Kärre, K. (1985) 'Host resistance directed selectively against H-2-deficient lymphoma variants. Analysis of the mechanism', *The Journal of experimental medicine*, 162(6), pp. 1745–1759.

References

Ljunggren, H.G. and Kärre, K. (1990) 'In search of the "missing self": MHC molecules and NK cell recognition', *Immunology Today*, 11(C), pp. 237–244.

Lopez-Vergès, S., Milush, J.M., *et al.* (2010) 'CD57 defines a functionally distinct population of mature NK cells in the human CD56dimCD16+ NK-cell subset', *Blood*, 116(19), pp. 3865–3874.

Magadán, J.G., Pérez-Victoria, F.J., *et al.* (2010) 'Multilayered mechanism of CD4 downregulation by HIV-1 Vpu involving distinct ER retention and ERAD targeting steps', *PLoS pathogens*, 6(4), pp. 1–18.

Malim, M.H., Hauber, J., *et al.* (1989) 'The HIV-1 rev trans-activator acts through a structured target sequence to activate nuclear export of unspliced viral mRNA', *Nature*, 338(6212), pp. 254–257.

Mandelboim, O., Reyburn, H.T., *et al.* (1996) 'Protection from lysis by natural killer cells of group 1 and 2 specificity is mediated by residue 80 in human histocompatibility leukocyte antigen C alleles and also occurs with empty major histocompatibility complex molecules.', *The Journal of experimental medicine*, 184(3), pp. 913–22.

Manohar, S.M., Shah, P. and Nair, A. (2021) 'Flow cytometry: principles, applications and recent advances', *Bioanalysis*, 13(3), pp. 185–202.

Margottin, F., Bour, S.P., *et al.* (1998) 'A novel human WD protein, h-beta TrCp, that interacts with HIV-1 Vpu connects CD4 to the ER degradation pathway through an F-box motif', *Molecular cell*, 1(4), pp. 565–574.

De Maria, A., Fogli, M., *et al.* (2003) 'The impaired NK cell cytolytic function in viremic HIV-1 infection is associated with a reduced surface expression of natural cytotoxicity receptors (NKp46, NKp30 and NKp44)', *European Journal of Immunology*, 33(9), pp. 2410–2418.

Martin, M.P., Gao, X., *et al.* (2002) 'Epistatic interaction between KIR3DS1 and HLA-B delays the progression to AIDS', *Nature Genetics*, 31(4), pp. 429–434.

Martin, M.P., Qi, Y., *et al.* (2007) 'Innate partnership of HLA-B and KIR3DL1 subtypes against HIV-1', *Nature genetics*, 39(6), pp. 733–740.

Mavilio, D., Benjamin, J., *et al.* (2003) 'Natural killer cells in HIV-1 infection: Dichotomous effects of viremia on inhibitory and activating receptors and their functional correlates', *Proceedings of the National Academy of Sciences*, 100(25), pp. 15011–15016.

Maxwell, L.D., Wallace, A., Middleton, D. and Curran, M.D. (2002) 'A common KIR2DS4 deletion variant in the human that predicts a soluble KIR molecule analogous to the KIR1D molecule observed in the rhesus monkey', *Tissue Antigens*, 60(3), pp. 254–258.

McNatt, M.W., Zang, T. and Bieniasz, P.D. (2013) 'Vpu binds directly to tetherin and displaces it from nascent virions', *PLoS pathogens*, 9(4), p. e1003299.

Mela, C.M., Burton, C.T., *et al.* (2005) 'Switch from inhibitory to activating NKG2 receptor expression in HIV-1 infection: lack of reversion with highly active antiretroviral therapy', *AIDS*, 19(16), pp. 1761–1769.

Mela, C.M. and Goodier, M.R. (2007) 'The Contribution of Cytomegalovirus to Changes in NK Cell Receptor Expression in HIV-1–Infected Individuals', *The Journal of Infectious Diseases*, 195(1), pp. 158–159.

Merino, A.M., Dugast, A.S., *et al.* (2014) 'KIR2DS4 promotes HIV-1 pathogenesis: new evidence from analyses of immunogenetic data and natural killer cell function', *PloS one*, 9(6), p. e99353.

Mhandire, K., Tshabalala, M., *et al.* (2018) 'HLA-C*18:01 and KIR2DL2+C1 genetic variants are associated with low viral load in cART naïve HIV-infected adult Zimbabweans', *Journal of Infection in Developing Countries*, 12(12), pp. 1105–1111.

Mhandire, K., Zijenah, L.S., *et al.* (2016) 'KIR Gene Content Diversity in a Zimbabwean Population: Does KIR2DL2 Have a Role in Protection Against Human Immunodeficiency Virus Infection?', *OMICS: A Journal of Integrative Biology*, 20(12), pp. 727–735.

Migueles, S.A., Osborne, C.M., *et al.* (2008) 'Lytic granule loading of CD8+ T cells is required for HIV-infected cell elimination associated with immune control', *Immunity*, 29(6), pp. 1009–1021.

Migueles, S.A., Sabbaghian, M.S., *et al.* (2000) 'HLA B*5701 is highly associated with restriction of virus replication in a subgroup of HIV-infected long term nonprogressors', *Proceedings of the National Academy of Sciences*, 97(6), pp. 2709–2714.

Mingari, M.C., Vitale, C., *et al.* (1995) 'Cytolytic T lymphocytes displaying natural killer (NK)-like activity: expression of NK-related functional receptors for HLA class I molecules (p58 and CD94) and inhibitory effect on the TCR-mediated target cell lysis or lymphokine production', *International immunology*, 7(4), pp. 697–703.

Moesta, A.K., Norman, P.J., *et al.* (2008) 'Synergistic Polymorphism at Two Positions Distal to the Ligand-Binding Site Makes KIR2DL2 a Stronger Receptor for HLA-C Than KIR2DL3', *The Journal of Immunology*, 180(6), pp. 3969–3979.

Mori, M., Leitman, E., *et al.* (2019) 'Impact of HLA Allele-KIR Pairs on HIV Clinical Outcome in South Africa', *Journal of Infectious Diseases*, 219(9), pp. 1456–1463.

Mori, M., Wichukchinda, N., *et al.* (2015) 'The effect of KIR2D–HLA-C receptor–ligand interactions on clinical outcome in a HIV-1 CRF01_AE-infected Thai population', *AIDS*, 29(13), pp. 1607–1615.

Münch, J., Rajan, D., *et al.* (2007) 'Nef-mediated enhancement of virion infectivity and stimulation of viral replication are fundamental properties of primate lentiviruses', *Journal of virology*, 81(24), pp. 13852–13864.

Naranbhai, V., Altfeld, M., *et al.* (2012) 'Natural killer cell function in women at high risk for HIV acquisition', *AIDS*, 26(14), pp. 1745–1753.

Naranbhai, V., Altfeld, M., *et al.* (2013) 'Changes in Natural Killer Cell Activation and Function during Primary HIV-1 Infection', *PLoS ONE*. 8(1), p. e53251.

Naranbhai, V., de Assis Rosa, D., *et al.* (2016) 'Killer-cell Immunoglobulin-like Receptor (KIR) gene profiles modify HIV disease course, not HIV acquisition in South African women', *BMC infectious diseases*, 16(1), p. 27.

Nattermann, J., Nischalke, H.D., *et al.* (2005) 'HIV-1 infection leads to increased HLA-E expression resulting in impaired function of natural killer cells', *Antiviral therapy*, 10(1), pp. 95–107.

Nedvetzki, S., Sowinski, S., *et al.* (2007) 'Reciprocal regulation of human natural killer cells and macrophages associated with distinct immune synapses', *Blood*, 109(9), pp. 3776–3785.

Neil, S.J.D. (2013) 'The antiviral activities of tetherin', *Current topics in microbiology and immunology*, 371, pp. 67–104.

Norman, P.J., Abi-Rached, L., *et al.* (2009) 'Meiotic recombination generates rich diversity in NK cell receptor genes, alleles, and haplotypes', *Genome research*, 19(5), pp. 757–769.

Oliviero, B., Varchetta, S., *et al.* (2009) 'Natural killer cell functional dichotomy in chronic hepatitis B and chronic hepatitis C virus infections', *Gastroenterology*, 137(3), pp. 1151-1160.

Otten, H.G., Verhaar, M.C., *et al.* (2013) 'The significance of pretransplant donor-specific antibodies reactive with intact or denatured human leucocyte antigen in kidney transplantation', *Clinical and Experimental Immunology*, 173(3), pp. 536–543.

Overbaugh, J. and Bangham, C.R.M. (2001) 'Selection Forces and Constraints on Retroviral Sequence Variation', *Science*, 292(5519), pp. 1106–1109.

References

Pacyniak, E., Gomez, M.L., *et al.* (2005) 'Identification of a Region within the Cytoplasmic Domain of the Subtype B Vpu Protein of Human Immunodeficiency Virus Type 1 (HIV-1) That Is Responsible for Retention in the Golgi Complex and Its Absence in the Vpu Protein from a Subtype C HIV-1', *AIDS Research and Human Retroviruses*, 21(5), pp. 379–394.

Paladino, N., Flores, A.C., *et al.* (2007) 'Increased frequencies of activating natural killer receptors are associated with liver injury in individuals who do not eliminate hepatitis C virus', *Tissue Antigens*, 69(SUPPL. 1), pp. 109–111.

Papúchová, H., Meissner, T.B., *et al.* (2019) 'The Dual Role of HLA-C in Tolerance and Immunity at the Maternal-Fetal Interface', *Frontiers in Immunology*, 10(December), pp. 1–14.

Parham, P. (2005) 'MHC class I molecules and KIRs in human history, health and survival.', *Nature reviews. Immunology*, 5(3), pp. 201–14.

Parham, P. and Moffett, A. (2013) 'Variable NK cell receptors and their MHC class I ligands in immunity, reproduction and human evolution.', *Nature reviews. Immunology*, 13(2), pp. 133–44.

Paximadis, M., Minevich, G., *et al.* (2011) 'KIR-HLA and maternal-infant HIV-1 transmission in sub-Saharan Africa.', *PloS one*, 6(2), p. e16541.

Pegram, H.J., Andrews, D.M., *et al.* (2011) 'Activating and inhibitory receptors of natural killer cells', *Immunology and cell biology*, 89(2), pp. 216–224.

Pelak, K., Need, A.C., *et al.* (2011) 'Copy number variation of KIR genes influences HIV-1 control', *PLoS biology*, 9(11), p. e1001208.

Pende, D., Falco, M., *et al.* (2019) 'Killer Ig-Like Receptors (KIRs): Their Role in NK Cell Modulation and Developments Leading to Their Clinical Exploitation', *Frontiers in immunology*, 10(MAY).

Pende, D., Parolini, S., *et al.* (1999) 'Identification and molecular characterization of NKp30, a novel triggering receptor involved in natural cytotoxicity mediated by human natural killer cells', *The Journal of experimental medicine*, 190(10), pp. 1505–1516.

Pennock, N.D., White, J.T., *et al.* (2013) 'T cell responses: naïve to memory and everything in between', *Advances in Physiology Education*, 37(4), pp. 273–283.

Petitdemange, C., Becquart, P., *et al.* (2011) 'Unconventional repertoire profile is imprinted during acute chikungunya infection for natural killer cells polarization toward cytotoxicity.', *PLoS pathogens*, 7(9), p. e1002268.

Pfeifer, C., Highton, A.J., *et al.* (2018) 'Natural Killer Cell Education Is Associated With a Distinct Glycolytic Profile', *Frontiers in Immunology*, 9, p. 3020.

Pickering, S., Hué, S., *et al.* (2014) 'Preservation of Tetherin and CD4 Counter-Activities in Circulating Vpu Alleles despite Extensive Sequence Variation within HIV-1 Infected Individuals', *PLoS Pathogens*, 10(1), p. e1003895.

Pornillos, O., Ganser-Pornillos, B.K. and Yeager, M. (2011) 'Atomic-level modelling of the HIV capsid', *Nature*, 469(7330), pp. 424–427.

Prabakaran, P., Dimitrov, A.S., Fouts, T.R. and Dimitrov, D.S. (2007) 'Structure and Function of the HIV Envelope Glycoprotein as Entry Mediator, Vaccine Immunogen, and Target for Inhibitors', in *Advances in Pharmacology*, pp. 33–97.

Pyo, C.W., Guethlein, L.A., *et al.* (2010) 'Different patterns of evolution in the centromeric and telomeric regions of group A and B haplotypes of the human killer cell Ig-like receptor locus', *PLOS ONE*, 5(12), p. e15115.

Raulet, D.H. and Vance, R.E. (2006) 'Self-tolerance of natural killer cells', *Nature reviews. Immunology*, 6(7), pp. 520–531.

Ravet, S., Scott-Algara, D., *et al.* (2007) 'Distinctive NK-cell receptor repertoires sustain high-level constitutive NK-cell activation in HIV-exposed uninfected individuals.', *Blood*, 109(10), pp. 4296–305.

Reeves, R.K., Li, Haiying, *et al.* (2015) 'Antigen-specific NK cell memory in rhesus macaques', *Nature immunology*, 16(9), pp. 927–932.

Renard, V., Cambiaggi, A., *et al.* (1997) 'Transduction of cytotoxic signals in natural killer cells: a general model of fine tuning between activatory and inhibitory pathways in lymphocytes', *Immunological reviews*, 155, pp. 205–221.

Roeth, J.F., Kasper, M.R., Filzen, T.M. and Collins, K.L. (2004) 'HIV-1 Nef disrupts MHC-I trafficking by recruiting AP-1 to the MHC-I cytoplasmic tail', *The Journal of cell biology*, 167(5), pp. 903–913.

Rose, K.M., Marin, M., Kozak, S.L. and Kabat, D. (2004) 'The viral infectivity factor (Vif) of HIV-1 unveiled', *Trends in molecular medicine*, 10(6), pp. 291–297.

Ross, T.M., Oran, A.E. and Cullen, B.R. (1999) 'Inhibition of HIV-1 progeny virion release by cell-surface CD4 is relieved by expression of the viral Nef protein', *Current Biology*, 9(12), pp. 613–621.

Salzwedel, K., West, J.T. and Hunter, E. (1999) 'A conserved tryptophan-rich motif in the membrane-proximal region of the human immunodeficiency virus type 1 gp41 ectodomain is important for Env-mediated fusion and virus infectivity', *Journal of virology*, 73(3), pp. 2469–2480.

Sauter, D., Schindler, M., *et al.* (2009) 'Tetherin-driven adaptation of Vpu and Nef function and the evolution of pandemic and nonpandemic HIV-1 strains', *Cell host & microbe*, 6(5), pp. 409–421.

Schiralli Lester, G.M. and Henderson, A.J. (2012) 'Mechanisms of HIV Transcriptional Regulation and Their Contribution to Latency', *Molecular Biology International*, 2012, pp. 1–11.

Schönberg, K., Sribar, M., *et al.* (2011) 'Analyses of HLA-C-specific KIR repertoires in donors with group A and B haplotypes suggest a ligand-instructed model of NK cell receptor acquisition', *Blood*, 117(1), pp. 98–107.

Schwartz, O., Maréchal, V., *et al.* (1996) 'Endocytosis of major histocompatibility complex class I molecules is induced by the HIV–1 Nef protein', *Nature Medicine*, 2(3), pp. 338–342.

Serra-Moreno, R., Jia, B., *et al.* (2011) 'Compensatory changes in the cytoplasmic tail of gp41 confer resistance to tetherin/BST-2 in a pathogenic nef-deleted SIV', *Cell host & microbe*, 9(1), pp. 46–57.

Sharp, P.M. and Hahn, B.H. (2010) 'The evolution of HIV-1 and the origin of AIDS', *Philosophical Transactions of the Royal Society B: Biological Sciences*, 365(1552), pp. 2487–2494.

Shilling, H.G., Guethlein, L.A., *et al.* (2002) 'Allelic Polymorphism Synergizes with Variable Gene Content to Individualize Human KIR Genotype', *The Journal of Immunology*, 168(5), pp. 2307–2315.

Shimizu, Y. and DeMars, R. (1989a) 'Production of human cells expressing individual transferred HLA-A,-B,-C genes using an HLA-A,-B,-C null human cell line.', *Journal of immunology (Baltimore, Md. : 1950)*, 142(9), pp. 3320–8.

Shimizu, Y., Geraghty, D.E., *et al.* (1988) 'Transfer and expression of three cloned human non-HLA-A,B,C class I major histocompatibility complex genes in mutant lymphoblastoid cells.', *Proceedings of the National Academy of Sciences*, 85(1), pp. 227–231.

Sim, M.J.W., Malaker, S.A., *et al.* (2017) 'Canonical and Cross-reactive Binding of NK Cell Inhibitory Receptors to HLA-C Allotypes Is Dictated by Peptides Bound to HLA-C', *Frontiers in immunology*, 8(MAR).

Simon, F., Mauclère, P., *et al.* (1998) 'Identification of a new human immunodeficiency virus type 1 distinct from group M and group O', *Nature medicine*, 4(9), pp. 1032–1037.

References

Sivori, S., Vacca, P., *et al.* (2019) 'Human NK cells: surface receptors, inhibitory checkpoints, and translational applications', *Cellular & Molecular Immunology*, 16(5), pp. 430–441.

Sivori, S., Vitale, M., *et al.* (1997) 'p46, a novel natural killer cell-specific surface molecule that mediates cell activation', *The Journal of experimental medicine*, 186(7), pp. 1129–1136.

Smyth, M.J., Cretney, E., *et al.* (2001) 'Tumor necrosis factor-related apoptosis-inducing ligand (TRAIL) contributes to interferon gamma-dependent natural killer cell protection from tumor metastasis', *The Journal of experimental medicine*, 193(6), pp. 661–670.

Sodroski, J., Goh, W.C., *et al.* (1986) 'A second post-transcriptional trans-activator gene required for HTLV-III replication', *Nature*, 321(6068), pp. 412–417.

van Stigt Thans, T., Akko, J.I., *et al.* (2019) 'Primary HIV-1 Strains Use Nef To Downmodulate HLA-E Surface Expression', *Journal of virology*, 93(20).

Stranger, B.E., Forrest, M.S., *et al.* (2005) 'Genome-Wide Associations of Gene Expression Variation in Humans', *PLOS Genetics*, 1(6), p. e78.

Stranger, B.E., Nica, A.C., *et al.* (2007) 'Population genomics of human gene expression', *Nature Genetics*, 39(10), pp. 1217–1224.

Strauss-Albee, D.M. and Blish, C.A. (2016) 'Human NK Cell Diversity in Viral Infection: Ramifications of Ramification', *Frontiers in immunology*, 7(MAR).

Sullivan, N., Sun, Y., *et al.* (1998) 'CD4-Induced conformational changes in the human immunodeficiency virus type 1 gp120 glycoprotein: consequences for virus entry and neutralization', *Journal of virology*, 72(6), pp. 4694–4703.

Sun, J.C., Beilke, J.N. and Lanier, L.L. (2009) 'Adaptive immune features of natural killer cells', *Nature*, 457(7229), pp. 557–561.

Sundquist, W.I. and Kräusslich, H.G. (2012) 'HIV-1 assembly, budding, and maturation', *Cold Spring Harbor perspectives in medicine*, 2(7).

Van Teijlingen, N.H., Hölzemer, A., *et al.* (2014) 'Sequence variations in HIV-1 p24 Gag-derived epitopes can alter binding of KIR2DL2 to HLA-C*03:04 and modulate primary natural killer cell function', *AIDS (London, England)*, 28(10), pp. 1399–1408.

Thomas, R., Apps, R., *et al.* (2009) 'HLA-C cell surface expression and control of HIV/AIDS correlate with a variant upstream of HLA-C', *Nature Genetics*, 41(12), pp. 1290–1294.

le Tortorec, A., Willey, S. and Neil, S.J.D. (2011) 'Antiviral inhibition of enveloped virus release by tetherin/BST-2: action and counteraction', *Viruses*, 3(5), pp. 520–540.

Traherne, J.A., Martin, M., *et al.* (2010) 'Mechanisms of copy number variation and hybrid gene formation in the KIR immune gene complex', *Human molecular genetics*, 19(5), pp. 737–751.

Uhrberg, M., Valiante, N.M., *et al.* (1997) 'Human Diversity in Killer Cell Inhibitory Receptor Genes', *Immunity*, 7(6), pp. 753–763.

Ulmer, A.J., Scholz, W., *et al.* (1984) 'Isolation and subfractionation of human peripheral blood mononuclear cells (PBMC) by density gradient centrifugation on Percoll', *Immunobiology*, 166(3), pp. 238–250.

Vallari, A., Holzmayer, V., *et al.* (2011) 'Confirmation of putative HIV-1 group P in Cameroon', *Journal of virology*, 85(3), pp. 1403–1407.

Venzke, S., Michel, N., *et al.* (2006) 'Expression of Nef downregulates CXCR4, the major coreceptor of human immunodeficiency virus, from the surfaces of target cells and thereby enhances resistance to superinfection', *Journal of virology*, 80(22), pp. 11141–11152.

Vilches, C. and Parham, P. (2002) 'KIR: diverse, rapidly evolving receptors of innate and adaptive immunity', *Annual review of immunology*, 20, pp. 217–251.

Vince, N., Li, H., *et al.* (2016) 'HLA-C Level Is Regulated by a Polymorphic Oct1 Binding Site in the HLA-C Promoter Region', *American Journal of Human Genetics*, 99(6), pp. 1353–1358.

Vitale, M., Bottino, C., *et al.* (1998) 'NKp44, a novel triggering surface molecule specifically expressed by activated natural killer cells, is involved in non-major histocompatibility complex-restricted tumor cell lysis', *The Journal of experimental medicine*, 187(12), pp. 2065–2072.

Vivier, E., Tomasello, E., *et al.* (2008) 'Functions of natural killer cells', *Nature Immunology*, 9(5), pp. 503–510.

Vollmers, S., Lobermeyer, A. and Körner, C. (2021) 'The New Kid on the Block: HLA-C, a Key Regulator of Natural Killer Cells in Viral Immunity', *Cells*, 10(11), p. 3108.

Walker-Sperling, V.E., Pohlmeyer, C.W., *et al.* (2017) 'Factors Associated With the Control of Viral Replication and Virologic Breakthrough in a Recently Infected HIV-1 Controller.', *EBioMedicine*, 16, pp. 141–149.

Walzer, T., Dalod, M., *et al.* (2005) 'Natural-killer cells and dendritic cells: "l'union fait la force"', *Blood*, 106(7), pp. 2252–2258.

Wan, F. and Lenardo, M.J. (2009) 'Specification of DNA binding activity of NF-kappaB proteins', *Cold Spring Harbor perspectives in biology*, 1(4), p. a000067.

Willey, R.L., Maldarelli, F., Martin, M.A. and Strebel, K. (1992) 'Human immunodeficiency virus type 1 Vpu protein induces rapid degradation of CD4', *Journal of virology*, 66(12), pp. 7193–7200.

Williams, A., Peh, C.A. and Elliott, T. (2002) 'The cell biology of MHC class I antigen presentation.', *Tissue antigens*, 59(1), pp. 3–17.

Williams, T.M. (2001) 'Human leukocyte antigen gene polymorphism and the histocompatibility laboratory', *The Journal of molecular diagnostics : JMD*, 3(3), pp. 98–104.

Wilson, M.J., Torkar, M., *et al.* (2000) 'Plasticity in the organization and sequences of human KIR/ILT gene families', *Proceedings of the National Academy of Sciences*, 97(9), pp. 4778–4783.

Winter, C.C., Gumperz, J.E., *et al.* (1998) 'Direct binding and functional transfer of NK cell inhibitory receptors reveal novel patterns of HLA-C allotype recognition.', *Journal of immunology*, 161(2), pp. 571–7.

Winter, C.C. and Long, E.O. (1997) 'A single amino acid in the p58 killer cell inhibitory receptor controls the ability of natural killer cells to discriminate between the two groups of HLA-C allotypes.', *Journal of immunology*, 158(9), pp. 4026–8.

Wittlich, M., Koenig, B.W. and Willbold, D. (2008) 'Structural consequences of phosphorylation of two serine residues in the cytoplasmic domain of HIV-1 VpU', *Journal of Peptide Science*, 14(7), pp. 804–810.

Wong, A.H.W., Williams, K., *et al.* (2010) 'Alterations in natural killer cell receptor profiles during HIV type 1 disease progression among chronically infected South African adults', *AIDS research and human retroviruses*, 26(4), pp. 459–469.

Yusim, K., Kesmir, C., *et al.* (2002) 'Clustering patterns of cytotoxic T-lymphocyte epitopes in human immunodeficiency virus type 1 (HIV-1) proteins reveal imprints of immune evasion on HIV-1 global variation', *Journal of virology*, 76(17), pp. 8757–8768.

Zhang, R., Xu, J., *et al.* (2007) 'Increased NKG2A found in cytotoxic natural killer subset in HIV-1 patients with advanced clinical status', *AIDS*, 21(Suppl 8), pp. 9–17.

Zhu, X. and Zhu, J. (2020) 'CD4 T Helper Cell Subsets and Related Human Immunological Disorders', *International Journal of Molecular Sciences*, 21(21), p. 8011.

References

Ziegler, M.C., Nelde, A., *et al.* (2020) 'HIV-1 induced changes in HLA-C∗03 : 04-presented peptide repertoires lead to reduced engagement of inhibitory natural killer cell receptors', *AIDS*, 34(12), pp. 1713–1723.

(a). Available at: https://www.unaids.org/en/resources/fact-sheet (Accessed: 22 November 2021).

(b). Available at: https://www.hiv.gov/hiv-basics/overview/about-hiv-and-aids/how-is-hiv-transmitted (Accessed: 1 December 2021).

(c). Available at: https://www.ebi.ac.uk/ipd/kir/about/statistics/ (Accessed: 7 March 2022).

(d). Available at: https://www.ebi.ac.uk/ipd/kir/alleles.html (Accessed: 1 December 2021).

(e). Available at: http://www.allelefrequencies.net/hla6006a.asp?hla_locus_type=Classical&hla_locus=C&hla_allele1=&hla_allele2=&hla_selection=&hla_pop_selection=&hla_population=3089&hla_country=&hla_dataset=&hla_region=&hla_ethnic=&hla_study=&hla_order=order_4&hla_sample_size_pattern=equal&hla_sample_size=&hla_sample_year_pattern=equal&hla_sample_year=&hla_level_pattern=equal&hla_level=&standard=a&hla_show= (Accessed: 29 December 2021).

(f). Available at: https://hivinfo.nih.gov/understanding-hiv/fact-sheets/stages-hiv-infection (Accessed: 1 December 2021).

List of Figures

List of tables

Acknowledgments

First of all, I would like to thank my supervisor **PD Dr. Christian Körner** for his excellent scientific advice and continuous support during my PhD study. I am very grateful for your guidance and feedback throughout my project.

I would like to thank **Prof. Dr. Marcus Altfeld** for the opportunity to conduct my PhD thesis in his department and for being the first reviewer of my dissertation.

I would also like to thank **Prof. Dr. Julia Kehr** for being the second reviewer of my dissertation.

A special thanks to **Dr. Annika Niehrs** for her scientific and non-scientific support and for critically reading my thesis.

I would like to thank **blood donors** for donating blood for my experiments, **Dr. Sven Peine** and everyone from the **Institute of Transfusion Medicine** at the University Medical Center Hamburg-Eppendorf, as well as the **Healthy Cohort Team** for the organisation of the blood donations.

I would also like to thank **Arne Düsedau** and **Jana Hennesen** for their support with flow cytometry and for their help with cell sorting.

I gratefully acknowledge the **TP-HIV Cohort** of the **DZIF** for the contribution of the PBMC and plasma samples of HIV-1^{+} individuals.

A special thanks to the **DFG** for funding my PhD project.

I want to thank the **DKMS** for the KIR/HLA genotyping.

Special thanks to **Pia Fittje** and **Kerri Hagemann** and all other PhD students for their scientific but especially emotional support. It was a great pleasure to do my PhD thesis together with you.

I would like to thank **Heike Hildebrandt** for her organisation and support that helped with the scientific work.

Lastly, I want to thank my parents, sister and friends for their encouragement and mental support during the time of my thesis.

Declaration of oath

I hereby declare, on oath, that I have written the present dissertation by my own and not used other than the acknowledged resources and aids.

Hamburg, May 17th, 2022

_____	_____
City and date	Signature student

Confirmation of English language authenticity

Bestätigung der Korrektheit der englischen Sprache

I, Andrew Highton, born on March 29th, 1989 in London, United Kingdom, hereby declare that the thesis with the title “Impact of KIR/HLA-C Interactions on the anti-HIV-1 Activity of NK Cells” written by Sarah Vollmers is written in grammatically correct English.

Hiermit erkläre ich, Andrew Highton, geboren am 29. März 1998 in London, Vereinigtes Königreich, dass die Dissertation mit dem Titel „Impact of KIR/HLA-C Interactions on the anti-HIV-1 Activity of NK Cells“ geschrieben on Sarah Vollmers in einem korrekten Englisch verfasst wurde.

Dunedin, May 17th, 2022

City and date Ort und Datum	Signature Unterschrift

Appendix

Appendix A: *HLA/KIR* genotyping of HIV-1$^-$ individuals for CD107a degranulation assays

	HLA-A		HLA-B			HLA-C			CCR5		KIR			
No.	**A_1**	**A_2**	**B_1**	**B_2**	**haplotype**	**allele_1**	**allele_2**	**haplotype**	**1**	**2**	**2DL1**	**2DL2**	**2DL3**	**3DL1**
1	02:01	03:02	07:02	35:01	66	04:01	07:DCGFH	**12**	WT	WT	*003/*034	*003	*001	*002+*015/*017
2	24:02	24:02	07:02	44:03	46	07:DJVBW	16:01	**11**	Del32	WT	*001/*002 +*003/*034	0	*001 +*002	*004+*005
3	01:01	03:01	50:01	51:01	46	06:02	15:DJVAR	**22**	Del32	WT	*003/*034 +*003/*034	0	*001 +*030	*002+*005
4	01:01	31:01	08:01	51:01	46	07:01	15:CZJFH	**12**	WT	WT	*001/*002 +*001/*002	0	*002 +*002	*001/*095+*004
5	01:01	03:01	08:01	15:01	66	03:DJUJX	07:01	**11**	WT	WT	*003/*034 +*004/*035|*006+*010	*001	*001	*002+*021
6	31:01	68:01	40:01	57:01	44	03:CZJEH	07:01	**11**	WT	WT	*003/*034 +*003/*034	0	*001 +*001	*004+*015/*017
7	01:01	02:01	07:02	15:01	66	03:CZJEE	07:DCGFH	**11**	WT	WT	*003/*034	*001	*001	*001/*095+*005
8	02:01	24:02	44:03	57:01	44	06:02	07:01	**12**	WT	WT	*001/*002 +*003/*034	0	*001 +*002	*004+*008
9	02:01	02:01	15:01	39:01	66	03:CZJEH	07:DCGFH	**11**	WT	WT	*001/*002	*003	*002	*NEW+*004
10	03:01	03:01	13:02	39:01	46	06:02	07:DCGFH	**12**	WT	WT	*001/*002 +*004/*035	*001	*002	*005
11	02:01	02:01	15:01	56:01	66	01:02:01	03:DJUJX	**11**	WT	WT	*003/*034 +*004/*035|*006+*010	*001	*001	*015/*017
12	02:01	02:01	13:02	49:01	44	06:02	07:01	**12**	Del32	WT	*001/*002	*003	*002	*002+*008
13	03:01	24:02	07:02	27:05	46	02:DJUJS	07:DJVBW	**12**	WT	WT	*003/*034	*003	*001	*001/*095+*004

14	02:01	11:01	08:01	44:02	46	05:01:01	07:01	**12**	WT	WT	*001/*002 +*004/*035	*003	*002	*001/*095 +*015/*017
15	03:01	29:02	40:01	44:03	46	03:DJUJX	16:01	**11**	WT	WT	*003/*034	*003	*POS	*001/*095+*004
16	02:01	30:01	13:02	27:05	44	02:CVHVF	06:02	**22**	WT	WT	*001/*002 +*001/*002	0	*002 +*002	*004+*005
17	02:01	02:03	44:02	51:01	44	02:CVHVF	05:01	**22**	WT	WT	*001/*002	*003	*002	*005
18	02:22	03:01	08:01	39:05	66	07:01	07:DCGFH	**11**	WT	WT	*001/*002 +*003/*034	0	*001 +*002	*005
19	24:02	24:03	07:02	08:01	46	07:DJVBW	12:03	**11**	WT	WT	*003/*034 +*004	*001	*NEW	*005+*005
20	02:01	03:01	35:01	37:01	46	04:01	06:02	**22**	Del32	WT	*003/*034 +*003/*034	0	*001 +*001	*001/*095+*005

Appendix B: *HLA* genotyping of HIV-1$^-$ individuals for phenotypic characterization

	HLA-A		**HLA-B**			**HLA-C**			**CCR5**	
No.	**A_1**	**A_2**	**B_1**	**B_2**	**haplotype**	**C_1**	**C_2**	**haplotype**	**1**	**2**
1	24:02	26:01	35:01	44:02	46	04:01	05:09	22		
2	01:01	02:01	08:01	51:01	46	07:01	14:02	11	WT	Del32
3	02:01	03:01	07:02	18:01	66	07:01	07:02	11		
4	01:01	02:01	15:18	57:01	46	06:02	07:04	12		
5	32:01	68:01	38:01	44:02	44	12:03	16:04	11		
6	01:01	11:01	56:01	57:01	46	01:02	06:02	12		
7	02:01	11:01	40:01	44:03	44	03:DJUJX	16:01	11	WT	WT
8	02:01	03:01	39:01	44:03	46	04:01	12:03	12		
9	02:01	68:01	07:02	37:01	46	06:02	07:02	12		
10	02:01	02:01	27:05	40:01	46	02:02	03:04	12		
11	02:01	03:01	07:02	15:01	66	03:04	07:02	11		
12	03:01	24:02	15:228	35:03	66	03:03	12:03	11		
13	01:01	02:01	14:01	39:01	66	07:02	08:02	11		

14	01:01	24:02	08:01	55:01	66	03:03	07:01	11	WT	D32
15	01:01	02:01	18:01	57:01	46	06:02	07:01	12		
16	03:01	29:02	35:01	44:03	46	04:01	16:01	12		
17	02:01	31:01	07:02	08:01	66	07:01	07:02	11	WT	WT
18	01:01	24:02	15:01	37:01	46	03:03	06:02	12		
19	02:01	02:01	44:02	44:02	44	05:01	05:01	22	WT	D32
20	01:01	26:01	08:01	44:02	46	05:01	07:01	12	WT	WT
21	01:01	01:01	15:17	35:01	46	06:02	07:01	12	WT	WT
22	01:01	02:01	07:02	51:01	46	07:CENAH	15:CEJYE	12	Del32	WT
23	03:01	03:01	07:02	42:01	66	07:BRXNC	17:01	12	WT	
24	03:01	11:01	35:03	49:01	46	04:01	07:01	12	WT	WT
25	03:01	24:02	35:01	44:02	46	04:01:01G	07:04	12	WT	WT
26	02:01	03:01	39:01	44:02	46	05:01	12:03	12	WT	WT
27	02:01	02:01	07:02	57:01	46	06:02	07:BRNXC	12	WT	WT
28	01:01	02:01	08:01	57:01	46	06:02	07:01	12	WT	WT
29	02:01	68:01	07:02	35:08	66	04:01	07:BRXNC	12	WT	WT
30	26:01	30:01	07:02	38:01	46	07:CENAH	12:03	11	Del32	WT
31	01:01	11:01	08:01	51:01	46	07:01	15:02	12	WT	WT
32	02:01	26:01	07:02	51:01	46	07:02	14:02	11		
33	01:01	02:01	08:01	57:01	46	07:01	07:01	11	WT	Del32
34	02:01	24:02	07:02	44:02	46	05:01	07:02	12	WT	WT
35	24:02	31:01	13:02	15:01	46	03:03	06:02	12	Del32	Del32
36	01:01	31:01	44:02	57:01	44	05:01	06:02	22	WT	Del32
37	01:01	23:01	08:01	45:01	66	07:01	16:01	11	WT	WT
38	02:01	03:01	07:02	15:01	66	03:04	07:02	11	WT	WT
39	03:01	30:01	13:02	51:01	44	06:02	14:02	12	WT	WT
40	02:01	02:01	15:01	44:02	46	03:04	05:01	12	WT	WT
41	02:01	02:01	15:01	51:01	46	03:04	14:02	11	WT	WT

42	02:01	23:01	15:01	44:03	46	03:04	04:01	12	WT	WT
43	03:01	26:15	07:02	38:01	46	07:02	12:03	11	WT	Del32
44	02:01	03:01	35:01	57:01	46	04:01	06:02	22	WT	WT
45	01:01	23:01	37:01	44:03	44	04:01	06:02:01	22	WT	WT
46	02:05	24:02	18:01	50:01	66	06:02	07:01	12	WT	WT
47	02:01	68:02	14:02	27:05	46	02:DJUJS	08:02	12	WT	WT
48	02:01	11:01	35:01	44:02	46	01:02	04:01	12	WT	WT
49	02:01	26:01	38:01	44:02	44	05:01	12:03	12	WT	WT
50	31:01	68:01	27:03	35:01	46	02:DJUJS	04:01	22	WT	WT
51	03:01	25:01	07:02	08:01	66	07:01	07:DJVBW	11	WT	WT
52	11:01	31:01	35:01	51:01	46	04:01	15:DJVAR	22	WT	WT
53	24:02	68:02	13:02	44:05	44	02:DJUJS	06:02	22	WT	WT
54	02:01	11:01	35:01	39:01	66	04:01	07:DJVBW	12	Del32	WT
55	02:01	66:01	40:01	41:02	66	03:DJUJX	17:01	12	WT	WT
56	11:01	24:02	39:06	51:01	46	07:DJVBW	15:DJVAR	12	WT	WT
57	11:01	24:02	35:01	51:01	46	04:01	16:02	22	WT	WT
58	01:01	23:01	50:01	58:01	46	06:02	07:01	12	WT	WT
59	03:01	24:02	44:03	50:01	46	02:DJUJS	06:02	22	Del32	WT
60	01:01	02:01	08:01	15:01	66	03:DJUJX	07:01	11	WT	WT

Appendix C: *KIR* genotyping of HIV-1$^-$ individuals for phenotypic characterization

No.	2DL1	2DL2	2DL3	2DS1	2DS4	3DL1
1	1	1	1	1	197	1
2	1	0	1	0	197	1
3	1	1	1	1	197	1
4	1	0	1	0	197	1
5	1	1	1	1	219	1

6	1	1	0	1	197	1
7	*003/*034 +*003/*034	0	*NEW+*001	*002	*006	*004
8	1	1	1	1	0	0
9	1	0	1	0	197	1
10	*001/*002 +*003/*034	0	*001+*002	0	0	*001+*005
11	1	1	1	0	197/219	1
12	1	1	1	1	219	1
13	1	0	1	0	197/219	1
14	1	0	1	0	1	1
15	*003/*009/*015/ *018/*033/*034	*001/*002/*005	*001/*003/*007/*012/*021/*024	*002	0	*004/*091
16	1	0	1	0	197/219	1
17	*001/*002+*003/*009/ *015/*018/*033/*034	0	*001/*003/*007/*012/*021/*024 + *002/*003/*007/*012/*021/*024	*002+*002	0	0
18	*001/*002 +*003/*034	0	*001+*005	*002	0	*053
19	*001/*002 +*003/*034	0	*001+*002	*002	*010	*005
20	*001/*002 +*003/*034	0	*001+*002	*002	*001/*017	*020
21	*003/*034 +*004/*035| *006+*010	*001	*001	*002	*003	*001/*095
22	*001/*002 +*003/*034	0	*001+*002	0	*003+*006	*001/*095+*004
23	1	1	1	1	1	1
24	*003/*034	*001	*001	0	*NEW+*001/*017 |*NEW+*017	*002+*008
25	*003/*034 +*004/*035|*003/*034 +*035|*006+*010	*001	*001	*NEW|*002	*004	*007/*102

26	*001/*002 +*003/*034	0	*001+*002	0	*NEW+*004	*007/*102+*008
27	*003/*034 +*003/*034	0	*001+*001	0	*003+*006	*001/*095+*004
28	*001/*002 +*003/*034	0	*001+*002	*002	*001/*017	*015/*017
29	*001/*002 +*004/*035	*001	*002	*NEW	*NEW	*005
30	*003/*034 +*003/*034	0	*001+*001+*001|*001+*001	0	*001/*017+*003	*POS
31	*001/*002 +*003/*034	0	*001+*002	*002	0	*005
32	*003/*009/*015 /*018/*033/*034	*003	*001/*003/*007/*012/*021/*024	0	*POS	*POS
33	*003/*034	*003	*001	*002|*NEW	0	*005
34	*001/*002	*003	*002	0	*001/*017/*006N	*POS
35	*003/*009/*015/*018/*033/*034 +*003/*009/*015/ *018/*033/*034	0	*001/*003/*007/*012/*021/*024 + *001/*003/*007/*012/*021/*024	0	0	*001/*016/*026/*067/ *095+*019
36	*004|*010	*001/*002/*005+ *003|*003+*008/*010	0	*002	0	*002
37	*001/*002 +*003/*034	0	*001+*002	*002	0	*008
38	*003/*009/*015/*018/*033/*034 +*003/*009/*015/*018/033/*034	0	*001/*003/*007/*012/*021/*024 + *001/*003/*007/*012/*021/*024	*002	0	*005/*044/*097/*109
39	0	*POS	0	0	*POS	*POS
40	*003/*009/*015/*018/*033/*034 +*004|*003/*009/*015/*018/*033/*03 4 +*010|*006 +*010	*001/*002/*005 |*008/*010	*001/*003/*007/ *012/*021/*024	0	0	*004/*091+*004/*091
41	*003/*034 +*004|*006+*010	*001	*001	*006	0	*004
42	*001/*002+*003/*009/ *015/*018/*033/*034	0	*001/*003/*007/*012/*021/*024 + *002/*003/*007/*012/*021/*024	0	0	*004/*091+*008
43	*001/*002	*003	*002	0	*001/*017/*003N	*001+*002

44	*006+*NEW| *NEW+*NEW	*001	*001	0	*NEW/*NEWN	*005+*015/*017
45	*003/*034 +*003/*034	0	*001+*001	*002	0	*015/*017
46	*003/*034 +*003/*034	0	*001+*001	0	*006+*010	*004+*053
47	*003/*034 +*003/*034	0	*001+*001	0	*NEW+*010	*005+*005
48	*003/*034 +*003/*034	0	*001+*001	0	*NEW+*NEW|*NEW+*001/*017 |*NEW+*010|*001/*017+*010	*005+*015/*017
49	*001/*002 +*003/*034	0	*001+*002	0	*003+*003	*001/*095+ *001/*095
50	*001/*002+*003/*034 +*003/*034|*001/*002 +*003/*034	0	*POS	0	*003+*006	*001/095+ *004
51	*001/*002 +*032N	0	*001+*002	*002	*004	*007/*102
52	*NEW+*004/*035	*001+*001	0	*NEW| *002	*006	*004
53	*004/*035	*001+*003	0	*NEW| *002	*001/*017|*011|*017	*015/*017
54	*001/*002	*003	*002	0	*NEW+*001/*017|*NEW+*011| *NEW+*017	*002+*002
55	*003/*034 +*003/*034	0	*001+*001	0	*003+*006	*001/*095+*004
56	*003/*034 +*004/*035| *006+*010	*001	*001	0	*003+*003	*001/*095+*001/*095
57	*001/*002 +*004/*035	*001	*002	0	*004+*006	*004+*007/*102
58	*001/*002 +*003/*034	0	*001+*002	0	*001/*017+*010	*005+*015/*017
59	1*003/*034	*003	*009	*005	*001/*017|*011|*017	*029
60	*001/*002 +*003/*034	0	*002+*003	0	*003+*006	*001/*095+*004

Appendix D: *HLA* genotyping of HIV-1^{+} individuals

	HLA-A		HLA-B			HLA-C			CCR5	
No.	**A_1**	**A_2**	**B_1**	**B_2**	**haplotype**	**C_1**	**C_2**	**haplotype**	**1**	**2**
1	02:01	03:01	18:01	35:01	66	04:01	07:01	21	WT	WT
2	02:01	24:02	07:02	27:05	64	02:CVHVF	07:DCGFH	21	WT	WT
3	02:01	32:01	40:02	44:02	64	02:CVHVF	05:01	22	WT	WT
4	01:01	29:02	40:01	57:01	64	03:DJUJX	06:02	12	WT	WT
5	01:01	68:02	08:01	53:01	64	04:01	07:01	21	WT	WT
6	02:01	03:01	40:01	44:02	64	03:CZJEH	05:01	12	WT	WT
7	03:01	24:02	35:01	51:01	64	01:02	04:01	12	Del32	WT
8	02:01	02:01	13:02	18:01	46	06:02	07:01	21	Del32	WT
9	11:01	31:01	35:01	45:01	66	04:01	06:02	22	WT	WT
10	03:01	68:01	27:05	51:01	44	02:CVHVF	14:02	21	WT	WT
11	02:01	03:01	07:02	15:01	66	03:CZJEE	07:DCGFH	11	WT	WT
12	03:01	68:02	53:01	58:02	44	04:01	06:02	22	WT	WT
13	01:01	30:04	41:02	52:01	64	12:02	17:01	12	WT	WT
14	03:01	32:01	15:01	44:02	64	03:CZJEE	05:01	12	WT	WT
15	11:01	11:01	27:05	51:01	44	01:02	15:CZJFH	12	WT	WT
16	02:01	02:11	40:06	40:06	66	15:CZJFH	15:CZJFH	22	WT	WT
17	01:01	32:01	18:01	52:01	64	07:01	12:02	11	WT	WT
18	02:01	03:01	15:01	35:03	66	03:DJUJV	04:01	12	WT	WT
19	02:01	02:01	15:01	15:01	66	03:CZJEE	03:CZJEH	11	WT	WT
20	02:01	03:01	07:05	15:01	66	03:CZJEH	15:05:00	12	WT	WT
21	02:01	02:01	07:02	57:01	64	06:02	07:DCGFH	21	WT	WT
22	02:01	03:01	07:02	40:01	66	03:CZJEH	07:DCGFH	11	WT	WT
23	4:02	26:01	08:01	40:02	66	02:CVHVF	07:01	21	WT	WT
24	03:01:00	03:01	07:02	40:01	66	03:CZJEH	07:DCGFH	11	WT	WT

25	01:01:00	31:01	44:02	57:01	44	02:CVHVF	06:02	22	WT	WT
26	01:01:00	02:01	51:01	57:01	44	06:02	14:02	21	Del32	WT
27	68:02	74:01	07:02	15:03	66	02:10	07:DCGFH	21	WT	WT
28	02:01	26:01	07:02	44:05	44	02:CVHVF	02:CVHVF	22	WT	WT
29	01:01	68:01	08:01	57:01	64	06:02	07:01	21	WT	WT
30	01:01	26:01	27:05	35:01	46	02:CVHVF	04:01	22	Del32	WT
31	02:01	11:01	40:02	51:01	64	02:DJUJS	02:DJUJS	22	WT	WT
32	26:01	68:01	35:03	37:01	64	04:01	06:02	22	WT	WT
33	02:01	03:01	07:02	44:02	64	05:01	07:DJVBW	21	WT	WT
34	02:01	32:01	13:02	39:01	46	06:02	12:03	21	WT	WT
35	02:01	24:02	07:02	44:02	64	05:01	07:DJVBW	21	WT	WT
36	01:01	33:03	35:01	35:01	66	04:01	16:02	22	WT	WT
37	02:01	26:01	44:02	55:01	46	03:DJUJV	05:01	12	Del32	Del32
38	02:11	02:211	35:05	35:09	66	04:01	04:01	22	WT	WT
39	03:01	68:02	18:01	53:01	64	04:01	07:01	21	WT	WT
40	02:01	31:01	40:01	44:02	64	03:DJUJX	05:01	12	WT	WT
41	03:01	24:02	15:01	44:02	64	03:DJUJV	05:01	12	WT	WT
42	02:01	02:01	44:02	55:01	46	03:DJUJV	05:01	12	WT	WT
43	01:01	33:03	52:01	58:01	44	03:02	12:02	11	WT	WT
44	01:01	26:01	39:01	40:06	46	12:03	15:DJVAR	12	WT	WT
45	26:01	31:01	35:01	51:01	64	04:01	15:DJVAR	22	WT	WT
46	02:01	30:02	49:01	55:01	46	01:02	03:DJUJV	11	WT	WT
47	31:01	32:01	15:01	40:01	66	03:DJUJV	03:DJUJX	11	WT	WT
48	24:02	24:02	07:02	15:01	66	03:DJUJV	07:DJVBW	11	Del32	WT
49	01:01	02:01	40:01	57:01	64	03:DJUJX	06:02	12	WT	WT
50	24:02	30:02	07:02	18:01	66	05:01	07:DJVBW	21	WT	WT
51	30:02	66:01	57:02	58:02	44	06:02	18:01	22	WT	WT
52	03:01	23:01	35:03	44:03	64	04:01	04:01	22	WT	WT

53	03:01	11:01	07:02	35:01	66	04:01	07:DJVBW	21	WT	WT
54	26:01	68:01	38:01	40:01	46	03:DJUJX	12:03	11	Del32	WT
55	03:01	31:01	27:05	67:01	46	02:DJUJS	12:03	21	Del32	WT
56	24:02	66:01	18:01	35:02	66	12:03	17:01	12	WT	WT
57	02:01	03:01	07:02	07:02	66	07:DJVBW	07:DJVBW	11	WT	WT
58	03:01	11:01	07:02	14:02	66	07:DJVBW	08:02	11	WT	WT
59	11:01	24:02	07:02	35:01	66	04:01	07:DJVBW	21	Del32	WT
60	01:02	33:01	49:01	50:02	46	06:02	07:01	21	Del32	WT
61	01:01	32:01	07:02	38:01	64	07:DJVBW	12:03	11	WT	WT
62	02:01	02:01	15:01	44:02	64	03:DJUJV	05:01	12	WT	WT
63	01:01	02:06	07:02	39:01	64	07:DJVBW	12:03	11	WT	WT
64	01:01	02:01	15:01	51:01	64	03:DJUJV	15:DJVAR	12	WT	WT
65	02:05	66:01	40:02	49:01	64	07:01	15:DJVAR	12	Del32	WT
66	02:01	23:01	18:01	44:03	64	04:01	07:01	21	WT	WT
67	01:01	01:01	08:01	08:01	66	07:01	07:01	11	WT	WT
68	02:01	02:01	44:02	58:01	44	03:02	05:01	12	WT	WT
69	01:01	01:01	08:01	18:01	66	06:02	07:01	21	WT	WT
70	02:01	11:01	49:01	51:01	44	04:01	07:01	21	WT	WT
71	02:01	03:01	07:02	44:02	64	05:01	07:DJVBW	21	Del32	WT
72	02:01	31:01	44:03	55:01	46	03:DJUJV	04:01	12	WT	WT
73	01:01	24:02	07:02	57:01	64	06:02	07:DJVBW	21	WT	WT
74	02:01	25:01	18:01	27:05	64	03:DJUJV	12:03	11	Del32	WT
75	01:01	25:01	27:05	57:01	44	02:DJUJS	06:02	22	WT	WT
76	01:01	03:01	07:02	39:01	64	07:DJVBW	12:03	11	Del32	WT
77	01:01	03:01	44:03	51:01	44	04:01	14:02	21	Del32	WT
78	01:01	02:01	18:01	35:02	66	04:01	07:01	21	Del32	WT
79	01:01	03:02	39:01	51:01	44	12:03	15:DJVAR	12	WT	WT
80	01:01	68:01	35:02	51:01	64	04:01	05:01	22	WT	WT

81	02:40	25:01	07:02	40:01	66	03:DJUJX	07:DJVBW	11	WT	WT
82	02:01	02:01	07:02	18:01	66	07:01	07:DJVBW	11	WT	WT
83	24:07	25:01	18:01	35:05	66	04:01	12:03	21	WT	WT
84	01:01	03:01	07:02	08:01	66	07:01	07:DJVBW	11	WT	WT
85	02:01	31:01	15:01	38:01	64	03:DJUJV	12:03	11	WT	WT
86	02:01	02:11	44:03	48:02	46	04:01	04:01	22	WT	WT
87	02:01	24:02	51:01	51:01	44	01:02	15:DJVAR	12	WT	WT
88	02:01	03:01	07:02	51:01	64	07:DJVBW	14:02	11	Del32	WT
89	02:01	02:01	07:02	40:01	66	03:DJUJX	07:DJVBW	11	WT	WT
90	02:01	03:01	07:02	50:01	66	06:02	07:DJVBW	21	WT	WT
91	02:07	30:01	13:02	46:01	46	01:02	06:02	12	WT	WT
92	02:01	02:01	57:01	57:01	44	06:02	06:02	22	WT	WT
93	02:01	29:02	44:02	44:03	44	05:01	16:01	21	Del32	WT
94	03:01	32:01	35:01	40:02	66	02:DJUJS	04:01	22	WT	WT
95	01:01	02:01:	35:01	57:01	64	06:02	16:04	21	WT	WT
96	03:01	30:01	13:02	35:01	46	04:01	06:02	22	Del32	WT
97	01:01	01:01	08:01	57:01	64	06:02	7:01	21	WT	WT
98	01:01	02:01	13:02	27:05	44	01:02	07:01	11	WT	WT
99	11:01	32:01	35:01	38:01	64	04:01	12:03	21	WT	WT
100	01:01	02:01	07:02	08:01	66	07:01	07:DJVBW	11	Del32	WT
101	01:01	33:XXX	07:05	40:06	66	03:DJUJX	15:DJVAR	12	WT	WT
102	01:01	25:01	18:01	35:02	66	06:02	12:03	21	WT	WT
103	03:01	32:01	15:01	40:02	66	02:DJUJS	03:DJUJV	21	WT	WT
104	02:01	68:01	08:01	44:02	64	07:01	07:04	11	WT	WT
105	24:02	30:02	18:01	44:03	64	05:01	16:01	21	WT	WT
106	01:01	01:01	08:01	15:01	66	03:DJUJV	07:01	11	Del32	WT
107	02:01:0	11:01	27:05	40:01	46	02:DJUJS	03:DJUJX	21	WT	WT
108	01:01	01:01	08:01	55:01	66	03:DJUJV	07:01	11	WT	WT

109	02:01	02:01	07:02	15:01	66	03:DJUJV	07:DJVBW	11	WT	WT
110	02:01	24:02	07:02	40:01	66	03:DJUJX	07:DJVBW	11	Del32	WT
111	25:01	32:01	18:01	44:02	64	05:01	12:03	21	WT	WT
112	02:01	03:01	15:01	40:01	66	03:DJUJX	03:DJUJX	11	Del32	WT
113	02:01	32:01	18:01	56:01	66	01:02	12:03	11	Del32	WT
114	01:01	26:01	08:01	38:01	64	07:01	12:03	11	Del32	WT
115	25:01	30:01	18:01	58:01	64	03:02	07:01	11	WT	WT
116	11:01	33:01	14:02	40:02	66	02:DJUJS	08:02	21	Del32	WT
117	2:01	68:01	13:02	39:01	44	06:02	12:03	21	WT	WT
118	03:01	03:01	07:02	35:01	66	04:01	07:DJVBW	21	WT	WT
119	24:02	29:02	37:01	44:03	44	06:02	16:01	21	WT	WT
120	01:01	02:01	08:01	40:01	66	03:DJUJX	07:01	11	WT	WT
121	02:01	26:01	07:02	38:01	64	07:DJVBW	12:03	11	WT	WT
122	02:01	69:01	40:02	51:01	64	02:DJUJS	15:DJVAR	21	WT	WT

Appendix E: *KIR* genotyping of HIV-1^{+} individuals

No.	2DL1	2DL2	2DL3	2DS1	2DS4	3DL1
1	*003/*034+*032N	0	*001+*001	0	*NEW+*010	*005+*008
2	*001/*002+*003/*034	0	*001+*002	*NEW	*010	*005
3	*001/*002	*001	*002	*NEW|*002	*NEW|*001/*017|*011|*017	*002
4	*003/*034	*003	*001	0	*001/*017+*003|*003+*011|*003+*017	*001/*095+*002
5	*003/*034+*003/*034	0	*001+*001	0	*003+*010	*001/*095+*053
6	*001/*002+*001/*002	0	*002+*002	0	*001/*017+*006	*002+*004
7	*003/*034	*003	*001	0	*001/*017+*001/*017|*001/*017 +*011|*001/*017+*017|*011+*017	*NEW+*002|*NEW+*015/*017
8	*003/*034	*003	*003	*NEW|*002	*003	*001/*095

9	*POS	0	*POS	0	*010+*010	*005+*005
10	*003/*034+*003/*034	0	*001+*001	*002+*002	0	0
11	*003/*034+*003/*034	0	*001+*003	0	*006+*006	*004+*019
12	*004/*035+*054|*007+*051	*001+*001	0	0	*001/*017+*001/*017|*001/*017+*011|*001/*017 +*017|*011+*011|*011+*017|*017+*017	*015/*017+*015/*017
13	*003/*034	*001	*001	0	*003+*006	*001/*095+*004
14	*001/*002	*003	*002	0	*001/*017+*003|*003+*011|*003+*017	*001/*095+*002
15	*001/*002+*001/*002	0	*002+*002	*002+*002	0	0
16	*003/*034+*003/*034	0	*001+*001	*002	*004	*007/*102
17	*001/*002+*003/*034	0	*001+*002	0	*004+*006	*007/*102+*019
18	*003/*034 +*004/*035|*006+*010	*001	*001	*NEW|*002	*003	*001/*095
19	*001/*002+*003/*034	0	*001+*005/*036	0	*001/*017+*001/*017	*002+*015/*017
20	*001/*002+*004/*035	*001	*002	*NEW|*002	*003	*001/*095
21	*003/*034 +*004/*035|*006+*010	*003	*001	0	*006+*010	*NEW+*004
22	*001/*002+*003/*034	0	*002+*003	*002	*006	*004
23	*003/*034 +*004/*035|*006+*010	*001	*NEW	*002	*001/*017|*011|*017	*015/*017
24	*001/*002+*003/*034	0	*001+*002	*002	*010	*005
25	*001/002+*004/*035	*001	*002	*002	*004	*007/*102
26	*001/*002+*001/*002	0	*002+*002	0	*006+*010	*004+*005
27	*003/*034+*004/*035|*006+*010	*001	*001	0	*NEW+*010|*010+*011|*010+*017	*005+*015/*017

28	*001/*002	*003	*002	0	*NEW+*003	*001/*095+*008
29	*POS	*001	*002	0	*003+*006	*001/*095+*004
30	*001/*002 +*003/*034	0	*001+*002	0	*006+*010	*004+*005
31	0	*001+*003	0	0	*003+*006	*001/*095+*004
32	*003/*034	0	*001+*001	*005	*NEW	*008
33	*003/*034+*004/*035|*006+*010	*001	*001	*NEW|*002	*001/*017|*011|*017	*002
34	*001/*002+*001/*002	0	*002+*002	0	*003+*006	*001/*095+*004
35	*001/*002+*004/*035	*001	*005/*036	0	K*003+*010	*001/*095+*005
36	*001/*002+*004/*035	*001	*002	0	*NEW+*003	*001/*095+*005
37	*003/*034+*004/*035|*006+*010	*001	*001	*002	*006	*004
38	*003/*034+*003/*034	0	*001+*001	0	*001/*017+*010	*005+*015/*017
39	*003/*034	*003	*001	0	*001/*017+*001/*017|*001/*017 +*011|*001/*017+*017|*011+*017	*002+*002
40	*001/*002	*003	*002	*NEW|*002	*001/*017|*011|*017	*002
41	*003/*034+*004/*035|*006+*010	*001	*001	*NEW|*002	*001/*017|*011|*017	*015/*017
42	*003/*034	*003	*001	0	*010+*010	*POS
43	*003/*034+*003/*034	0	*001+*001	*006	*006	*004
44	*003/*034+*003/*034	0	*001+*001	0	*NEW+*003	*001/*095+*008
45	0	*001+*003	0	*NEW+*NEW |*NEW+*002	0	0

46	*NEW+*003/*034|*NEW+*004/*035 |*NEW+*006|*006+*010	*001	*001	0	*NEW+*NEW|*NEW+*001/*017|*NEW+*010|*NEW+*011 |*NEW+K*017|*001/*017+*010|*010+*011|*010+*017	*005+*020
47	*001/*002/*060+*003/*009/ *015/*018/*033/*034/*043/ *063	0	*001/*003/3*007/*012 /*021/*024 +*002/*003/*007/*012/*021/*024	0	*003+*010	*001/*016/*026/*067/*095/*118+*005/ *044/*097/*109
48	*001/*002+*004/*035	*001	*002	0	*003+*006	*001/*095+*004
49	*004/*035	*001+*003	0	0	*003+*006	*001/*095+*004
50	*001/*002+*001/*002	0	*002+*005/*036	0	*003+*006	*004+*009
51	*003/*034+*004/*035|*006+*010	*NEW+*001 |*001+*001	0	0	*001/*017+*006|*006+*011|*006+*017	*004+*015/*017
52	*003/*034	*003	*001	0	*003+*003	*001/*095+*001/*095
53	*001/*002	*003	*POS	0	*NEW+*001/*017|*NEW+*011|*NEW+*017	*002+*008
54	*003/*034+*003/*034	0	*001+*001	0	*001/*017+*006	*004+*015/*017
55	*003/*034+*003/*034	0	*001+*001	0	*010+*010	*005+*005
56	*001/*002+*003/*034	0	*001+*002	0	*004+*006	*004+*007/*102
57	*003/*034	0	*001+*001	*005	*010	*005
58	*POS	*001	*002	0	*NEW+*006	*004+*008
59	*001/*002+*003/*034	0	*001+*002	0	*003+*006	*001/*095+*004
60	*003/*034+*003/*034	0	*001+*001	0	*001/*017+*003	*001/*095+*015/*017
61	*003/*034+*003/*034	0	*001+*001	*002	*003	*001/*095
62	*003/*034+*007	*001	*001+*001	*NEW|*002	*003	*POS
63	*001/*002+*003/*034	0	*001+*002	0	*NEW+*NEW|*NEW+*001/*017 |*NEW+*010|*001/*017+*010	*002+*005

64	*003/*034	*001	*001	0	*010+*010	*005+*005
65	*004/*035	*001+*003	0	0	*001/*017+*003|*003+*011|*003+*017	*001/*095+*002
66	*003/*034	*003	*001	*NEW|*002	*001/*017|*011|*017	*002
67	*001/*002+*003/*034	0	*001+*002	0	*001/*017+*001/*017	*002+*015/*017
68	*003/*034+*004/*035|*006+*010	*001	*001	*002+*002	0	0
69	*003/*034+*003/*034	0	*001+*003	0	*NEW+*006|*NEW+*010	*004+*005
70	*001/*002+*001/*002	0	*002+*005/*036	0	*001/*017+*006	*POS
71	*008	*003	*002	0	*001/*017+*010|*010+*011|*010+*017	*002+*053
72	*001/*002+*003/*034	0	*POS	0	*003+*003	*001/*095+*009
73	*003/*034+*004/*035|*006+*010	*005	*001	*002	*004	*007/*102
74	*003/*034	*001	*001	0	*001/*017+*010|*010+*011 |*010+*017	*005+*020
75	*003/*034+*003/*034	0	*001+*001	*002	*001/*017	*015/*017
76	0	*003+*003	0	0	*003+*006	*004+*009
77	*003/*034+*003/*034+*004/*035 |*003/*034+*004/*035|*003/*034 +*006+*010	0	*001+*001	*002+*006	0	0
78	*003/*034+*003/*034	0	*NEW+*001	0	*NEW+*001/*017	*008+*015/*017

79	*003/*034+*004/*035|*006+*010	*001	*001	*NEW|*002	*006	*004
80	*001/*002+*004/*035	*001	*002	*002	*006	*NEW
81	*POS	0	*002+*005/*036	0	*003	*001/*095
82	*003/*034	*001	*001	*006	*003	*009
83	*001/*002+*004/*035	*003	*002	0	*004+*010	*005+*007/*102
84	*003/*034	*003	*001	*NEW|*002	*010	*005
85	*001/*002+*003/*034	0	*001+*002	0	*003+*010	*001/*095+*005
86	*003/*034+*004/*035|*006+*010	0	*POS	0	*001/*017+*001/*017	*020+*029
87	*003/*034	*003	*001	*NEW|*002	*010	*005
88	*003/*034+*004/*035|*006+*010	*001	*001	0	*001/*017+*001/*017|*001/*017+*011 |*001/*017+*017|*011+*017	*002+*015/*017
89	*003/*034+*032N	0	*001+*001	0	*006+*010	*POS
90	*001/*002+*003/*034	0	*001+*005/*036	*002	*006	*004
91	*003/*034+*003/*034	0	*001+*001	0	*001/*017+*010	*005+*015/*017
92	*001/*002+*003/*034	0	*001+*002	0	*006+*010	*004+*005
93	*001/*002+*037	0	*001+*002	0	*001/*017+*010	*002+*005
94	*001/*002+*004/*035	*001	*002	0	*001/*017+*006|*006+*011|*006+*017	*004+*020

95	*001/*002+*003/*034	0	*001+*002	0	*003+*004	*001/*095+*007/*102
96	*003/*034+*003/*034	0	*001+*001	0	*NEW+*006	*004+*008
97	*003/*034+*004/*035|*003/*034 +*035|*006+*010	*001	*001	0	*NEW+*006	*004+*008
98	*001/*002+*004/*035	*001	*002	*NEW|*002	*010	*005
99	*001/*002+*003/*034	0	*001+*002	*002	*001/*017	*015/*017
100	*001/*002+*001/*002	0	*002+*002	*002+*002	0	0
101	*NEW+*004/*035	*001+*001	0	0	*003+*006	*001/*095+*004
102	*003/*034	*003	*001	0	*001/*017+*003|*003+*011|*003+*017	*001/*095+*002
103	*001/*002+*004/*035	*001	*002	0	*006+*006	*004+*004
104	*003/*034+*004/*035|*006+*010	*001	*001	*NEW|*002	*010	*109
105	*001/*002+*004/*035	*001	*002	*NEW|*002	*006	*004
106	*001/*002+*003/*034	0	*001+*002	0	*003+*010	*001/*095+*005
107	*001/*002+*003/*034	0	*001+*002	*NEW|*002	*NEW|*010	*005
108	*001/*002	*003	*002	0	*006+*006	*004+*004
109	*001/*002/*060 +*003/*009/*015/*018/*033/*034/*043/*063	0	*001/*003/*007/*012/ *021/*024+*005/*036	*002	*006	*004/*091

110	*001/*002 +*003/*034	0	*001+*002	*002	*001/*017	*002
111	*001/*002 +*003/*034	0	*001+*002	0	*004+*010	*005+*007/*102
112	*003/*034 +*003/*034	0	*001+*001	0	*NEW+*001/*017	*002+*008
113	*003/*034 +*004/*035 |*006+*010	*001	*001	*NEW|*002	*001/*017|*011|*017	*002
114	*003/*034 +*003/*034	0	*001+*001	0	*006+*010	*004+*005
115	*003/*034+*004	*001	*001	*006	*003	*001/*095
116	0	*003+*003	0	*NEW|*002	*NEW|*010	*005
117	*004/*035	*001+*001	0	0	*003+*003	*001/*095+ KIR3DL1*001 /KIR3DL1*095
118	*001/*002 +*003/*034	0	*001+*002	0	*001/*017+*006	*004+*015/*017
119	*004/*035 +*004/*035	*001+*001	0	*NEW|*002	*003	*001/*095
120	*001/*002 +*001/*002	0	*002+*002	*002	*001/*017	*002
121	*003/ *034+*007	*001	*001	*NEW	*010	*005
122	*037	*001	*001	0	*NEW+*006	*004+*008

Appendix F: Clinical and demographic data of HIV-1$^+$ individuals

No.	Sex	Age	1. viral load (copies/ml)	1. CD4 (absolute)	1. CD4 (%)	1. CD8 (absolute)	1. CD8 (%)	1. CD4/CD8 (ratio)
1	Male	28	5030	151	15	-	-	-
2	Male	36	38000	389	26	-	-	-
3	Male	43	4960	476	28	-	-	-
4	Female	27	49900	231	23	-	-	-
5	Male	29	10500	390	16	-	-	-
6	Male	33	129000	165	16	-	-	-
7	Male	34	21600	338	29	-	-	-
8	Male	23	6510	400	27	-	-	-
9	Male	26	11500	357	30	-	-	-
10	Male	48	6510	470	27	-	-	-
11	Female	48	120000	291	25	-	-	-
12	Female	31	77600	273	14	-	-	-
13	Male	73	2080	426	22	-	-	-
14	Female	48	500	512	42	-	-	-
15	Male	47	8540	380	14	-	-	-
16	Male	32	13000	1400	39	-	-	-
17	Male	41	6400	509	22	-	-	-
18	Male	49	1690	381	16	-	-	-
19	Female	21	1750	514	30	-	-	-
20	Male	57	460	969	49	-	-	-
21	Male	20	102000	619	33	-	-	-
22	Male	40	88800	371	12	-	-	-
23	Male	27	60200	480	29	-	-	-
24	Male	45	162000	338	15	-	-	-
25	Female	40	800	810	40	-	-	-
26	Male	42	814	677	32	-	-	-
27	Female	30	8778	221	14	-	-	-
28	Male	36	1400000	1200	8	-	-	-
29	Male	35	54883	474	30	-	-	-
30	Male	33	65808	464	19	-	-	-
31	Male	42	5480000	528	11	3613	73	0.1
32	Male	44	235000	2601	31	3486	42	0.8
33	Male	28	>10000000	355	21	836	49	0.4
34	Male	32	10000000	380	27	690	-99	0.6
35	Male	41	39000000	651	22	1393	47	0.5
36	Female	26	>1000000	269	9	2167	nd	0.1
37	Male	49	10000000	221	18	649	52	0.3
38	Male	51	896000	228	9	2057	nd	0.1
39	Male	37	3490000	-	-	-	-	-
40	Male	33	57100	633	33	942	49	0.7

41	Male	24	230000	184	11	1238	72	0.1
42	Male	49	1500000	479	16	1820	-	0.3
43	Male	45	170000000	363	30	661	55	0.5
44	Male	52	10000000	291	31	401	-	0.7
45	Male	37	>10000000	408	11	2386	66	0.2
46	Male	48	4700000	490	-	-	-	-
47	Male	33	5220	795	24	1960	59	0.4
48	Male	43	516000	476	18	1439	55	0.3
49	Male	40	6080	363	22	894	-	0.4
50	Male	37	880000	450	30	818	54.47	0.55
51	Male	32	13000000	320	30	403	37	0.79
52	Male	37	1000000	179	25	405	56	0.44
53	Male	31	>10000000	498	29	727	43	0.69
54	Male	38	6807872	193	15	957	74	0.2
55	Male	49	>10000000	484	43	339	30	1.43
56	Male	27	4170	369	17	1361	64	0.27
57	Male	27	67400	565	26	1248	57	0.45
58	Male	53	2000000	550	46	400	34	1.4
59	Male	48	10000000	522	20	1096	42	0.48
60	Male	25	1360000	460	11	3284	76	0.14
61	Male	26	1250000	182	12	1065	68	0.17
62	Male	26	55843	769	29	1405	53	0.55
63	Male	26	<40	1602	54	863	29	1.86
64	Male	31	2980000	290	32	370	41	0.8
65	Male	27	4280000	394	33	548	46	0.72
66	Male	56	32000000	335	41	259	31	1.29
67	Male	54	478000	281	17	808	49	0.35
68	Male	29	42000000	560	19	1320	45	0.4
69	Male	20	135000	515	31	791	47	0.65
70	Male	25	54457	577	29	953	49	0.61
71	Male	22	1460000	427	17	1387	56	0.31
72	Male	33	250000	70	15	220	51	0.3
73	Male	40	174224	492	19	1885	71	0.26
74	Male	31	2960000	808	8	6636	69	0.12
75	Male	29	<40	767	32	863	36	0.89
76	Male	33	9740	1124	48	743	31	1.51
77	Male	37	3160000	449	36	377	30	1.19
78	Male	39	288000	520	20	1620	63	0.3
79	Male	25	1430000	478	27	930	52	0.51
80	Male	30	1260	660	19	2310	65	0.3
81	Male	40	1140000	1149	40	1266	44	0.91
82	Male	39	>10000000	212	44	177	37	1.19
83	Male	40	6240	550	31	651	36	0.84
84	Male	40	1000000	280	22.6	770	62.2	0.36
85	Male	42	24208	591	28.3	994	47.6	0.6
86	Male	32	60200	727	20	2087	57	0.35

87	Male	25	539000	388	24	757	46.9	0.51
88	Male	39	201000	840	27	1490	48	0.6
89	Male	42	1254740	503	22	1201	52	0.42
90	Male	24	1831509	490	21	1219	51	0.4
91	Male	35	576000	400	3	800	67	0.1
92	Male	42	>10000000	361	23	1080	68	0.33
93	Male	39	4550000	470	18	1880	71	0.3
94	Male	28	1090000	405	42	334	34	1.21
95	Male	39	31000	544	44	523	42	1.04
96	Male	31	-	609	30	950	48	0.64
97	Male	49	>10000000	650	23	1660	1660	0.4
98	Male	25	3949	-	-	-	-	-
99	Male	30	90600	200	7.4	2320	85.9	0.1
100	Male	41	192484	182	14.6	829	66.3	0.22
101	Male	35	151000	167	11	717	48	0.23
102	Male	46	25607	793	27.4	1528	52.8	0.52
103	Male	29	1904189	332	24.2	614	44.8	0.54
104	Male	49	4010 000	-	-	-	-	-
105	Male	32	9734980	249	23	638	58.8	0.39
106	Male	26	39300000	369	30	552	45	0.67
107	Male	32	5027195	675	15	2228	50	0.3
108	Male	42	5340000	376	6	4900	72	0.1
109	Male	45	>1000000	-	-	-	-	-
110	Male	48	21100000	565	27	1012	49	0.6
111	Male	60	41000	807	41	854	43	0.9
112	Male	24	10000000	156	-	792	-999	0.2
113	Male	49	>10000000	406	16	1701	66	0.2
114	Male	57	1310000	838	28	1738	58	0.5
115	Male	30	5710000	397	35	438	38	0.9
116	Male	47	>10000000	416	29	756	53	0.5
117	Male	29	282000	420	31	613	45	0.7
118	Male	43	10000000	227	25	305	33	0.7
119	Male	48	1860000	22	22	602	58	0.4
120	Male	30	181000	478	34	639	49	0.7
121	Male	38	4690000	321	25	630	49	0.5
122	Male	24	897000	389	12	2473	76	0.2

Appendix G: *HLA-C* allotype sequences for 721.221 cell lines

Signal peptide

Chain

HLA-C1^{asn80} (Asparagin, **N**)

HLA-C2^{lys80} (Lysin, **K**)

C*01:2 (C1)

MRVMAPRTLILLLSGALALTETWACSHSMKYFFTSVSRPGRGEPRFISVGYVDDTQFVRFDSDAASPRGEPRAPWVEQEGPEYWDRETQKYKRQAQTDRVSLRN
LRGYYNQSEAGSHTLQWMCGCDLGPDGRLLRGYDQYAYDGKDYIALNEDLRSWTAADTAAQITQRKWEAAREAEQRRAYLEGTCVEWLRRYLENGKETLQRAEH
PKTHVTHHPVSDHEATLRCWALGFYPAEITLTWQWDGEDQTQDTELVETRPAGDGTFQKWAAVMVPSGEEQRYTCHVQHEGLPEPLTLRWEPSSQPTIPIVGIV
AGLAVLAVLAVLGAVVAVVMCRRKSSGGKGGSCSQAASSNSAQGSDESLIACKA

C*02:2 (C1)

MRVMAPRTLLLLLSGALALTETWACSHSMRYFYTAVSRPSRGEPHFIAVGYVDDTQFVRFDSDAASPRGEPRAPWVEQEGPEYWDRETQKYKRQAQTDRVNLRK
LRGYYNQSEAGSHTLQRMYGCDLGPDGRLLRGYDQSAYDGKDYIALNEDLRSWTAADTAAQITQRKWEAAREAEQWRAYLEGECVEWLRRYLENGKETLQRAEH
PKTHVTHHPVSDHEATLRCWALGFYPTEITLTWQRDGEDQTQDTELVETRPAGDGTFQKWAAVVVPSGEEQRYTCHVQHEGLPEPLTLRWEPSSQPTIPIVGIV
AGLAVLAVLAVLGAVVAVVMCRRKSSGGKGGSCSQAASSNSAQGSDESLIACKA

C*03:03 (C1)

MRVMAPRTLILLLSGALALTETWAGSHSMRYFYTAVSRPGRGEPHFIAVGYVDDTQFVRFDSDAASPRGEPRAPWVEQEGPEYWDRETQKYKRQAQTDRVSLRN
LRGYYNQSEARSHIIQRMYGCDVGPDGRLLRGYDQYAYDGKDYIALNEDLRSWTAADTAAQITQRKWEAAREAEQLRAYLEGLCVEWLRRYLKNGKETLQRAEH
PKTHVTHHPVSDHEATLRCWALGFYPAEITLTWQWDGEDQTQDTELVETRPAGDGTFQKWAAVVVPSGEEQRYTCHVQHEGLPEPLTLRWEPSSQPTIPIVGIV
AGLAVLAVLAVLGAVVAVVMCRRKSSGGKGGSCSQAASSNSAQGSDESLIACKA

C*03:04 (C1)

MRVMAPRTLILLLSGALALTETWAGSHSMRYFYTAVSRPGRGEPHFIAVGYVDDTQFVRFDSDAASPRGEPRAPWVEQEGPEYWDRETQKYKRQAQTDRVSLRN
LRGYYNQSEAGSHIIQRMYGCDVGPDGRLLRGYDQYAYDGKDYIALNEDLRSWTAADTAAQITQRKWEAAREAEQLRAYLEGLCVEWLRRYLKNGKETLQRAEH
PKTHVTHHPVSDHEATLRCWALGFYPAEITLTWQWDGEDQTQDTELVETRPAGDGTFQKWAAVVVPSGEEQRYTCHVQHEGLPEPLTLRWEPSSQPTIPIVGIV
AGLAVLAVLAVLGAVVAVVMCRRKSSGGKGGSCSQAASSNSAQGSDESLIACKA

C*04:01 (C2)

MRVMAPRTLILLLSGALALTETWAGSHSMRYFSTSVSWPGRGEPRFIAVGYVDDTQFVRFDSDAASPRGEPREPWVEQEGPEYWDRETQKYKRQAQADRVNLRK
LRGYYNQSEDGSHTLQRMFGCDLGPDGRLLRGYNQFAYDGKDYIALNEDLRSWTAADTAAQITQRKWEAAREAEQRRAYLEGTCVEWLRRYLENGKETLQRAEH
PKTHVTHHPVSDHEATLRCWALGFYPAEITLTWQWDGEDQTQDTELVETRPAGDGTFQKWAAVVVPSGEEQRYTCHVQHEGLPEPLTLRWKPSSQPTIPIVGIV
AGLAVLAVLAVLGAMVAVVMCRRKSSGGKGGSCSQAASSNSAQGSDESLIACKA

C*05:01 (C2)

MRVMAPRTLILLLSGALALTETWACSHSMRYFYTAVSRPGRGEPRFIAVGYVDDTQFVQFDSDAASPRGEPRAPWVEQEGPEYWDRETQKYKRQAQTDRVNLRK
LRGYYNQSEAGSHTLQRMYGCDLGPDGRLLRGYNQFAYDGKDYIALNEDLRSWTAADKAAQITQRKWEAAREAEQRRAYLEGTCVEWLRRYLENGKKTLQRAEH
PKTHVTHHPVSDHEATLRCWALGFYPAEITLTWQRDGEDQTQDTELVETRPAGDGTFQKWAAVVVPSGEEQRYTCHVQHEGLPEPLTLRWGPSSQPTIPIVGIV
AGLAVLAVLAVLGAVMAVVMCRRKSSGGKGGSCSQAASSNSAQGSDESLIACKA

C*06:02 (C2)

MRVMAPRTLILLLSGALALTETWACSHSMRYFDTAVSRPGRGEPRFISVGYVDDTQFVRFDSDAASPRGEPRAPWVEQEGPEYWDRETQKYKRQAQADRVNLRK
LRGYYNQSEDGSHTLQWMYGCDLGPDGRLLRGYDQSAYDGKDYIALNEDLRSWTAADTAAQITQRKWEAAREAEQWRAYLEGTCVEWLRRYLENGKETLQRAEH
PKTHVTHHPVSDHEATLRCWALGFYPAEITLTWQRDGEDQTQDTELVETRPAGDGTFQKWAAVVVPSGEEQRYTCHVQHEGLPEPLTLRWEPSSQPTIPIVGIV
AGLAVLAVLAVLGAVMAVVMCRRKSSGGKGGSCSQAASSNSAQGSDESLIACKA

C*07:01 (C1)

MRVMAPRALLLLLSGGLALTETWACSHSMRYFDTAVSRPGRGEPRFISVGYVDDTQFVRFDSDAASPRGEPRAPWVEQEGPEYWDRETQNYKRQAQADRVSLRN
LRGYYNQSEDGSHTLQRMYGCDLGPDGRLLRGYDQSAYDGKDYIALNEDLRSWTAADTAAQITQRKLEAARAAEQLRAYLEGTCVEWLRRYLENGKETLQRAEP
PKTHVTHHPLSDHEATLRCWALGFYPAEITLTWQRDGEDQTQDTELVETRPAGDGTFQKWAAVVVPSGQEQRYTCHMQHEGLQEPLTLSWEPSSQPTIPIMGIV
AGLAVLVVLAVLGAVVTAMMCRRKSSGGKGGSCSQAACSNSAQGSDESLITCKA

C*07:02 (C1)

MRVMAPRALLLLLSGGLALTETWACSHSMRYFDTAVSRPGRGEPRFISVGYVDDTQFVRFDSDAASPRGEPRAPWVEQEGPEYWDRETQKYKRQAQADRVSLRN
LRGYYNQSEDGSHTLQRMSGCDLGPDGRLLRGYDQSAYDGKDYIALNEDLRSWTAADTAAQITQRKLEAARAAEQLRAYLEGTCVEWLRRYLENGKETLQRAEP
PKTHVTHHPLSDHEATLRCWALGFYPAEITLTWQRDGEDQTQDTELVETRPAGDGTFQKWAAVVVPSGQEQRYTCHMQHEGLQEPLTLSWEPSSQPTIPIMGIV
AGLAVLVVLAVLGAVVTAMMCRRKSSGGKGGSCSQAACSNSAQGSDESLITCKA

C*12:03 (C1)

MRVMAPRTLILLLSGALALTETWACSHSMRYFYTAVSRPGRGEPRFIAVGYVDDTQFVRFDSDAASPRGEPRAPWVEQEGPEYWDRETQKYKRQAQADRVSLRN
LRGYYNQSEAGSHTLQWMYGCDLGPDGRLLRGYDQSAYDGKDYIALNEDLRSWTAADTAAQITQRKWEAAREAEQWRAYLEGTCVEWLRRYLENGKETLQRAEH
PKTHVTHHPVSDHEATLRCWALGFYPAEITLTWQRDGEDQTQDTELVETRPAGDGTFQKWAAVVVPSGEEQRYTCHVQHEGLPEPLTLRWEPSSQPTIPIVGIV
AGLAVLAVLAVLGAVMAVVMCRRKSSGGKGGSCSQAASSNSAQGSDESLIACKA

C*14:02 (C1)

MRVMAPRTLILLLSGALALTETWACSHSMRYFSTSVSRPGRGEPRFIAVGYVDDTQFVRFDSDAASPRGEPRAPWVEQEGPEYWDRETQKYKRQAQTDRVSLRN
LRGYYNQSEAGSHTLQWMFGCDLGPDGRLLRGYDQSAYDGKDYIALNEDLRSWTAADTAAQITQRKWEAAREAEQRRAYLEGTCVEWLRRYLENGKETLQRAEH
PKTHVTHHPVSDHEATLRCWALGFYPAEITLTWQWDGEDQTQDTELVETRPAGDGTFQKWAAVVVPSGEEQRYTCHVQHEGLPEPLTLRWEPSSQPTIPIVGIV
AGLAVLAVLAVLGAVVAVVMCRRKSSGGKGGSCSQAASSNSAQGSDESLIACKA

C*16:01 (C1)

MRVMAPRTLILLLSGALALTETWACSHSMRYFYTAVSRPGRGEPRFIAVGYVDDTQFVRFDSDAASPRGEPRAPWVEQEGPEYWDRETQKYKRQAQTDRVSLRN
LRGYYNQSEAGSHTLQWMYGCDLGPDGRLLRGYDQSAYDGKDYIALNEDLRSWTAADTAAQITQRKWEAARAAEQQRAYLEGTCVEWLRRYLENGKETLQRAEH
PKTHVTHHLVSDHEATLRCWALGFYPAEITLTWQRDGEDQTQDTELVETRPAGDGTFQKWAAVVVPSGEEQRYTCHVQHEGLPEPLTLRWEPSSQPTIPIVGIV
AGLAVLAVLAVLGAVVAVVMCRRKSSGGKGGSCSQAASSNSAQGSDESLIACKA

Appendix H: *KIR2DL-CD3ζ* sequences for β2m-KO Jurkats cell lines

Signalpeptide

extracellular domain

transmembrane domain

CD3ζ cytoplasmatic domain

KIR2DL1*001-CD3ζ

MSLLVVSMACVGFFLLQGAWPHEGVHRKPSLLAHPGPLVKSEETVILQCWSDVMFEHFLLHREGMFNDTLRLIGEHHDGVSKANFSISRMTQDLAGTYRCYGSV
THSPYQVSAPSDPLDIVIIGLYEKPSLSAQPGPTVLAGENVTLSCSSRSSYDMYHLSREGEAHERRLPAGPKVNGTFQADFPLGPATHGGTYRCFGSFHDSPYE
WSKSSDPLLVSVTGNPSNSWPSPTEPSSKTGNPRHLHILIGTSVVIILFILLFFLLRVKFSRSADAPAYQQGQNQLYNELNLGRREEYDVLDKRRGRDPEMGGK
PQRRKNPQEGLYNELQKDKMAEAYSEIGMKGERRRGKGHDGLYQGLSTATKDTYDALHMQALPPR

KIR2DL1*004 -CD3ζ

MSLLVVSMACVGFFLLQGAWPHEGVHRKPSLLAHPGRLVKSEETVILQCWSDVMFEHFLLHREGMFNDTLRLIGEHHDGVSKANFSISRMTQDLAGTYRCYGSV
THSPYQVSAPSDPLDIVIIGLYEKPSLSAQPGPTVLAGENVTLSCSSRSSYDMYHLSREGEAHERRLPAGTKVNGTFQANFPLGPATHGGTYRCFGSFRDSPYE
WSKSSDPLLVSVTGNPSNSWPSPTEPSSETGNPRHLHILIGTSVVIILFILLFFLLRVKFSRSADAPAYQQGQNQLYNELNLGRREEYDVLDKRRGRDPEMGGK
PQRRKNPQEGLYNELQKDKMAEAYSEIGMKGERRRGKGHDGLYQGLSTATKDTYDALHMQALPPR

KIR2DL1*020-CD3ζ

LVVSMACVGFFLLQGAWPHEGVHRKPSLLAHPGRLVKSEETVILQCWSDVMFEHFLLHREGMFNDTLRLIGEHHDGVSKANFSIGRMTQDLAGTYRCYGSVTHS
PYQVSAPSDPLDIVIIGLYEKPSLSAQLGPTVLAGENVTLSCSSRSSYDMYHLSREGEAHERRLPAGPKVNGTFQADFPLGPATHGGTYRCFGSFHDSPYEWSK
SSDPLLVSVTGNPSNSWPSPTEPSSKTGNPRHLHILIGTSVVIILFILLFFLLRVKFSRSADAPAYQQGQNQLYNELNLGRREEYDVLDKRRGRDPEMGGKPQR
RKNPQEGLYNELQKDKMAEAYSEIGMKGERRRGKGHDGLYQGLSTATKDTYDALHMQALPPR

KIR2DL1*022-CD3ζ

MSLLVVSMACVGFFLLQGAWPHEGVHRKPSLLAHPGPLVKSEETVILQCWSDVMFEHFLLHREGKFNDTLRLIGEHHDGVSKANFSISRMTQDLAGTYRCYGSV
THSPYQVSAPSDPLDIVIIGLYEKPSLSAQPGPTVLAGENVTLSCSSRSSYDMYHLSREGEAHERRLPAGPKVNGTFQADFPLGPATHGGTYRCFGSFHDSPYE
WSKSSDPLLVSVTGNPSNSWPSPTEPSSKTGNPRHLHILIGTSVVIILFILLFFRVKFSRSADAPAYQQGQNQLYNELNLGRREEYDVLDKRRGRDPEMGGKPQ
RRKNPQEGLYNELQKDKMAEAYSEIGMKGERRRGKGHDGLYQGLSTATKDTYDALHMQALPPR

KIR2DL2*001 -CD3ζ

MSLMVVSMACVGFFLLQGAWPHEGVHRKPSLLAHPGRLVKSEETVILQCWSDVRFEHFLLHREGKFKDTLHLIGEHHDGVSKANFSIGPMMQDLAGTYRCYGSV
THSPYQLSAPSDPLDIVITGLYEKPSLSAQPGPTVLAGESVTLSCSSRSSYDMYHLSREGEAHECRFSAGPKVNGTFQADFPLGPATHGGTYRCFGSFRDSPYE
WSNSSDPLLVSVIGNPSNSWPSPTEPSSKTGNPRHLHILIGTSVVIILFILLFFLLRVKFSRSADAPAYQQGQNQLYNELNLGRREEYDVLDKRRGRDPEMGGK
PQRRKNPQEGLYNELQKDKMAEAYSEIGMKGERRRGKGHDGLYQGLSTATKDTYDALHMQALPPR

KIR2DL2*003-CD3ζ

MSLMVVSMACVGFFLLQGAWPHEGVHRKPSLLAHPGRLVKSEETVILQCWSDVRFEHFLLHREGKFKDTLHLIGEHHDGVSKANFSIGPMMQDLAGTYRCYGSV
THSPYQLSAPSDPLDIVITGLYEKPSLSAQPGPTVLAGESVTLSCSSRSSYDMYHLSREGEAHECRFSAGPKVNGTFQADFPLGPATHGGTYRCFGSFRDSPYE
WSNSSDPLLVSVTGNPSNSWPSPTEPSSKTGNPRHLHILIGTSVVIILFILLFFLLRVKFSRSADAPAYQQGQNQLYNELNLGRREEYDVLDKRRGRDPEMGGK
PQRRKNPQEGLYNELQKDKMAEAYSEIGMKGERRRGKGHDGLYQGLSTATKDTYDALHMQALPPR

KIR2DL2*009-CD3ζ

MSLMVVSMACVGFFLLQGAWPHEGVHRKPSLLAHPGRLVKSEETVILQCWSDVRFEHFLLHREGKFKDTLHLIGEHHDGVSKANFSIGPMMQDLAGTYRCYGSV
THSPYQLSAPSDPLDIVITGLYEKPSLSAQPGPTVLAGESVTLSCSSRSSYDMYHLSREGEAHERRFSAGPKVNGTFQADFPLGPATHGGTYRCFGSFRDSPYE
WSNSSDPLLVSVTGNPSNSWPSPTEPSSKTGNPRHLHILIGTSVVIILFILLFFLLRVKFSRSADAPAYQQGQNQLYNELNLGRREEYDVLDKRRGRDPEMGGK
PQRRKNPQEGLYNELQKDKMAEAYSEIGMKGERRRGKGHDGLYQGLSTATKDTYDALHMQALPPR

KIR2DL3*001-CD3ζ

MSLMVVSMVCVGFFLLQGAWPHEGVHRKPSLLAHPGPLVKSEETVILQCWSDVRFQHFLLHREGKFKDTLHLIGEHHDGVSKANFSIGPMMQDLAGTYRCYGSV
THSPYQLSAPSDPLDIVITGLYEKPSLSAQPGPTVLAGESVTLSCSSRSSYDMYHLSREGEAHERRFSAGPKVNGTFQADFPLGPATHGGTYRCFGSFRDSPYE
WSNSSDPLLVSVTGNPSNSWPSPTEPSSETGNPRHLHVLIGTSVVIILFILLLFFLLRVKFSRSADAPAYQQGQNQLYNELNLGRREEYDVLDKRRGRDPEMGG
KPQRRKNPQEGLYNELQKDKMAEAYSEIGMKGERRRGKGHDGLYQGLSTATKDTYDALHMQALPPRLPPR

KIR2DL3*002-CD3ζ

MSLMVVSMVCVGFFLLQGAWPHEGVHRKPSLLAHPGPLVKSEETVILQCWSDVRFQHFLLHREGKFKDTLHLIGEHHDGVSKANFSIGPMMQDLAGTYRCYGSVTHSPYQLSAPSDPLDIVITGLYEKPSLSAQPGPTVLAGESVTLSCSSRSSYDMYHLSREGEAHERRFSAGPKVNGTFQADFPLGPATHGGTYRCFGSFRDSPYEWSNSSDPLLVSVTGNPSNSWLSPTEPSSETGNPRHLHVLIGTSVVIILFILLLFFLLRVKFSRSADAPAYQQGQNQLYNELNLGRREEYDVLDKRRGRDPEMGGKPQRRKNPQEGLYNELQKDKMAEAYSEIGMKGERRRGKGHDGLYQGLSTATKDTYDALHMQALPPR

KIR2DL3*009-CD3ζ

MSLMVVSMVCVGFFLLQGAWPHEGVHRKPSLLAHPGPLVKSEETVILQCWSDVRFQHFLLHREGKFKDTLHLIGEHHDGVSKANFSIGPMMQDLAGTYRCYGSVTHSPYQLSAPSDPLDIVITGLYEKPSLSAQPGPTVLAGESVTLSCSSRSSYDMYHLSREGEAHEPRFSAGPKVNGTFQADFPLGPATHGGTYRCFGSFRDSPYEWSNSSDPLLVSVTGNPSNSWPSPTEPSSETGNPRHLHVLIGTSVVIILFILLLFFLLRVKFSRSADAPAYQQGQNQLYNELNLGRREEYDVLDKRRGRDPEMGGKPQRRKNPQEGLYNELQKDKMAEAYSEIGMKGERRRGKGHDGLYQGLSTATKDTYDALHMQALPPR

KIR2DL3*016-CD3ζ

MSLMVVSMVCVGFFLLQGAWPHEGVHRKPSLLAHPGPLVKSEETVILQCWSDVRFQHFLLHREGKFKDTLHLIGEHHDGVSKANFSIGPMMQDLAGTYRCYGSVTHSPYQLSAPSDPLDIVITGLYEKPSLSAQPGPTVLAGENVTLSCSSRSSYDMYHLSREGEAHERRFSAGPKVNGTFQADFPLGPATHGGTYRCFGSFRDSPYEWSNSSDPLLVSVTGNPSNSWPSPTEPSSETGNPRHLHVLIGTSVVIILFILLLFFLLRVKFSRSADAPAYQQGQNQLYNELNLGRREEYDVLDKRRGRDPEMGGKPQRRKNPQEGLYNELQKDKMAEAYSEIGMKGERRRGKGHDGLYQGLSTATKDTYDALHMQALPPR

Appendix I: KIR2DL sequences for KIR2DL-Fc fusion proteins

KIR2DL extracellular domain
human Fc fragment/ IgG heavy chain

KIR2DL1*001

HEGVHRKPSLLAHPGPLVKSEETVILQCWSDVMFEHFLLHREGMFNDTLRLIGEHHDGVSKANFSISRMTQDLAGTYRCYGSVTHSPYQVSAPSDPLDIVIIGLYEKPSLSAQPGPTVLAGENVTLSCSSRSSYDMYHLSREGEAHERRLPAGPKVNGTFQADFPLGPATHGGTYRCFGSFHDSPYEWSKSSDPLLVSVTGNPSNSWPSPTEPSSKTGNPRHLHEPKSCDKTHTCPPCPAPELLGGPSVFLFPPKPKDTLMISRTPEVTCVVVDVSHEDPEVKFNWYVDGVEVHNAKTKPREEQYNSTYRVVSVLTVLHQDWLNGKEYKCKVSNKALPAPIEKTISKAKGQPREPQVYTLPPSRDELTKNQVSLTCLVKGFYPSDIAVEWESNGQPENNYKTTPPVLDSDGSFFLYSKLTVDKSRWQQGNVFSCSVMHEALHNHYTQKSLSLSPGK

KIR2DL1*003

HEGVHRKPSLLAHPGRLVKSEETVILQCWSDVMFEHFLLHREGMFNDTLRLIGEHHDGVSKANFSISRMTQDLAGTYRCYGSVTHSPYQVSAPSDPLDIVIIGLYEKPSLSAQLGPTVLAGENVTLSCSSRSSYDMYHLSREGEAHERRLPAGPKVNGTFQADFPLGPATHGGTYRCFGSFHDSPYEWSKSSDPLLVSVTGNPSNSWPSPTEPSSKTGNPRHLHEPKSCDKTHTCPPCPAPELLGGPSVFLFPPKPKDTLMISRTPEVTCVVVDVSHEDPEVKFNWYVDGVEVHNAKTKPREEQYNSTYRVVSVLTVLHQDWLNGKEYKCKVSNKALPAPIEKTISKAKGQPREPQVYTLPPSRDELTKNQVSLTCLVKGFYPSDIAVEWESNGQPENNYKTTPPVLDSDGSFFLYSKLTVDKSRWQQGNVFSCSVMHEALHNHYTQKSLSLSPGK

KIR2DL1*004

HEGVHRKPSLLAHPGRLVKSEETVILQCWSDVMFEHFLLHREGMFNDTLRLIGEHHDGVSKANFSISRMTQDLAGTYRCYGSVTHSPYQVSAPSDPLDIVIIGLYEKPSLSAQLGPTVLAGENVTLSCSSRSSYDMYHLSREGEAHERRLPAGPKVNGTFQANFPLGPATHGGTYRCFGSFRDSPYEWSKSSDPLLVSVTGNPSNSWPSPTEPSSETGNPRHLHEPKSCDKTHTCPPCPAPELLGGPSVFLFPPKPKDTLMISRTPEVTCVVVDVSHEDPEVKFNWYVDGVEVHNAKTKPREEQYNSTYRVVSVLTVLHQDWLNGKEYKCKVSNKALPAPIEKTISKAKGQPREPQVYTLPPSRDELTKNQVSLTCLVKGFYPSDIAVEWESNGQPENNYKTTPPVLDSDGSFFLYSKLTVDKSRWQQGNVFSCSVMHEALHNHYTQKSLSLSPGK

KIR2DL1*020

HEGVHRKPSLLAHPGRLVKSEETVILQCWSDVMFEHFLLHREGMFNDTLRLIGEHHDGVSKANFSIGRMTQDLAGTYRCYGSVTHSPYQVSAPSDPLDIVIIGLYEKPSLSAQLGPTVLAGENVTLSCSSRSSYDMYHLSREGEAHERRLPAGPKVNGTFQADFPLGPATHGGTYRCFGSFHDSPYEWSKSSDPLLVSVTGNPSNSWPSPTEPSSKTGNPRHLHEPKSCDKTHTCPPCPAPELLGGPSVFLFPPKPKDTLMISRTPEVTCVVVDVSHEDPEVKFNWYVDGVEVHNAKTKPREEQYNSTYRVVSVLTVLHQDWLNGKEYKCKVSNKALPAPIEKTISKAKGQPREPQVYTLPPSRDELTKNQVSLTCLVKGFYPSDIAVEWESNGQPENNYKTTPPVLDSDGSFFLYSKLTVDKSRWQQGNVFSCSVMHEALHNHYTQKSLSLSPGK

KIR2DL1*022

HEGVHRKPSLLAHPGPLVKSEETVILQCWSDVMFEHFLLHREGKFNDTLRLIGEHHDGVSKANFSISRMTQDLAGTYRCYGSVTHSPYQVSAPSDPLDIVIIGLYEKPSLSAQPGPTVLAGENVTLSCSSRSSYDMYHLSREGEAHERRLPAGPKVNGTFQADFPLGPATHGGTYRCFGSFHDSPYEWSKSSDPLLVSVTGNPSNSWPSPTEPSSKTGNPRHLHEPKSCDKTHTCPPCPAPELLGGPSVFLFPPKPKDTLMISRTPEVTCVVVDVSHEDPEVKFNWYVDGVEVHNAKTKPREEQYNSTYRVVSVLTVLHQDWLNGKEYKCKVSNKALPAPIEKTISKAKGQPREPQVYTLPPSRDELTKNQVSLTCLVKGFYPSDIAVEWESNGQPENNYKTTPPVLDSDGSFFLYSKLTVDKSRWQQGNVFSCSVMHEALHNHYTQKSLSLSPGK

KIR2DL2*001

HEGVHRKPSLLAHPGRLVKSEETVILQCWSDVRFEHFLLHREGKFKDTLHLIGEHHDGVSKANFSIGPMMQDLAGTYRCYGSVTHSPYQLSAPSDPLDIVITGLYEKPSLSAQPGPTVLAGESVTLSCSSRSSYDMYHLSREGEAHECRFSAGPKVNGTFQADFPLGPATHGGTYRCFGSFRDSPYEWSNSSDPLLVSVIGNPSNSWPSPTEPSSKTGNPRHLHEPKSCDKTHTCPPCPAPELLGGPSVFLFPPKPKDTLMISRTPEVTCVVVDVSHEDPEVKFNWYVDGVEVHNAKTKPREEQYNSTYRVVSVLTVLHQDWLNGKEYKCKVSNKALPAPIEKTISKAKGQPREPQVYTLPPSRDELTKNQVSLTCLVKGFYPSDIAVEWESNGQPENNYKTTPPVLDSDGSFFLYSKLTVDKSRWQQGNVFSCSVMHEALHNHYTQKSLSLSPGK

KIR2DL2*003

HEGVHRKPSLLAHPGRLVKSEETVILQCWSDVRFEHFLLHREGKFKDTLHLIGEHHDGVSKANFSIGPMMQDLAGTYRCYGSVTHSPYQLSAPSDPLDIVITGL
YEKPSLSAQPGPTVLAGESVTLSCSSRSSYDMYHLSREGEAHECRFSAGPKVNGTFQADFPLGPATHGGTYRCFGSFRDSPYEWSNSSDPLLVSVTGNPSNSWP
SPTEPSSKTGNPRHLHEPKSCDKTHTCPPCPAPELLGGPSVFLFPPKPKDTLMISRTPEVTCVVVDVSHEDPEVKFNWYVDGVEVHNAKTKPREEQYNSTYRVV
SVLTVLHQDWLNGKEYKCKVSNKALPAPIEKTISKAKGQPREPQVYTLPPSRDELTKNQVSLTCLVKGFYPSDIAVEWESNGQPENNYKTTPPVLDSDGSFFLY
SKLTVDKSRWQQGNVFSCSVMHEALHNHYTQKSLSLSPGK

KIR2DL2*009

HEGVHRKPSLLAHPGRLVKSEETVILQCWSDVRFEHFLLHREGKFKDTLHLIGEHHDGVSKANFSIGPMMQDLAGTYRCYGSVTHSPYQLSAPSDPLDIVITGL
YEKPSLSAQPGPTVLAGESVTLSCSSRSSYDMYHLSREGEAHERRFSAGPKVNGTFQADFPLGPATHGGTYRCFGSFRDSPYEWSNSSDPLLVSVTGNPSNSWP
SPTEPSSKTGNPRHLHEPKSCDKTHTCPPCPAPELLGGPSVFLFPPKPKDTLMISRTPEVTCVVVDVSHEDPEVKFNWYVDGVEVHNAKTKPREEQYNSTYRVV
SVLTVLHQDWLNGKEYKCKVSNKALPAPIEKTISKAKGQPREPQVYTLPPSRDELTKNQVSLTCLVKGFYPSDIAVEWESNGQPENNYKTTPPVLDSDGSFFLY
SKLTVDKSRWQQGNVFSCSVMHEALHNHYTQKSLSLSPGK

KIR2DL3*001

HEGVHRKPSLLAHPGPLVKSEETVILQCWSDVRFQHFLLHREGKFKDTLHLIGEHHDGVSKANFSIGPMMQDLAGTYRCYGSVTHSPYQLSAPSDPLDIVITGL
YEKPSLSAQPGPTVLAGESVTLSCSSRSSYDMYHLSREGEAHERRFSAGPKVNGTFQADFPLGPATHGGTYRCFGSFRDSPYEWSNSSDPLLVSVTGNPSNSWP
SPTEPSSETGNPRHLHEPKSCDKTHTCPPCPAPELLGGPSVFLFPPKPKDTLMISRTPEVTCVVVDVSHEDPEVKFNWYVDGVEVHNAKTKPREEQYNSTYRVV
SVLTVLHQDWLNGKEYKCKVSNKALPAPIEKTISKAKGQPREPQVYTLPPSRDELTKNQVSLTCLVKGFYPSDIAVEWESNGQPENNYKTTPPVLDSDGSFFLY
SKLTVDKSRWQQGNVFSCSVMHEALHNHYTQKSLSLSPGK

KIR2DL3*002

HEGVHRKPSLLAHPGPLVKSEETVILQCWSDVRFQHFLLHREGKFKDTLHLIGEHHDGVSKANFSIGPMMQDLAGTYRCYGSVTHSPYQLSAPSDPLDIVITGL
YEKPSLSAQPGPTVLAGESVTLSCSSRSSYDMYHLSREGEAHERRFSAGPKVNGTFQADFPLGPATHGGTYRCFGSFRDSPYEWSNSSDPLLVSVTGNPSNSWL
SPTEPSSETGNPRHLHEPKSCDKTHTCPPCPAPELLGGPSVFLFPPKPKDTLMISRTPEVTCVVVDVSHEDPEVKFNWYVDGVEVHNAKTKPREEQYNSTYRVV
SVLTVLHQDWLNGKEYKCKVSNKALPAPIEKTISKAKGQPREPQVYTLPPSRDELTKNQVSLTCLVKGFYPSDIAVEWESNGQPENNYKTTPPVLDSDGSFFLY
SKLTVDKSRWQQGNVFSCSVMHEALHNHYTQKSLSLSPGK

KIR2DL3*009

HEGVHRKPSLLAHPGPLVKSEETVILQCWSDVRFQHFLLHREGKFKDTLHLIGEHHDGVSKANFSIGPMMQDLAGTYRCYGSVTHSPYQLSAPSDPLDIVITGL
YEKPSLSAQPGPTVLAGESVTLSCSSRSSYDMYHLSREGEAHEPRFSAGPKVNGTFQADFPLGPATHGGTYRCFGSFRDSPYEWSNSSDPLLVSVTGNPSNSWP
SPTEPSSETGNPRHLHEPKSCDKTHTCPPCPAPELLGGPSVFLFPPKPKDTLMISRTPEVTCVVVDVSHEDPEVKFNWYVDGVEVHNAKTKPREEQYNSTYRVV
SVLTVLHQDWLNGKEYKCKVSNKALPAPIEKTISKAKGQPREPQVYTLPPSRDELTKNQVSLTCLVKGFYPSDIAVEWESNGQPENNYKTTPPVLDSD
GSFFLYSKLTVDKSRWQQGNVFSCSVMHEALHNHYTQKSLSLSPGK

KIR2DL3*016

HEGVHRKPSLLAHPGPLVKSEETVILQCWSDVRFQHFLLHREGKFKDTLHLIGEHHDGVSKANFSIGPMMQDLAGTYRCYGSVTHSPYQLSAPSDPLDIVITGL
YEKPSLSAQPGPTVLAGENVTLSCSSRSSYDMYHLSREGEAHERRFSAGPKVNGTFQADFPLGPATHGGTYRCFGSFRDSPYEWSNSSDPLLVSVTGNPSNSWP
SPTEPSSETGNPRHLHEPKSCDKTHTCPPCPAPELLGGPSVFLFPPKPKDTLMISRTPEVTCVVVDVSHEDPEVKFNWYVDGVEVHNAKTKPREEQYNSTYRVV
SVLTVLHQDWLNGKEYKCKVSNKALPAPIEKTISKAKGQPREPQVYTLPPSRDELTKNQVSLTCLVKGFYPSDIAVEWESNGQPENNYKTTPPVLDSDGSFFLY
SKLTVDKSRWQQGNVFSCSVMHEALHNHYTQKSLSLSPGK

Appendix J: Vpu sequences of HIV-1 strains

HIV-1 JRCSF wt

MQPLQILAIVALVVAGIIAIIVWSIVLIEYRKILRQRKIDRLIDKIRERAEDSGNESEGDQEELSALVERGHLAPWDINDL

HIV-1 JRCSF Vpu mutant (L4IQ5del)

MQPIILAIVALVVAGIIAIIVWSIVLIEYRKILRQRKIDRLIDKIRERAEDSGNESEGDQEELSALVERGHLAPWDINDL

HIV-1 NL4-3

MQPIIVAIVALVVAIIIAIVVWSIVIIEYRKILRQRKIDRLIDRLIERAEDSGNESEGEVSALVEMGVEMGHHAPWDIDDL

Appendix K: *HLA-C* allele frequencies

Appendix Table 1: HLA-C allele frequencies. Source: (e).

	Allele	Frequency
1	**C*07:01**	0.14697
2	**C*07:02**	0.13418
3	**C*04:01**	0.12506
4	**C*06:02**	0.10005
5	**C*03:04**	0.07408
6	**C*05:01**	0.06380
7	**C*12:03**	0.06317
8	**C*02:02**	0.05407
9	**C*03:03**	0.05105
10	**C*01:02**	0.03574
11	C*15:02	0.02618
12	C*08:02	0.02380
13	**C*16:01**	0.02246
14	**C*14:02**	0.01519
15	C*12:02	0.01075
16	C*17:01	0.01014
17	C*16:02	0.00602
18	C*15:05	0.00489
19	C*08:01	0.00073
20	C*02:10	0.00031

Appendix L: *KIR2DL* allele frequencies

Appendix Table 2: *KIR2DL* allele frequencies. Source: DKMS.

Locus: *KIR2DL1**		Locus: *KIR2DL2**		Locus: *KIR2DL3**	
Allele	**Frequency**	**Allele**	**Frequency**	**Allele**	**Frequency**
003	0.373410	NEG	0.452898	**001**	0.469908
001	0.168364	**001**	0.274612	**002**	0.323055
002	0.168355	**003**	0.225329	POS	0.079708
004	0.107953	POS	0.033997	NEG	0.064636
POS	0.052174	NEW	0.003303	005	0.016848
010	0.028033	005	0.002338	003	0.014284
NEW	0.027851	008	0.002296	NEW	0.007083
006	0.025908	002	0.002139	021	0.005758
NEG	0.018643	010	0.001661	007	0.005729
007	0.010940	012	0.000996	012	0.005726
008	0.005399	006	0.000262	024	0.005723
009	0.003847	**009**	0.000167	015	0.000695
018	0.003836	013	0.000002	030	0.000240
015	0.003834	004	0.000002	006	0.000191
020	0.000973			027	0.000129
012	0.000236			**009**	0.000095
005	0.000081			013	0.000045
014	0.000049			011	0.000045
011	0.000042			023	0.000023
017	0.000027			028	0.000020

Appendix M: *Vpu* sequences of PBMC samples

PBMC_1	MQTIQIVAIAALVVVGIIAIVVWSIVLIEYRKILRQRKIDRLVNRIIERAEDSGNESEGEVSALVAMVVEMGHHAPWDVNDQ*
PBMC_3	MQQLYLLTIVAFVVALLLAIIVWSIVLIEYRKILRQRKIDRLLDRIRERAEDSGNESDGDQEELSILVDRGHLAPWDIDDQ*
PBMC_4	MQPIIVAIVALVVAIIIAIVVWSIVIIEYRKILRQRKIDRLIDRLIERAEDSGNESEGEVSALVEMGVEMGHLAPWDIDDQ*
PBMC_5	MQSTVVAAIVALVIAAIIAIVVWTIVLIEYRKILRQRKIDRLLERIIERAEDSGNESEGDQEELSALVEMGHHAPWDVNDL*
PBMC_7	MQLSPVITIIALVVAAIIAIIVWTIVLIEYRKILRQRKIDRLIDRIAERAEDSGNESEGEVSALVEMGVEMGHHAPWDIDDL*
PBMC_8	MNSLTIVAVVALVVAAIIAIVVWSIVIIEYRKILRQRKIDRLIDRLIERAEDSGNESEGEVSALVEMGVEMGHHAPWDIDDL*
PBMC_9	MQPIIVAIVALVVAAIIAIVVWSIVFIEYRKILRQRKIDRLIDRLIERAEDSGNESEGEVSALVEMGVEMGHHAPWDIDDL*
PBMC_12	MQLLIISIVALVVAAILAIIVWTIVFIEYRKILRQRKIDRLIDRLIERAEDSGNESEGEVSALVEMGVEMGHHAPWDIDDL*
PBMC_15	MQPIIVAIVALVVAIGILAIVVWTIVLLEYRKILRQRKIDRLIDRIGDREEDSGNESDGDQDEVSALVEMGVEMGHDAPWNVDDL*
PBMC_17	MTPEAILSIVALVIVAILAIVVWTIVLLEYKKILRQRKIDRLIDRIADREEDSGNESDGDQDELSAIMEKGHLAPWNVGDL*
PBMC_19	MQPIIVAIVALVVAIILAIVVWTIVLLEYRKILRQRKIDRLIDRLIERAEDSGNESEGEVSALVEMGVEMGHHAPWDIDDL*
PBMC_20	MQPIIVAIVALVVATILAIVVWTIVLLEYRKILRQRKIDRLIDRIAERAEDSGNESDGDQDELSAIMEKGHLAPWNVDDL*
PBMC_21	MQPIIVAIVALVVAIIIAIVVWSIVIIEYRKILRQRKIDRLLDRIIERAEDSGNESEGEVSALVEMGVEMGHHAPWDIDDL*
PBMC_22	MQLLIISIVALVVAAILAIIVWTIVFIEYRKILRQRKIDRLIDRLIERAEDSGNESEGEVSALVEMGVEMGHHAPWDIDDL*
PBMC_23	MQLLIISIVALVVAAILAIIVWTIVFIEYRKILRQRKIDRLIDRISERAEDSGNESEGDREEEELSALMEMGHHAPWDVNDL*
PBMC_25	MQLLIISIVALVVAAILAIIVWTIVFIEYRKILRQRKIDRLIDRISERAEDSGNESEGDQEELSALMEMGHHAPWDVNDL*
PBMC_26	MQPLQIVAIAALVVVAIIAIVVWTIVLIEYRKLLRQRKIDRLIDRLIERAEDSGNESDGDQEELSALMEMGHHAPWNVDDL*
PBMC_30	MQPIIVAIVALVVAIIIAIVVWSIVIIEYRKILRQRKIDRLFERIRERAEDSGNESEGEVSALVEMGVEMGHHAPWDIDNL*
PBMC_31	MQPIIVAIVALVVAGIIAIVVWSIVIIEYRRILKQRKIDRIIDRLIERAEDSGNESEGEVSALVEMGVEMGHHAPWDIDDL*
PBMC_32	MQPIIVAIVALVVAIIIAIVVWSIVIIEYRKILRQRKIDRLIDRLIERAEDSGNESEGEVSALVEMGVEMGHHAPWDIDDL*
PBMC_33	MKSIQIAAIVALVVAAIIAIVVWSIVLIEYRKILRQRKIDRLINRIAERAEDSGNESEGDQEELSALVEMGHDAPWDVDDL*
PBMC_34	MTLSIISIVALVVVAILAIIVWTIVLIEYKKILRQRKIDKLLDRISERAEDSGNESEGEVSALVEMGVEMGHHAPWDIDDL*
PBMC_35	MQPIIVAIVALVVAAIIAIVVWSIVIIEYRKILRQRKIDRLIDRLIERAEDSGNESEGEVSALVEMGVEMGHHAPWDIDDL*

PBMC_36	MTLLILSIVALVVAFLLAVVIWTLVFIEYRKILRQRRIDRLIERIRERAEDSGNESEGEVSALVEMGVEMGHHAPWDIDDL*
PBMC_40	MQPIIVAIVALVVAIIIAIVIWSLVLIEYKKILRQRKIDRLIERIIERAEDSGNESEGEVSALVEMGVEMGHHAPWDIDDL*
PBMC_42	MQPIIVAIVALVVAIILAIVVWTIVFIEYRKILRQRKIDRLIDRIRERAEDSGNESEGEVSALVEMGVEMGHHAPWDIDDL*
PBMC_47	MQPIIVAIVALVVAIILAIVVWTIVLLEYKKILRQRKIDRLIDRIIERAEDSGNESEGEVSALVEMGVEMGHHAPWDIDDL*
PBMC_48	MTPLTIAAIVALVVATIIAIVVWTIVFIEYRKILRERRIDRLIDRIRERAEDSGNESEGDQEELSGLMELGHHAPWNVDDL*
PBMC_49	MTPLTILSIVALVVVAIIIAIVVWSIVLIEYKKILRQRKIDRLIERISDREEDSGNESEGEVSALVEMGVEMGHHAPWDIDDL*
PBMC_54	MQPIIVAIVALVVATILAIIVWTIVLLEYRKILRQRKIDRLIDRLIERAEDSGNESEGEVSALVEMGVEMGHHAPWDIDDL*
PBMC_55	MQSLIILAIAALVVAAILAIVVWTIVFIEYRKILRQRKIDRLIDRIRERAEDSGNESDGDQEELSALVERGHLAPWDVDDQ*
PBMC_56	MNSLTIVAVVALVVAAIIAIVVWSIVIIEYRKILRQRKIDRLIDRIRERAEDSGNESEGDHEELSALVEMGHNAPWDVDDL*
PBMC_58	MTLLVTVSIVALVVAAIIAIVVWTLAFIEYRKILRQKKIDRIIDRIRERAEDSGNESEGDQEELSALVERGHLEMGHHAPWDVNDL*
PBMC_59	MQPIIVAIVALVVAGIIAIVVWSIVIIEYRKILRQRKIDRLIDRLIERAEDSGNESEGEVSALVEMGVEMGHHAPWDIDDL*
PBMC_65	MQLLIISIVALVVAAILAIIVWTIVFIEYRKILRQRKIDRLIDRLIERAEDSGNESEGEVSALVEMGVEMGHHAPWDIDDL*
PBMC_68	MQPIIVAIVALVVAGIIAIVVWSIVIIEYRKILRQRKIDRLIDRLIERAEDSGNESEGDQEEVSALVEMGVEMGHHAPWDIDDL*
PBMC_69	MQPIIVAIVALVVAIIIAIVVWSIVIIAYRKILRQRKIDRLIERLIERAEDSGNESEGEVSALVEMGVEMGHHAPWDIDDL*
PBMC_70	MTPLTIVSIVALVVAIIIAIVVWSIVLIEYKKILRQRKIDRLIDRIRDREEDSGNESEGEVSALVEMGVEMGHHAPWDIDDL*
PBMC_72	MQLLIISIVALVVAAILAIIVWTIVFIEYRKILRQRKIDRLIDRISERAEDSGNESEGDQEELSALMEMGHHAPWDVNDL*
PBMC_75	MQPIIVAIVALVVAIIIAIVVWSIVLIEYRRILRQKKIDRLIDRIRERAEDSGNESEGDQEELSALVERGHLAPWDITDR*
PBMC_76	MQSLQIAAIVGLVVAVILAIVVWTIVFIEYRKILRQRKIDRLIDRIAERAEDSGNESEGETIISTGGDGASCSLEC*
PBMC_77	MQLSPVITIIALVVAAIIAIIVWTIVLIEYRKILRQRKIDRLIDRLIERAEDSGNESEGEVSALVEMGVEMGHLAPWDVNDL*
PBMC_81	MQPIIVAIVALVVAIIIAIVVWSIVIIEYRKILRQRKIDRLIDRLIERAEDSGNESEGEVSALVERGHLAPWDVNDL*
PBMC_82	MQPIIVAIVALVVAIIIAIVVWSIVIIEYRKILRQRKIDRLIDRLIERAEDSGNESEGEVSALVERGHLAPWHIDDM*
PBMC_83	MQPIIVAIVALVVAGIIAIVVWSIVTIEYRKILRQRKIDRLIDRLIERAEDSGNESEGEVSALVEMGVEMGHHAPWDIDDL*
PBMC_84	MQPIIVAIVALVVAGIIAIVVWSIVIIEYRKILRQRKIDRLIDRIRERAEDSGNESEGEVSALVEMGVEMGHHAPWDVNDL*
PBMC_85	MQPIIVAIVAFVVAIIIVIVVWTIVLIEYRKLLRQRKIDRLIDRIQERAEDSGNESEGEVSALVDGNGAPCSSGC*
PBMC_87	MQPIIVAIVALVVAGIIAIVVWSIVIIEYRKILRQRKIDRLIDRLIERAEDSGNESEGEVSALVEMGVEMGHHAPWDIDDL*
PBMC_88	MQPLEIVAIVALVVAIIIAIVVWSIVIIEYRKILRQRKIDRLIDRLIERAEDSGNESEGEVSALVEMGVEMGHHAPWDIDDL*
PBMC_89	MQPIIVAIVALVVAGIIAIIVWSIVLIEYRKILRQRKIDRLIDRLIERAEDSGNESEGEVSALVEMGVEMGHHAPWDIDDL*
PBMC_90	MQPIIVAIVALVVAGIIAIVVWSIVIIEYRKILRQRKIDRLIDRLIERAEDSGNESEGEVSALVEMGVEMGHHAPWDIDDL*
PBMC_91	MQPIIVAIVAFVVAIIIVIVVWTIVLIEYRKLLRQRKIDRLIDRLQERAEDSGNESEGEVSALVEMGVEMGHHAPRDVNDL*
PBMC_92	MHTSEIAVIVAFVVAIIIVIVVWTIVLIEYRKLLRQRKIDRLIERIQERAEDSGNESEGDQEELSALMEMGHHAPRDVNDL*
PBMC_93	MQPIIVAIVALVVAGIIAIVVWSIVIIEYRKILRQRKIDRLIDRLIERAEDSGNESEGEVSALVEMGVEMGHHAPWDIDDL*
PBMC_94	MQPIIVAIVALVVAIIIAIVVWSIVFIEYRRIVKQRKIDRLITRIIERAEDSGNESEGEVSALVEMGVEMGHHAPWDVDDL*
PBMC_96	MQSLQIAAIVALVVAAIIAIVVWSIVIIEYKKILKQRRIDRLIDRIRERAEDSGNESEGEVSALVEMGVEMGHHAPWDVNDM*
PBMC_97	MQPIIVAIVALVVAGIIAIVVWSIVIIEYRKILRQRKIDRLIDRLIERAEDSGNESEGEVSALVEMGVEMGHHAPWDIDDL*
PBMC_98	MQPIIVAIVALVVAGIIAIVVWSIVIIEYRKILRQRKIDRLIDRLIERAEDSGNESEGEVSALVEMGVEMGHHAPWDIDDL*
PBMC_99	MQPIIVAIVALVVGIIAIIVWSIVFIEYRKILRQRKINRILDKIRERAEDSGNESDGDQEELSALVDRGHVAPWDVNDL*
PBMC_100	MQPIILAIVALVVAGIIAIVVWSIVLIEYRKILRQRKIDRLIDKIRERAEDSGNESEGDQEELSALVERGHLAPWDINDL*
PBMC_101	MQPIIVAIVALVVAGIIAIVVWSIVIIEYRKILRQRKIDRLIDRLIERAEDSGNESEGEVSALVEMGVEMGHHAPWDIDDL*
PBMC_102	MQPIILAIVALVVAGIIAIIVWSIVLIEYRKILRQRKIDRLIDKIRERAEDSGNESEGDQEELSALVERGHLAPWDINDL*
PBMC_103	MQPIILAIVALVVAGIIAIIVWSIVLIEYRKILRQRKIDRLIDRLIERAEDSGNESEGDQEELSALVERGHLAPWDINDL*
PBMC_104	MQPIIVAIVALVVAGIIAIVVWSIVIIEYRKILRQRKIDRLIDRLIERAEDSGNESEGEVSALVEMGVEMGHHAPWDIDDL*
PBMC_105	MQPIIVAIVALVVAGIIAIVVWSIVIIEYRKILRQRKIDRLIDRLIERAEDSGNESEGEVSALVEMGVEMGHHAPWDIDDL*
PBMC_106	MQPIIVAIVALVVAGIIAIVVWSIVIIEYRKILRQRKIDRLIDRLIERAEDSGNESEGEVSALVEMGVEMGHHAPWDIDDL*
PBMC_107	MQPIIVAIVALVVAGIIAIIVWSIVFIEYRKILRQRKIDRLIDRLIERAEDSGNESEGEVSALVEMGVEMGHHAPWDIDDL*

Appendix N: *Vpu* sequences of plasma samples

Plasma_1	MQTIQIVAIAALVVVGIIAIVVWSIVLIEYRKILRQRKIDRLVNRIIERAEDSGNESEGEVSALVEMGHLVPWDVNDQ*
Plasma_2	MQPLLIYSIVALVVVGIIAIVVWTIVFIEYRKILRQRKIDRLIERIRERAEDSGNESEGDQEELSELIVERGYDAPWDIDDL*
Plasma_3	MQQLYLLTIVAFVVALLLAIIVWSIVLIEYRKILRQRKIDRLLDRIRERAEDSGNESDGDQEELSILVDRGHLAPWDIDDQ*
Plasma_5	MQTLQIVAIVALVVAAIIAIVVWTIVGIEYRKILRQRKIDKLIDRIRERAEDSGNESEGDQEELSALVEMGHHAPWDVNDL*
Plasma_6	MQPLVIATIVGLIVAAILAVVVWTIVFIEYRKILRQRRIDRLIDRITERAEDSGNESDGDHEALLVEMGNHAPWDVDDL*
Plasma_7	MQLSPVITIIALVVAAIIAIIVWTIVLIEYRKILRQRKIDRLIDRIAERAEDSGNESEGDQVSALVEMGVEMGHHAPWDVNDL*

Plasma_9	MQPIILSIVALVVAAIIAIIVWTIVYIEYRKILRQRRIDRLIDRITERAEDSGNESEGEVSALVEMGVEMGHYAHHAPWDVDDL*
Plasma_10	MQALPIVSITALVIVGIIAIIVWTIVLIEYRKILRERKIDRLIDRLIERAEDSGNESEGEVSALVEMGRHAPWVDNAL*
Plasma_11	MQPLLIYSIVALVVVGIIAIVVWTIVFIEYRKILRQRKIDRLIERIRERAEDSGNESEGDQEELSELIVERGYDAPWDIDDL*
Plasma_12	MQALTIVAIAALVVVAIIAIVVWSIVLIEYRKILRQRKIDRLIDRIRERAEDSGNESEGEVSALVEMGVEMGHHAPWDIDDL*
Plasma_13	MQSLKIAAIVGLVVAAIIAIVVWSIVLIEYRKILRQKRIDRLIDRIRERAEDSGNESEGDQEELSALVERGHLAPWAIDDL*
Plasma_14	MQPLEILAVVALVVALILAIVVWTIVYIEYRKIQKQKKIDRLIDRIRERAEDSGNESDGDQEELSALVEMGHHAPWDVNDE*
Plasma_15	MTLIIAIVALVIVGIIAIVVWTIVFIEYRKIVRQKKIDRLIDRIRDRAEDSGNDSDGDQEELSGLVGRGHLAPWDVNDL*
Plasma_16	MHPLVIVSIAALVIVTIIAIVVWSIVLIEYMKILKQRKIDRLLARILERAEDSGNESEGEVSALVEVGHDAPGNVDDL*
Plasma_17	MTLLVTVSIVALVVAAIIAIVVWTLAFLEIRKFLRQKKIDRIIDRIRERAEDSGNESEGDQEELSALVERGHLEMGHNAPWDVNDL*
Plasma_18	MQPLVIGTIVALIVAAIIAIVVWSIVLIEYRKILRQRKIDRLINKIRERAEDSGNESDGEVSALVEMGVEMGHHAPWDIDDL*
Plasma_19	MQALTHNINSSFNSSSAILAIVVWTIVLLEYRKILRQRKIDRLIDRIAERAEDSGNESDGDQDEVSAIMEKGHLAPWNVDDL*
Plasma_20	MQPIIVAIVALVVAIIIAIVVWSIVIIEYRKILRQRRIDRLIDRIRERAEDSGNESEGEVSALVEMGVEMGHHAPWDVNDL*
Plasma_21	MQSLQIAAIVGLVVVGIIAIVVWSIVLIEYRKILRQREIDRLIDRITERAEDSGNESEGDQEVSALVEMGVERGHLAPGNVNDR*
Plasma_22	MQPLIIASIVALVVVGIIAIVVWTIVLLEYRKILRQRKIDRLIDRIRERAEDSGNESEGDQEELSKLVEMGPDDLWDVDDL*
Plasma_23	MQSLIVLAIVALVVAAILAIVVWIIVFIEYRKILRQRKIDRLIDRIRERAEDSGNESEGDQEALLELGYDAPWGIDDL*
Plasma_24	MQSLEILSIVALVVAGLIAIVVWTIVLIEYRKILRQRKIDRLIDRIRERAEDSGNDSDGDQEELSALVERGHLAPWDIDDL*
Plasma_25	MQLLIISIVALVVAAILAIIVWTIVFIEYRKILRQRKIDRLIDRISERAEDSGNESEGDQEELSALMEMGHHAPWDVNDL*
Plasma_26	MQPLQIVAIAALVVVAIIAIVVWTIVLIEYRKLLRQRKIDKLIDRLIERAEDSGNESEGEVSALMEMGHHAPWNVDDL*
Plasma_27	MQPIIVAIVALVVAGIIAIVVWSIVIIEYRKILRQRKIDRLIDRLIERAEDSGNESEGDQEEVSALVEMGVEMGHHAPWDIDDL*
Plasma_28	MQPIIVAIVALVVAIIIAIVVWSIVIIEYRKILRQRKIDRLIDRLIERAEDSGNESEGEVSALVEMGVEMGHHAPWDIDDL*
Plasma_29	MQPIIVAIVALVVATGIIAIIVWTIVFIEYIKILKQRKIDRLLTKIIERAEDSGNESEGEVSALVEMGVEMGHHAPWDIDDL*
Plasma_30	MQPIIVAIVALVVAIIIAIVVWSIVIIEYRKILRQRKIDRLIDRIRERAEDSGNESEGEVSALVEMGHLVLGDIDNL*
Plasma_31	MQPIIVAIVALVVAAILAIVVWSIVIIEYRKILRQRKIDRLIDRLIERAEDSGNESEGEVSALVEMGVEMGHHAPWDIDDL*
Plasma_32	MQPLEIVSIAALVAVTIIAIVVWSIVLIEYRKILRQRKIDRLIDRIRERAEDSGNESEGDEEQLAALVERGHLAPWGVDDL*
Plasma_33	MKSIQIAAIVALVVAAIIAIVVWSIVLIEYRKILRQRKIDRLINRIAERAEDSGNESEGDQEELSALVEMGHDAPWDVDDL*
Plasma_34	MTPLTIVSIVALVVVTIIAIVVWSIVLIEYKKILRQRKIDRLIDRIIDREEDSGNESEGDQEELSAIVEMGHLAPWDITD*
Plasma_35	MTPEVILAIVALVIVAIIAIVIWSLVLIEYRKILRQRKIDRLIERISERAEDSGNESEGEVSALVEMGVEMGHHAPWDVDDQ*
Plasma_37	MQPIIVSIVALVVAALIAIIVWTIVFIEYRKILRQKKIDRLLDRIRERAEDSGNESDGDNEELSALVERGHLAPWDIDDR*
Plasma_38	MQSLTILAIVALVVASIIAIVVWTIVYIEYRKILRQRKIDRLIDRIRERAEDSGNESEGDQEELSELVERGHLAPWDVNDL*
Plasma_39	MQSIQIAGIVALVIAAILAIVVWSIVFIEYRKILRQRRIDKLLDRIIERAEDSGNESDGDQEELSALVEMGHHAPWVVNDL*
Plasma_40	MIPLAVLSIVALVVVAIIAIAVWTIVFIEYRKILRQRKIDRLIDRIRDRAEDSGNESEGDQEQLSALLEMGHDAPWNVDDL*
Plasma_41	MQPIIVAIVALVVAALIAIIVWTIVLIEYRKILRQRKIDKLLDRIRERAEDSGNESDGDHEELSALVERGHLAPWDIDDQ*
Plasma_42	MNSLTIVAVVALVVAGIIAIVVWSIVIIEYRKILRQRKIDRLIDRIRERAEDSGNESEGDHEELSALVEMGHNAPWDVDDL*
Plasma_43	MIPLQIAALVGLVVAAISAVVVWTIVGLEYRKILRQRKIDRLIDRIAERAEDSGNESDGDQDELSALVVEMGHHAPWNIDD*
Plasma_44	MQPLVVGIVALVVAGILAIVVWTIVFLEYRKILRQRKIDRLINRIAERAEDSGNESEGDQEELSALVDMGHDAPWDVDDL*
Plasma_45	MQPIIVAIVALVVAIIIAIIVWTIVLIEYRKILRERRIDRLINRIGERAEDSGNESEGDQGNQEVSALVEMGVEMGHHAPWDIDDL*
Plasma_46	MQPIIVAIVALVVAIIIAIVVWSIVIIEYRKILRQRKIDRLIERIRERAEDSGNESEGEVSALVEMGVEMGHHAPWDYDNL*
Plasma_48	MTPLTIAAIVALVVATIIAIVVWTIVFIEYRKILRERRIDRLIDRIRERAEDSGNESEGDQEELSGLMELGHHAPWNVDDL*
Plasma_49	MQPIIVAIVALVVATILAIVVWSIVFIEYRKIRKQRKIDKLIDRIRERAEDSGNESDGDQEQLSALMEMGHHAPWDIDDE*
Plasma_50	MQSLQILAIVALVVVAIIAIVVWTIVLIEYRKILRQRKIDRLIDRIRERAEDSGNESEGEVSALVEMGVEMGHHAPWDIDDL*
Plasma_51	MTPLQISAIVGLVVAFIIAIFVWSIVLIEYRRILRQRKIDRLINRIRDRAEDSGNESEGEVSALVEMGVEMGHHAPWDIDDL*
Plasma_52	MQALTIVAIAALVVVAIIAIVVWSIVLIEYRKILRQRKIDRLIDRIRERAEDSGNESEGEVSALLGVERGHDAPWDVNDL*
Plasma_53	MQLLIISIVALVVAAILAIIVWTIVFIEYRKILRQRKIDRLIDRLIERAEDSGNESEGEVSALVEMGVEMGHHAPWDIDDL*
Plasma_55	MQSLIILAIAALVVAAILAIVVWTIVFIEYRKILRQRKIDRLIDRIRERAEDSGNESDGDQEELSALVERGHLAPWDVDDQ*
Plasma_56	MNSLTIVAVVALVVAAIIAIVVWSIVIIEYRKILRQRKIDRLIDRIRERAEDSGNESEGDHEELSALVEMGHNAPWDVDDL*
Plasma_57	MQPIIVAIVALVVAIIIAIVVWSIVIIEYRKIIRQRKIDRLIERIRERAEDSGNESEGEVSALVEMGVEMGHHAPWDIDDL*
Plasma_58	MTLLVTVSIVALVVAAIIAIVVWTLAFIEIRKFLRQRKIDRLIDRLIERAEDSGNESEGELSALVERGHLEMGHNAPWDVNDL*
Plasma_59	MQPIIVAIVALVVAIIIAIVVWSIVFIEYRRIVKQRKIDRLITRLIERAEDSGNESEGEVSALVEMGVEMGHHAPWDIDDL*
Plasma_60	MQPIIVAIVALVVVAIIAIIVWTIVLIEYRKLLRQKRIDRLIDRIRERAEDSGNESEGDQDELSTLVLEMGHDAPWNVNDL*
Plasma_61	MNSLTIVAVVALVVAAIIAIVVWSIVIIEYRKILRQRKIDRLIDRLIERAEDSGNESEGEVSALVEMGVEMGHHAPWDIDDL*
Plasma_62	MQPIIVAIVALVVAGIIAIVVWSIVIIEYRKILRQRKIDRLIDRLIERAEDSGNESEGEVSALVEMGVEMGHHAPWDIDDL*
Plasma_63	MQPLVIVSIVALVVVGLIAIVVWSIVFIEYRKLLRQRKVDRLLTRIAERAEDSGNESEGDEEELSALVVEMGHHAPWNVDDQ*
Plasma_64	MQPIIVAIVALVVAIIIAIVVWSIVSIEYRKILRQRRIDWLVDKILGKEQKTVAMRVKEKRNYQHLWRWGWRASCSLGC*
Plasma_65	MQLLIISIVALVVAAIIAIVVWSIVFIEYRKILRQRKIDRLIDRLIERAEDSGNESEGEVSALMEMGHHAPWDVNDL*

Plasma_66	MSSLYVLSIVALVVAAIIAIIVWTIVFIEYRRILREKRIDRLIDRIAERAEDSGNESEGEVSALVEMGASCSLEC*
Plasma_67	MLTLHIIAIVALVIAAILAIVVWSIVFIEYRRIVKQRKIDRLITRIAERAEDSGNESEGDQEELSALVERGHYAHHAPWDVDDL*
Plasma_68	MQPIIVAIVALVVAIIIAIVVWSIVIIEYRKILRQRKIDRLIERIRERAEDSGNESEGEVSALVEMGVEMGHHAPWDIDDL*
Plasma_69	MQPIIVAIVALVVAIIIAIVVWSIVYIEYRKIQKQKKIDRLIERIGERAEDSGNESEGEVSALVEMGVERGYDAPWDIDDE*
Plasma_71	MQPIIVAIVALVVAIIIAIVVWSMVIIEYRKILRQRKIDRLIDRLIERAEDSGNESEGEVSALVEMGVEMGHHAPWDIDDL*
Plasma_72	MKSIQIAAIVALVVVAIIAIVVWSIVLIEYRKILRQRKIDRLINRIAERAEDSGNESEGDQEELSALVEMGHDAPWNVDDL*
Plasma_73	MQSTVVAAIVALVIATILAIVVWTIVLIEYRKILRQRKIDRLLERIIERAEDSGNESEGDQEELSALVEMGHHAPWDVNDL*
Plasma_74	MQSLQILAIVALVVVAIIAIVVWTIVLIEYRKILRQRKIDRLIDRIRERAEDSGNESDGDREELSLLVEMGHDAHWDVDDL*
Plasma_76	MQSLQIAAIVGLVVAVILAIVVWTIVFIEYRKILRQRKIDRLIDRIAERAEDSGNESEGETIISTGGDGASCSLEC*
Plasma_78	MQALTIVAIAALVVVAIIAIVVWSIVFIEYRKILRQRKIDRLIDRLIERAEDSGNESEGEVSALVEMGVEMGHHAPWDIDDL*
Plasma_79	MQPLVILAIVALVVVSIIAIVVWSIVLIEYRKILRQRRIDRLIDRIRDRAEDSGNESEGEVSALVEMGVEMGHHAPWDVDDL*
Plasma_80	MQLLIVSIVALVVAFLLAVVVWTIVFIEYRKILRQRRIDRLIDRIRERAEDSGNESEGEVSALVEMGVEMGHHAPWVVDDQ*
Plasma_81	MQPIIVAIVALVVAGIIAIVVWSIVIIEYRKILRQRKIDRLIDRLIERAEDSGNESEGEVSALVEMGVEMGHHAPWDIDDL*
Plasma_82	MQPIIVAIVALVVAGIIAIVVWSIVIIEYRKILRQRKIDRLIDRLRERAEDSGNESEGEELLALEEMGHLEMGHHAPWDVNDL*
Plasma_83	MQPLEIVAIVALVVAGIIAIVVWSIVIIEYRKILRQRKIDRLIDRLIERAEDSGNESEGEVSALVEMGVEMGHHAPWDIDDL*
Plasma_84	MQSIIVAIVALVVVGIIAIVVWSIVIIEYRKILRQRKIDRLIDRLIERAEDSGNESEGEVSALVEMGVEMGHHAPWDIDDL*
Plasma_86	MQPIIVAIVALVVAGIIAIVVWSIVIIEYRKILRQRKIDRLIDRLIERAEDSGNESEGEVSALVEMGVEMGHHAPWDIDDL*
Plasma_87	MQPIIVAIVALVVAGIIAIVVWSIVIIEYRKILRQRKIDRLIDRLIERAEDSGNESEGEVSALVEMGVEMGHHAPWDIDDL*
Plasma_88	MQPIIVAIVALVVAGIIAIVVWSIVIIEYRKILRQRKIDRLIDRLIERAEDSGNESEGEVSALVEMGVEMGHHAPWDIDDL*
Plasma_89	MQPIIVAIVALVVAGIIAIVVWSIVIIEYRKILRQRKIDRLIDRLIERAEDSGNESEGEVSALVEMGVEMGHHAPWDIDDL*
Plasma_90	MQPIIVAIVALVVAGIIAIVVWSIVIIEYRKILRQRKIDRLIDRLIERAEDSGNESEGEVSALVEMGVEMGHHAPWDIDDL*
Plasma_91	MQPIIVAIVALVVAGIIAIIVWSIVLIEYRKILRQRKIDRLIDRLIERAEDSGNESEGDQEEVSALVEMGVERGHHAPWDIDDL*
Plasma_92	MQPIILAIVALVVAGIIAIIVWSIVLIEYRKILRQRKIDRLIDKLIERAEDSGNESEGDQEEVSALVEMGVERGHLAPWDINDL*
Plasma_93	MIPLTILAIVALVVAVIIAIVVWSIVLIEYRKILRQRKIDRLIDRIRERAEDSGNESEGDQEEVSALVEMGVEMGHLAPWHINDM*
Plasma_94	MQPIIVAIVALVVAGIIAIVVWSIVIIEYRKILRQRKIDRLIDRLIERAEDSGNESEGEVSALVEMGVEMGHHAPWDIDDL*
Plasma_95	MQPIIVAIVALVVAGIIAIVVWSIVIIEYRKILRQRKIDRLIDRLIERAEDSGNESEGEVSALVEMGVEMGHHAPWDIDDL*
Plasma_96	MQPIIVAIVALVVAGIIAIVVWSIVIIEYRKILRQRKIDRLIDRLIERAEDSGNESEGEVSALVEMGVEMGHHAPWDIDDL*
Plasma_97	MQPIIVAIVALVVAGIIAIIVWSIVLIEYRKILRQRKIDRLIDRLIERAEDSGNESEGDQEEVSALVEMGVERGHLAPWDIDDL*
Plasma_98	MQLLTTLSIVALVVAIIIAIVVWSIVIIEYRKILRQRKIDRLIDRLIERAEDSGNESEGDQEVSALVEMGVEMGHHAPWDIDDL*
Plasma_99	MQPIILAIVALVVAGIIAIIVWSIVLIEYRKILRQRKIDRLIDRLIERAEDSGNESEGDQEEVSALVEMGVERGHLAPWDINDL*
Plasma_100	MQPIIVAIVALVVAGIIAIVVWSIVIIEYRKILRQRKIDRLIDRLIERAEDSGNESEGEVSALVEMGVEMGHHAPWDIDDL*
Plasma_101	MQPIIVAIVALVVAGIIAIIVWSIVLIEYRKILRQRKIDRLIDRLIERAEDSGNESEGDQEEVSALVEMGVERGHHAPWDIDDL*
Plasma_106	MQPIIVAIVALVVAGIIAIVVWSIVIIEYRKILRQRKIDRLIDRLIERAEDSGNESEGEVSALVEMGVEMGHHAPWDIDDL*
Plasma_108	MQPIIVAIVALVVAGIIAIVVWSIVIIEYRKILRQRKIDRLIDRLIERAEDSGNESEGEVSALVEMGVEMGHHAPWDIDDL*
Plasma_109	MQPLQILAIVALVVAIIIAIIVWSIVLIEYRKILRQRKIDRLIDKLIERAEDSGNESEGDQEEVSALVEMGVEMGHHAPWDIDDL*